The Dissertation Committee for Jeffrey Douglas Williams Certifies that this is the approved version of the following dissertation

The Flavonoids and Phenolic Acids of the Genus *Silphium* and Their Chemosystematic and Medicinal Value

Committee:

Tom J. Mabry, Supervisor

Stanley Roux, Co-Supervisor

Ben Shoulders

Jennifer Clevinger

Enamel Huq

The Flavonoids and Phenolic Acids of the Genus *Silphium* and Their Chemosystematic and Medicinal Value

by

Jeffrey Douglas Williams, B.A.

Dissertation

Presented to the faculty of the Graduate School

Of the University of Texas at Austin

in Partial Fulfillment

of the Requirements

for the degree of

Doctor of Philosophy

The University of Texas at Austin

December, 2006

Dedication

I would like to dedicate this dissertation to Professor Tom J. Mabry. Without his encouragement and support for my family and his ability to open numerous doors, this project would not have been possible. Dr. Mabry has been emotionally supportive and always available.

I would like to express sincere thanks to my parents for always providing an example of hard work and sacrifice.

I would like to thank Dr. Małgorzata Wojcińska and Dr. Nabil El-Sayed for their guidance, patience and the long summer evenings spent tirelessly spotting TLC plates.

Finally, I thank Amy, *für die große Segnungen das Du zur meinem Leben bringt. Ich bin auch dankbar für der Zeit und das herrliechen Unterstuntzen daß Du mit unseren Kindern teilst.*

Liebe und Ewigkeit

Acknowledgements

I would like to express my appreciation to those individuals and institutions that provided intellectual advice, time, financial support and friendship, especially my Dissertation Committee: Dr. Tom Mabry, Dr. Stan Roux, Dr. Ben Shoulders, Dr. Jennifer Clevinger and Dr. Enamel Huq. I am grateful to Dr. Małgorzata Wojcińska for her instruction, diligence and friendship, to Dr. Roux for introducing me to a higher form of teaching and Dr. Shoulders for his instruction and help in NMR technologies. I would like to thank Steve Sorey, Jim Wallin and Howard Johnson for guidance in Dr. Shoulder's NMR chemistry analysis labs. Others I appreciate for their assistance and understanding are Dr. Klaus Linse, UT Institute for Cellular and Molecular Biology, Dr. Surangani Dharmawardhane and Dr. Nicolas Azios when they were both here at UT and later at the Universidad Central del Caribe, Puerto Rico; Dr. Nabil El-Sayed from the National Research Center, Cairo, Egypt for his optimism, patience and love for children; Dr. Mabry's graduate students Lalita Calabra, Jason Avent and Michael Woodward, as well as Barry Davis from Dr. Jennifer Brodbelt's lab; along with the UT- Austin Plant Biology Graduate Program and MCDB: Tamra Rogers, Francisco Valladares, Tamara Thomas, Maureen Meko, Kendrick Weld and Arthur De la Cruz.

The Robert A. Welch Foundation (F-130)

The Undergraduate Research Fellowship (URF), University Co-operative Society, University of Texas at Austin 2004-2006

The Flavonoids and Phenolic Acids of the Genus *Silphium* and Their Chemosystematic and Medicinal Value

Publication No._____

Jeffrey Douglas Williams, Ph.D.

The University of Texas at Austin, 2006

Supervisors: Tom J. Mabry, Stanley Roux

My chemistry studies of the genus *Silphium* involved the flavonoids and phenolic acids among eleven species. In the course of these investigations, five new flavonol triglycosides were isolated and characterized: isorhamnetin 3-*O*-α-L-rhamnosyl (1'''→6'')-*O*-*β*-D-galactopyranoside 7-*O*-β-L-apiofuranoside (**1A**), quercetin 3-*O*-α-L-rhamnosyl (1'''→6'')-*O*-*β*-D-galactopyranoside 7-*O*-β-L-apiofuranoside (**2A**), quercetin 3-*O*-*β*-L-galactosyl (1'''→6'')-*O*-*β*-D-rhamnopyranoside 7-*O*-α-L-apiofuranoside (**3A**), kaempferol 3-*O*-*β*-D-apiofuranoside 7-*O*-α-L-rhamnosyl (1''''→6''')-*O*-*β*-D-galactopyranoside (**4A**) and kaempferol 3-*O*-*β*-D-apiofuranoside 7-*O*-α-L-rhamnosyl (1''''→6''')-*O*-*β*-D (2'''-*O*-*E*-

caffeoylgalactopyranoside) (**5A)**. Many other known mono and diglycosidic flavonoids were also isolated and identified. The structures of all these compounds were established by chemical methods and spectral analyses using ^{1}H NMR, ^{13}C NMR, HMQC, HMBC, ROESY, TOCSY and LC/MS techniques. The distribution of the flavonoids and phenolic acids in all eleven members were compared with Dr. Jennifer Clevinger's DNA-based revision of the genus. In addition to the detailed chemical investigations, I present my evaluations of the chemosystematic and medicinal value of the compounds I characterized; moreover, the new flavonoids are now being made available for medicinal and pharmaceutical studies.

Table of Contents

List of Figures

List of Tables

Abbreviations

Caco-2 Cells: Human Colon Cancer Cells

COSY: Homonuclear shift correlation (**CO**rrelated **S**pectroscop**Y**) While ^{1}H, ^{1}H-COSY simply identifies which protons are coupled to each other and ^{1}H, ^{13}C-COSY identifies which protons are coupled to specific carbons, the latter is also of particular use in assigning proton resonances when the carbon resonances for the same sites are known, and vice versa.

cpDNA: **c**hloro**p**last **DNA**

DEPT: **D**istortion less **E**nhancement by **P**olarization **T**ransfer produces separate carbon subspectra for methyl, methylene and methane signals.

DOSY Experiments: The DOSY (**D**iffusion **O**rdered **S**pectroscop**Y**) application separates the NMR signals of mixture components based on different diffusion coefficients.

ETS: **E**xternal **T**ranscribed **S**pacer

FAB MS: **F**ast **A**tom **B**ombardment **M**ass **S**pectrometry

HMBC: **H**eteronuclear **M**ultiple-**B**ond **C**orrelation provides means to identify H-C connectivity through two or more bonds.

HMQC: **H**eteronuclear **M**ultiple-**Q**uantum **C**oherence provides direct H-C shift correlations from data related to the connectivity of the proton to the carbon to which it is directly bound.

ITS: **I**nternal **T**ranscribed **S**pacer

LC/MS: **L**iquid **C**hromatography/**M**ass **S**pectrometry

MAPK: **M**itogen-**A**ctivated **P**rotein **K**inase

MS: **M**ass **S**pectrometry

NMR: **N**uclear **M**agnetic **R**esonance

NOESY: (**N**uclear **O**verhauser 2D **E**nhancement **S**pectroscop**Y**) A contour projection of the one dimensional ^{1}H-NMR spectrum displayed along the diagonal, with correlated signals indicated by off-diagonal cross-peaks; this is particularly helpful in the assignment of glycosylation sites.

PCR: **P**olymerase **C**hain **R**eaction

ROESY: (**R**otating frame **O**verhauser **E**ffect **S**pectroscop**Y)** determines which signals arise from protons that are close to each other even if they are not bonded. ROESY also detects chemical and conformational exchanges.

TLC: **T**hin **L**ayer **C**hromatography

TOCSY: (**TO**tal **C**orrelated **S**pectroscop**Y**) is useful for dividing the proton signals into groups based on coupling networks used in large molecules with many separated coupling networks, which include oligo and polysaccharides.

UV: **U**ltra**V**iolet Light Spectrophotometry

TGF: **T**ransforming **G**rowth **F**actor

Introduction

The Goals of This Dissertation

The goals of this dissertation were to establish the flavonoid and phenolic acid chemistry of the genus *Silphium* and to compare the chemical findings for each species with the molecular-based assignments provided by Dr. Jennifer Clevinger (Clevinger, 1999). Thus, in addition to expanding our knowledge of the chemistry of the genus *Silphium*, these studies provide the first opportunity to compare the systematic conclusions based on both the natural product chemical findings and those deduced from DNA molecular analyses.

The application of patterns of structurally **unidentified** compounds, especially flavonoids, for systematics was initiated at the University of Texas at Austin by two botanists, the late Dr. Ralph Alston and the recently retired Dr. Billie Turner, under a program entitled "Biochemical Systematics." Chemist Dr. Tom Mabry joined the group in 1962 to bring **structural identification** to the biochemical systematic program leading to the detailed information on how to isolate, purify and structurally characterize flavonoids. These efforts resulted in a book for use by both chemists and non-chemists (especially botanists) to quickly structurally identify any and all flavonoids: **The Systematic Identification of Flavonoids, Mabry, Markham and Thomas, 1970**. Over the years using modern NMR, UV and MS spectral findings, Dr. Mabry's group assembled detailed structural data not only for flavonoids but also for many other classes of natural products including terpenoids and alkaloids; furthermore, they determined the chemical patterns for species obtained from different ecosystems and established the

biosynthetic pathways to different classes of natural products, including notably the betalains, which are the unique red and yellow pigments distinguishing most families of the Order Caryophyllales (Benke and Mabry). Since the birth and rise of molecular studies for taxonomy there have been few attempts to compare the two approaches (chemical and molecular) for the systematic treatment of taxa at the species level. The studies presented here use flavonoid and phenolic acid chemistry to support the revision of *Silphium* species made by Dr. Clevinger as described in her detailed DNA-based arrangement of the genus.

Finally, it should be noted that several of the newly discovered flavonoids isolated from both sections of the genus belong to a class of flavonoids that have important medicinal properties which include antioxidant and chemotherapeutic activities. These compounds are being made available to our contacts in other labs for bioassays involving breast, ovarian and colon cancer.

Before I describe my investigations of the chemistry in *Silphium*, I should recount how I came to be involved with this genus. In the fall of 2000, I began graduate school here at The University of Texas at Austin in order to study under the supervision of Dr. Tom Mabry. Dr. Mabry assigned me to serve as an assistant to Małgorzata ("Margaret") Wojcińska from the Department of Pharmacognosy, Medical University of Poznań in Poland. Margaret was in the process of completing her Ph.D. on the flavonoids in one species, namely *S. perfoliatum*. Originally, this species attracted special attention due to indigenous Native American reports of its uses for various medicinal purposes hundreds of years ago.

I quickly learned that carefulness and commitment of time were necessary requirements for natural products extractions and chemical analysis. Large quantities of foliage were collected and extracted in aqueous methanol. Selected columns where then prepared for the isolation steps of the flavonoids. The fractions obtained from the first columns were purified over still other columns until very pure compounds were obtained. All of the samples from each isolation were monitored by thin layer chromatography (TLC) to determine their purity. The samples were finally subjected to modern spectral analyses in UT's Chemistry and Cellular and Molecular Biology Programs using the facilities made available by Dr. Ben Shoulders (NMR), Dr. Mehdi Moini (Mass Spectrometry) and Dr. Klaus Linse (LC-MS). Without the help of these specialists, the availability of their facilities and their close connections to Dr. Mabry, I could not have finished my research in a reasonable period!

I later learned that the medicinal plant that initiated the work, *Silphium perfoliatum*, was a member of an exclusive North American genus consisting of about a dozen species distributed from Southeastern Canada down through the Appalachian Mountains and extending west on into the state of Texas. When I read that six *Silphium* species were native to Texas and that molecular taxonomists in our Plant Biology Program here at UT (Jennifer Clevinger and her supervisor Dr. José Panero) had revised the genus, I made the decision to conduct a broad scale investigation of the flavonoids in eleven *Silphium* species. I later added the phenolic acid chemistry to my studies. It has been my goal to obtain chemical data that would either support or challenge the systematic conclusions of Clevinger and Panero based on their molecular findings. I now

present the chemical findings, add a few of my chemosystematic conclusions and compare them with the Clevinger-Panero molecular-based revision for the genus. Finally, I want to thank Jennifer for her assistance in plant collecting and identification; moreover, she has provided Lalita and I with advice and support throughout our studies for which I am grateful. Although the detailed chemical studies have occupied most of my time and constitute the majority of this dissertation, I, nevertheless, comment on the chemosystematic and medicinal value of the chemical data in the final chapters.

Chapter 1: Introduction to *Silphium*:

Secondary metabolites, including flavonoids and phenolic acids, have many functions. These compounds are important for a plants survival and reproductive fitness although the activity of many of these secondary metabolites remains unknown. Along with protection against herbivores, microbes and competing vegetation, many phenolic compounds are active biochemicals, protecting organisms against cancer and other diseases by their ability to absorb UV light and inactivate dangerous free radicals. The latter topic is especially popular today as flavonoids are respected as one of the most important of the dietary antioxidants.

Molecular phylogenies from several plant families have been used in an attempt to map the distribution of major secondary metabolites distinctive to specific plant families. The distributions of these compounds are consistent with phylogenetic patterns and have taxonomic value even though their occurrences often reflect specific environmental adaptations (Wink, 2003).

The Asteraceae (Compositae) family, which contains approximately one thousand genera with over 25,000 species, is represented on almost every continent of the globe. The members of this family consist of annual and perennial herbs with a few woody varieties. The name Compositae itself refers anatomically to the numerous florets that form involucrated heads during reproduction; moreover, the plants in this family are described as erect, twining, or drooping and occasionally contain milky lactone-like substances (Bailey, 1951). At least thirty species have established uses as drugs with sixteen currently listed in modern pharmacopeias. Many more species either have been used and or are currently used for various purposes in different cultures (Pcolinski, 1992).

Many plant systematists continue to classify members of this family using morphology, anatomy and even reproductive cycles, while modern chromosomal and DNA analysis are the most accurate forms of analyses used today. I believe my studies show that comparative analysis of secondary metabolites such as flavonoids and phenolics can provide additional clarifications for these classifications.

1.1 The Genus *Silphium*: History

The word "Silphion" was first used by the ancient Greeks to describe a now extinct form of the resinous African *Ferula*. During the early nineteenth century, Carl Linnaeus assigned the name *Silphium* to a genus within the tribe Heliantheae in reference to the resinous-like exudates that members of the genus excrete when damaged (Linnaeus, 1826). Over the past century many revisions to Linnaeus' classification have been made.

In 1933, John Kunkel Small revised the *Silphium* species into five sections *Composita, Dentate, Integrifolia, Laciniata and Perfoliata* and characterized 33 species using morphological data which included foliar shape, arrangement and phyllary anatomy (Small, 1933). A few years later, Lily Perry (1937) reduced the genus to 23 species. In reviewing her notes on *Silphium*, it is clear that Perry concluded that several of the species recognized by Small showed no more than minor variations in anatomical features including leaf-margins and achene characters; she noted that, "Too often in this genus a single specimen or two or three plants will appear to have distinctive characters which, as a matter of fact, break down in a good series of representative material" (Perry, 1937).

In the past few decades, taxonomists have again turned their attention to this complex genus. In 1977, Tod Stuessy removed several genera, including *Silphium* due to its staminate disc florets and compressed ray cypsela, from the sub-tribe Melampodinnae adding them to the sub-tribe Engelmanniinae (Clevinger, 1999). In 1980, Arthur Cronquist in his text *Vascular Flora of the Southern United States* further revised the genus to 15 species and in 1989, M.E. Medley added the species *Silphium wasiotense* to the genus based on collections discovered in Kentucky and Tennessee (Cronquist, 1980). Medley later grouped this new species with the plants of *S. brachiatum* and *S. mohrii*, eventually placing it among the species of section *Dentata* (Medley, 1989).

Dr. Clevinger, who used DNA analysis for her Ph. D. studies on *Silphium* at UT Austin, currently continues her molecular investigations on *Silphium* and the tribe Heliantheae at Walsh University, North Canton, Ohio. Data collected from the Internal

Transcribed Spacer (ITS) and External Transcribed Spacer (ETS) regions of nuclear ribosomal DNA were used by Dr. Clevinger to construct a molecular-based phylogeny for the genus. Her chloroplast DNA analysis along with previous morphological cladistic data support *Silphium's* placement in the sub-tribe Engelmanniinae.

Dr. Clevinger's revision of section *Composita* establishes that *Silphium albiflorum* descends from and is a sister species to *S. laciniatum*. The clade also clarifies that both species, *S. albiflorum* and *S. laciniatum*, descend from *S. terebinthinaceum* with the species *S. compositum* being the oldest ancestral progenitor of the section (Figure 1.1).

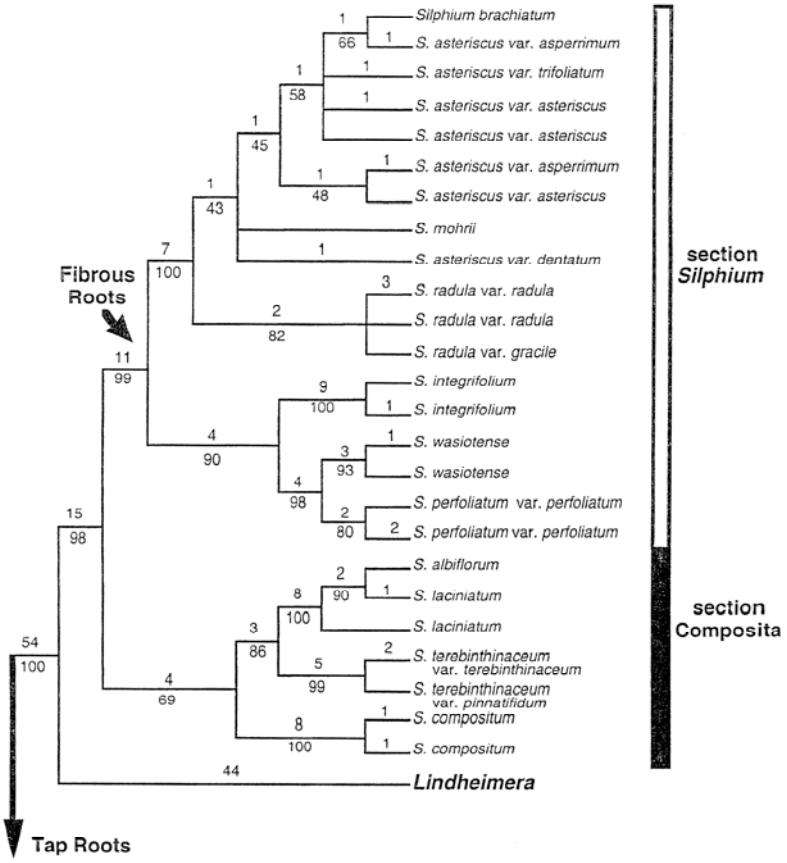

Figure 1.1: Dr. Clevinger's clade for the genus *Silphium* (Clevinger, 1999).

Among the seven species of section *Silphium*, three species *Silphium integrifolium*, *S. perfoliatum* and *S. wasiotense* clearly diverged earlier from the remaining four. Of these three species, *S. perfoliatum* and *S. wasiotense* are the closest related with *S. integrifolium* being sister too and diverging from the later two. The remaining species *S. brachiatum*, *S. asteriscus* and *S. mohrii* are all sister to species *S. radula* with *S. asteriscus* being considered the closet species related to the uniquely cream pigmented *Silphium mohrii* (Figure 1.1).

1.2 Habit and Distribution of *Silphium*

Silphium species are perennial and begin growth as a basal rosette. For several of these plants, the first growing season only involves the slow emergence of the basal rosette. The rosettes are persistent throughout the genus with the species from section *Composita* typically exhibiting the largest in size.

On exposure to full sun, members of *S. laciniatum* display leaf tips pointing in a north-south direction; thus, early European pioneers commonly referred to this species as "compass" or "pilot weed". It has been observed that after summer maturity, the basal leaves may or may not recede into late fall (Zhang *et al*., 1991). Dr. Clevinger's molecular analysis supports two clades with two distinct morphologic growth forms. The species from section *Composita* produce taproots with above ground scapiform development, whereas those in section *Silphium* exhibit fibrous roots having caulescent apical growth.

Seedlings from all *Silphium* species grow in close proximity to the parent plant and germination involves a single outgrowth with subsequent years providing several stems as a clump. The large cypselae lacks wind adaptations and the average distance for dispersal is typically 1.0 m; these narrow pollination and dispersal factors have created spatially isolated populations leading to considerable variation causing, as mentioned previously, earlier taxonomists to improperly use minor morphological differences as evidence for additional species (Pleasant and Jurik, 1992). *Silphium* species show rapid growth and flowering when carefully cultivated; in fact, several varieties of *Silphium asteriscus* have been classified using these criteria (Clevinger, 1999).

Figure 1.2: *Silphium albiflorum* growing in the poor nutrient soil of Bosque County, TX.

Early taxonomic confusion may have also originated from the failure to recognize variations due to ecological factors such as climate. In 1887, Halsted recorded that the leaves of *S. laciniatum* appeared strikingly different when compared with their shape the previous year (Halsted, 1887). Annual temperatures and precipitation affect the phenology, number of capitula, capitulescences and height of several species. Some plants, especially in section *Composita,* may remain in a dormant state until climatic conditions promote germination and growth; thus, years

with little precipitation promote a shorter flowering season with smaller inflorescences.

Silphium species are found in diverse habitats and, moreover, are rarely collected south of the central Texas Hill country. The lack of lower winter temperatures along with the need for consistent moisture patterns may prevent germination (Auffenorde and Wistendahl, 1982); in fact, a few species require more than three months of increased precipitation at 40˚ F in order to initiate germination (Clevinger, 1999).

Silphium albiflorum (Fig. 1.1), the only white flowering species, is located exclusively in the hill country of central Texas; this species is particularly abundant in the low nutrient, calcareous soils of Bosque County, TX, approximately 200 miles west of Waco. Each plant flourishes in full sun with *Silphium albiflorum* sometimes growing in as much as a two foot radius with complete isolation. During years of low precipitation, Bosque County, TX, is one of the few areas in which *S. albiflorum* thrives.

The species *S. laciniatum*, *S. integrifolium* and *S. terebinthinaceum* are found in northeast Texas with several populations spread across the Gulf southern states. *Silphium laciniatum* and *S. terebinthinaceum* are referred to as keystone species due to the fact that they can remain on a stretch of land for years despite limited human disturbance; indeed, their presence allows ecologists to monitor environmental changes among several southwestern prairies (Clevinger, 1999). *Silphium astericus*, the last of the six Texas natives, can be found along the borders of northeastern Texas oak forests and in open meadows. Ranching and roadway cuttings have reduced many populations to limited numbers including the two keystone species mentioned above; *Silphium* rarely reoccupies fields that are plowed or grazed. Today, plant collection sites for *Silphium* primarily

involve either lowland ravines or new habitats created along highways and rail furrows; indeed the actual expansion of one species, *S. laciniatum*, occurs in the state of New York due to these transportation avenues (Gleason and Cronquist, 1991).

Morphologically, several species within *Silphium* appear very closely related. Local speciation dictates that individual isolated populations may form paraphyletic progenitor species along with monophyletic derivatives (Riesenberg and Brouillet, 1994). Gene flow between the species increases the time required for progenitor species to become monophyletic, a process that may explain the evolutionary divergence of several species. DNA analysis indicates that the six nativeTexas species are derived from species having considerably larger populations. For example, *Silphium albiflorum* evolved from S. *laciniatum*, although the two species now occur on completely different substrates. *Silphium brachiatum*, *S. mohrii* and *S. wasiotensis* are found in localized patches throughout the southern Gulf coastal states. *Silphium mohrii* and *S. brachiatum* appear more rudimentary as sister species to the Texas native *S. asteriscus* while *Silphium wasiotense* appears more closely linked to the widely distributed Midwestern species, *S. perfoliatum* (Clevinger, 1999).

1.3 Dr. Clevinger's Systematic Treatment of *Silphium*

PCR sequencing was performed by Dr. Clevinger on 14 species of *Silphium,* which were recognized at the initiation of her studies as well as members of several other closely related genera. In her studies, DNA was extracted from leaf tissue collected in the field and isolated using a hexadecyltrimethylammonium method. Material from the

Internal Transcribed Spacer or ITS region and the 3´ end of the External Transcribed Spacer were generated through polymerase chain reactions (PCR). The ITS region was sequenced and along with the phylogenetic ETS data they were combined using a partition homogeneity test (Clevinger, 1999).

The ITS and ETS findings support a monophyly of the genus *Silphium*. Base change analysis provided clade information supporting root and growth form morphologies. Section *Composita* includes the tap rooted species: *S. albiflorum*, *S. laciniatum*, *S. compositum* and *S. terebinthinaceum* while section *Silphium* contains the fibrous root species *S. asteriscus*, *S.brachiatum*, *S. integrifolium*, *S. mohrii*, *S. perfoliatum*, *S. radula* and *S. wasiotense,* together providing the eleven species in Clevinger's revision of the genus (Clevinger, 1999).

1.4 Traditional Medicinal Uses of *Silphium* Extracts

During the late nineteenth century, extracts of various parts of *Silphium laciniatum, S. compositum, S. integrifolium* and *S. perfoliatum* were all used as folk remedies (Fielder, 1975). Treatments for liver, spleen and stomach ulcers along with internal hemorrhaging with material used from several *Silphium* species afforded both diaphoretic and restorative results (Dragondorff, 1898; Heilpflanzen, 1996; King's Amercan Dispensatory, 1898). The Cherokee of the northern Mississippi territories smoked *S. compositum* to treat colds and neuralgia (Mallorn, 1999). Migratory tribes from Arkansas and Texas where recorded as chewing resins taken from *S. laciniatum* and the stems from this species were useful for teeth cleaning (Felter, 1898).

Aerial collections of *Silphium perfoliatum* are reported to possess diaphoretic, expectorant and diuretic properties, usefulness for treating upper respiratory illnesses including fever, cough and asthma. The Native American Chippewa tribe employed the root extracts of *S. perfoliatum* for chest pain including pulmonary hemorrhaging (Densmore, 1928). The northwestern Winnebago nation used a decoction made from *S. perfoliatum* during spiritual rituals to increase adrenalin levels prior to hunting and warfare (Mallorn, 1999). The administration of root extracts for abdominal liver and spleen enlargements have been recorded with the resins from *S. perfoliatum* having been used for both stimulative and antispasmodic activities (Davidyants and Abubakirov, 1992 Steinmetz, 1954).

Dermatological testing with different *Silphium* extracts for burn injuries have shown increased regenerative healing when applied as a poultice or administered as an ointment. Tissue healing was observed as occurring as quickly as the ninth day post application (Davidyants and Abubakirov, 1992).

1.5 The Medicinal Properties of Kaempferol and Quercetin

The antiproliferative effects of quercetin and kaempferol demonstrate not only the influence of dietary nutrients *in vivo*, but also show positive trends in the death of several types of cancer cells (Figure 1.2). Breast (PMC42) and human intestinal cells (HuTu-80) in combined treatments with kaempferol and quercetin showed a decreased expression of a specific antigen and decreased total protein levels (Akland, 69)

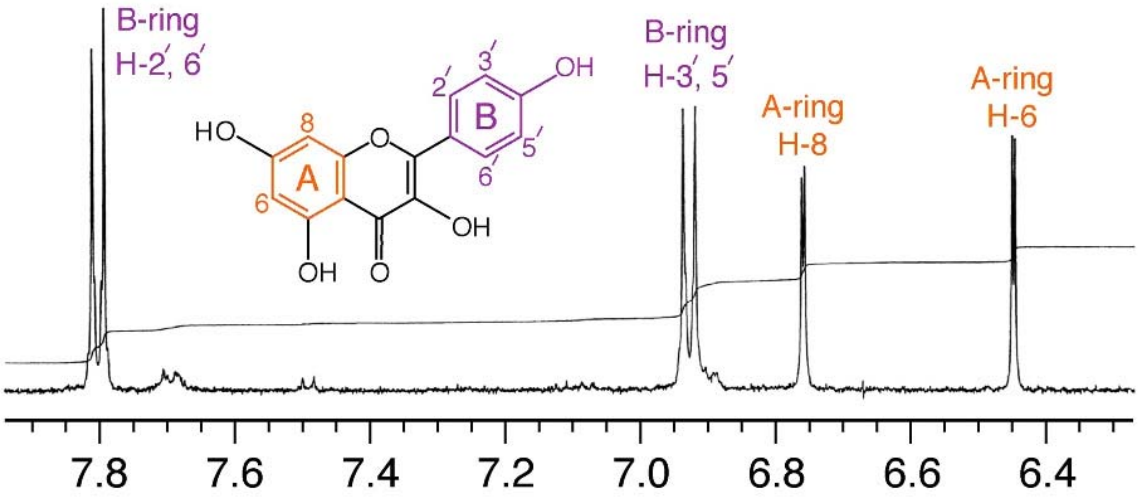

Figure 1.3: The approximate ^{1}H NMR resonance peaks for the flavonol kaempferol as measured in ppm's (Mabry, Markham and Thomas, 1970, the basic guide for my NMR studies).

The flavonol quercetin has been shown to inhibit the proliferation of tumor cells through induced cell cycle arrest, up regulation of tumor suppressor genes and influence MAPK signal transduction (Van Erk, 2005). Quercetin (3, 3', 4', 5, 7-pentahydroxyflavone) has been shown to interfere with the expression of both onco and the tumor suppressor genes in human mammary carcinoma cells (Avila, 1996). Analysis involving ovarian cancer suggests that quercetin-induced inhibition may be mediated through the control of the growth factor TGF β1 adding new information to carcinoma developmental pathways and mechanisms (Ferrandina, 1994).

Studies with quercetin and kaempferol involving colon cancer show that these flavonols inhibit proliferation of the tumor cells thus providing a reduction in the number of atypical or abnormal crypt foci. Differentially expressed genes involving the pathogenic cells were categorized and analyzed. Quercetin, at as low as 5um aliquots,

was found to down regulate the expression of cell cycle genes, down regulate proliferation and induce cell cycle arrest. Quercetin alone has also been found to up-regulate the expression of several tumor suppressor genes, effect beta catenin/ TCF signaling and MAPK signal transduction (van Erk, 2005).

Quercetin and other flavonoids are also being investigated in relation to currently used chemotherapy agents. The agent *cis*-DDP (*cis*-diaminedichloroplatinum (II)), is one of the most effective drugs used for chemotherapy, although its use must be monitored carefully due to multiple side effects. Synergistic effects of quercetin and *cis*-DDP were analyzed in *cis*-DDP-sensitive cancer cells resulting in the lower toxicity of *cis*-DDP. Also, introduction of the flavonol ligand altered the DNA-binding properties of the complex as compared to *cis*-DDP alone. The T6 synergistic activities of these compounds have sparked further research involving other routinely applied chemotherapeutic agents (Kosmider and Osiecka, 2004).

Finally, Dr. Kiminori Matsubara at Okayama Prefectural University, Japan, using isoquercetin (quercetin 3-*O*-*β*-D-glucopyranoside), has been able to show that this compound produces a strong inhibition of *ex vivo* angiogenesis in comparison to other glycosylated quercetin derivatives (Matsubara, 2004). Our isolation and identification of several new glycosylated derivatives of not only quercetin, but also isorhamnetin and kaempferol, provide a new series of triglycosylated flavonoid agents that need to be further investigated for their medicinal properties.

Structures of the five new compounds (**1A**, **2A**, **3A**, **4A** and **5A**) that have been isolated and identified from *Silphium* are shown in Figs. 1.3-1.7:

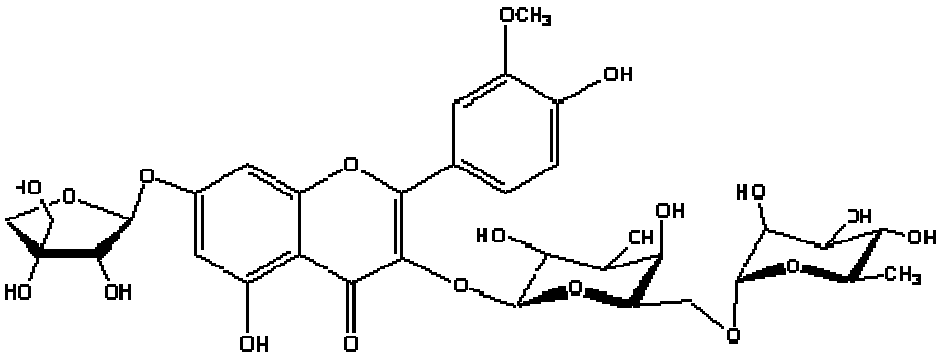

Figure 1.4: Isorhamnetin 3-*O*-*α*-L-rhamnosyl (1'''→6'') –*O*-*β*-D-galactopyranoside 7-*O*-*β*-L-apiofuranoside (**1A**).

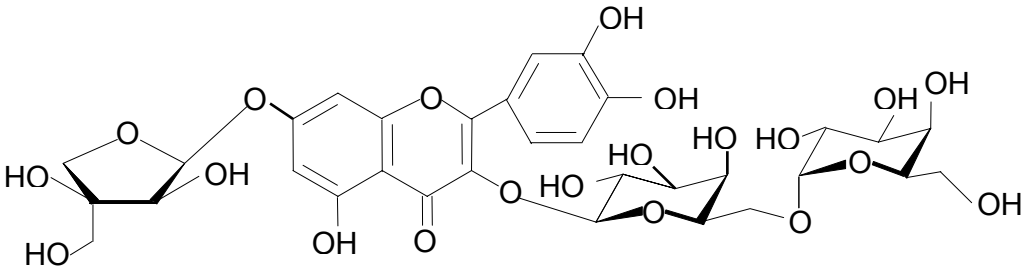

Figure 1.5: Quercitin 3-*O*-*α*-L-rhamnosyl (1'''→6'') –*O*-*β*-D-galactopyranoside 7-*O*-*β*-L-apiofuranoside (**2A**).

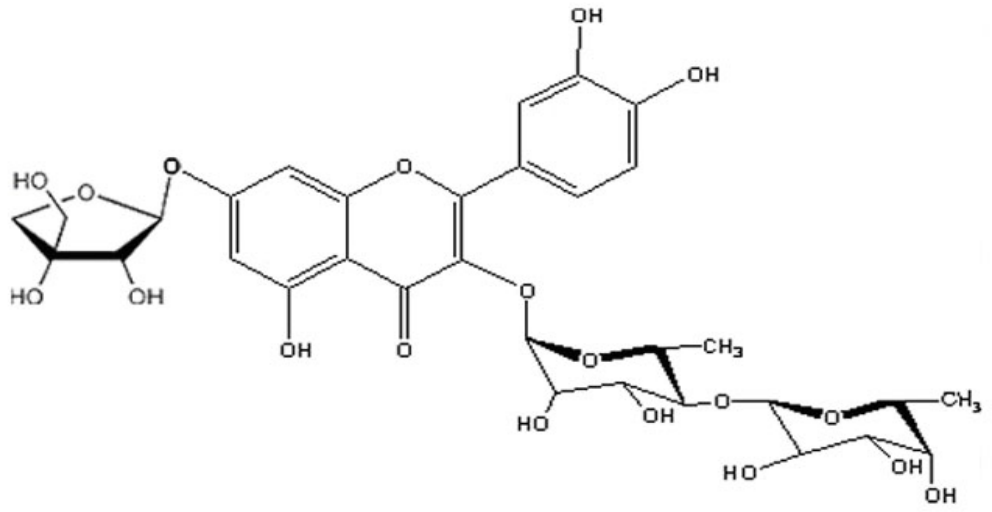

Figure 1.6: Quercetin 3-*O*-*β*-L-galactosyl (1'''→6'') –*O*-*β*-D-rhamnopyranoside 7-*O*-*α*-L-apiofuranoside (**3A**).

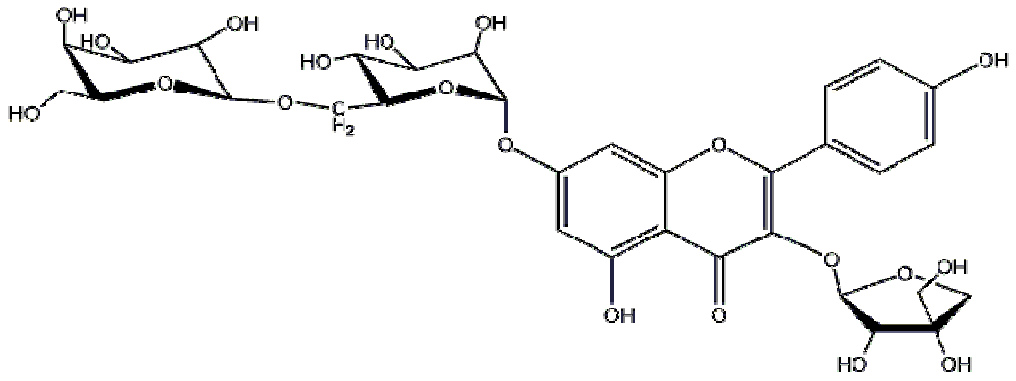

Figure 1.7: Kaempferol 3-*O*-*β*-D-apiofuranoside 7-*O*-*α*-L-rhamnosyl-(1''''→6''')-*O*-*β*-D-galactopyranoside (**4A**).

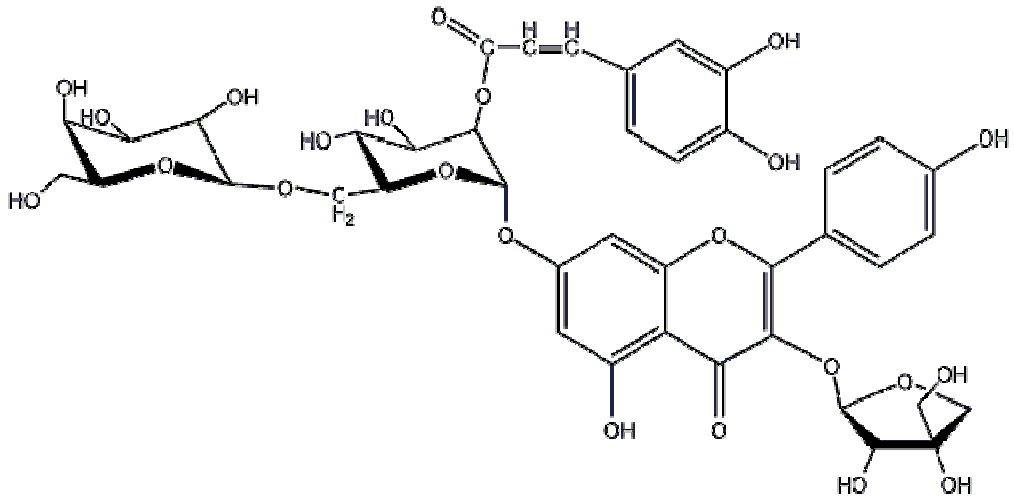

Figure 1.8: Kaempferol 3-*O*- *β*-D-apiofuranoside 7-*O*-*α*-L-rhamnosyl (1''''→6''')-*O*- *β*-D-(2'''-*O*-*E*-caffeoylgalactopyranoside) (**5A**).

Chapter 2

The Flavonoid Investigations of *Silphium* section *Composita*

2.1 Preliminary Chromatography Analysis for section *Composita*

Initial two dimension paper chromatography of all eleven species showed distinctive flavonoid and phenolic acid R_f spot distributions (Mabry *et al*., 1970). The individual images of similarly patterned *Silphium* species have been overlapped (Figures. 2.1-2.2).

Among the four species of section *Composita*, the flavonoid spots from *Silphium albiflorum*, *S. laciniatum*, *S. compositum* and *S. terebinthinaceum* not only showed a wider distribution of mono- and disaccharide flavonoids, but the larger sized regions also suggested greater extractable quantities of these compounds (Figure 2.1). The species *S. terebinthinaceum* showed the presence of three distinct flavonoid regions with higher R_f values when eluted in acetic acid (lower right corner, Figure 2.2). These spots may suggest that this species contains more un-extracted unknown triglycosidic flavonoids.

Based on preliminary two dimensional chromatography, individual and overlapping flavonoid patterns were apparent. Concerning *Silphium* section *Composita*, the spot distributions of *S. albiflorum* and *S. laciniatum* showed larger sized regions with similar overlapping patterns in the mono and disaccharide regions (Figure 2.1). The species *S. compositum* and *S. terebinthinaceum* showed greater distribution of mono and disaccharide compounds including larger areas having even greater overlap (Figure 2.2).

Figure 2.1: The TLC flavonoid/phenolic distributions for the species *S. albiflorum* and its sister species *S. laciniatum*, section *Composita.*

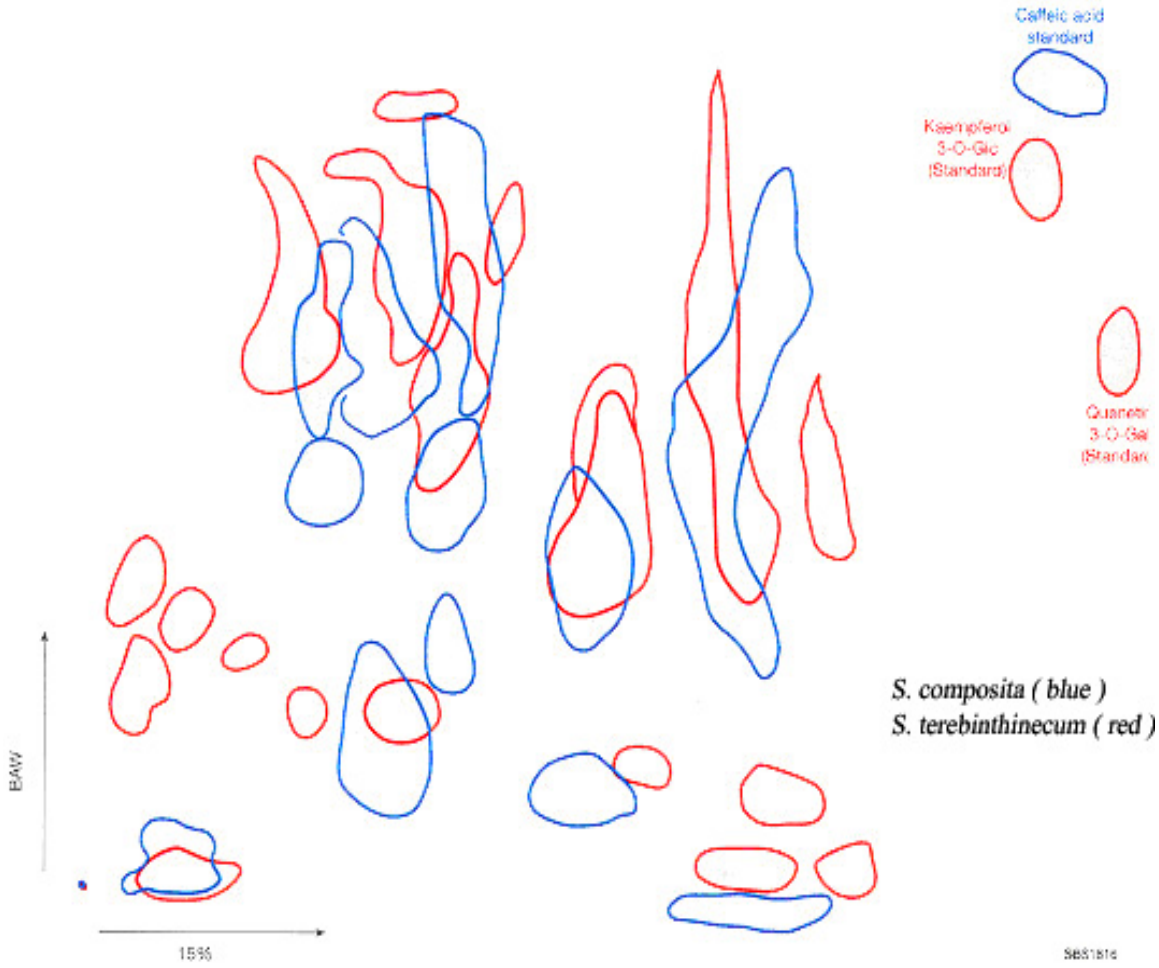

Figure 2.2: The strong mono and diglycosidic flavonoid distributions of the species *S. compositum* and *S. terebinthinaceum,* section *Composita.*

2.2 Introduction to the Flavonoid Chemistry of *Silphium* section *Composita*:

Using comparative LC/MS analysis, the four species comprising section *Composita* showed the presence of various derivatives of the flavonols quercetin, isorhamnetin and kaempferol. The flavonoid quercetin was prevalent among all four species. *Silphium albiflorum* and *S. laciniatum* contained the same monosaccharide flavonoids quercetin 3-*O*-*β*-D-glucopyranoside, kaempferol 3-*O*-*β*-D-glucopyranoside and the newly isolated triglycosidic compound isorhamnetin 3-*O*-*α*-L-rhamnosyl

(1'''→6'')-*O*-*β*-D-galactopyranoside 7-*O*- *β*-L-apiofuranoside (**1A**). The second isolated quercetin triglycoside, quercetin 3-*O*-*α*-L-rhamnosyl (1'''→6'') –*O*-*β*-D-galactopyranoside-7-*O*-*β*-L-apiofuranoside (**2A**) was detected in both *Silphium albiflorum* and *S. compositum* but not *S. laciniatum.* The pentose sugar apiose (*m/z* 132) was prevalent among the quercetin glycosides for all four species of the section, while *S. laciniatum* also contained this sugar bound to kaempferol.

Silphium albiflorum and *S. terebinthinaceum* contained similiar isorhamnetin mono and disaccharide derivatives. *Silphium compositum* also shared the isorhamnetin disaccharides isorhamnetin 3-*O*-*α*- rhamnosyl (1'''→6'')-*O*-*β*-D-galactopyranoside and isorhamnetin 3-*O*-*α*- rhamnosyl (1'''→6'')-*O*-*β*-D-glucopyranoside with *S. albiflorum* and *S. terebinthinaceum*. The detection of the less common, highly polar triglycosidic compounds found in *S. albiflorum*, *S. laciniatum* and *S. compositum* were not detected in *S. terebinthinaceum*. It is possible that the newly isolated kaempferol triglycosides **4A** and kaempferol 3-*O*- *β*-D-apiofuranoside 7-*O*-*α*-L-rhamnosyl (1''''→6''')-*O*- *β*-D-(2'''-*O*-*E*-caffeoylgalactopyranoside) (**5A**) were also detected for the first time in a member of section *Composita*. Both LC peaks for these compounds appeared with masses two hydrogen units less than what the actual values should have been *m/z* 724.6 $[M-2H]^+$ (21.0 min.) and *m/z* 886.0 $[M-2H]^+$ (21.0 min). The only known identification of compound **5A** was in the section *Silphium* species *S. perfoliatum* and *S. wasiotense*. It is also important to note that the two-dimensional paper chromatograms revealed large extractable concentrations of three and possibly four glycosidic flavonoids in the species *S. terebinthinaceum*- more than found in any other *Silphium* species (Figure 2.2).

2.3 *Silphium albiflorum* (Fig. 2.3), the first discussed of the six native Texas species, is exclusive to the central Texas Hill Country. Populations of the plant are abundant in the low nutrient calcareous soil of Bosque County, TX that is located approximately 250 miles northwest of Austin. Individual plants grow in full sun with low precipitation and are often found flourishing among sparse outcroppings of *Centaurium beyrichii* and *Juniperus ashei*. During years of little rainfall, this county is one of the few regions where this species of *Silphium* thrives when undisturbed.

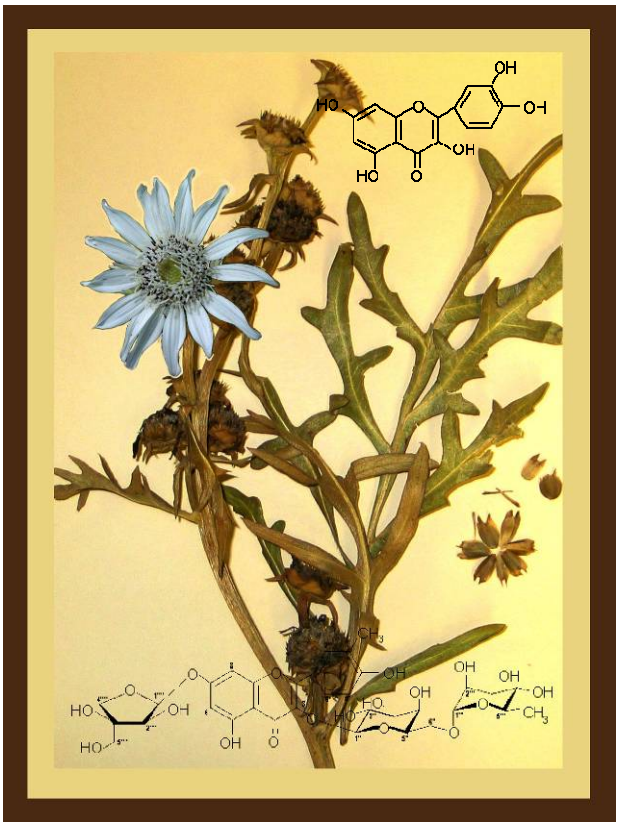

Figure 2.3: *Silphium albiflorum* dried sample with superimposed inflorescence collected from Bosque Co. June 2002.

Silphium albiflorum is described as a scapiform, tap rooted perennial. As mentioned in chapter one, the leaves consist of 90-400 mm long blades, with up to 13 deeply set primary lobes (Clevinger, 1999). Of the eleven species in the genus, *S. albiflorum* is the only plant containing white corollas (Dings *et al*., 1999). DNA and cladistic analysis assign *S. albiflorum* to the ancestral species *S. laciniatum* (Clevinger and Panero, 2000). Flower color, pubescence, along with a shorter stockier growth form represents the major morphological differences as compared with *S. laciniatum*.

Results and Discussion

The LC/MS of *Silphium albiflorum* extracts along with those of two of the other species within section *Composita* all showed the newly isolated compound, isorhamnetin 3-*O*-α-L-rhamnosyl (1'''→6'')-*O*-*β*-D-galactopyranoside 7-*O*-β-L-apiofuranoside (**1A**). *Silphium albiflorum* and *S. compositum* also shared the triglycoside quercetin 3-*O*-*α*-L-rhamnosyl (1'''→6'') –*O*-*β*-D- galactopyranoside-7-*O*-*β*-L-apiofuranoside (**2A**). Along with the isorhamnetin triglycoside, *Silphium albiflorum* contained the diglycosidic isorhamnetin compounds isorhamnetin 3-*O*-*α*- rhamnosyl (1'''→6'')-*O*-*β*-D-glucopyranoside (**5**) and isorhamnetin 3-*O*-*α*- rhamnosyl (1'''→6'')-*O*-*β*-D-galactopyranoside (**4**). Fewer derivatives of the flavonols quercetin and kaempferol were detected in this species compared with the other species in the genus although kaempferol 3-*O*-*β*-D-glucopyranoside (**6**) and kaempferol 3-*O*-*β*-D-galactopyranoside (**7**), were identified.

The chemistry of *Silphium albiflorum* includes the isolation and identification of two new flavonols whose structures were established by spectral analysis (^{1}H NMR, ^{13}C NMR, HMQC, HMBC, ROESY and TOCSY). **I mention that throughout this dissertation, the reports of compounds detected by LC/MS are described with their accompanying name, mass spectral data and retention time.** This is the first report of compounds **1A** and **2A** from the plant kingdom. Isorhamnetin 3-*O*-*α*-L-rhamnosyl (1'''→6'') –*O*-*β*-D-galactopyranoside 7-*O*-*β*-L-apiofuranoside (**1A**), *m/z* 757.4 $[M+H]^{+}$, (22.2 min) and quercetin 3-*O*-*α*-L-rhamnosyl (1'''→6'') –*O*-*β*-D- galactopyranoside-7-*O*-*β*-

L-apiofuranoside (**2A**), *m/z* 743.4 $[M+H]^+$, (20.2 min). MS/MS fractionation in positive mode shows the mass detection of both compounds as *m/z* 757.4 and *m/z* 743.4, respectively (Figures 2.6 and 2.7).

. In addition, five known flavonol glycosides were detected from the leaf extracts including quercetin 3-*O*-*β*-D-glucopyranoside (**3**), *m/z* 463.4 $[M+H]^+$, (21.0 min); isorhamnetin 3-*O*-*α*- rhamnosyl (1'''→6'')-*O*-*β*-D-galactopyranoside (**4**), *m/z* 625.2 $[M+H]^+$, (23.7 min); isorhamnetin 3-*O*-*α*- rhamnosyl (1'''→6'')-*O*-*β*-D-glucopyranoside (**5**), *m/z* 625.4 $[M+H]^+$, (25.8 min); kaempferol 3-*O*-*β*-D-glucopyranoside (**6**), *m/z* 447.4 $[M+H]^+$, (19.8 min) and the galactopyranoside (**7**), *m/z* 447.4 $[M+H]^+$, (19.4 min).

Characteristic ^1H NMR and ^{13}C NMR shift values and coupling constants support the structure for compound **1A** based on the literature data for the flavonol isorhamnetin and its derivatives (Mabry *et al*. 1970; Markham, 1982; Markham and Geiger, 1994). For both of the two new compounds **1A** and **2A**, ^1H NMR and ^{13}C NMR experiments confirmed the presence of three sugar moieties, which are attached at the 3 and 7 carbon positions of each aglycone (Figures 2.8 and 2.9).

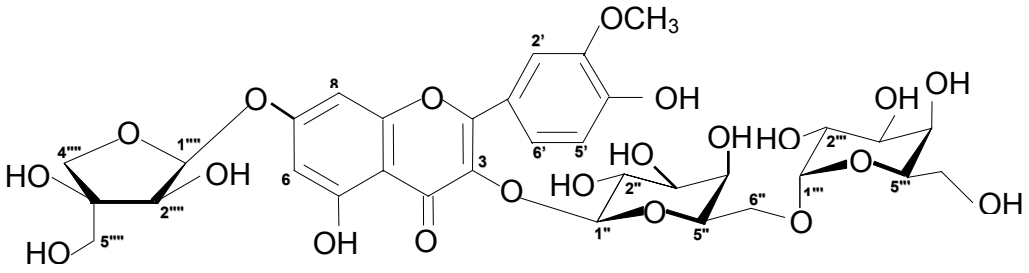

Figure 2.4: The structure for isorhamnetin 3-*O*-*α*-L-rhamnosyl (1'''→6'')-*O*-*β*-D-galactopyranoside 7-*O*-*β*-L-apiofuranoside (**1A**).

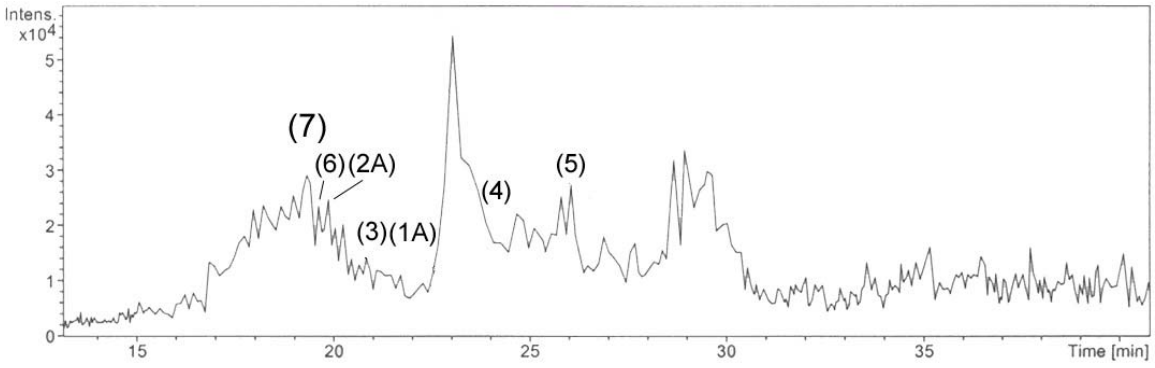

Figure 2.5: The LC/MS spectrum for the species *Silphium albiflorum.*

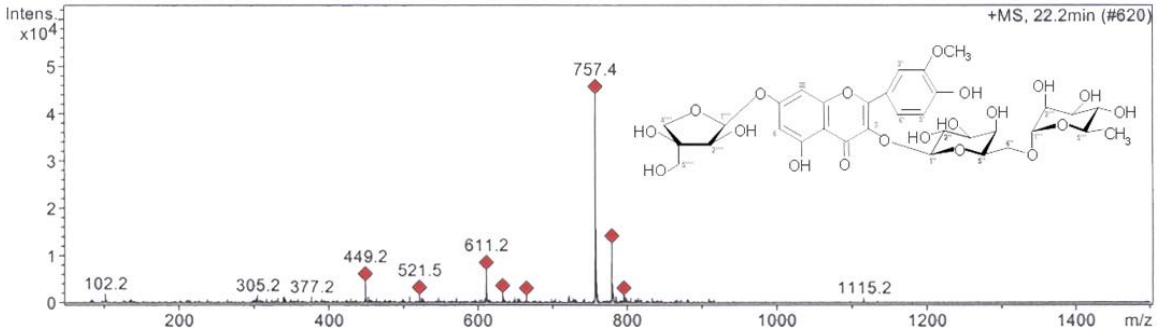

Figure 2.6: The LC/MS detection of the isorhamnetin glycoside **1A,** *m/z* 757.4 $[M+H]^+$

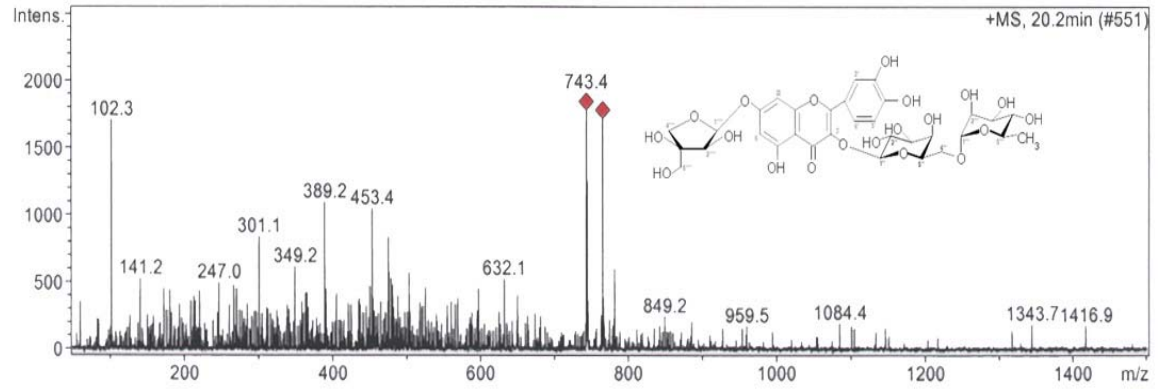

Figure 2.7: The LC/MS spectrum for a quercetin triglycoside **2A,** *m/z* 743.4 $[M+H]^+$

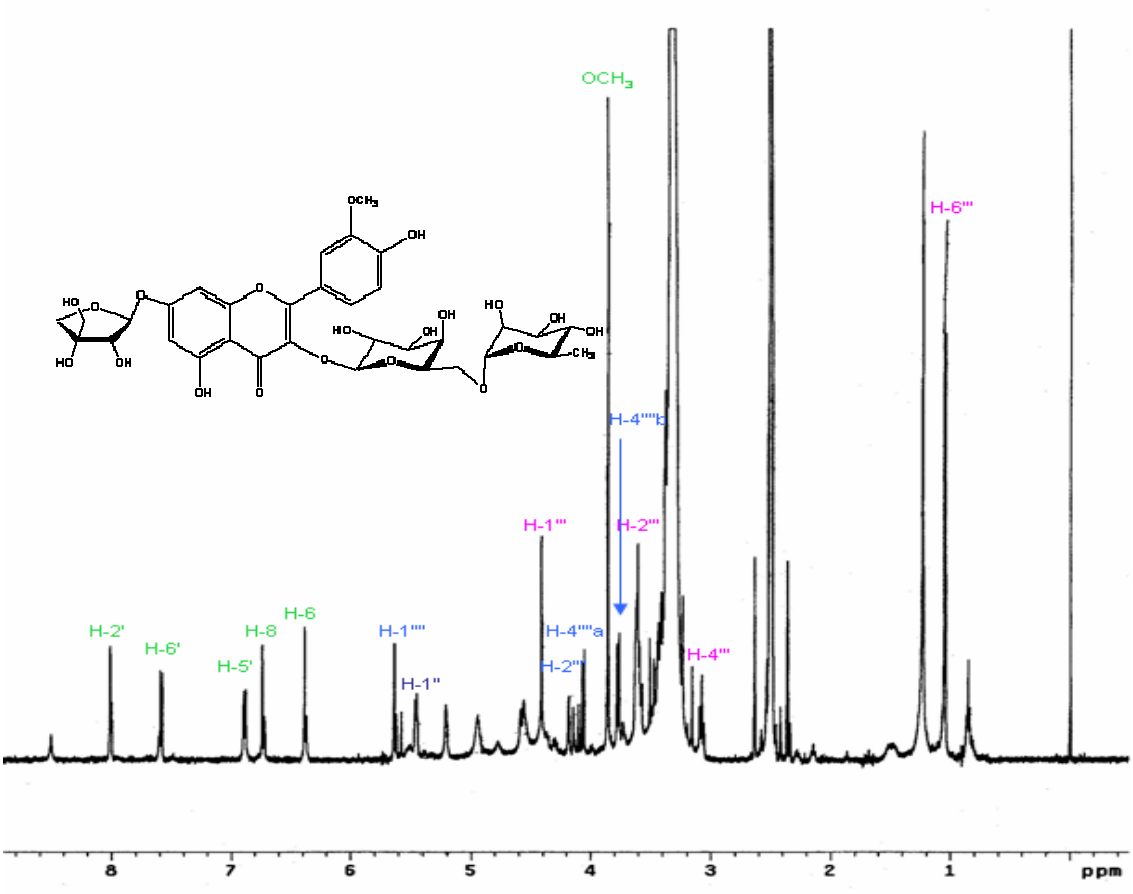

Figure 2.8: The ^{1}H NMR spectrum of the isorhamnetin 3-*O*-*α*-L-rhamnosyl (1'''→6'')-*O*-*β*-D-galactopyranoside 7-*O*-*β*-L-apiofuranoside (**1A**).

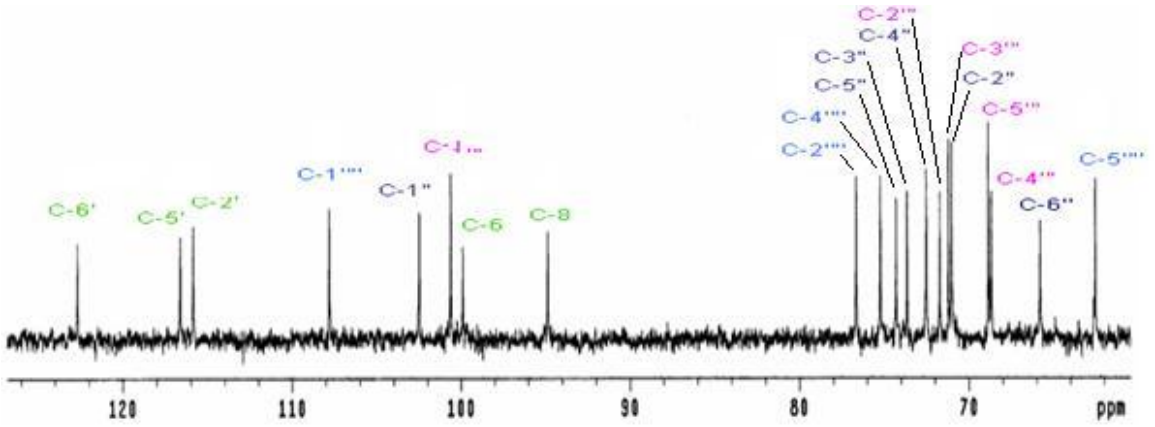

Figure 2.9: The ^{13}C NMR spectrum of compound **1A**.

Compound **1A** from *Silphium albiflorum* was purified to a yellow amorphous powder. On TLC analysis, under UV light, the compound appeared as a dull brown spot, changing to yellow on exposure to Naturstoffreagenz A, indicating the presence of 3'- and 4' hydroxyl attachment's and the lack of a *meta*-dihydroxyl pattern in the B-ring. The hydroxyl positions were also confirmed by the lack of UV shifts on addition of diagnostic reagents (Mabry *et al*., 1970; Markham, 1982). Proton and carbon NMR spectra, UV spectroscopic analysis and LC/MS ion fragmentation patterns all suggested compound **1A** to be a 3, 7-di-*O*-substituted isorhamnetin triglycoside (Mabry *et al*., 1970; Markham, 1982; Markham and Geiger, 1994). Acid hydrolysis yielded the sugars galactose, rhamnose and apiose, all identified using cellulose plates. Since isorhamnetin 3-*O*-rhamnosyl (1''' →6'') galactoside has been already identified from this species, it was considered likely that compound **1A** might be the 7-*O*-apiose derivative; this was confirmed by modern NMR spectral analysis. The MS experiments suggested the molecular formula to be $C_{33}H_{40}O_{20}$. The mass, supported by HR-FABMS $[M+Na]^+$ (*m/z* 779.01779), together with the fragmentation ions of *m/z* 735 $[M-H+Na-43]^-$ (due to the loss of CH_3CO) aided in the identification. The appearance of ions at *m/z* 623 $[M-H-132]^-$ as well as *m/z* 315 $[M-H-132-162-146]^-$ resulted from the losses of pentose, hexose and deoxyhexose, respectively (Markham, 1982). These findings were supported by the LC-MS^2 spectrum (positive mode) by the ions at *m/z* 757. Significant fragmentation ions were observed at *m/z* 611 $[M+H-146]^+$ and *m/z* 449 $[M+H-146-162]^+$, both corresponding to the successive elimination of two sugar moieties. The characteristic ^1H and ^{13}C

chemical shift values along with the coupling constant analysis all support the structure shown in figure 2.4 for compound **1A.**

In the ^{1}H NMR spectrum of isorhamnetin 3-*O*-*α*-L-rhamnosyl (1'''→6'')-*O*-*β*-D-galactopyranoside 7-*O*-*β*-L-apiofuranoside (**1A**), two narrow doublets resembling *meta*-coupled protons resonated at around *δ* 6.74 and 6.39 ppm (*J* = 1.6 Hz). These signals, through HMQC analysis, correlate with the carbon of (C-8) *δ* 94.5 and (C-6) 99.3 ppm indicating the 5-OH and 7-OH substituted pattern for ring A. The slight downfield shifts of the aglycone protons H-6 and H-8 also suggested the presence of a glycosidic substituent on the 7-hydroxyl group. This was further supported by the upfield shift in the C-7 signal and downfield shifts in the *ortho*- and *para*-related carbon signals (C-6 and C-10), all observed in the ^{13}C NMR spectrum (Markham and Ternai, 1976; Markham *et al*., 1978; Markham *et al*., 1982), all in accord with a sugar moiety attached to the 7-hydroxyl. The aglycone proton signals well established for the isorhamnetin skeleton appear at *δ* 8.01(s), 7.58 (*dd*; *J* = 8.4, 2.0 Hz) and 6.92 ppm (*d*; *J* = 8.6 Hz). These signals correlate with the carbons of C-2' (*δ* 113.4), C-6' (122.3) and C-5' (115.2), respectively. Finally, a singlet signal for three protons at *δ* 3.86 ppm showed from the cross peak analysis of C-3' (HMBC) and C-2' (COSY), support the presence of a 3',4'-dioxygenated B-ring with one methoxyl group positioned at C-3'; isorhamnetin being the aglycone for compound **1A**.

The ^{1}H and ^{13}C NMR experiments confirmed the presence of three sugar moieties in **1A**, which have been determined as being attached to the 3 and 7 positions of the

aglycone. UV analysis as well as one and two-dimensional NMR spectral studies aided in establishing the sites of glycosidic groups.

The assignments for all of the ^{1}H and ^{13}C sugar signals were supported using TOCSY and 2D NMR experiments. Three anomeric proton signals resonated at δ 5.64, 5.46 and 4.41 ppm and through HMQC analysis these protons were correlated to the carbons located at δ 107.2, 101.8 and 100.1 ppm, respectively. The first anomeric proton at δ 5.64 appeared as a doublet (J = 3.7 Hz) and from the HMQC studies cross linked with the δ 107.2 ppm carbon. The other protons from that sugar were located at δ 4.18 (*d*; J = 3.7 Hz), 3.77 (*d*; J = 9.4 Hz), 4.06 (*d*; J = 9.4 Hz), 3.39 and 3.43 ppm and were assigned to C-2"", C-4a"", C-4b"", C-5a"" and C-5b"", respectively. DEPT experiments showed that two of the carbons were of the methane type (C-1"" and C-2""), two were methylenes (C-4""and C-5"") and one quarternary (C-3"") type.

A correlation between the H-1"" (δ 5.64) and H-8 (δ 6.74) and H-6 (δ 6.39) was observed in the ROESY experiment as well as the cross peak intersection of the H-8 (δ 6.74) and H-6 (δ 6.39) and C-1"" (δ 107.2) (recorded in the HMBC spectrum). These analyses supported the attachment of a sugar at C-7 (Figure 2.10).

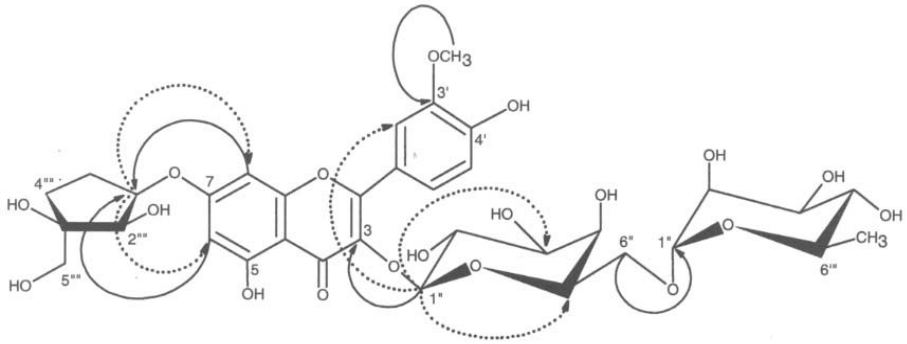

Figure 2.10: Shown are the ROESY (dotted displayed arrows) and HMBC (solid displayed arrows) correlations of compound **1A**.

	1				2					
Position	**δc**	**HMBC**	**δH**	**COSY**	**δc**	**HMBC**		**δH**	**COSY**	
Aglyc 2	156.9 *s*				156.8 *s*					
3	133.4 *s*				133.7 *s*					
4	177.6 *s*				177.4 *s*					
5	160.9*s*				160.8 *s*					
6	99.3 *d*	5,7,8,10, 1""	6.39 *d* (1.6)	8	99.3 *d*	5,7,8,10		6.38 *d* (2.0)	8	
7	162.5 *s*				162.5 *s*					
8	94.5 *d*	6,7,9,10,1""	6.74 *d*	6	94.2 *d*	6,7,9,10		6.69 *d* (2.0)	6	
9	156.0 *s*				155.9 *s*					
10	105.5 *s*				105.4 *s*					
1'	120.8 *s*				120.8 *s*					
2'	113.4 *d*	2, 1',3',4', 6'	8.01 *s*	6', Ome	116.0 *d*	2, 1',3',4', 6'		7.59 *d* (2.1)	5',6'	
3'	147.1 *s*				144.9 *s*					
4'	149.7 *s*				148.9 *s*					
5'	115.2 *d*	1',3',4'	6.92 *d* (8.6)	6'	115.2 *d*	1',3',4'		6.82 *d* (8.4)	6'	
6'	122.3 *d*	2,2',3',4'	7.58 *dd* (8.4, 2.0)	2',5'	122.1 *d*	2,2',4',5'		7.69 *dd* (8.5, 2.0)	2',5'	
3'-OMe	56.0 *q*	3'	3.86 *s*	2'						
Gal 1"	101.8 *d*	3,2",5"	5.46 *d* (7.7)	2"	101.9 *d*	3		5.35 *d* (7.7)	2"	
2"	71.2 *d*		3.60 *t* (8.4)		73.7 *d*	4",6"		3.54 *t* (6.1)	1"	
3"	73.0 *d*		3.44 *d* (9.3)		73.0 *d*			3.42	4"	
4"	68.0 *d*		3.64 *s*		68.0 *d*	3",5"		3.6		
5"	73.7 *d*		3.61		71.1 *d*	3"		3.59	6b"	
6" a	65.3 *t*		3.34		65.2 *t*	3",4",5"		3.25 *dd* (6.0, 6.1)	6a"	
b			3.61					3.61		
Rha 1""	100.1 *d*	6",3"",5""	4.41 *d* (1.0)	2""	100.0 *d*	6",2"",3"",5""		4.41 *d* (not res.)	2""	
2""	70.4 *d*		3.39		70.4 *d*	4",6",3"",5""		3.39	1"",3""	
3""	70.6 *d*		3.30 *dd* (9.4, 3.2)		70.6 *d*	1"",4"",5""		3.30 *dd* (9.4,3.2)	2"",4""	
4""	71.9 *d*		3.09 *t* (9.4)		71.9 *d*	3"",5"",6""		3.07 *t* (9.3,9.4)	3"",5""	
5""	68.3 *d*		3.37	5""	68.2 *d*	4""		3.38	4""	
6""	17.9 *q*	4"",5""	1.05 *d* (6.2)		17.9 *q*	4"",5""		1.06 *d* (6.0)		
Api 1""	107.2 *d*	4""	5.64 *d* (3.7)	2""	107.2 *d*	7,4""		5.63 *d* (3.5)	2""	
2""	76.1 *d*	1""	4.18 *d* (3.7)	1""	76.0 *d*	1""		4.18 *d* (3.5)	1""	
3""	78.7 *s*				78.7*s*					
4"" a	74.6 *t*	1"",2"",3""	3.77 *d* (9.4)		74.6 *t*	1"",2"",3"",5""		3.77 *d* (9.5)	4b""	
b		5""	4.06 *d* (9.4)					4.06 *d* (9.5)	4a""	
5"" a	62.0 *t*		3.39		61.9 *t*	2"",3"",4""		3.36	5b""	
b			3.43					3.44	5a""	

Table 2.1: The HMBC/COSY analysis for both isorhamnetin 3-*O*-*α*-L-rhamnosyl (1"'→6")-*O*-*β*-D-galactopyranoside 7-*O*-*β*-L-apiofuranoside (**1A**) and quercetin 3-*O*-*α*-L-rhamnosyl (1"'→6") –*O*-*β*-D- galactopyranoside 7-*O*-*β*-L-apiofuranoside (**2A**)**.**

The proton shift of H-5"" and ^{13}C chemical shift values and coupling constants of apiose were nonequivalent suggesting an L configuration for apiose, where as the $^{3}J_{1'''', 2''''}$ at 3.7 Hz showed the β configuration for the apiofuranoside ring (Ishii and Yanagisawa, 1998; Ranganathan *et al*., 1980). The second anomeric proton (H-1") at δ 5.46 ppm appeared as a doublet with a diaxial coupling constant (J = 7.7 Hz) (Mabry *et al*., 1970; Markham and Geiger, 1994), and its location in the ^{1}H NMR spectrum was in accordance with the data reported for a 3-*O*- galactoside (Markham and Geiger, 1994). The presence of galactose was also confirmed using ^{13}C NMR and DEPT analysis. The long range ^{13}C - ^{1}H correlation between H-1" and C-3, as well as a weak ROESY connectivity between H-1" and C-2', indicated that galactose is attached to the hydroxyl group at the C-3 position. The $J_{1,2}$ value and the ROESY connectivity's for H-1" to H-3" and H-5" provided support for the β-configuration of the galactose moiety. The chemical shift values for all of the recorded galactose carbons as well as the H-1"/H-2" coupling constant (J = 7.7 Hz) confirms the pyranose form of galactose (Agrawal, 1992; Markham and Geiger, 1994). A downfield shift for C-6" (near 5 ppm) and an upfield shift of the neighboring C-5" (near 2.2 ppm), compared to the corresponding signals for compound (**8**), indicates the attachment of the next sugar, namely rhamnose (Agrawal and Bansal, 1989). The H-1''' anomeric proton of rhamnose resonated at approximately δ 4.41 ppm, the region characteristic for terminal sugars. Further evidence that rhamnose is the terminal sugar was supported by the LC/MS^2 spectrum, showing the initial independent loss of -146u. The cross peak intersection between rhamnose H-1''' and galactose C-6" observed in the HMBC spectrum confirms the linkage between the two sugar moieties.

Moreover, the location of H-1" and H-1'" as well as the three proton doublet for the rhamnosyl methyl group appearing at δ 1.05 (J = 6.2 Hz), coincide with literature values for the rhamnosyl (1→6) galactoside linkage (Mabry *et al*., 1970). All of the individual glycosidic carbon signals were in agreement with the attachment of the rhamnosyl moiety to the 3-*O*-galactosyl through a (1→6) linkage (Halim *et al*., 1995). Analysis of HR-FAMS, ^{1}H NMR and ^{13}C NMR, H-H-COSY, HMQC, HMBC, ROESY, TOCSY and UV spectra all confirmed that compound **1A** is isorhamnetin 3-*O*-α-L-rhamnosyl (1'" → 6")-*O*-*β*-D-galactopyranoside 7-*O*-*β*-L-apiofuranoside (Figure 2.4). The selected HMBC and ROESY connectivity's, especially those indicative of sugar location, are presented in figure 2.10.

The second new compound, quercetin 3-*O*-*α*-L-rhamnosyl (1'"→6") –*O*-*β*-D-galactopyranoside 7-*O*-*β*-L-apiofuranoside **(2A)** (Figure 2.11) was identified by similar analyses procedures as used for **1A**. This quercetin derivative differs from compound **1A** only in the aglycone, namely it contains a 3' hydroxyl group. Unlike **1A**, TLC markers for the quercetin derivative changed to orange on exposure to Naturstoffreagenz A supporting an *ortho*-dihydroxyl pattern in the B-ring. Additionally, the UV absorption spectrum in methanol of **2A**, along with shifts observed on addition of diagnostic reagents, showed the presence of three free hydroxyl groups at positions 5, 3', 4', along with the presence of substituted 3 and 7 position hydroxyl groups. These data support the conclusion that compound **2A** is a 3, 7-di-*O*-substituted quercetin glycoside (Mabry *et al*., 1970; Markham, 1982; Markham and Geiger, 1994).

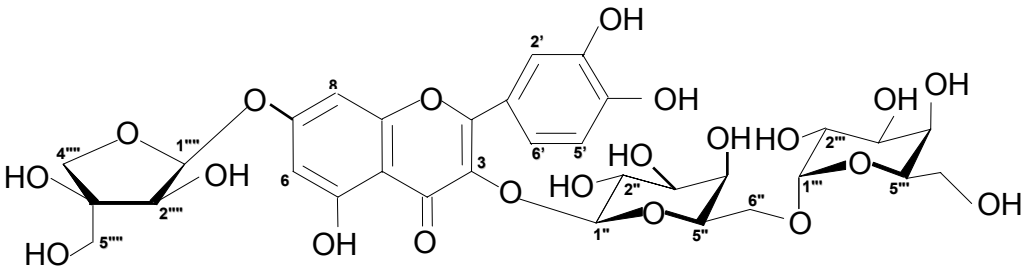

Figure 2.11: The structure for quercetin 3-*O*-*α*-L-rhamnosyl (1'''→6") –*O*-*β*-D-galactopyranoside 7-*O*-*β*-L-apiofuranoside (**2A**)**.**

Acid hydrolysis of **2A** released quercetin, together with the three sugar moieties: galactose, rhamnose and apiose.

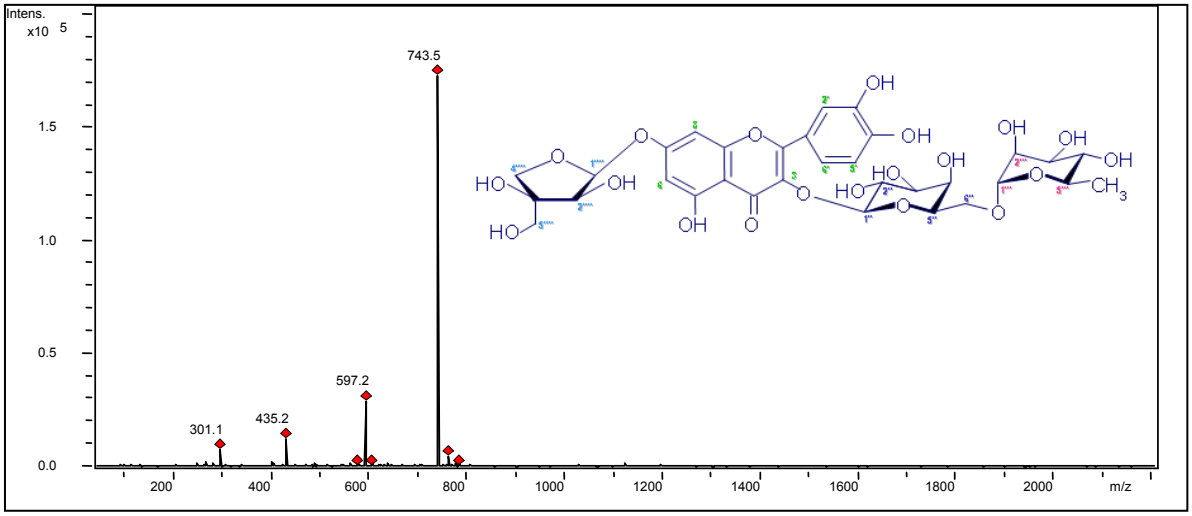

Figure 2.12: An additional LC/MS run for quercetin 3-*O*-*α*-L-rhamnosyl (1''' → 6")-*O*-*β*-D-galactopyranoside 7-*O*-*β*-L-apiofuranoside (**2A**)**.**

The FAB-MS of **2A** (positive mode) showed a quasimolecular ion $[M+H]^+$ at *m/z* 743. The LC-MS^2 spectrum (positive mode) for the ion at *m/z* 743 gave three fragment ions at *m/z* 597 $[M+H-146]^+$, *m/z* 435 $[M+H-146-162]^+$ and *m/z* 303 $[M+H-146-162-132]^+$, corresponding to the successive loss of three sugar moieties. Finally, a high resolution

negative ion FAB mass spectrum of **2A** showed a $[M-H]^-$ peak at *m/z* 741.191663, which was consistent with a molecular formula of $C_{32}H_{37}O_{20}$. The ^{1}H and ^{13}C NMR spectra of **2A** were similar to those for **1A,** with the exception of the aglycone signals, which indicate quercetin. The identification of the three sugars of **2A** and their sites of attachment were further deduced from the NMR experiments in the same manner as for **1A**. Thus, compound **2A** was identified as quercetin 3-*O*-α-L-rhamnosyl (1'''→6")-*O*-*β*-D-galactopyranoside 7-*O*-*β*-L-apiofuranoside (Figure 2.11).

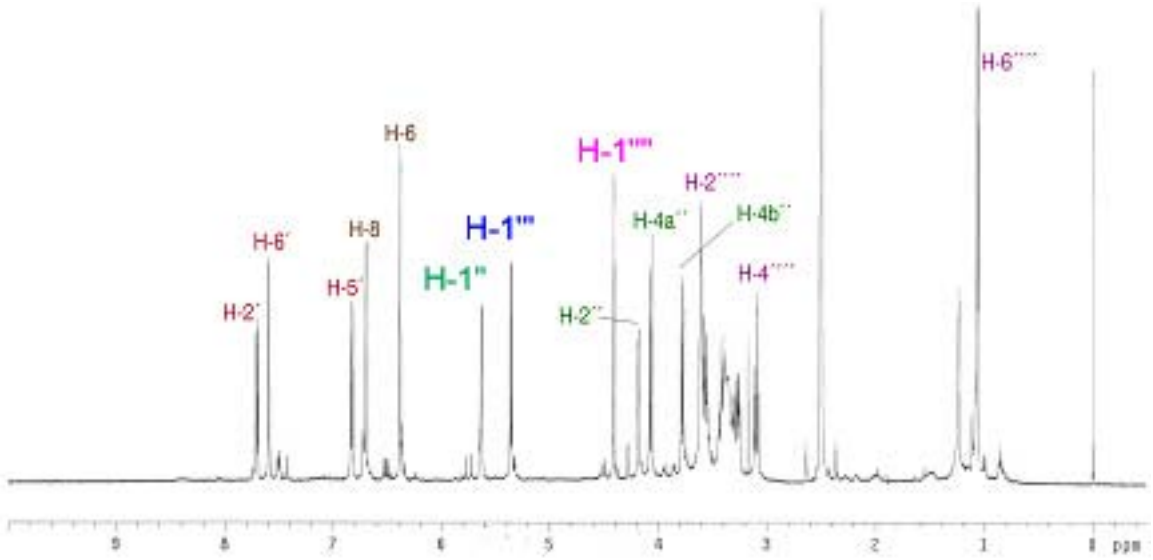

Figure 2.13: The ^{1}H NMR spectrum for compound **2A** highlighting the three anomeric carbons along with the doublet signals identified for the anomeric proton at the 4 position of galactose.

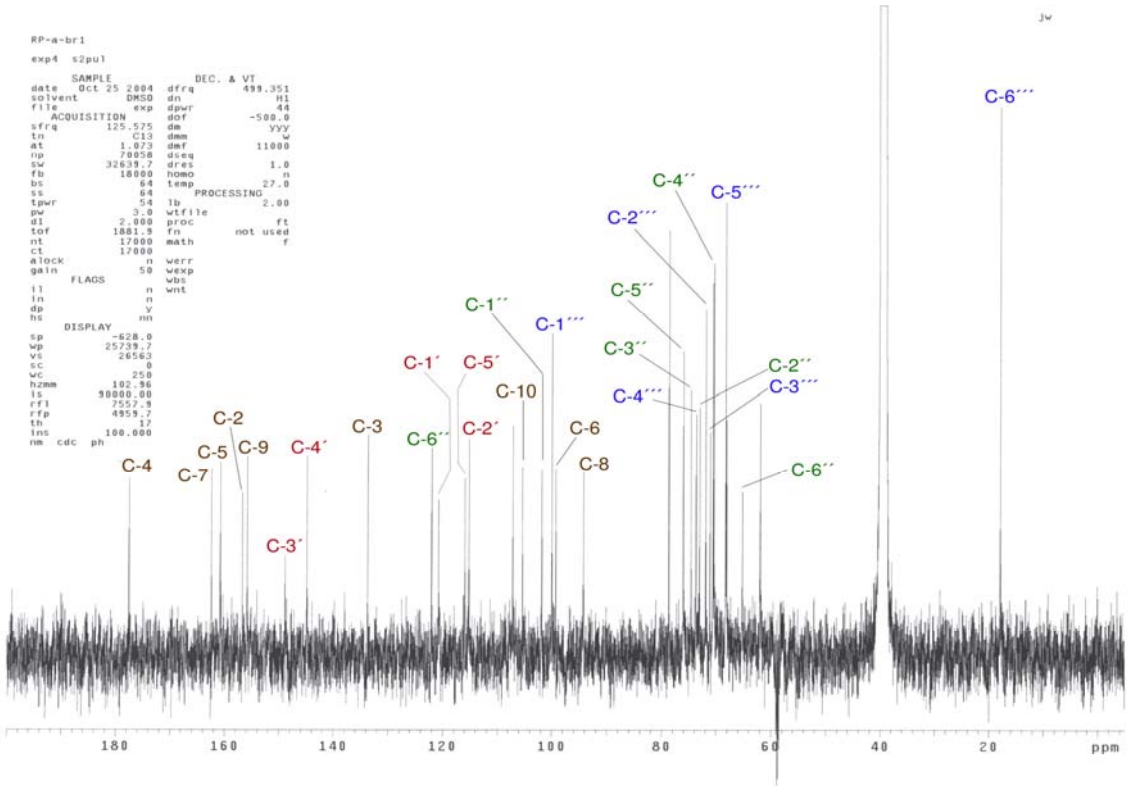

Figure 2.14: The ^{13}C NMR spectrum for quercetin 3-*O*-*α*-L-rhamnosyl (1'''→6'') –*O*-*β*-D-galactopyranoside 7-*O*-*β*-L-apiofuranoside (**2A**)**.**

^{1}H NMR for compound **2A** exhibited A and B ring signals typical of quercetin 3, 7-di-*O*-substituted glycosides (Mabry *et al*., 1970). The signals for the anomeric protons were detected at δ 5.63 as *d*, J = 3.48 Hz for the 3 position galactose, δ 5.36 *d*, J = 7.69 Hz and for the 7-*O* apiose at 4.41 Hz. The doublet of doublet signals for both the H-2' and H-5' protons were at δ 7.70, J = 10.81 Hz and 6.83, J = 8.4 Hz, respectively. The H-6' doublet, influenced by both the *meta* and *ortho* effects of the H-5' and H-2 protons was observed at δ 7.59, J = 2.04 Hz. The glycoside protons all appear in the characteristic region between 3.0 and 4.5 with the H-6''' methyl protons of rhamnose appearing at δ 1.06, J = 0.01 Hz (Figure 2.14).

The ^{13}C and DEPT analysis indicated 3 methylene, one methyl and 17 methine carbons for compound **2A** with an additional methyl group for the isorhamnetin aglycone of compound **1A** (Figure 2.3j).

The LC-MS analysis of a mixture of the compounds (**6**) and (**7**) revealed the presence of two compounds with molecular weights of 447. In negative ion mode, collisional activated dissociation (CAD) resulted in the loss of one hexose moiety (-162 u) from each compound. Compounds (**6**) and (**7**) were identified as kaempferol derivatives by comparing the fragmentation patterns of the aglycone components with commercial standards. In order to determine the locations and identities of the hexose moieties, LC-MS^n with post-column manganese complexation was used according to recently described methods (Davis and Brodbelt, 2005). The four compounds produced complexes of the form $[Mn (II) (M-H) (M)]^+$, where M is the unknown flavonoid glycoside. Performing CAD on these complexes yielded a single fragmented ion corresponding to the loss of one hexose moiety, thus resulting in a 3-*O*-glycoside (Davis and Brodbelt, 2004, 2005).

Further dissociation of these ions allowed for the identification of each hexose moiety. Losses from the second hexose moiety and the main aglycone were observed for all four Mn complexes. This diagnostic fragmentation pattern appears exclusively in flavonoid galactosides (Davis and Brodbelt, 2005). Thus, the compounds were identified as: kaempferol 3-*O*-*β*-D-glucoside (**6**) and kaempferol 3-*O*-*β*-D-galactoside (**7**). The identities (**6**) and (**7)** were confirmed by retention time comparisons with commercial standards. The isorhamnetin identifications were supported from the observation that

flavonoid galactosides generally elute slightly earlier than flavonoid glucosides using reverse-phase HPLC (Robards and Antolovich, 1997; Santos-Buelga and Williamson, 2003; Schieber *et al*., 2002).

For the compounds isorhamnetin 3-*O*-robinobioside (**4**) and isorhamnetin hyperoside (identified through additional analysis)**, t**heir UV, MS, ^{1}H and ^{13}C NMR spectra were compared with the spectroscopic data available from the literature (Baberá *et al*., 1986; Buschi and Pomilio, 1982; Halim *et al*., 1995; Mabry *et al*., 1970; Rastrelli *et al*., 1995; Yasukawa and Takido, 1987). Acid hydrolysis followed by TLC of the aglycone and its sugars further confirmed the identities of these compounds.

Further analyses for each of the compounds above are included in the Appendix. Isorhamnetin 3-*O*-*α*-L-rhamnosyl (1'''→6'')-*O*-*β*-D-galactopyranoside 7-*O*-*β*-L-apiofuranoside (**1A**) was a dark yellow amorphous powder (10 mg); R_f: UV λ_{max} MeOH (nm) 255, 268 *sh*, 355; + NaOMe: 248 *sh*, 271, 406; + NaOAc: 260, 328 *sh*, 375, 417; + NaOAc-H_3BO_3: 256, 268 *sh*, 360; + $AlCl_3$: 270, 302 *sh*; + $AlCl_3$-HCl: 269, 302 *sh*, 364, 402 nm. ^{1}HNMR: Table 1; ^{13}CNMR: Table 1. FAB-MS (neg.) (rel. int.) *m/z* $[M-H]^-$ (14), *m/z* 623 $[M-H\text{-apio}]^-$ (21), CI-MS (neg.) *m/z* 778 $[M-H + Na]^-$ (35), *m/z* 735 $[M-H\text{-}CH3CO]^-$ (13), *m/z* 623 $[M-H\text{-apio}]^-$ (12), *m/z* 315 $[M-H\text{-gal-rha-apio}]^-$ (100); LS-MS^2 (for 757) (pos.) *m/z* 611 $[M+H\text{-rha}]^+$ (12), *m/z* 449 $[M+H\text{-rha-gal}]^+$ (58), *m/z* 317 $[M+H\text{-rha-gal-apio}]^+$ (30), HRFAB-MS (pos.) *m/z* 779.01779 $[M+Na]^+$, calculated for $C_{33}H_{40}O_{22}$ + Na, 779.01064.

Quercetin 3-*O*-*α*-L-rhamnosyl (1'''→6'')-*O*-*β*-D-galactopyranoside 7-*O*-*β*-L-apiofuranoside (**2A**) was a yellow amorphous powder (10 mg); R_f: UV λ_{max} MeOH (nm)

258, 271 *sh*, 292 *sh*, 358; + NaOMe 271, 397; + NaOAc 262, 293 *sh*, 380; + NaOAc-H_3BO_3 262, 300 *sh*, 380; + $AlCl_3$ 274, 300 *sh*, 340, 420; + $AlCl_3$-HCl 270, 297 *sh*, 341, 406 nm. ^{1}HNMR; ^{13}CNMR: Table 1. FAB MS (neg.) *m/z* (rel. int.): 741 $[M-H]^-$ (100), 609 [M-H-api]$^-$ (84); FAB-MS (pos.) *m/z* (rel. int.): 743 $[M+H]^+$ (19), 435 [M+H-rha-gal]$^+$ (39); LS-MS^2 (for 743) (pos.) *m/z* 597 $[M+H\text{-rha}]^+$ (20), *m/z* 435 $[M+H\text{-rha-gal}]^+$ (85), *m/z* 303 [M=H-rha-gal-apio]$^+$ (47); HRFAB-MS (neg.) *m/z* 741.91663 $[M-H]^-$, calculated for $C_{32}H_{37}O_{20}$ 741.87819.

UV analysis of quercetin 3-*O*-*β*-D-glucopyranoside (**3**) (SAMPLE SR 11-15) in MeOH exhibited two bands at 359 nm, band I, 258 nm, band II and a shoulder at 292 nm. On addition of $NaOCH_3$, both an increase in absorbance and wavelength occurred (+ 38 nm, band I**,** + 13 nm, II) consistent with a 4 position free OH. The compound, on addition of $AlCl_3$, showed a bathochromic shift of (+61 nm, band I, + 16 nm, band II) confirming the catecholic 3,4-OH presence. On addition of HCl, a decomposition and a return to the wavelengths 341 and 270 nm occurred. Addition of NaOAc showed a +21 nm, band I, +4 nm, band II suggestive of an OH at the 7 position, and on addition of boric acid, a reconfirmation of the ortho 3,4-OH presence, +13 nm, band I, - 8 nm, band II, occurred. ^{1}H NMR provided for the **A** ring signals 6 and 8 at δ ppm 5.8 and 5.9, respectively. The **B** ring 2', 5' and 6' signals can be identified at δ ppm 7.46, 7.42 (*d*, *J* ~1.0 Hz), (*dd*, *J* = 8.19, ~ 1.0 Hz), and 6.75 ppm (*d*, *J* = 8.34 Hz), respectively. The anomeric 3 position glucosidic proton H-1 was observed at δ 4.93 ppm (*d*, *J* = 7.49 Hz) with the remaining sugar protons appearing between δ ppm 3-4. FAB-MS, in negative mode, provided the strongest molecular peak at *m/z* 462.9 (M-1) consistent for quercetin

3-*O*-*β*-D–glucoside (**3**). ^{13}C NMR data for quercetin 3-*O*-*β*-D-glucoside includes 177 (C-4), 164 (C-7), 162 (C-9), 157 (C-2), 156.5 (C-5), 149 (C-4), 145 (C-3), 133 (C-3), 122 (C-1), 121.5 (C-6), 117 (C-5), 115.5 (C-2), 105 (C-10), 101.5 (C-1), 98 (C-6), 93.5 (C-8), 78 (C-5), 77 (C-3), 76 (C-2), 70 (C-4), 61.5 (C-6). The anomeric glycosidic carbon typical for this known compound appears at 101.5 ppm.

Additional LC analyses performed in the lab report the isorhamnetin monosides isorhamnetin 3-*O*-*β*-*D*-glucopyranoside, isorhamnetin 3-*O*-*β*-*D*-galactopyranoside and the aglycone quercetin.

Isorhamnetin 3-*O*-*β*-*D*-glucopyranoside**:** LC-MS: *m/z* 477 $[M-H]^-$, *m/z* 315 [M-H – gal]$^-$; MS^2: *m/z* 1010 $[Mn(II)\ (M)\ (M-H)]^+$, *m/z* 848 $[Mn(II)\ (M)\ (M-H) – glc]^+$; MS^3: *m/z* 848 $[Mn(II)\ (M)\ (M-H) – glc]^+$, *m/z* 686 $[Mn(II)\ (M)\ (M-H) – 2\ glc]^+$, *m/z* 532 $[Mn(II)\ (M)\ (M-H) – glc – A]^+$.

Isorhamnetin 3-*O*-*β*-*D*-galactopyranoside**:** LC-MS: *m/z* 477 $[M-H]^-$, *m/z* 315 [M-H – gal]$^-$; MS^2: *m/z* 1010 $[Mn(II)\ (M)\ (M-H)]^+$, *m/z* 848 $[Mn(II)\ (M)\ (M-H) – gal]^+$; MS^3: *m/z* 848 $[Mn(II)\ (M)\ (M-H) – gal]^+$, *m/z* 686 $[Mn(II)\ (M)\ (M-H) – 2\ gal]^+$, *m/z* 532 $[Mn(II)\ (M)\ (M-H) – gal – A]^+$, *m/z* 430 $[Mn(II)\ (M)\ (M-H) – gal – A – 102]^+$. FAB-MS, in positive mode, provided the strongest signal at *m/z* 625 (M+1) accounting for the aglycone, robinose and rhamnose sugars. ^{13}C NMR data included 178 (C-4), 165 (C-7), 162 (C-5), 157 (C-9), 150 (C-3), 148 (C-4'), 134 (C-3), 123 (C-6'), 122 (C-1'), 116 (C-5'), 114 (C-2'), 104 (C-10), 101 (C-1''), 100 (C-1'''), 99.5 (C-6), 95 (C-8), 74 (C-5''), 71.8 (C-4'''), 71.3 (C-2''), 71.1 (C-3'''), 68.9 (C-2'''), 68.6 (C-4''), 67.3 (C-5'''), 65.8 (C-6'') 18.5 (C-6'''). The identification of both isorhamnetin monosides were supported by the

observation that flavonoid galactopyranosides generally elute slightly earlier than flavonoid glucopyranosides using reversed-phase HPLC (Robards and Antolovich, 1997; Schieber *et al*., 2002; Santos-Buelga *et al*., 2003).

Isorhamnetin 3-*O*-*α*-L-rhamnosyl (1'''→6'')-*O*-*β*-D-galactopyranoside (**4**)**:** was a yellow amorphous powder (20 mg); R_f: UV λ_{max} MeOH (nm): 255, 267 *sh*, 300 *sh*, 365; + NaOMe: 273, 332, 416; + NaOAc: 274, 322, 374; + NaOAc-H_3BO_3: 256, 278 *sh*, 358; + $AlCl_3$: 269, 302, 363 *sh*, 404; + $AlCl_3$-HCl: 268, 300, 362, 402 nm; CI-MS (pos.) *m/z* 625 $[M+H]^+$ (16), 479 $[M+H\text{-rha}]^+$ (3), 317 $\{M+H\text{-gal-rha}]^+$ (100); ^{1}HNMR (500 MHz, DMSO-d_6, TMS as int. standard); aglycone: δ 8.01 (1H, *d*, *J* = 1.8 Hz, H-2′), 7.49 (1H, *dd*, *J* = 2.0, 8.4 Hz, H-6′), 6.89 (1H, *d*, *J* = 8.4 Hz, H-5′), 6.42 (1H, *d*, *J* = 1.54 Hz, H-8), 6.19 (1H, *d*, *J* = 1.54 Hz, H-6), 3.86 (AH, *s*, OMe), sugar moieties: 5.44 (1H, *d*, *J* = 7.7 Hz, H-1″), 4.43 (1H, *s*, H-1‴), 3.24-3.78 the other sugar protons, 1.05 (1H, *d*, *J* = 6., H-6‴); ^{13}CNMR: aglycone: δ 177.96 (C-4), 161.88 (C-5), 165.46 (C-7), 157.17 (C-2), 156.99 (C-9), 150.14 (C-3′), 147.68 (C-4′), 133.74 (C-3), 122.64 (C-6′), 121.73 (C-1′), 115.85 (C-5′), 114.12 (C-2′), 104.48 (C-10), 99.59 (C-6), 94.53 (C-8), 56.61 (CMe-3′); sugar moieties: 102.53 (C-1″), 100.74 (C-1‴), 74.24 (C-5″), 73.63 (C-3″), 72.58 (C-4‴), 71.83 (C-2″), 71.30 (C-2‴), 71.12 (C-3‴), 68.98 (C-4″), 68.66 (C-5‴), 65.86 (C-6″), 18.58 (C-6‴). All of the spectral data for **4** were comparable with those previously reported for isorhamnetin 3-O-robinobioside (Buschi and Pomilio, 1982; Halim *et al*., 1995; Rastrelli *et al*., 1995).

Kaempferol 3-*O*-*β*-*D*-glucopyranoside (**6**)**:** LC-MS: *m/z* 447 $[M-H]^-$; MS^2: *m/z* 950 [Mn(II) (M) (M-H)]$^+$, 788 [Mn(II) (M) (M-H) – glc]$^+$; MS^3: *m/z* 788 [Mn(II) (M) (M-

H) – glc]$^+$, *m/z* 626 [Mn(II) (M) (M-H) – 2 gcl]$^+$, *m/z* 502 [Mn(II) (M) (M-H) – glc – A]$^+$, where M is the parent compound and A is an aglycone.

Kaempferol 3-*O*-*β*-*D*-galactopyranoside (**7):** LC-MS: *m/z* 447 [M-H]$^-$; MS^2: *m/z* 950 [Mn(II) (M) (M-H)]$^+$, 788 [Mn(II) (M) (M-H) – gal]$^+$; MS^3: *m/z* 788 [Mn(II) (M) (M-H) – gal]$^+$, *m/z* 626 [Mn(II) (M) (M-H) – 2 gal]$^+$, *m/z* 502 [Mn(II) (M) (M-H) – gal – A]$^+$, *m/z* 400 [Mn(II) (M) (M-H) – gal – A – 102]$^+$.

Quercetin 3-*O*-*α*-*L*-rhamnosyl (1'''→6'')-*O*-*β*-*D*-glucopyranoside: Yellow amorphous powder (100 mg); CI-MS (pos.) *m/z* 465 [M+H]$^+$, 303 [M+H – glu]$^+$. All spectral data for the quercetin aglycone were comparable with those previously reported for hyperoside (Baberá *et al*., 1986; Mabry *et al*., 1970; Yusakawa and Takido, 1987).

2.4 *Silphium laciniatum* (Fig. 2.15) is native to Northeast Texas, where it can be found in prairies and sites cleared from underbrush (Clevinger, 1999). This species is considered the genetic precursor to *S. albiflorum* based on Dr. Clevinger's ITS DNA analysis (Clevinger, 1999). Similar to *S. albiflorum*, this plant is described as having a root tap, scapiform growth form, and bipinnately lobed blades; however unlike *S. albiflorum*, it is distinguished by its yellow corollas, thinner leaf blades and taller plant height (100-300 cm).

Figure 2.15: Early 1900th century botanical plate made for the species *Silphium laciniatum* (Chartingnature.com).

Results and Discussion

LC/MS analysis of *S. laciniatum* extracts showed the following 8 flavonoids: isorhamnetin 3-*O*-*α*-L-rhamnosyl (1'''→6'')-*O*-*β*-D-galactopyranoside 7-*O*-*β*-L-apiofuranoside (**1A**), *m/z* 757.4 $[M+H]^+$, (23.0 min); quercetin 3-*O*-*β*-D-galactopyranoside (**2**), *m/z* 465.0 $[M+H]^+$, (19.4 min); quercetin 3-*O*-*β*-D-glucopyranoside (**3**), *m/z* 465.1 $[M+H]^+$, (20.4 min); quercetin 3-*O*-*α*-L-rhamnosyl (1'''→6'')-*O*-*β*-D-glucopyranoside (**4**), *m/z* 611 $[M+H]^+$, (22.2 min); quercetin 3-*O*-*α*-L-rhamnosyl (1'''→6'')-*O*-*β*-D-galactopyranoside (**5**), *m/z* 611 $[M+H]^+$, (25.6 min);

kaempferol 3-*O*-*β*-D-glucopyranoside (**6**)**,** *m/z* 447 $[M+H]^+$, (21.5 min); kaempferol 3-*O*-*β*-D-apiopyranoside (**7**)**,** *m/z* 417.2 $[M+H]^+$, (22.6 min). An eighth flavonoid isorhamnetin 3-*O*-*α*-L-rhamnosyl (1'''→6'')-*O*-*β*-galactopyranoside (**8**) was identified separately through ^{1}H NMR analysis.

Compounds **1A**, **2**, **3**, **4**, **6** and **7** all shared corresponding masses and retention times with the compounds detected in *S. albiflorum.* The triglycoside isorhamnetin 3-*O*-*α*-L-rhamnosyl (1'''→6'')-*O*-*β*-D-galactopyranoside 7-*O*-*β*-L-apiofuranoside (**1A**) exhibited a mass *m/z* 757.5 and at approximately the same retention time as that of compound **1A** found in *S. albiflorum.* A quercetin triglycoside with a mass *m/z* 743, the same as observed for compound **2A,** was detected but at a much earlier retention time. Mass fractionation peaks correlated with those specific for quercetin derivatives and two showed consistent patterns for both kaempferol derivatives. While kaempferol 3-*O*-*β*-D-glucopyranoside (**6**) was detected, the accompanying 3 substituted glucopyranoside sister compound was not. At a retention time of 22.6 min, a compound with a mass of *m/z* 417.2 was, however, detected, suggesting the presence of kaempferol 3-*O*-*β*-D-apiopyranoside (**7**).

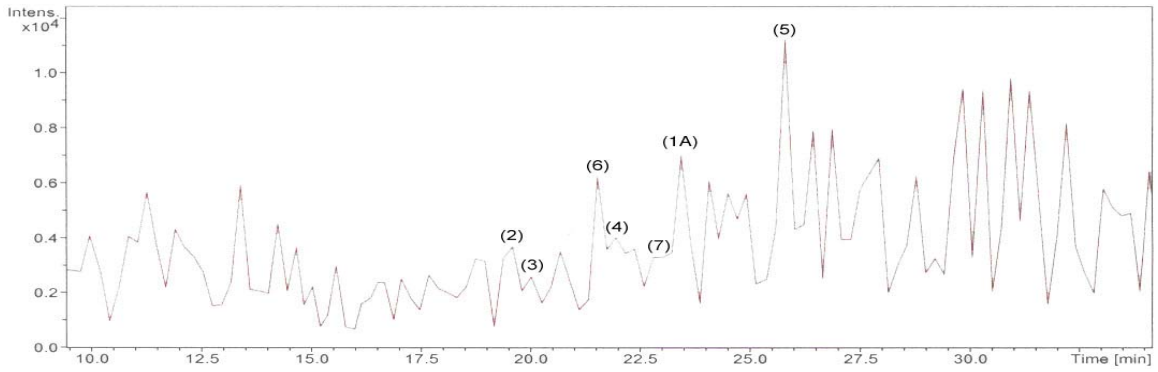

Figure 2.16: The seven flavonoid LC/MS peaks detected for extracts of *S. laciniatum* ranging between 15.0 and 30.0 minutes retention times.

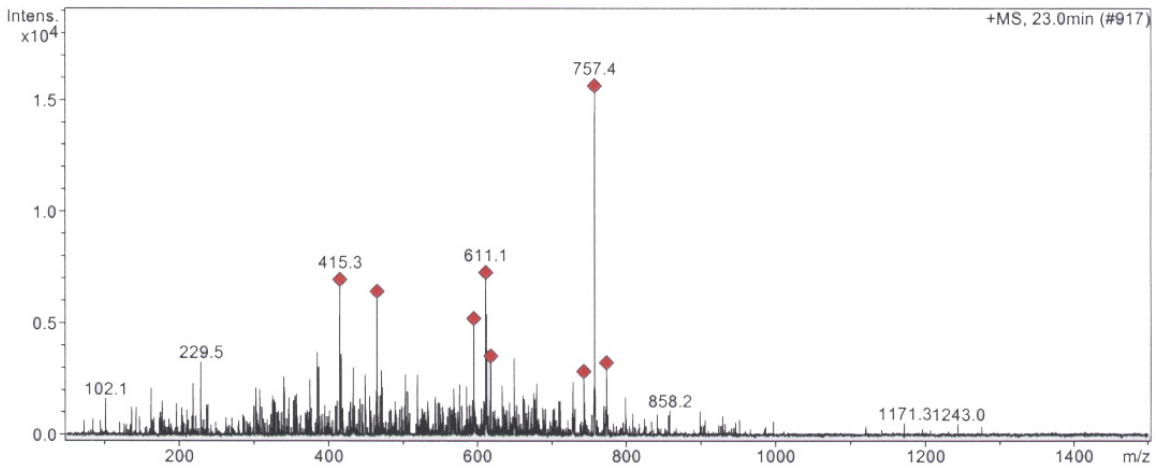

Figure 2.17: The *S. laciniatum* LC/MS fractionation peaks for isorhamnetin 3-*O*-*α*-L-rhamnosyl (1'''→6'')-*O*-*β*-D-galactopyranoside 7-*O*-*β*-L-apiofuranoside (**1A**)**.**

Quercetin 3-*O*-*β*-D-glucopyranoside (**3**) was identified using UV spectroscopy, ^{1}H NMR, HPLC, LC/MS and ESI-FAB MS along with sugar moiety identification through Mg^{+} complexation (Davis and Brodbelt, 2005).

The ^{1}H NMR provided identification for the **A** ring signals for H-6 and H-8 at *δ* ppm 5.8 and 5.9, respectively. The **B** ring 2′, 6′and 5′ signals were detected at *δ* ppm 7.4, 7.4 (*d*, *J* ~1.0 Hz), (*dd*, *J* = 8.19, ~ 1.0 Hz), and *δ* 6.7 ppm (*d*, *J* = 8.34 Hz), respectively. The anomeric proton (H-1") of the glycosidic group at the 3 position was observed at *δ* 4.9 ppm (*d*, *J* = 7.49 Hz), and the signals for the remaining sugar protons appeared between *δ* ppm 3-4.

The FAB-MS, in negative mode, provided the strongest molecular peak at *m/z* 464.0 (M-1) consistent for quercetin 3-*O*-*β*-D–glucopyranoside. UV analysis of quercetin 3-*O*-*β*-D–glucopyranoside (**3**) in MeOH exhibited two bands at λ 356 nm (band I), 260 nm (band II) and a shoulder at 306 nm. On addition of $NaOCH_3$, both bands I and II showed an increase in absorbance and a shift in their wavelength absorptions (+ 43 nm,

band I**,** + 10 nm, band II), results which establish a free 4′ OH. On addition of $AlCl_3$, the compound showed a bathochromic shift of +65 nm, band I, + 8 nm, band II, confirming the catecholic 3′, 4′ OH group presence. On addition of HCl hydrolysis, a return shift to the wavelengths λ 357 and 263 nm occurred. Addition of NaOAc showed a shift of +13 nm for band I and +10 nm for band II, suggestive of an OH presence at the 7 position; in addition, the introduction of boric acid confirmed the ortho 3′,4′ OH group (+13 nm, band I, - 8 nm, band II).

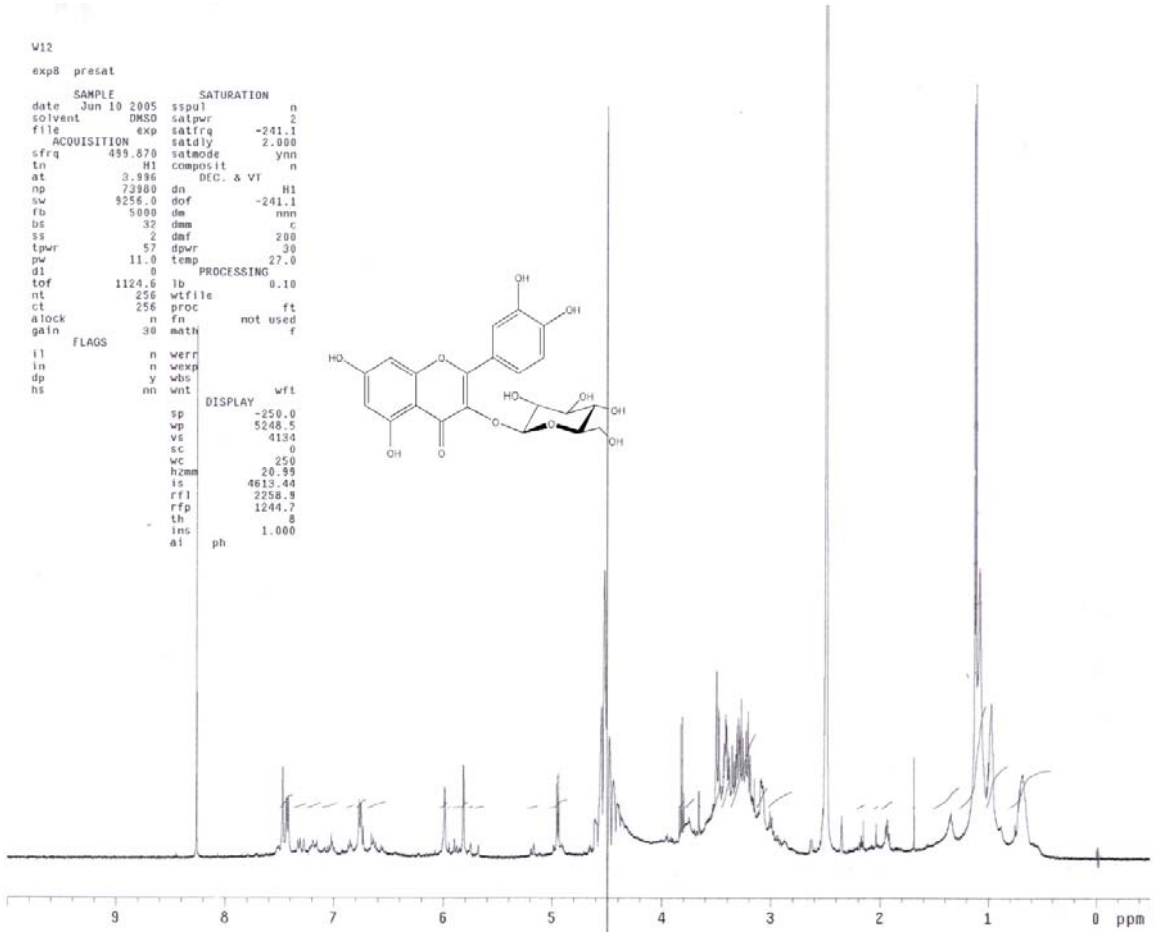

Figure 2.18: The ^{1}H NMR spectrum for quercetin 3-*O*-*β*-D–glucopyranoside (**3**).

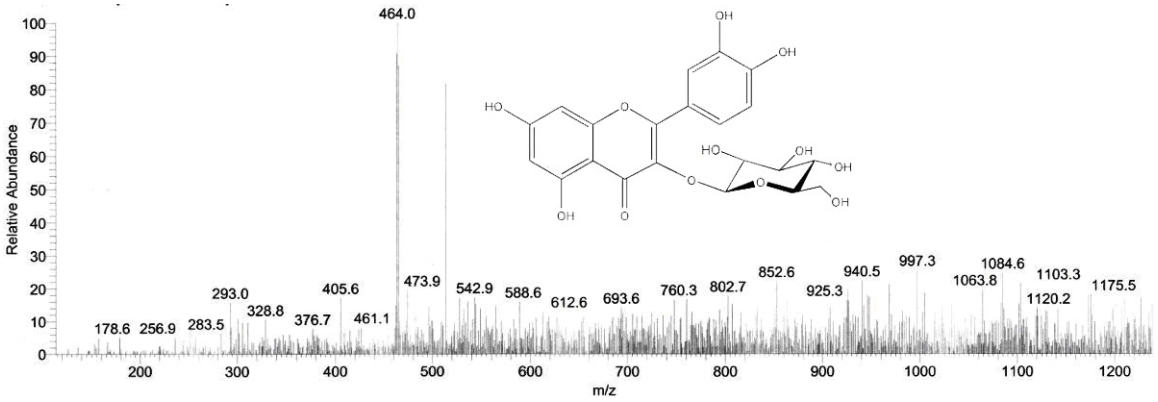

Figure 2.19: The FAB-MS spectrum for quercetin 3-*O*-*β*-D–glucopyranoside (**3**).

The second compound characterized through ^{1}HNMR analysis (Sample M19) was isorhamnetin 3-*O*-*α*-L-rhamnosyl (1'''→6'')-*O*-*β*-D-galactopyranoside (not observed in the LC/MS spectra). ^{1}HNMR showed the A ring signals for H-6 and H-8 at *δ* ppm 5.63 and 5.78 (*d*, *J* ~ 1.0 Hz), respectively. The B ring signals for H-2' and H-6' appeared at *δ* ppm 7.80 (*d*, *J* = 1.98 Hz) and 7.45 (*dd*, *J* = 8.19, ~ 1.0 Hz) along with a doublet for H-5' at 6.75 (*d*, *J* = 8.34 Hz). The protons of the characteristic OCH_3 methoxyl group of isorhamnetin can be seen at 3.80 ppm. The anomeric 3 position glucose doublet H-1'' appeared at *δ* ppm 5.22 (*d*, *J* = 6.78 Hz), and the rhamnose H-1''' was upfield at *δ* ppm 4.42. The *δ* ppm 4.4 position of the anomeric rhamnose proton indicates a terminal attachment to the glucose moiety.

UV analysis in MeOH provided for the wavelengths λ 352 nm band I and 257 nm band II. On addition of $NaOCH_3$, an increase in absorbance and wavelength (+ 62 nm, I, +15 nm, II) was observed, alluding to the **B** ring 4′ OH. On addition of $AlCl_3$ a drop in absorbance with an increase in wavelength (+ 43nm, band I, +33 nm, band II) was

observed indicating the **A** ring 5 position OH. The wavelength values remained the same on addition of HCl confirming the **A** ring 5 hydroxyl. On addition of NaOAc, an increase in wavelength from λ 257 to 273 nm in band II occurred (351 nm to 353 nm for band I) supporting a free OH at the 7 position of the **A** ring and addition of boric acid provided again for the same wavelength in band I of 353 nm confirming the absence of the 3', 4' hydroxyl groups.

FAB-MS, in negative mode, provided a signal at *m/z* 623 (M-1) accounting for the masses of the aglycone with its accompanying hexose and rhamnose sugars.

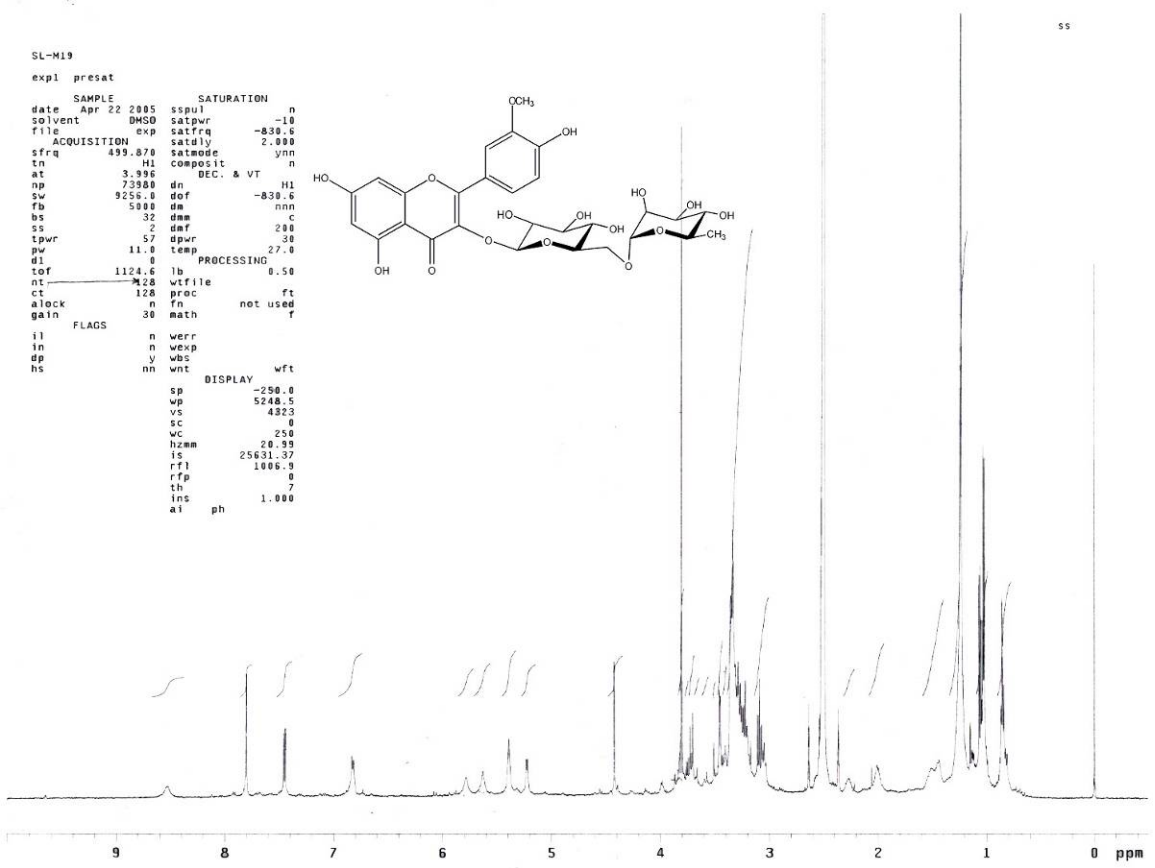

Figure 2.20: The ^{1}H NMR spectrum of isorhamnetin 3-*O*-*α*-L-rhamnosyl (1'''→6'')-*O*-*β*-D-galactopyranoside (**8**) in *S. laciniatum*.

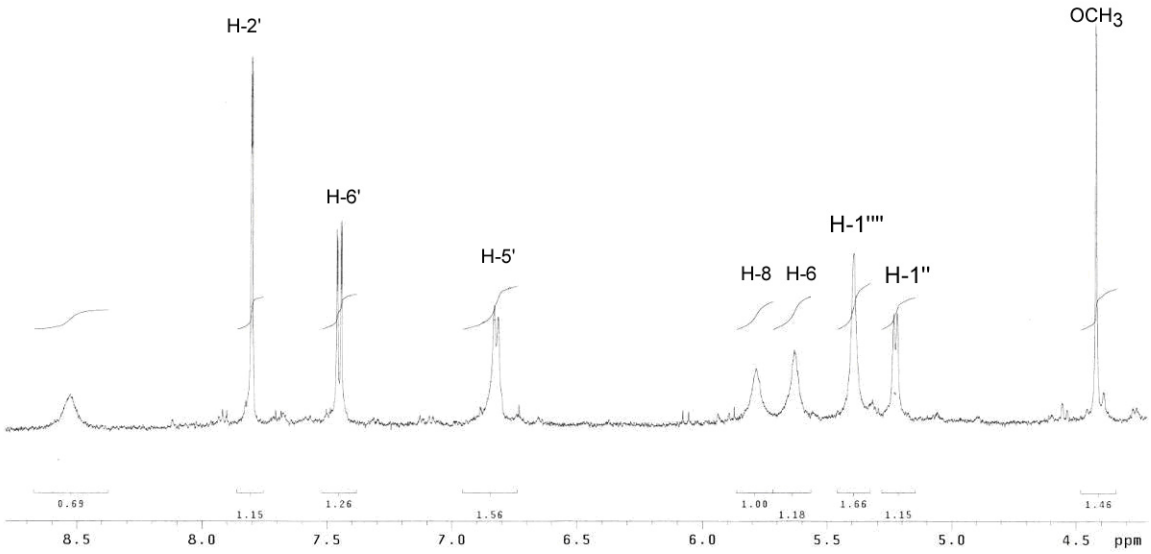

Figure 2.21: Increased resolution of the anomeric NMR signals characteristic for isorhamnetin 3-*O*-*α*-L-rhamnosyl (1'''→6'')-*O*-*β*-D-galactopyranoside (**8**) (Mabry *et al*., 1970).

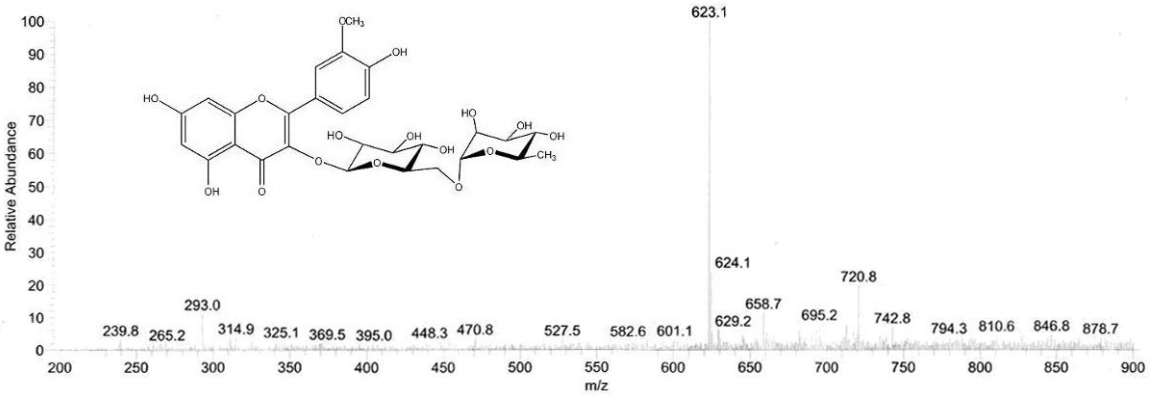

Figure 2.22: The FAB-MS (negative mode) for isorhamnetin 3-*O*-*α*-L-rhamnosyl (1'''→6'')-*O*-*β*-D-galactopyranoside (**8**) *m/z* 623.1.

2.5 *Silphium compositum* (Fig. 2.23)**,** also known as lesser basal-leaved rosinweed, thrives in the sandy soils of open pine and oak forests, roadsides, and meadows. The first of several Appalachian species, populations of this species are located in the lower nutrient soils of the Cherokee National Forest, Polk County, Tennessee.

Figure 2.23 Photographed dried leaves and superimposed flower of *S. compositum*

The plant is described as a scapiform, tap rooted perennial. The cauline leaves are basal persistent with up to 14 lobes per blade and range from entire to pinnately lobed (Clevinger, 1999). Easily distinguished from the other four tap-rooted species, *Silphium compositum* possesses smaller capitula comprising of 6 to 12 ray flowers per plant (Clevinger, 1999).

Results and Discussion

The LC/MS analysis of *S. compositum* extracts revealed the two new flavonoids observed in *S. albiflorum* along with six known flavonoids. These compounds were: isorhamnetin 3-*O*-*α*-L-rhamnosyl (1'''→6'')-*O*-*β*-D-galactopyranoside 7-*O*-*β*-L-apiofuranoside (**1A**)**,** *m/z* 757.4 $[M+H]^+$, (22.8 min); quercetin 3-*O*-*α*-L-rhamnosyl (1'''→6'')-*O*-*β*-D-galactopyranoside 7-*O*-*β*-L-apiofuranoside (**2A**)**,** *m/z* 743.4 $[M+H]^+$, (22.2 min); quercetin 3-*O*-*α*-L-rhamnosyl (1'''→6'')-*O*-*β*-D-galactopyranoside (**3**)**,** *m/z*

611.2 $[M+H]^+$, (27.8 min); quercetin 3-*O*-*α*-L-rhamnosyl (1'''→6'')-*O*-*β*-D-glucopyranoside (**4**), *m/z* 625.4 $[M+H]^+$, (20.2 min); isorhamnetin 3-*O*-*α*-L-rhamnosyl (1'''→6'')-*O*-*β*-D-galactopyranoside (**5**), *m/z* 625.2 $[M+H]^+$, (22.8 min); and quercetin 3-*O*-*β*-D-galactopyranoside (**6**)-identified separately through ^1H NMR analysis. Both of the newly isolated quercetin and isorhamnetin 3, 7 disubstituted triglycosides isolated from *S. albiflorum* were detected from *S. compositum*. Of the six total compounds found in *S. compositum*, an additional compound containing a mass of *m/z* 725.4 (**7**), a kaempferol triglycoside, had an unidentified retention time of 30.1 minutes.

Isorhamnetin 3-*O*-*α*-L-rhamnosyl (1'''→6'') *O*-*β*-D-galactopyranoside 7-*O*-*β*-L-apiofuranoside (**1A**) was detected in all of the species comprising *Silphium* section *Composita* except for the fourth, namely *S. terebinthinaceum*.

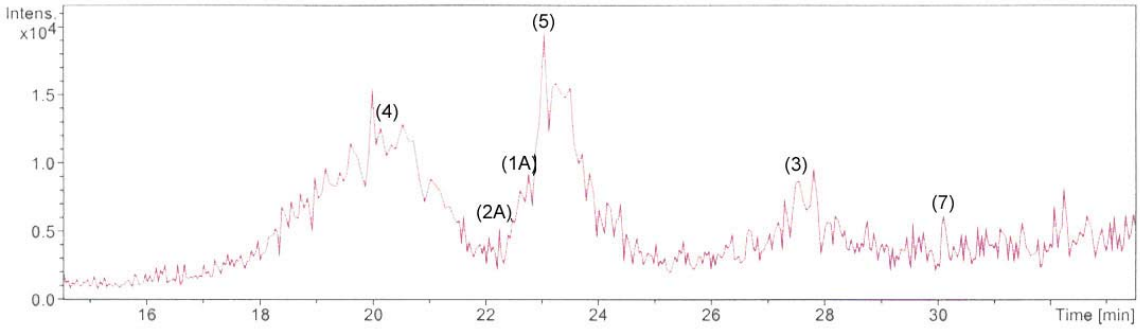

Figure 2.24: The LC/MS spectrum for the flavonoids of *S. compositum*.

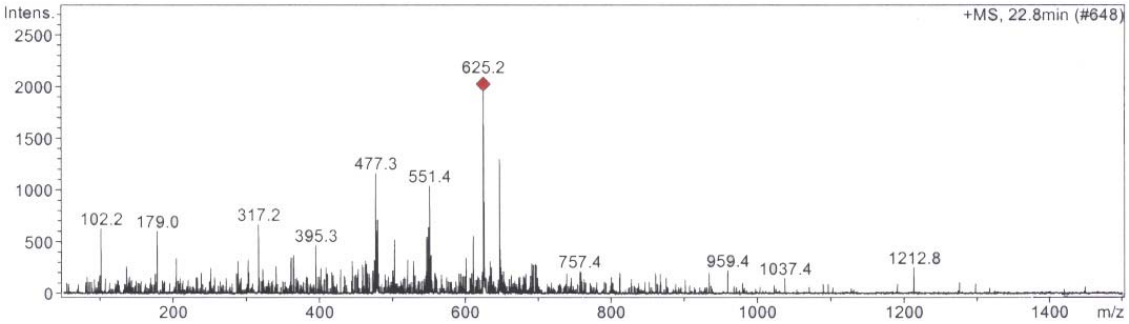

Figure 2.25: The LC/MS spectrum showing the isorhamnetin triglycoside isorhamnetin 3-*O*-*α*-L-rhamnosyl (1'''→6'')-*O*-*β*-D-galactopyranoside 7-*O*-*β*-L-apiofuranoside (**1A**), *m/z* 757.4 $[M+H]^+$, (22.8 min).

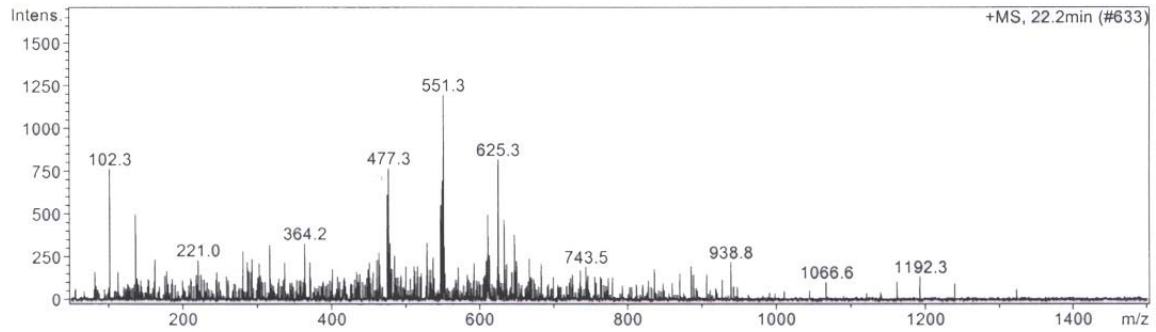

Figure 2.26: The LC/MS spectrum providing evidence for the quercetin triglycoside structure for quercetin 3-*O*-*α*-L-rhamnosyl (1'''→6'')-*O*-*β*-D-galactopyranoside 7-*O*-*β*-L-apiofuranoside (**2A**)**,** *m/z* 743.4 $[M+H]^+$, (22.2 min).

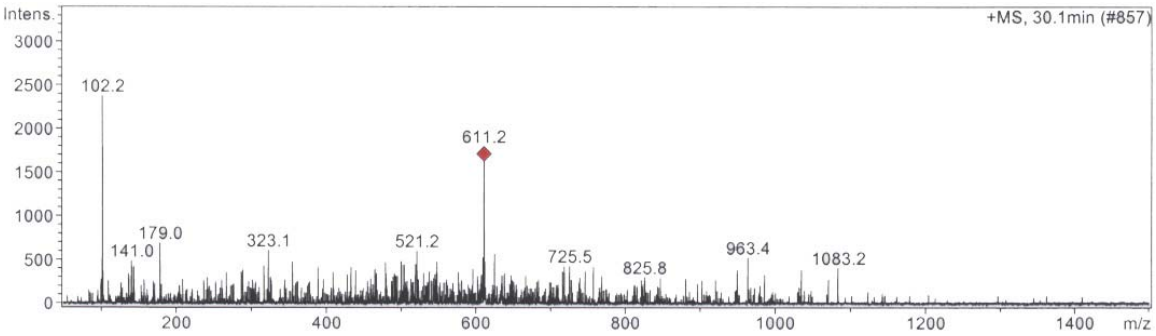

Figure 2.27: The LC/MS detection of what appears to be a new kaempferol triglycoside (**7**) with a retention time of 30.1 minutes.

The ^{1}H NMR analysis provided spectra for structural characterization of quercetin 3-*O*-*α*-L-rhamnosyl (1'''→6'')-*O*-*β*-D-galactopyranoside (**3**), quercetin 3-*O*-*α*-L-rhamnosyl (1'''→6'')-*O*-*β*-D-glucopyranoside (**4**) and isorhamnetin 3-*O*-*α*-L-rhamnosyl (1'''→6'')-*O*-*β*-D-galactopyranoside (**5**).

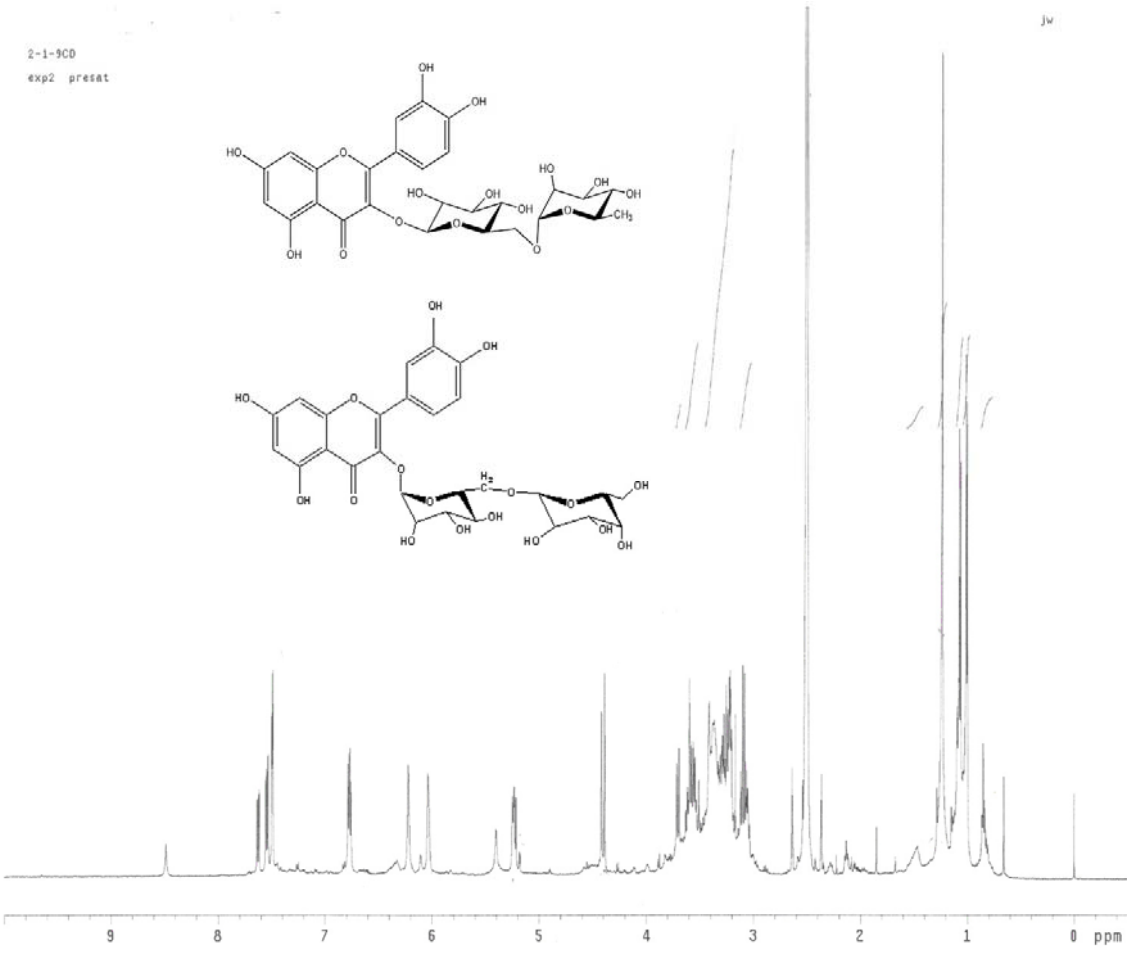

Figure 2.28: The ^{1}H NMR spectra for the compounds quercetin 3-*O*-*α*-L-rhamnosyl (1'''→6'')-*O*-*β*-D-galactopyranoside (**3**) and quercetin 3-*O*-*α*-L-rhamnosyl (1'''→6'')-*O*-*β*-D-glucopyranoside (**4**)**.**

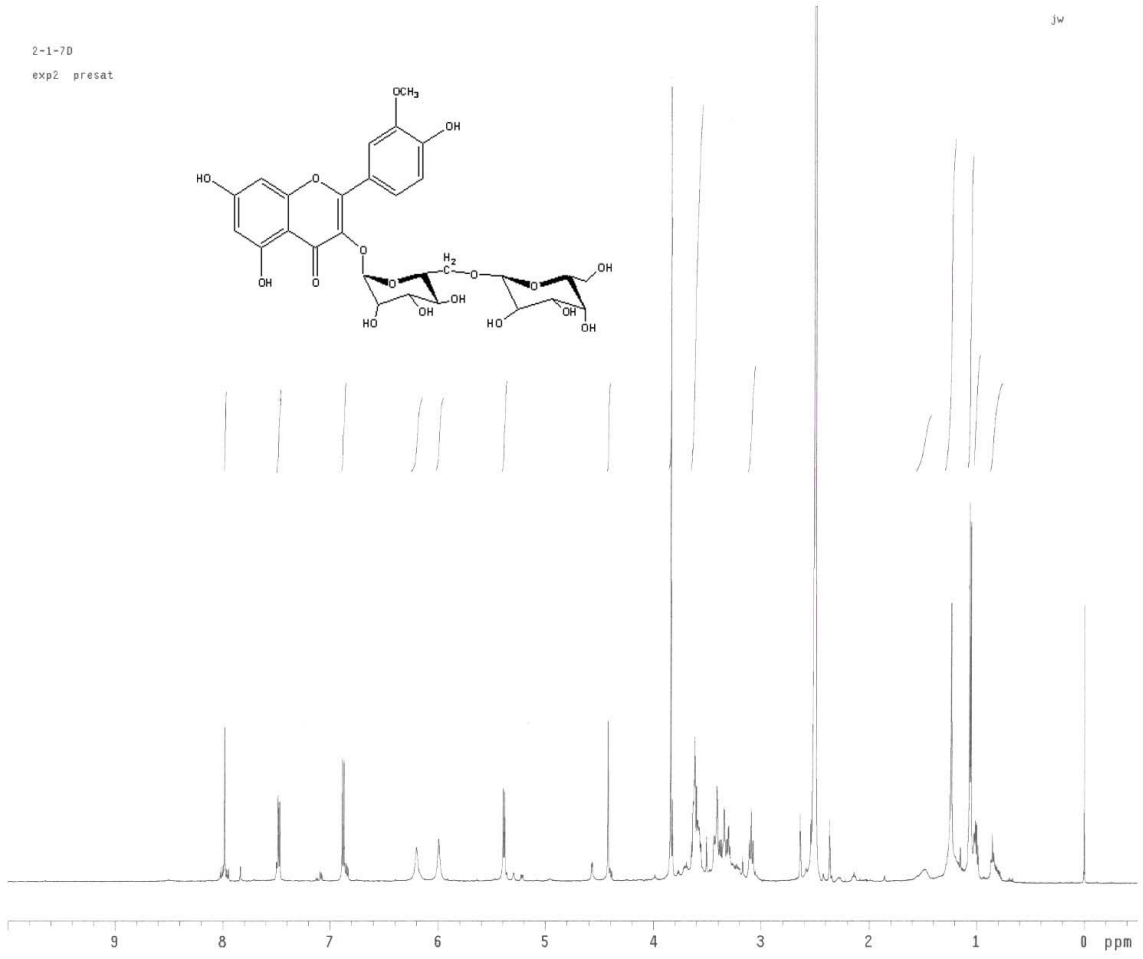

Figure 2.29: The ^{1}H NMR spectrum of isorhamnetin 3-*O*-α-L-rhamnosyl (1'''→6'')-*O*-β-D-galactopyranoside (**5**)**.**

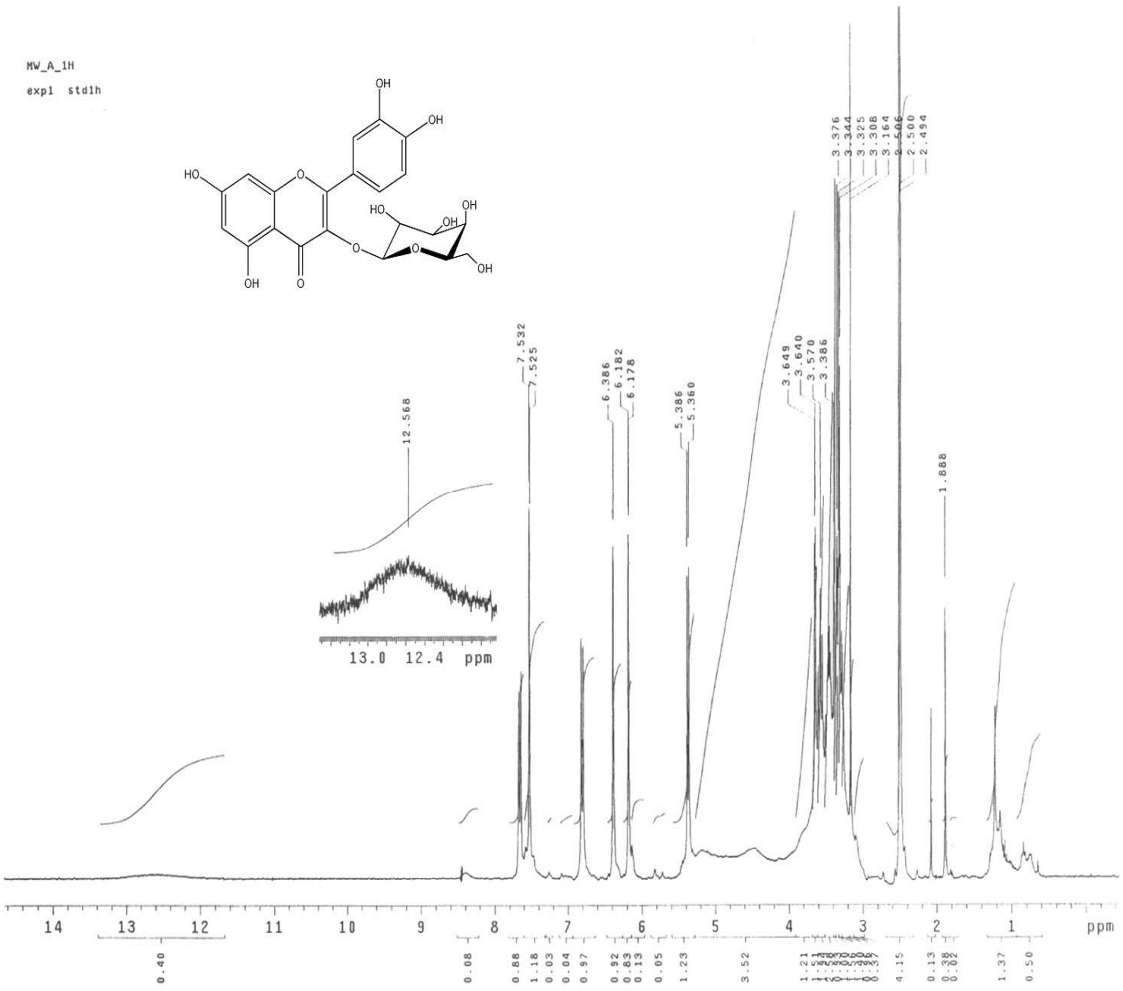

Figure 2.30: The ^{1}H NMR spectrum for quercetin 3-*O*-*β*-D-galactopyranoside (**6**).

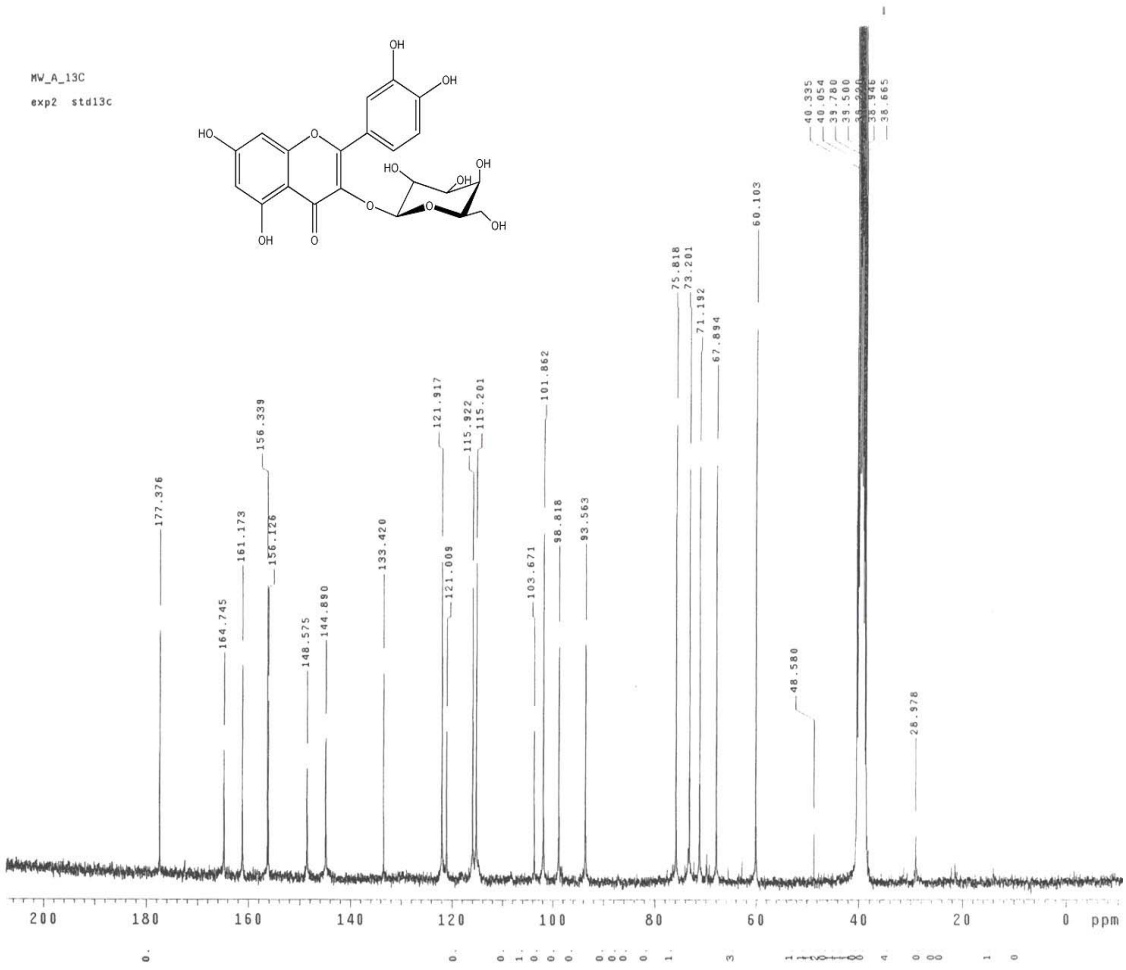

Figure 2.31: The ^{13}C NMR spectrum for quercetin 3-*O*-*β*-D-galactopyranoside (**6**).

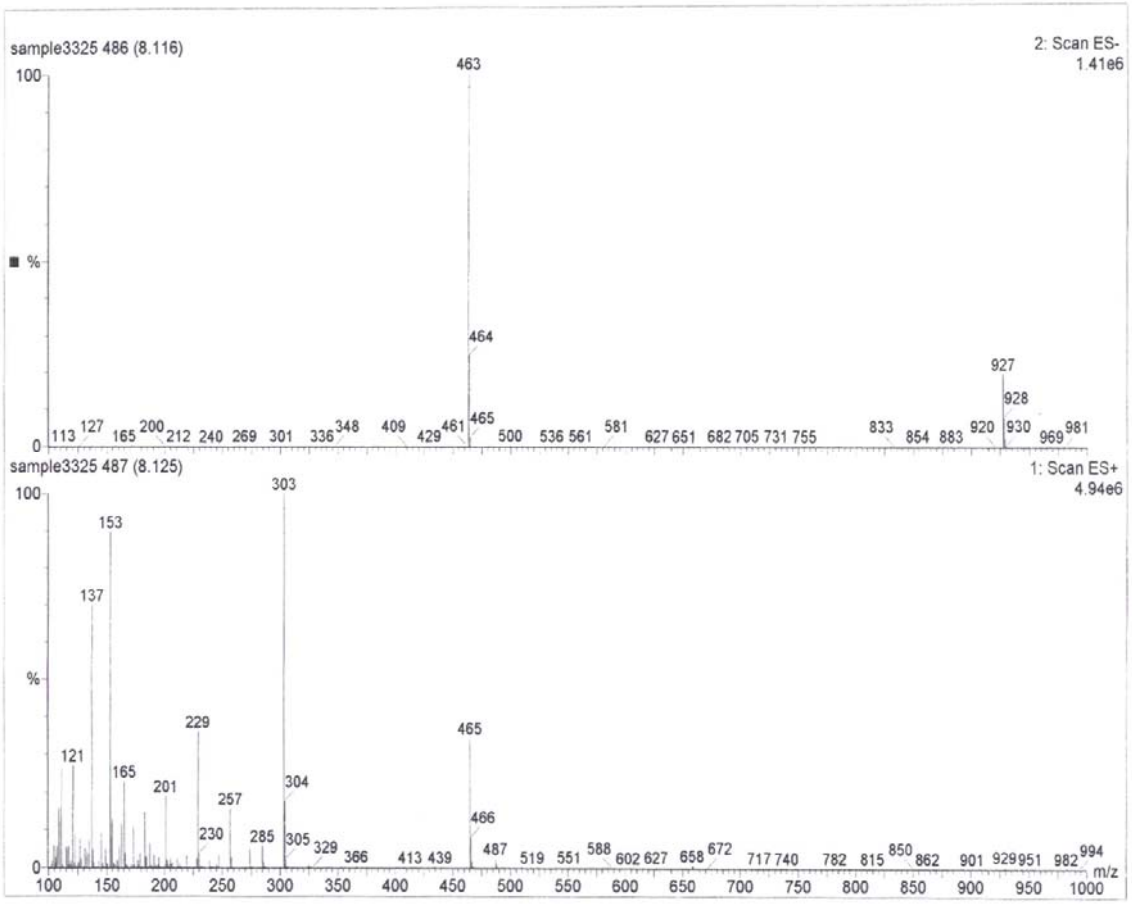

Figure 2.32: The FAB-MS for quercetin 3-*O*-*β*-D-galactopyranoside (**6)**.

2.6 *Silphium terebinthinaceum* var. *pinnatifidum* (Elliot) A. Gray (Fig. 2.33), the last of the four species discussed in *Silphium* section *Composita*, shares the common names prairie dock, basal-leaved rosinweed and dock rosinweed (Clevinger, 1999). This species ranges from Northwest Texas to Northern Michigan. The distribution of the species includes regions of wet prairies, and railway furrows.

Figure 2.33: Eighteenth century botanical plate of Prairie dock, *Silphium terebinthinaceum* (Curtis, 1836).

Past taxonomic analyses based on leaf shape suggest that this species includes intermediate hybrids consisting of *S. laciniatum* and *S. t.* var. *terebinthinaceum*. Dr. Clevinger's own molecular data indicates a closer relationship between *S. t.* var. *pinnatifidum* and *S. t.* var. *terebinthinaceum* coexisting as sister varieties.

Results and Discussion

The flavonoids detected in *Silphium terebinthinaceum* are again derivatives of the flavonoid aglycones quercetin, isorhamnetin and kaempferol. LC/MS analysis of *Silphium terebinthinaceum* extracts provided ten peaks with masses following the same

patterns as those for previously described flavonoids. The same masses and retention times as observed for quercetin 3-*O*-*β*-D-glucopyranoside (**2**) were detected for compounds from each of the species *S. terebinthinaceum, S. albiflorum* and *S. laciniatum*; similarly, isorhamnetin 3-*O*-*α*-L-rhamnosyl (1'''→6'')-*O*-*β*-D-glucopyranoside (**10**) was also detected in *S. laciniatum* and *S. compositum*. It is possible that the newly isolated kaempferol triglycosides **4A** and **5A** or similar derivative may also be present for the first time in a member of section *Composita*. The only confirmed detection of compound **5A** kaempferol 3-*O*- *β*-D-apiofuranoside 7-*O*-*α*-L-rhamnosyl (1''''→6''')-*O*- *β*-D-(2'''-*O*-*E*-caffeoylgalactopyranoside) is in the section *Silphium* species *S. perfoliatum* and *S. wasiotense*. Both LC peaks appeared with masses two hydrogen units less than what the actual masses should have been *m/z* 724.6 $[M-2H]^+$ (21.0 min.) and *m/z* 886.0 $[M-2H]^+$ (21.0 min). Several unknowns were also detected with masses matching an isorhamnetin diglycoside *m/z* 625, isorhamnetin monoside *m/z* 477, quercetin diglycoside *m/z* 609 and a kaempferol 3-apioside *m/z* 417.

The identified flavonoid compounds with their respective mass and retention times were: quercetin 3-*O*-D-galactopyranoside (**1**), *m/z* 465.1 $[M+H]^+$, (20.7 min); quercetin 3-*O*-D- glucopyranoside (**2**), *m/z* 487.1 $[M-22Na]^+$, (21.0 min); quercetin 3-*O*-rutinoside (**3**)**,** *m/z* 611.2 $[M+H]^+$, (22.1 min); kaempferol 3-*O*-*β*-D-apiofuranoside 7-*O*-*α*-L-rhamnosyl (1''''→6''')-*O*-*β*-D-galactopyranoside (**4A**)**,** *m/z* 886.0 $[M-2H]^+$, (21.0 min); and its caffeoyl ester (**5A**)**,** *m/z* 724.6 $[M-2H]^+$, (21.0 min); keampferol 3-*O*-*β*-D-rutinoside (**6**)**,** *m/z* 596.1 $[M-H]^+$, (21.0 min); isorhamnetin 3-*O*-*β*-D-galactopyranoside (**7**)**,** *m/z* 479.1 $[M+H]^+$, (24.5 min); isorhamnetin 3-*O*-*β*-D-glucopyranoside (**8**), *m/z*

477.1 $[M+H]^+$, (28.3 min); isorhamnetin 3-*O*-*β*-D-robinioside (**9**), *m/z* 625.2 $[M+H]^+$, (24.3 min); and isorhamnetin 3-*O*-*β*-D-rutinoside (**10**), *m/z* 625.3 $[M+H]^+$, (25.9 min).

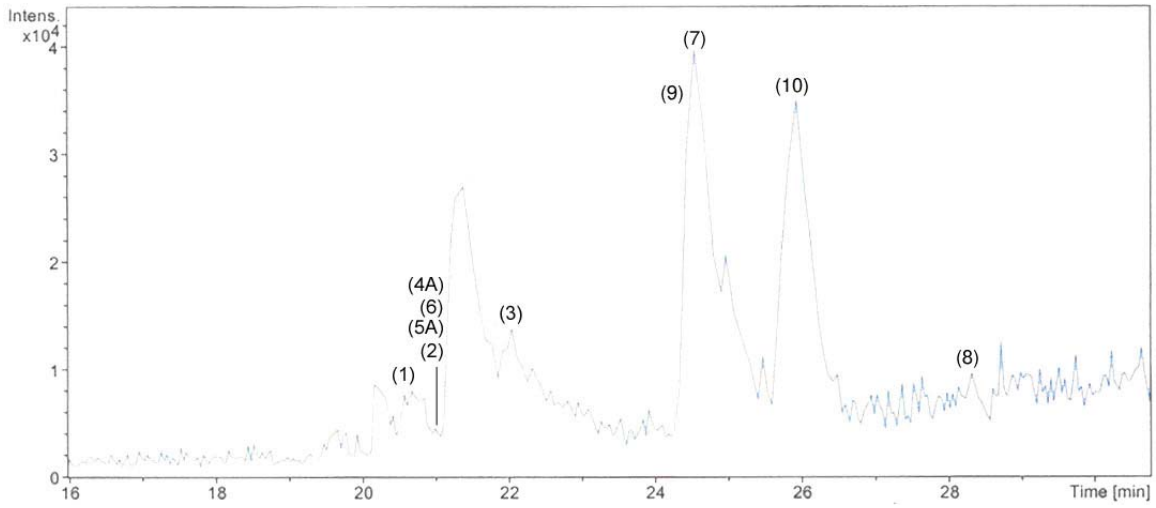

Figure 2.34: The LC/MS for the flavonoids of *S. terebinthinaceum.*

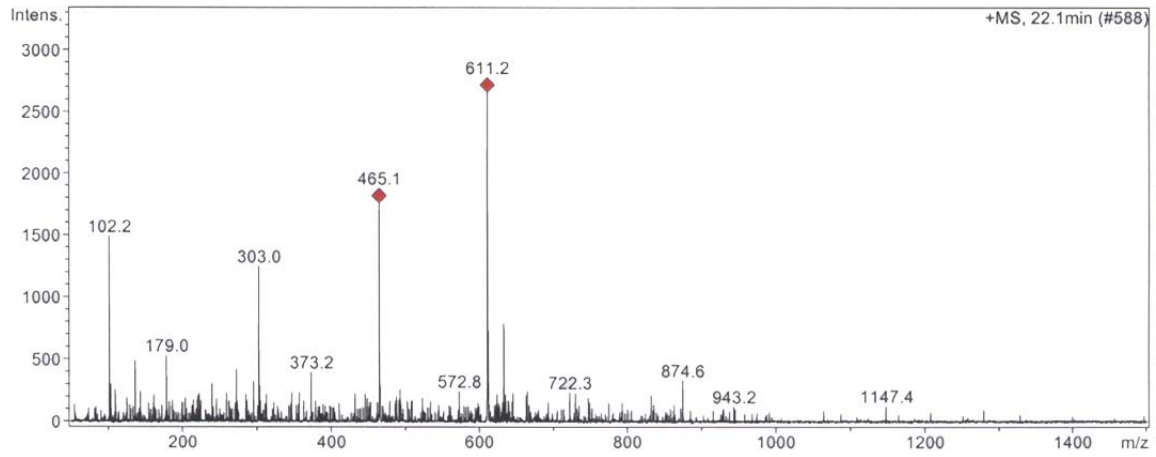

Figure 2.35: LC/MS peaks for quercetin 3-*O*-*α*-L-rhamnosyl (1'''→6'')-*O*-*β*-D-glucopyranoside (**3**).

The UV analysis of a mixture of the two known compounds quercetin-3-*O*-D-galactopyranoside **(1)** and quercetin-3-*O*-D-glucopyranoside **(2)** provided evidence that

both compounds where indeed quercetin based. In MeOH, band I was at λ 360 nm and band II at 258 nm. On addition of $NaOCH_3$, an increase in both bands was observed (+ 38 nm, band I, + 16 nm, band II) consistent with a 4′ free OH. On addition of $AlCl_3$, the compound showed a bathochromic shift of + 64 nm, band I, + 16 nm, band II, confirming the catecholic 3′, 4′ OH group. On addition of HCl, reductions of the shifts of the wavelengths λ 402 and 270 nm occurred. Addition of NaOAc showed a + 26 nm, band I, + 16 nm, band II, suggestive of an OH at the 7 position, and, on addition or boric acid, confirmation of an ortho 3′,4′ OH group (+ 20 nm, band I, + 4 nm, band II).

The ^{1}H NMR spectrum provided for the **A** ring signals of H-6 and H-8 at δ ppm 6.2 and 6.4, respectively. The **B** ring 2′, 6′ and 5′ signals can be seen at δ ppm 7.7 (*d*, *J* = 2.2 Hz), 7.6 (*dd*, *J* = 10.6, 2.24 Hz), and δ 6.9 ppm (*dd*, *J* = 10.8, 2.2 Hz), respectively. The anomeric 3 position glucosidic proton H-1″ was observed upfield at δ 5.2 ppm (*d*, J = 7.55 Hz) along with the second anomeric galactosidic H-1‴ proton at δ 5.1 ppm (*d*, *J* = 7.75 Hz).

The FAB-MS, in negative mode, provided for the molecular peak *m/z* 463 (M-1) consistent for quercetin-3-*O*-*β*-D-glucose/galactose along with the accompanying ESI-MS single peak at retention time=7.5 min.

The UV analysis of quercetin 3-*O*-*α*-L-rhamnosyl (1‴→6″)-*O*-*β*-D-glucopyranoside (**3**) in MeOH showed both bands characteristic for rutin at λ 364 nm, band I, and 258 nm, band II. On addition of $NaOCH_3$, both an increase in absorbance and wavelength occurred (+ 40 nm, band I, +10 nm, band II), consistent with a 4′ free OH. The compound, on addition of $AlCl_3$, showed a bathochromic shift of + 48 nm, band I, + 8

nm, band II, confirming the catecholic 3′,4′ OH group. On addition of HCl, a decomposition and return to the wavelengths of λ 360 nm and 266 nm occurred. Addition of NaOAc showed a + 30 nm, I, + 8 nm, II, suggestive of an OH at the 7 position, and on addition or boric acid, a confirmation of the ortho 3′,4′ OH group (+ 18 nm, band I, + 4 nm, band II) presence appeared.

The ^{1}H NMR spectrum provided for the H-6 and H-8 at δ ppm 6.2 and 6.4, respectively. The signals for H-2′, H-6′ and H-5′ were at δ ppm 7.7 (*d*, *J* = 2.3 Hz), 7.6 (*dd*, *J* = 6.21, 2.12 Hz), and δ 6.9 ppm (*d*, *J* = 8.46 Hz), respectively. The glucosidic anomeric proton (H-1″) signal was observed upfield at δ 5.1 ppm (*d*, J = 7.63 Hz), along with the remaining anomeric rhamnoside proton signal at δ 4.5 ppm (*d*, *J* = 1.56 Hz).

The FAB-MS, in negative mode, provided the molecular peak m/z 609 (M-1) consistent for quercetin 3-*O*-*β*-D-rutinoside along with the accompanying ESI-MS peak at *m/z* 609.50.

UV analysis of isorhamnetin-3-*O*-*β*-D-robinobioside (**9**) and isorhamnetin-3-*O*-*β*-D-rutinoside (**10**) in MeOH showed bands characteristic for isorhamnetin at λ 356 nm for band I and 256 nm for band II. On addition of $NaOCH_3$, both an increase in absorbance and wavelength occurred (+ 54 nm for band I, +18 nm for band II) consistent with a 4′ free OH. The compound, on addition of $AlCl_3$, showed a bathochromic shift of (+ 46 nm for band I, + 14 nm for band II) confirming the catecholic 3′,4′ OH group. On addition of HCl, decomposition occurred and the spectrum returned to the wavelengths of λ 356 and 256 nm. Addition of NaOAc showed a + 34 nm, band I, + 20 nm, band II, suggestive of

an OH presence at position 7, and on addition of boric acid, confirmation of the 4′ OH occurred with the return to the original wavelengths (358 nm, band I, 256 nm, band II).

The ^{1}H NMR provided for the **A** signals H-6 and H-8 at δ ppm 6.2 and 6.4, respectively. The H-2′, H-6′ and H-5′ signals appeared at δ ppm 7.9 (*d*, *J* = 2.0 Hz), 7.6 (*dd*, *J* = 10.4, 2.0 Hz), and δ 6.9 ppm (*d*, *J* = 8.4 Hz), respectively. The anomeric proton (H-1") for the glucosidic group appears upfield at δ 5.4 ppm (*d*, *J* = 7.5 Hz) along with the remaining anomeric rhamnoside proton at δ 4.5 ppm.

The FAB-MS, in negative mode, provided the molecular peak *m/z* 609.3 (M-1) consistent for quercetin 3-*O*-*β*-D-rutinoside along with the accompanying ESI-MS peak at *m/z* 609.5.

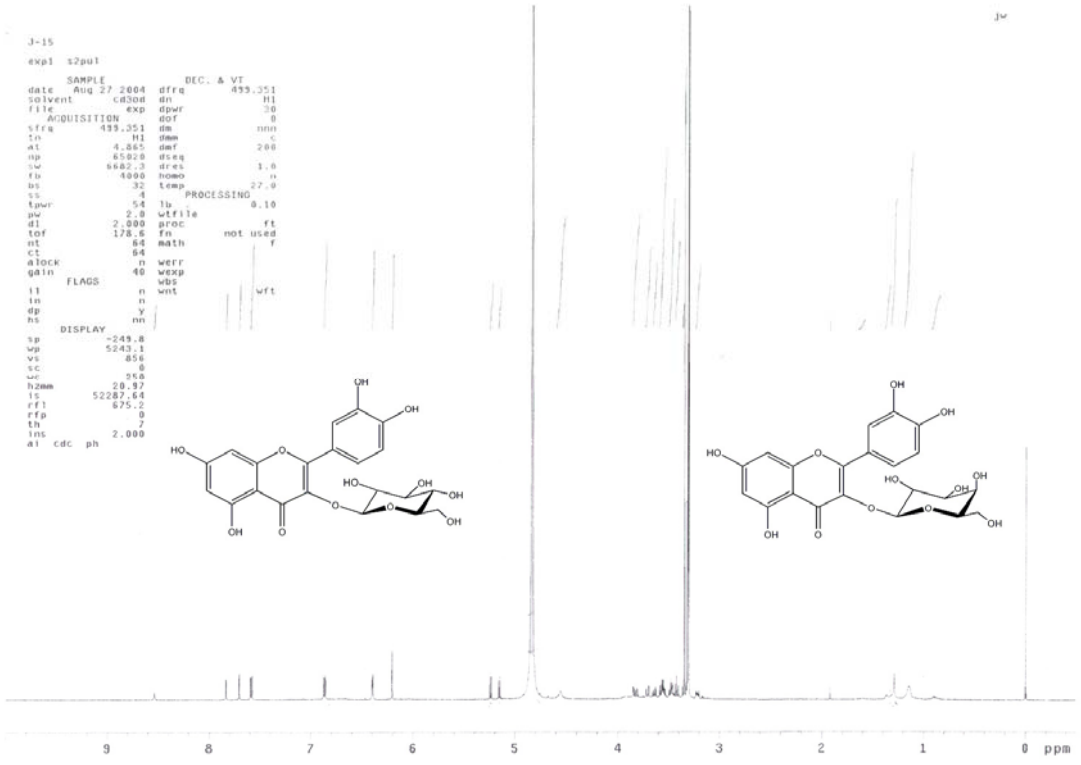

Figure 2.36: The ^{1}H NMR spectra for quercetin 3-*O*-*β*-D-galactopyranoside (**1**) and quercetin 3-*O*-*β*-D-glucopyranoside (**2**).

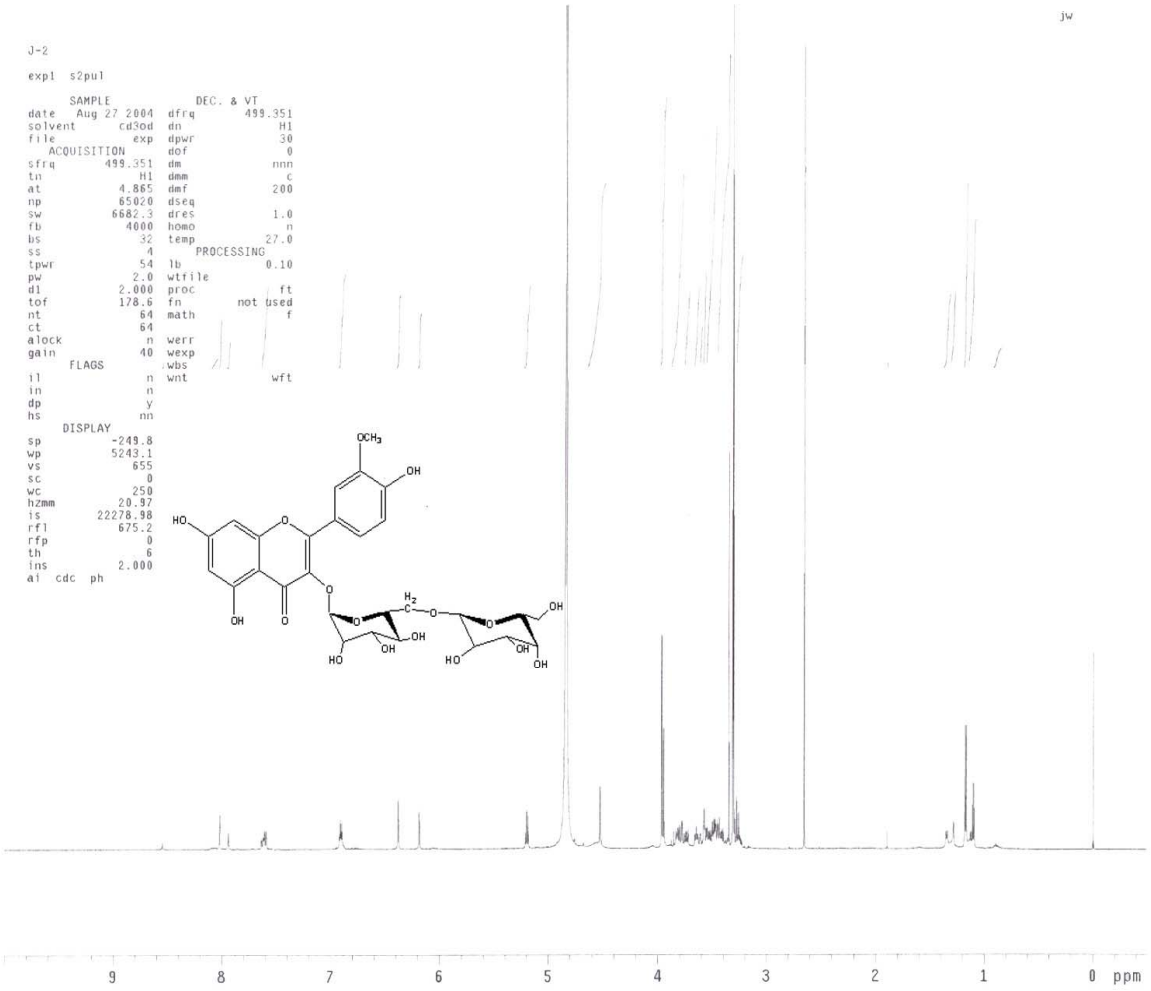

Figure 2.37: The ^{1}H NMR spectrum for isorhamnetin 3-O-α-L-rhamnosyl (1'''→6'')-*O*-*β*-D-galactopyranoside (**9**).

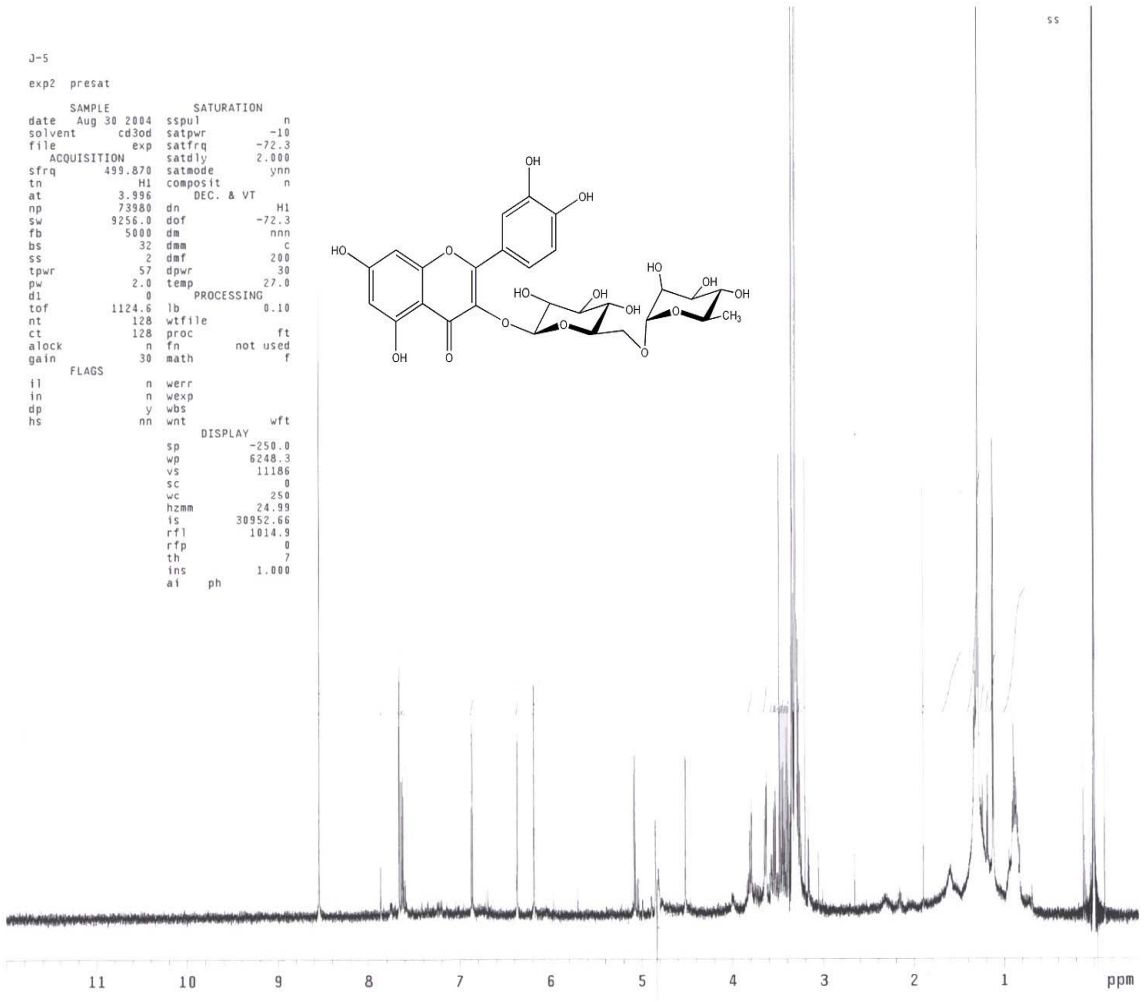

Figure 2.38: The ^{1}H NMR spectrum for quercetin 3-*O*-*α*-L-rhamnosyl (1'''→6'')-*O*-*β*-D-glucopyranoside (**3**).

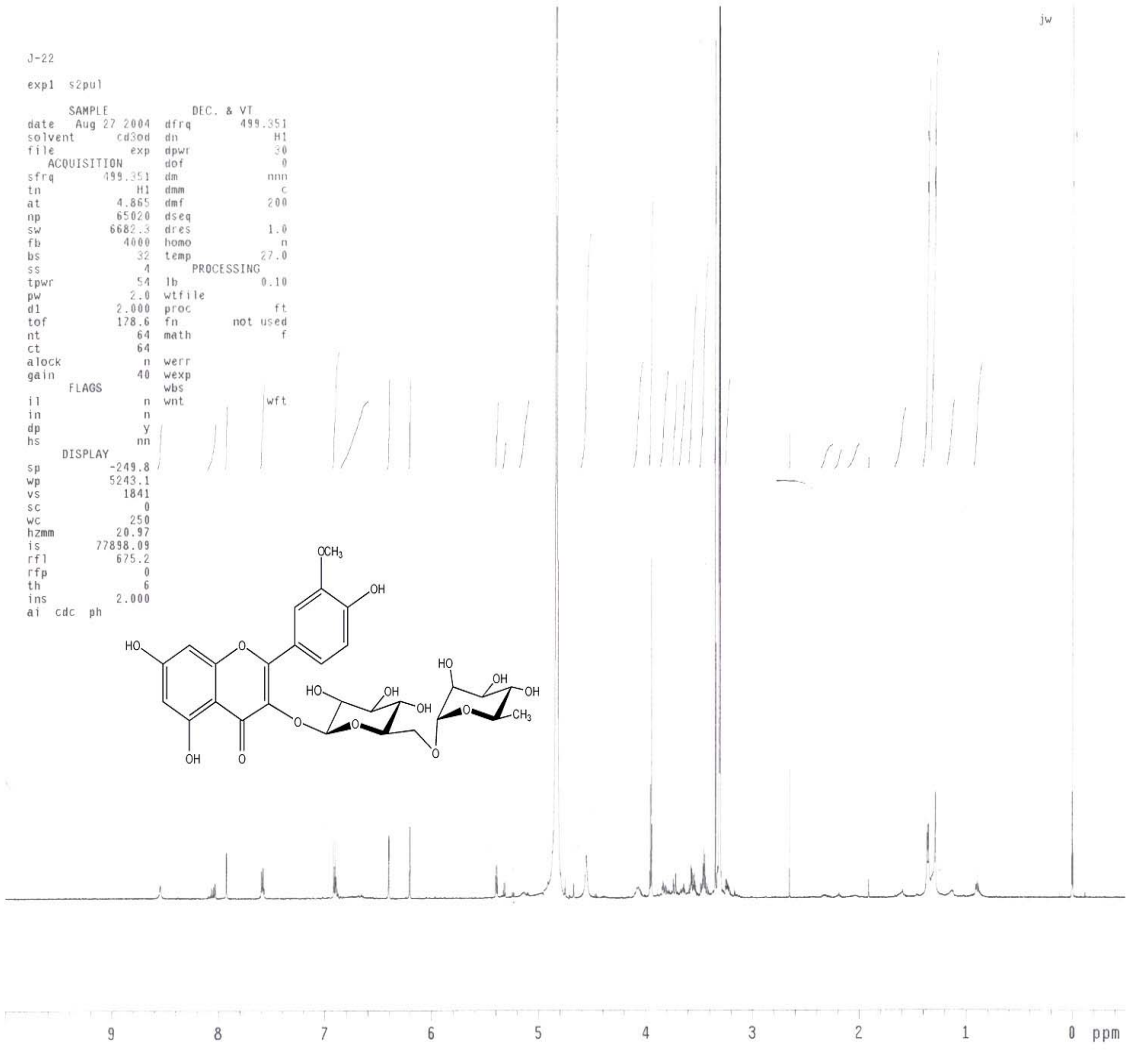

Figure 2.39: The ^{1}H NMR spectrum for isorhamnetin 3-*O*-*α*-L-rhamnosyl (1'''→6'')-*O*-*β*-D-galactopyranoside (**9**).

Chapter 3

Flavonoid Investigations of *Silphium* section *Silphium*

3.1 The flavonoid analysis of the seven species within *Silphium* section *Silphium*

In this section, the species *S. asteriscus*, *S. brachiatum*, and *S. integrifolium* all showed greater numbers of spots located in the center of the paper, indicative of a large number of disaccharide compounds (Figure 3.1). The regions circled in black represent the species *S. asteriscus*. These larger spots may again correlate with the greater milligram amounts of flavonoid compounds present in this species. Also notable from this chromatograph are the smaller blue regions representing the species *S. brachiatum*. The size of these spots directly correlated with the limitations experienced in extracting enough flavonoid compounds in order to run adequate NMR spectrum- although LC/MS analysis was performed.

The final chromatogram trends observed from section *Silphium* were the long traveled, closely grouped regions and/or R_f values for the four species *S. mohrii*, *S. perfoliatum*, *S. radula* and *S. wasiotense* (Figure 3.2). The species *S. wasiotense* showed the greatest number of spots wrapped around the right perimeter of the paper (violet). If one looks closely, there is considerable overlap occurring between the orange (*S. perfoliatum*) and the violet (*S. wasiotense*) colored regions. Also evident were the spots from the species *S. radula* (red) appearing in the same regions as the two species above. Although compound **5A** was not detected in *S. radula*, several known flavonoids from the species *S. perfoliatum* and *S. wasiotense* where shared by this species.

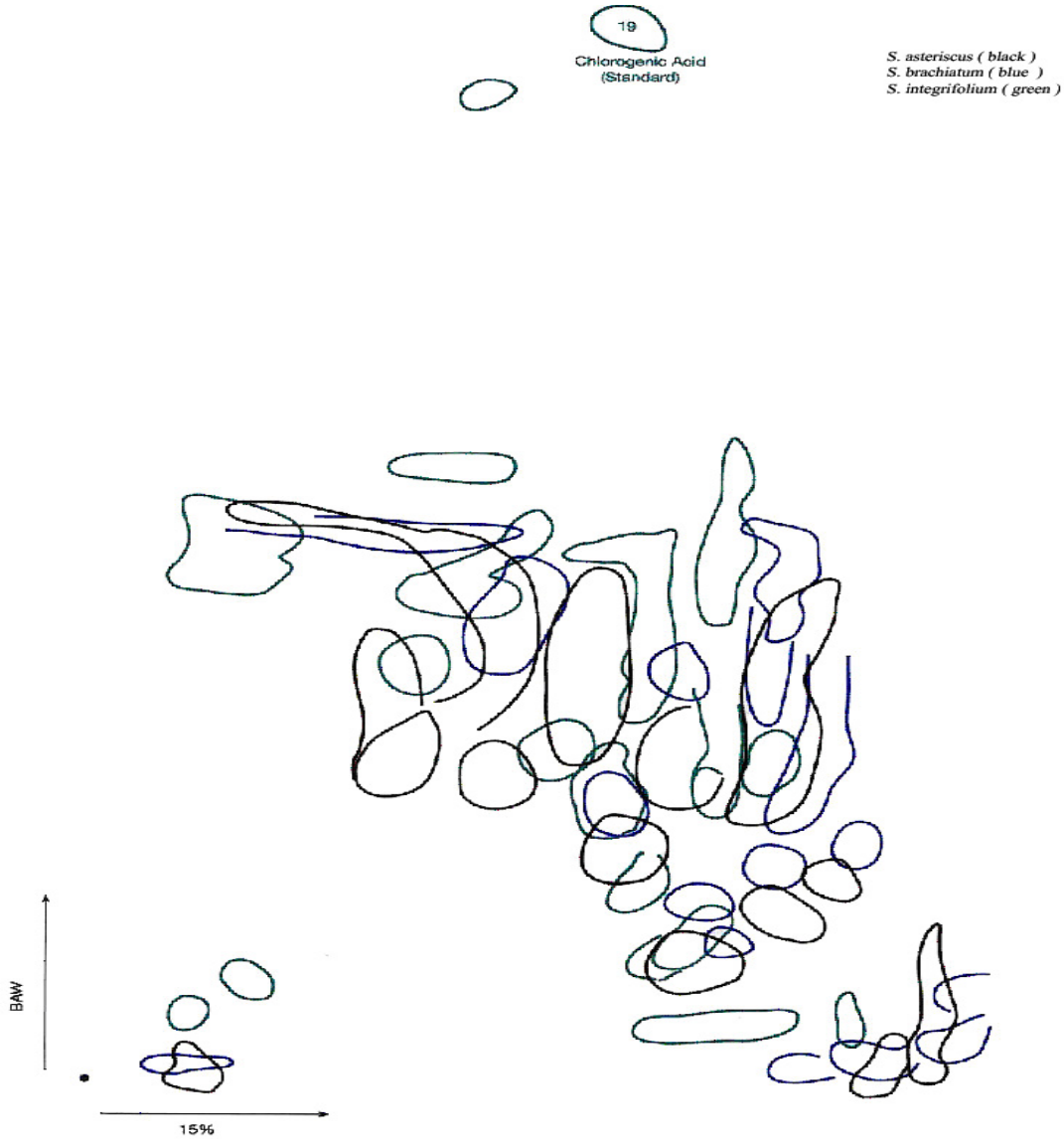

Figure 3.1: The systematic TLC flavonoid/phenolic distributions for the species *S. albiflorum* and its sister species *S. laciniatum* section *Composita.*

3.2 Introduction to the Flavonoid Chemistry of *Silphium* section *Silphium*:

Silphium asteriscus contained thirteen compounds, the highest number of flavonoids in the genus. A second quercetin triglycoside **3A** in addition to the compounds **1A** and **2A** was isolated containing the suspected reverse attachment of the sugars rhamnose and galactose.

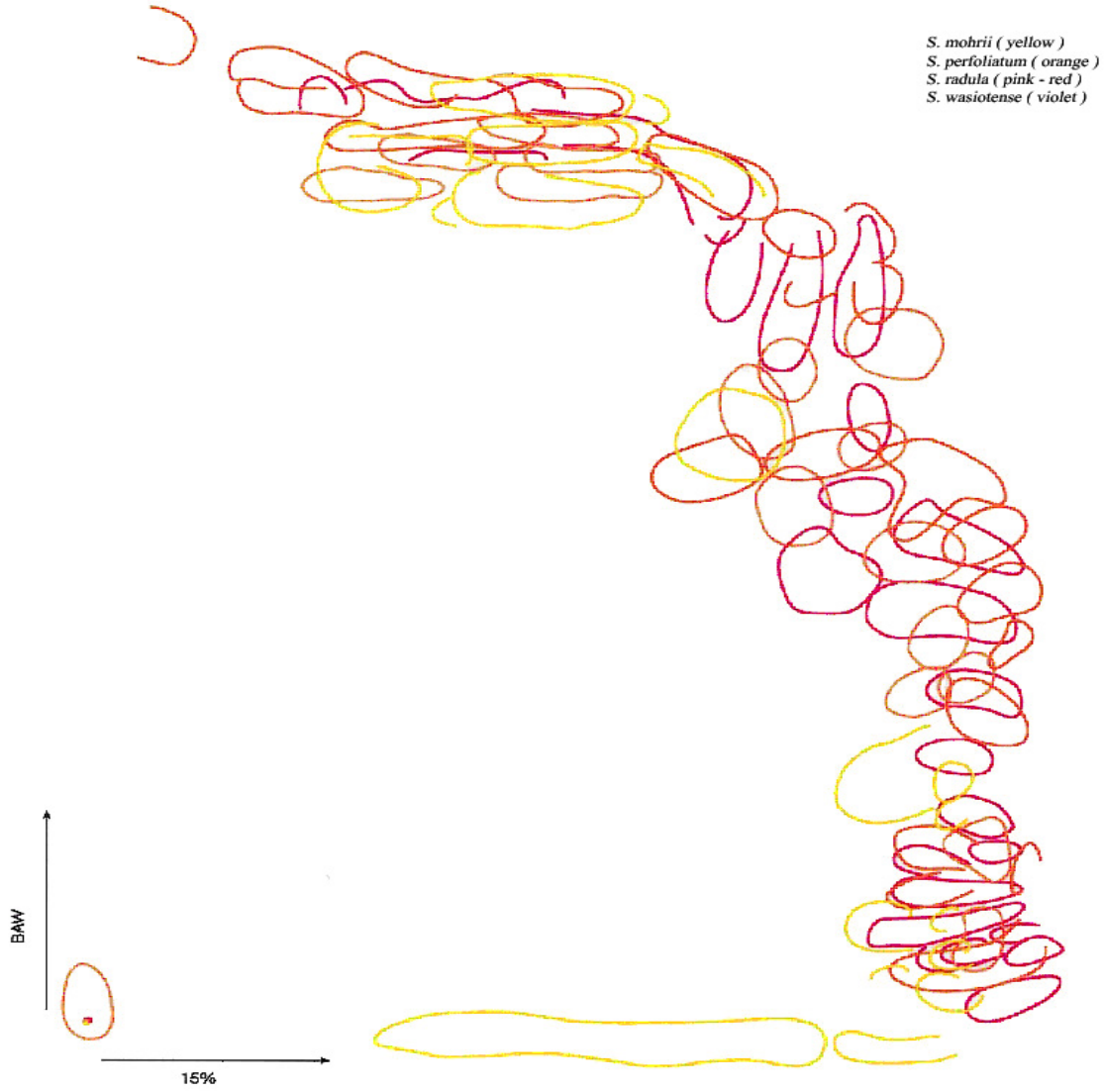

Figure 3.2: The "long-distance" two dimensional flavonoid migrations observed for four of the section *Silphium* species: *S. mohrii, S. perfoliatum*, *S. radula*, and *S. wasiotense*.

Of all eleven species, LC/MS detection of this compound was specific to this species appearing at a later retention time of 23.0 minutes. Five additional known quercetin flavonoids were also detected, again more than any other species. *Silphium asteriscus* shared the isorhamnetin triglycoside isorhamnetin 3-*O*-α-L-rhamnosyl (1'''→6")-*O*-*β*-D-galactopyranoside 7-*O*-*β*-L-apiofuranoside **(1A)** with the species *S. brachiatum*, *S.*

integrifolium, *S. mohrii* and *S. wasiotense*. It also exclusively shared the isorhamnetin monoside isorhamnetin 3-*O*-*β*-D-glucopyranoside with *S. brachiatum*. In addition to the isorhamnetin compounds above, *S. asteriscus* shared the new quercetin triglycoside quercetin 3-*O*-*α*-L-rhamnosyl (1'''→6'') –*O*-*β*-D- galactopyranoside-7-*O*-*β*-L-apiofuranoside **(2A)**, with the species *S. integifolium*, *S. mohrii* and *S. radula*.

Silphium brachiatum, containing the least number of flavonoids with four, contained the kaempferol triglycoside kaempferol 3-*O*-*β*-D-apiofuranoside 7-*O*-α-L-rhamnosyl (1''''→6''')-*O*-*β*-D-galactopyranoside **(4A)** with the species *S. mohrii*, *S. perfoliatum* and *S. radula*. *Silphium terebinthinaceum* in section *Composita* may also contain this compound (Figure 2.34). *Silphium integrifolium*, *S. perfoliatum* and *S. mohrii* contained the highest number of kaempferol mono and triglycoside flavonols in the genus.

Silphium perfoliatum and *S. wasiotense* exclusively shared the kaempferol caffeic acid linked triglycoside kaempferol 3-*O*-*β*-D-apiofuranoside 7-*O*-*α*-L-rhamnosyl-(1''''→6''')-*O*-*β*-D (2'''-*O*-*E*-caffeoylgalactopyranoside) **(5A)**. Both species also shared the quercetin monosides quercetin 3-*O*-*β*-D-galactopyranoside and quercetin 3-*O*-*β*-D-glucopyranoside. *Silphium wasiotense* contained the additional quercetin diglycosides quercetin 3-*O*-*β*-D-robinobioside and quercetin 3-*O*-*β*-D-rutinoside. Kaempferol 3-*O*-*β*-D-rutinoside at the retention times 25.1 min and 25.3 min were also present in both species (Figures 3.33 and 3.60)

3.3 *Silphium asteriscus* L. (Fig. 3.3), commonly known as Starry rosinweed, is reported here as the first species included in *Silphium* section *Silphium*. *S. asteriscus* characteristically grows in rocky open woodlands and is found along regions of the Southern Gulf Coast. This species is the fourth of the six Texas *Silphium* natives with *S. asteriscus* var. *asperrimum* found among plants of the central Texas Hill Country. Mature lower stem leaves are approximately 15 centimeters long tapering at the base. *S. asteriscus* produces eight to ten smaller yellow inflorescences from the months of May through September (Clevinger, 1999).

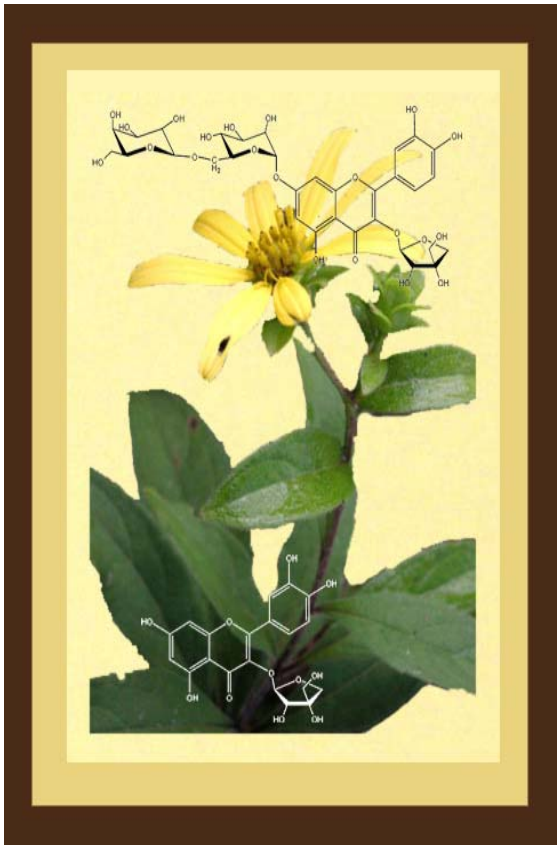

Figure 3.3: The superimposed plant and quercetin structures for the species *Silphium asteriscus*.

Of the eleven species included in the genus *Silphium*, the taxonomy of *S. asteriscus* appears the most complex. There are seven varieties of this species based on basal rosettes, phyllaries and other differentiating characters (Clevinger, 2004). ITS/ETS DNA analysis loosely relates *S. asteriscus* to the species *S. brachiatum* and *S. mohrii* (Clevinger, 1999). The most widely distributed species, including the Texas variety *S. asteriscus* var. *asperrimum*, have been distinguished by the pubescences of their phyllaries (Clevinger, 1999).

Results and Discussion

The third newly isolated flavonoid quercetin 3-*O*-α-L-galactosyl (1'''→6'') -*O*-*β*-D-rhamnopyranoside 7-*O*-*β*-L-apiofuranoside **(3A)** was obtained from *S. asteriscus*. The difference between this compound and the quercetin triglycoside first isolated from *S. albiflorum* is the reversal of the 3 position sugars rhamnose and galactose.

S. asteriscus contained more compounds than any other species in the genus. Thirteen known flavonoids were detected using comparative LC/MS and ^{1}H NMR analysis. These compounds were: isorhamnetin 3-*O*-α-L-rhamnosyl (1'''→6'')-*O*-*β*-D-galactopyranoside 7-*O*-*β*-L-apiofuranoside **(1A)**, *m/z* 799 [M-22 Na^{+}-18 H_2O]$^{+}$, (21.3 min); quercetin 3-*O*-*α*-L-rhamnosyl (1'''→6'') –*O*-*β*-D- galactopyranoside 7-*O*-*β*-L-apiofuranoside **(2A)**, *m/z* 741.3 [M+H]$^{+}$**,** (21.3 min); quercetin 3-O-*α*-L-galactosyl (1'''→6'') –O-*β*-D-rhamnosyl 7-O-*β*-L-apiofuranoside **(3A)**, *m/z* 743.7 [M+H]$^{+}$, (23.0 min); quercetin 3-*O*-*β*-D-apioside **(4),** *m/z* 433 [M+H]$^{+}$**,** (14.2 min); quercetin 3-*O*-*β*-D-galactopyranoside **(5),** *m/z* 462.4 [M+H]$^{+}$, (18.1 min); quercetin 3-*O*-robinobioside **(6),** *m/z* 627.6 [M-O]$^{+}$, (25.9 min); quercetin 3-*O*-rutinoside **(7)**, *m/z* 611.4 [M+H]$^{+}$, with retention times (14.5 and 22.3 min); quercetin 3-*O*-*α*-D-rhamnosyl 7-*O*-*β*-L-apiofuranoside **(8)**, *m/z* 583.5 [M+H]$^{+}$, (25.9 min); isorhamnetin 3-*O*-*β*-D-galactopyranoside **(9)**, *m/z* 477 [M+H]$^{+}$, (17.1 min); isorhamnetin 3-*O*-*β*-D-glucopyranoside **(10)**, *m/z* 495 [M-18 H_2O]$^{+}$, (17.1 min); kaempferol 3-*O*-*β*-L-apiosyl-(1''''→6''')-*O*-*β*-D-glucopyranoside **(11)**, *m/z* 581.2 [M+H] $^{+}$, (15.3 min); kaempferol 3-*O*-robinobioside **(12)**, *m/z* 595.3 [M+H]$^{+}$, (18.1 min); kaempferol 3-*O*-rutinoside **(13)**, *m/z* 595.3 [M-H] $^{+}$, (19.3 min).

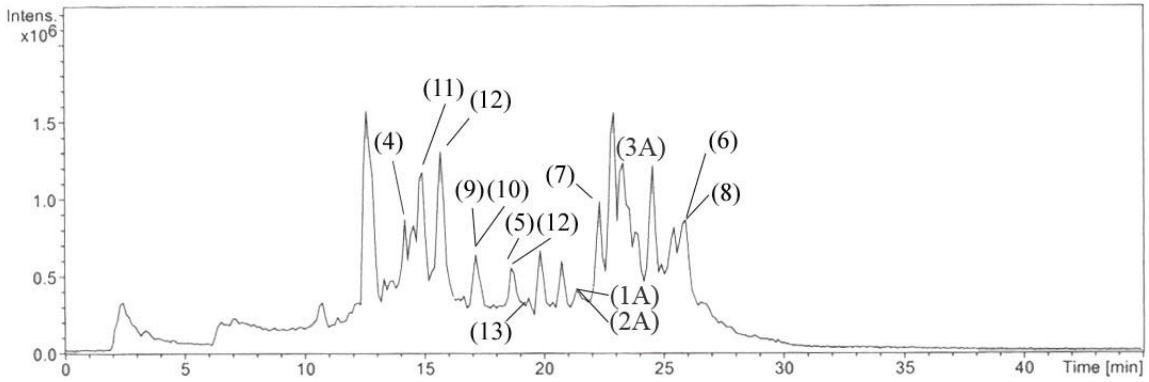

Figure 3.4: The flavonoid LC/MS *m/z* spectrum for the species *S. asteriscus*.

Three of the twelve known compounds from *S. asteriscus* along with the new quercetin triglycoside **(3A)** provided sufficient material for ^{1}H NMR, UV and LC/MS analysis.

The ^{1}H NMR analysis of the sample of quercetin 3-*O*-*α*-L-galactosyl (1'''→6'') -*O*-*β*-D-rhamnopyranoside-7-*O*-*β*-L-apiofuranoside **(3A)** (sample SA-186/5D2) detected the aglycone A ring signals 6 and 8 at δ 6.32 *d*, *J* = 2.12 Hz and 6.68 *d*, *J* = 1.83 Hz; the B ring 2' and 6' signals at δ 7.50 *d*, *J* = 2.4 Hz and 7.75 *dd*, *J* = 11.0 Hz, respectively, along with the 5' signal at ppm 6.45. The anomeric proton H-1'''' signal for apiose was located at δ 5.09 with both H-1'' (rhamnose) and H-1''' (galactose) appearing at 5.62 *d*, *J* = 3.53 Hz and 5.19 ppm (Figure 4.2).

The FAB/MS in positive mode provided an absorbance similar to that of compound **2A,** *m/z* 743 $[M+H]^{+}$ (Figure 4.3). The ^{13}C NMR, DEPT, HMBC, HMQC and ROESY analyses remain to be performed based on the limited quantity of the extract.

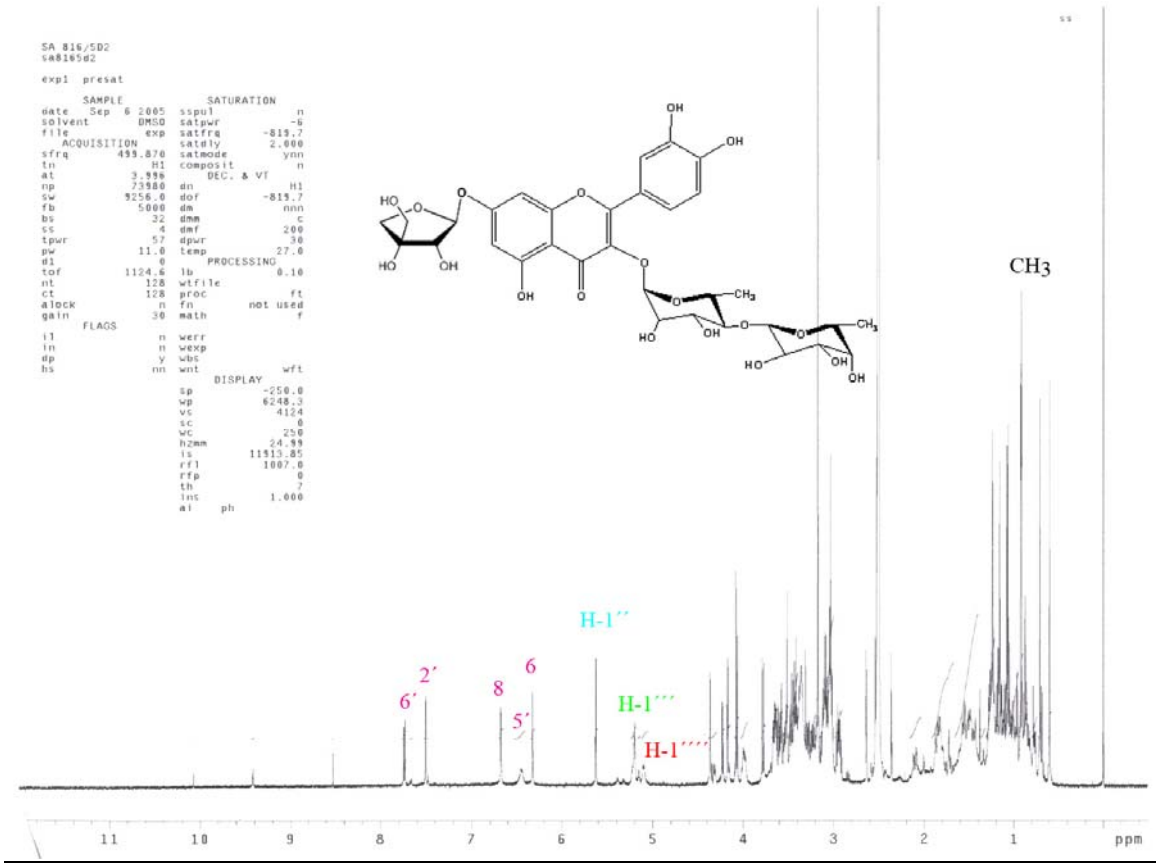

Figure 3.5: The ^{1}H NMR spectrum for the quercetin triglycoside (**3A**). The shift of the smaller peak at δ 5.09 to the left (positioned down field of the taller peak at δ 5.19) indicates the possible rearrangement of the two sugars rhamnose and galactose as compared with compound **2A (**El-Sayed, 2002).

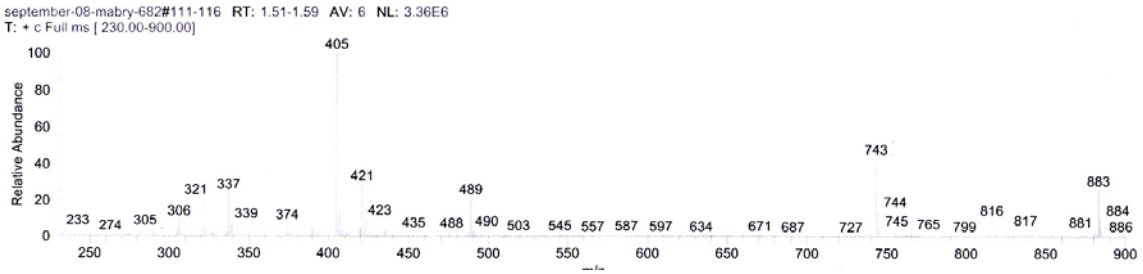

Figure 3.6: The FAB/MS for *m/z* 743 $[M+H]^{+}$, for quercetin 3-O-α-L-galactosyl (1‴→6″) -O-β-D-rhamnosyl 7-O-β-L-apiofuranoside **(3A)**.

The ^{1}H NMR spectrum for kaempferol 3-*O*-rutinoside **(13)** provided signals for H-6 and H-8 at δ 6.12 *d*, *J* = 1.92 Hz and 6.35 *d*, *J* = 1.80, respectively, and for H-2' and H-6' at δ 8.05 and 8.03 *d*, *J* = 2.04 Hz along with a doublet for H-5' at δ 6.84 *d*, *J* = 2.24 Hz, and a doublet for H-3' at δ 6.86 *d*, *J* = 2.04 Hz. The anomeric protons for the sugars glucose and rhamnose resonated at δ 5.28 *d*, *J* = 7.79 Hz and 4.40 *d*, *J* = 1.44 Hz. The methyl group of rhamnose appeared as a doublet at δ 1.06 *d*, *J* = 6.23 Hz.

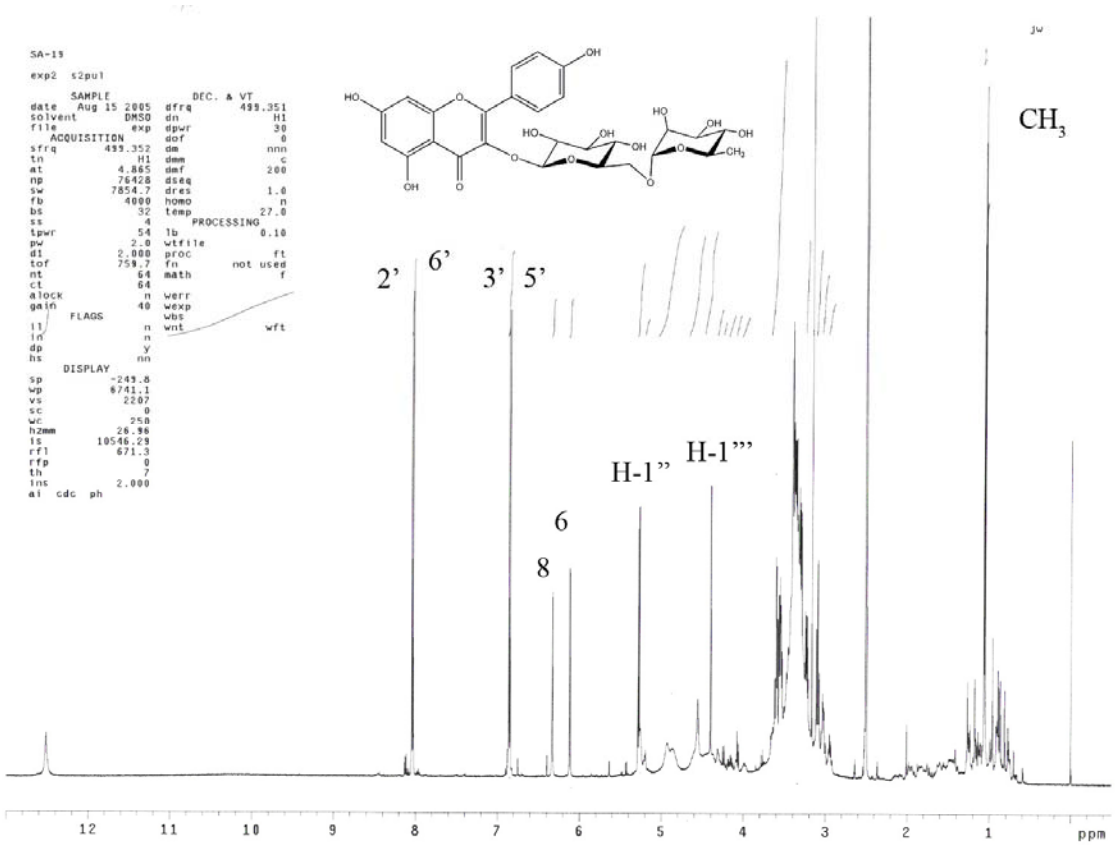

Figure 3.7: The ^{1}H NMR spectrum for the flavonol kaempferol 3-*O*-rutinoside **(13)**.

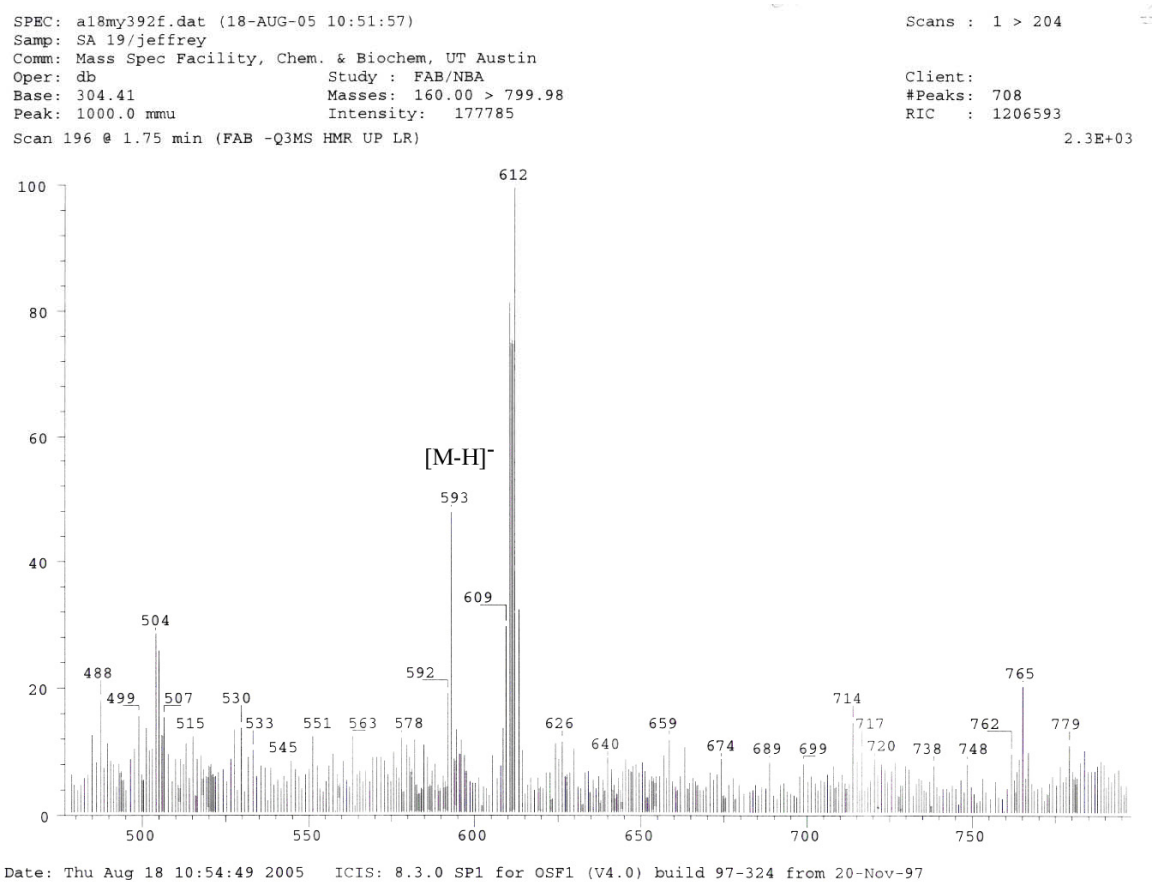

Figure 3.8: The FAB/MS in negative mode for kaempferol 3-*O*- rutinoside **(13),** *m/z* 593. The peak appearing at *m/z* 612 is one of several matrixes.

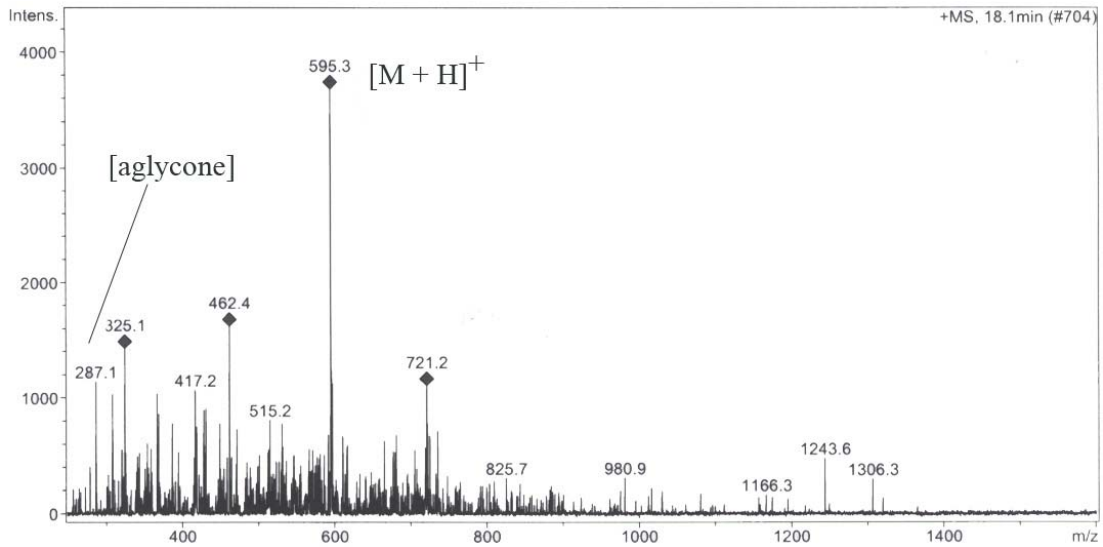

Figure 3.9: The independent LC/+MS detection of kaempferol 3-*O*- rutinoside **(13)** at a retention time of 18.1 minutes.

The ^{1}H NMR spectra for quercetin 3-*O*-*α*-L-rhamnosyl 7-*O*-*β*-L-apiofuranoside **(8)** provided for the flavonol A ring signals H-6 and H-8 at δ 6.36 and 6.68, respectively. The B ring 2' and 6' signals appear at δ 7.57 and 7.71 *d*, *J* = 9.1 Hz along with the proton 5' doublet at 6.72 ppm. The anomeric protons for the sugars apiose and rhamnose appeared at δ 5.63 *d*, *J* = 3.55 Hz and a singlet at 5.19 ppm. The methyl group from rhamnose appears as a singlet at ppm 1.15.

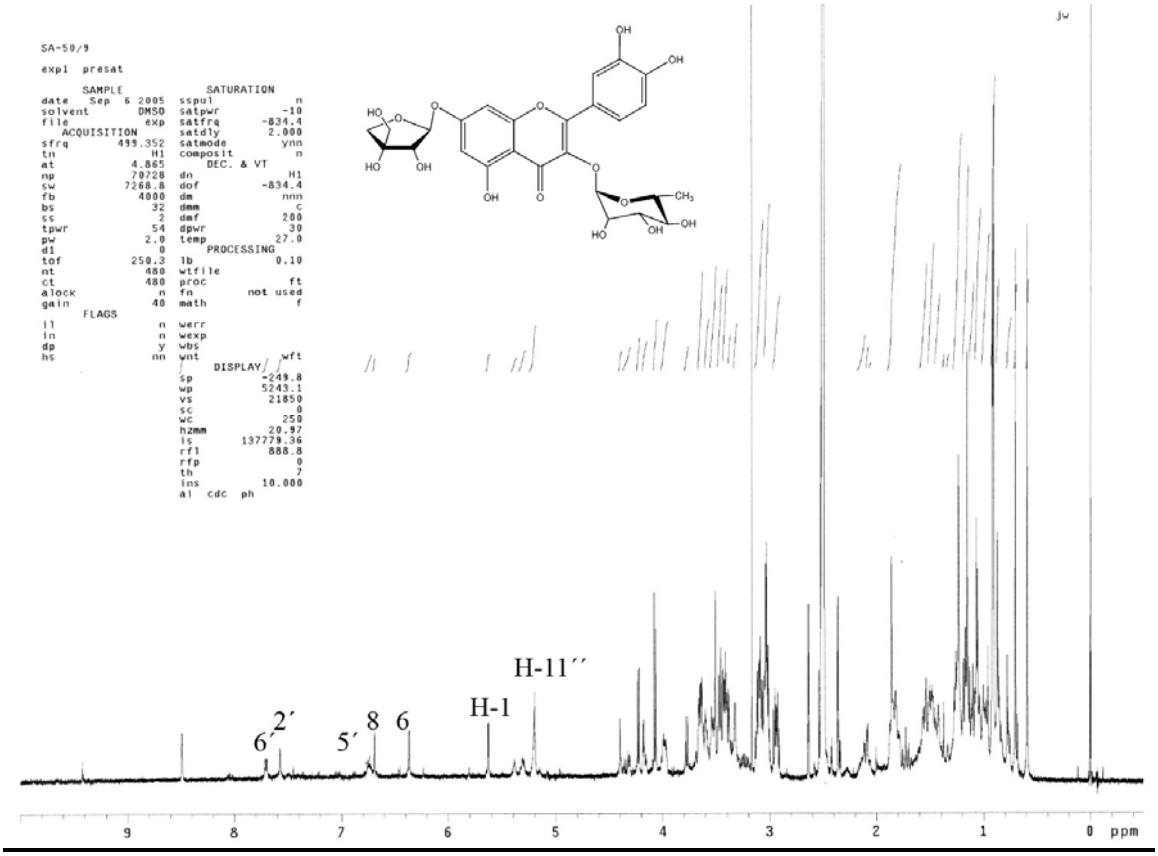

Figure 3.10: The ^{1}H NMR spectrum for quercetin 3-*O*-*α*-D-rhamnosyl 7-*O*-*β*-L-apiofuranoside **(8)**.

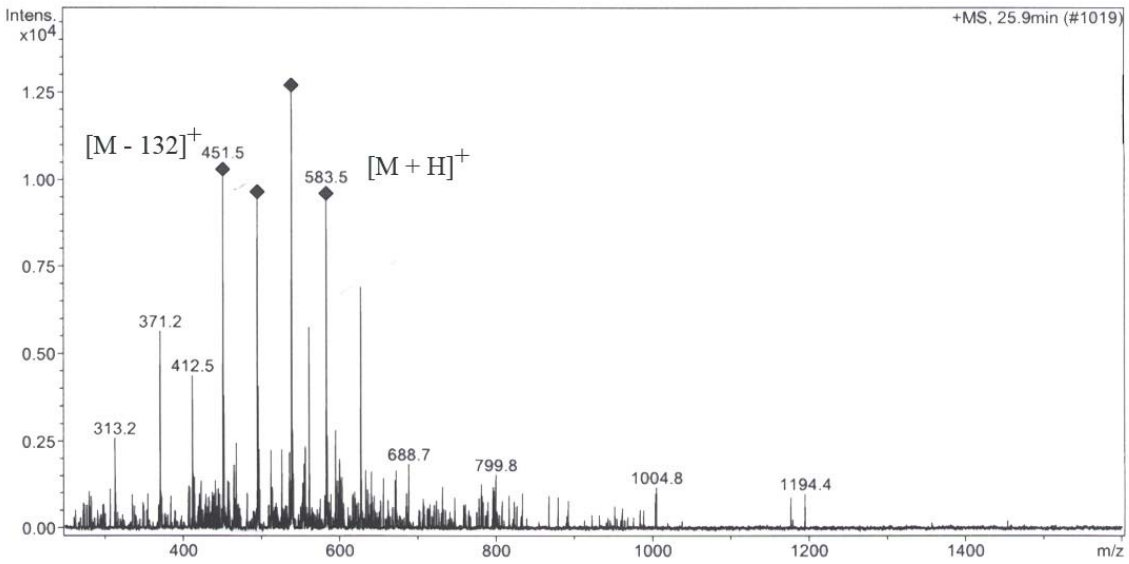

Figure 3.11: The LC/+MS for quercetin 3-*O*-*α*-D-rhamnosyl 7-*O*-*β*-L-apiofuranoside **(8)**.

The ^{1}H NMR for quercetin 3-*O*-apioside **(1)** provided the flavonol A ring signals 6 and 8 at δ 5.91 and 6.10, respectively. The H- 2' and H-6' signals appeared at δ 7.47 and 7.58 *d*, J = 2.27 Hz, respectively, along with a doublet for H-5' at δ 6.75 *d*, J = 8.45 Hz.

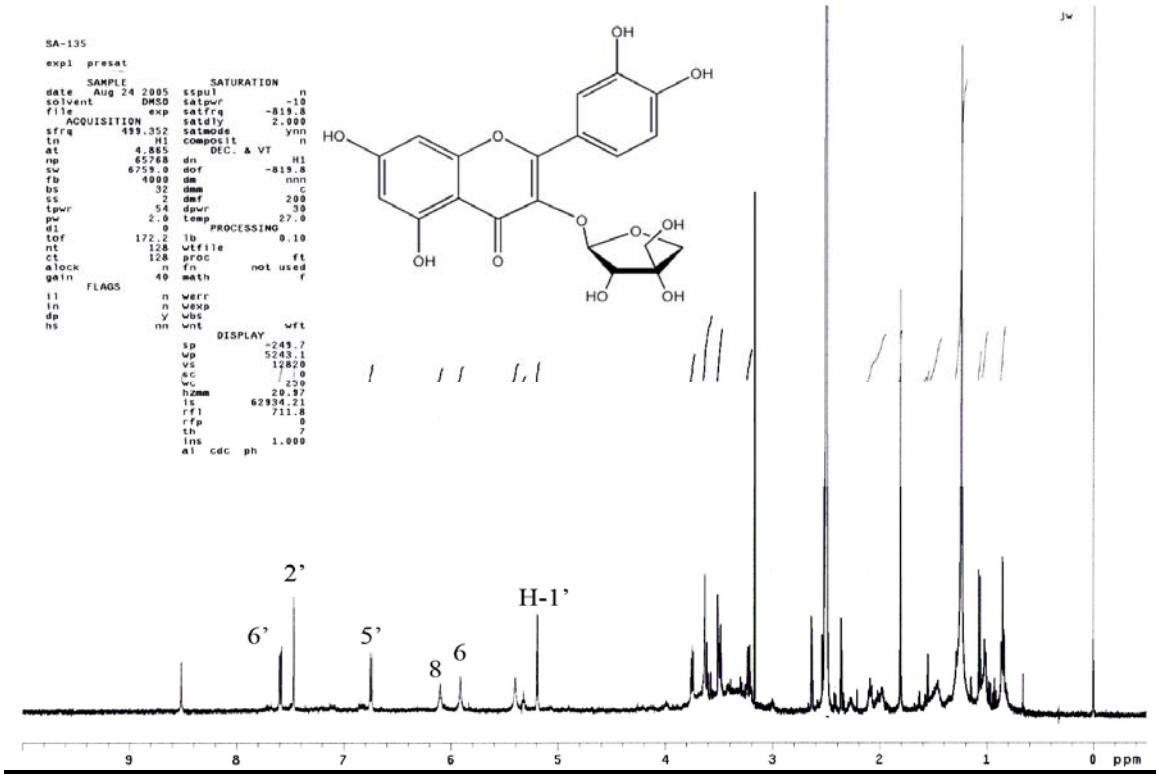

Figure 3.12: The ^{1}H NMR spectrum for quercetin 3-*O*-*α*-D-apioside **(4)**.

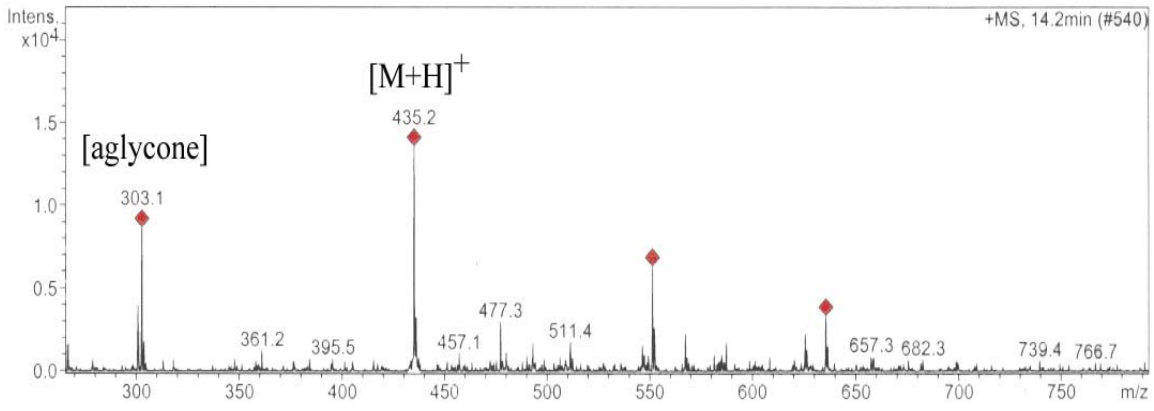

Figure 3.13: The LC/+MS provided for both the complete compound at *m/z* 435.2 $[M+H]^{+}$ and the aglycone **(4)** at *m/z* 303.1 (14.2 min).

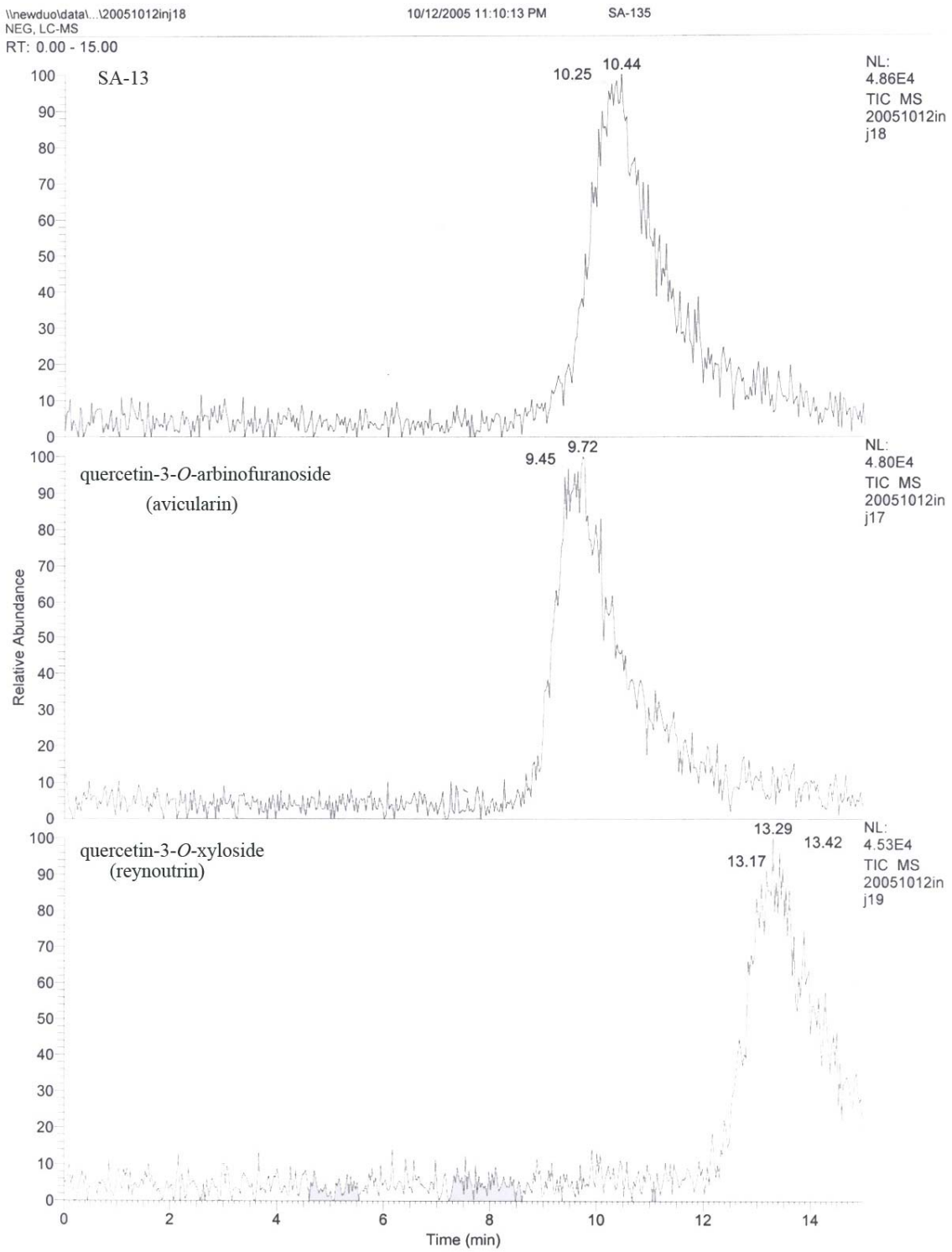

Figure 3.14: Additional LC/MC analysis of quercetin 3-*O*-*α*-D-apioside **(4)**. The compound was run against the standards avicularin and reynoutrin. While this analysis does not confirm the presence of apiose alone, it does support the lack of other similarly sized glycosides.

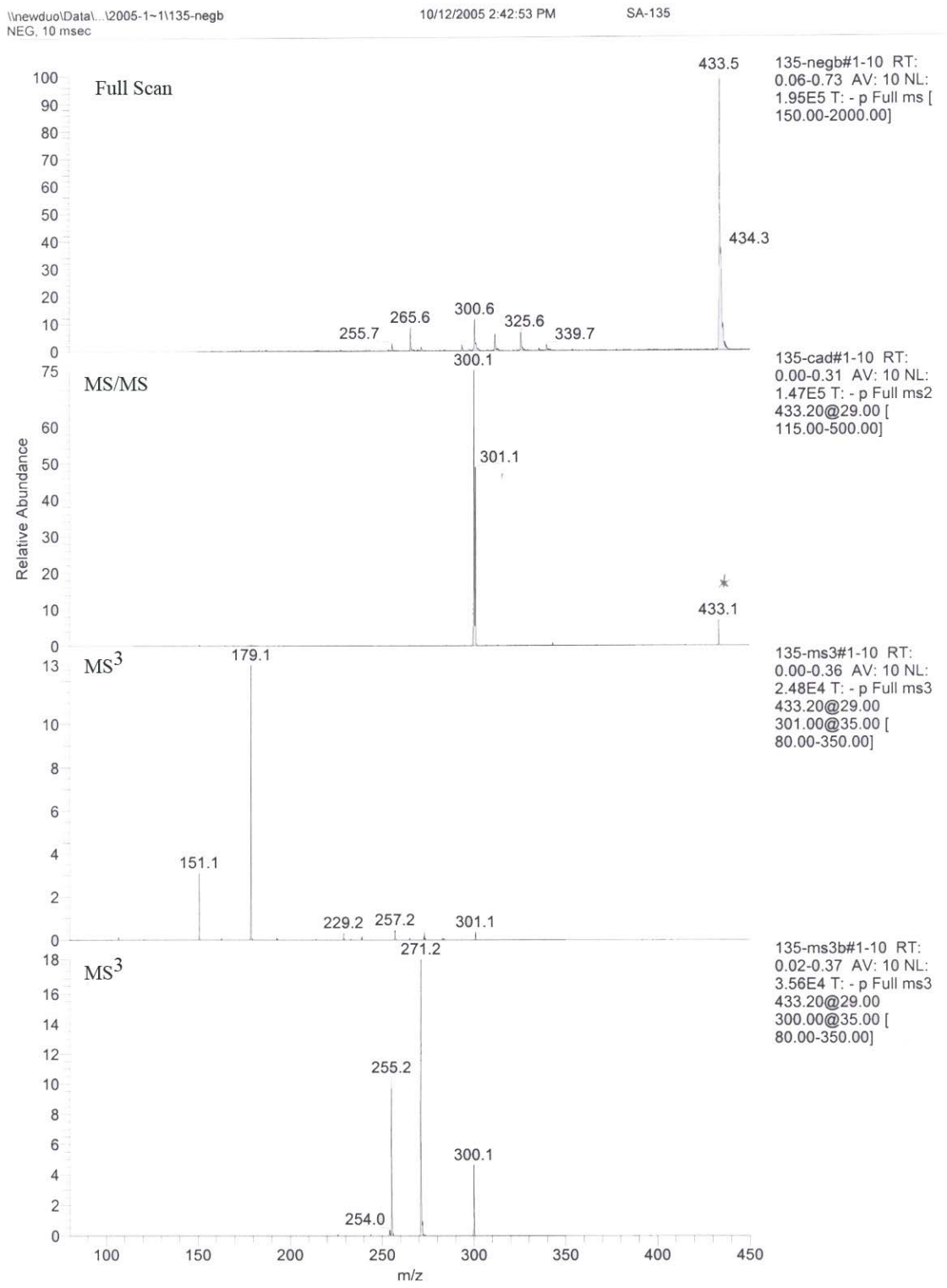

Figure 3.15: The MS/MS provided for quercetin 3-*O*-*α*-D-apioside **(4)** *m/z* 435.2 $[M-H]^-$ and the aglycone at *m/z* 300.1, in negative mode.

3.4 *Silphium brachiatum* (Fig 3.16), commonly known as Cumberland rosinweed, is found along road cuts, open forests, and rural fence lines (Clevinger 1999). This species is most prevalent in the lower Appalachian mountain regions of Alabama and Tennessee. Thus far to date, no chemical analyses on this species can be found in the literature. DNA molecular studies performed by Dr. Clevinger indicate a more distant relationship shared between this species and of *S. asteriscus* and *S. mohrii*

(Clevinger, 1999).

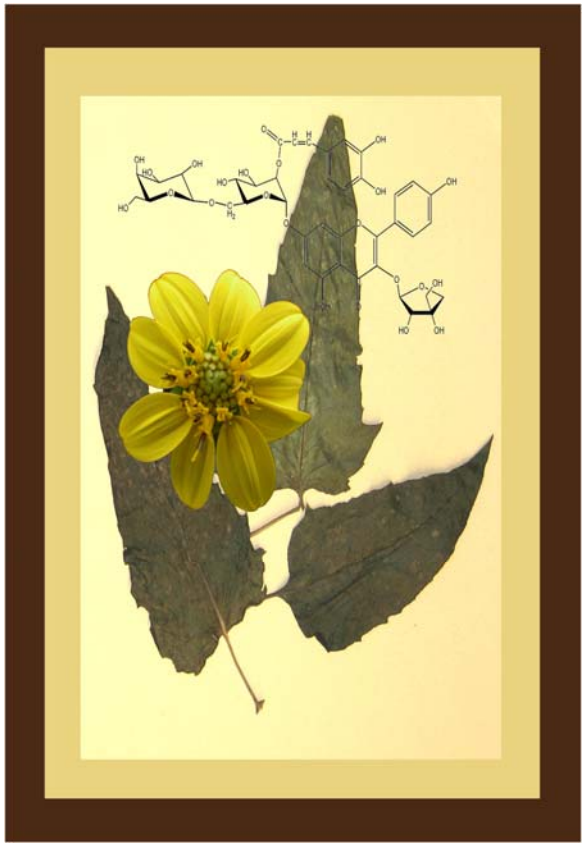

Figure 3.16: *Silphium brachiatum* dried leaves with superimposed flower (Clevinger, 1999).

Results and Discussion

Initial column chromatography of *S. brachiatum* revealed a highly polar, dark brown substance which crystallized upon drying and ^{1}H NMR analysis resulted in an inconclusive identification. Of the eleven species in the genus, this species produced the fewest flavonoids with a total number of four. Of these four compounds, two matched in masses and retention times with those of the new compounds isorhamnetin 3-*O*-α-L-rhamnosyl (1'''→6")-*O*-*β*-D-galactopyranoside 7-*O*-*β*-L-apiofuranoside **(1A)** and

kaempferol 3-*O*-*β*-D-apiofuranoside 7-*O*-α-L-rhamnosyl (1''''→6''')-*O*-*β*-D-galactopyranoside **(4A)**.

The LC/MS analysis of the four flavonoids resulted in the following compounds: isorhamnetin 3-*O*-α-L-rhamnosyl (1'''→6'')-*O*-*β*-D-galactopyranoside 7-*O*-*β*-L-apiofuranoside **(1A)**, *m/z* 757.4 $[M+H]^+$, (23.4 min); isorhamnetin 3-*O*-*β*-D-glucopyranoside **(2)**, *m/z* 517.4 $[M\text{-}22\ Na^+\text{-}18\ H_2O]^+$, (21.8 min); quercetin 3-*O*-*β*-D-galactopyranoside **(3)**, *m/z* 503.4 $[M\text{-}22\ Na^+\text{-}18\ H_2O]^+$, (18.1 min) and kaempferol 3-*O*-*β*-D-apiofuranoside 7-*O*-α-L-rhamnosyl (1'''→6''')-*O*-*β*-D-galactopyranoside **(4A)**, *m/z* 727.3 $[M+H]^+$, (20.7 min).

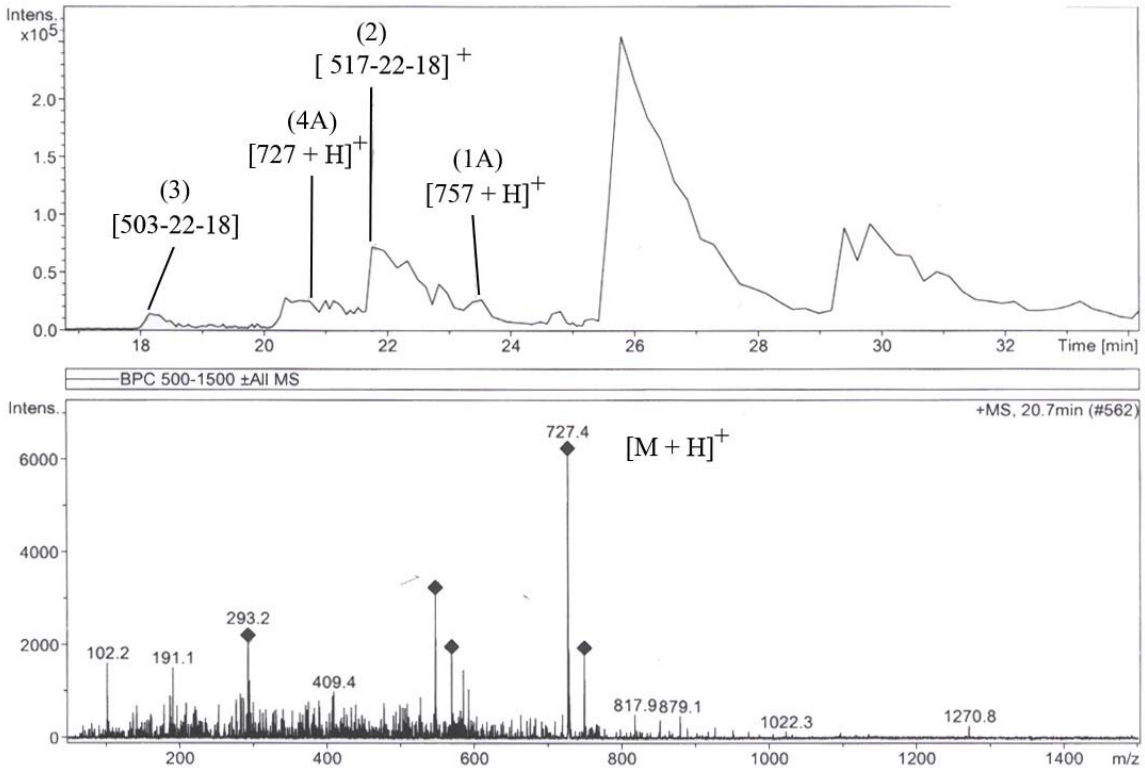

Figure 3.17: The LC/MS analysis of the species *S. brachiatum*, showing the isolated compounds isorhamnetin 3-*O*-α-L-rhamnosyl (1''''→6'')-*O*-*β*-D-galactopyranoside 7-*O*-*β*-L-apiofuranoside **(1A)** and **(4A)** along with the MS/MS of the compound kaempferol 3-*O*-*β*-D-apiofuranoside 7-*O*-α-L-rhamnosyl (1''''→6''')-*O*-*β*-D-galactopyranoside **(4A)**.

While this species was found to contain few flavonoids, three of the four compounds were similar to those detected in the species *S. asteriscus* and *S. mohrii***.**

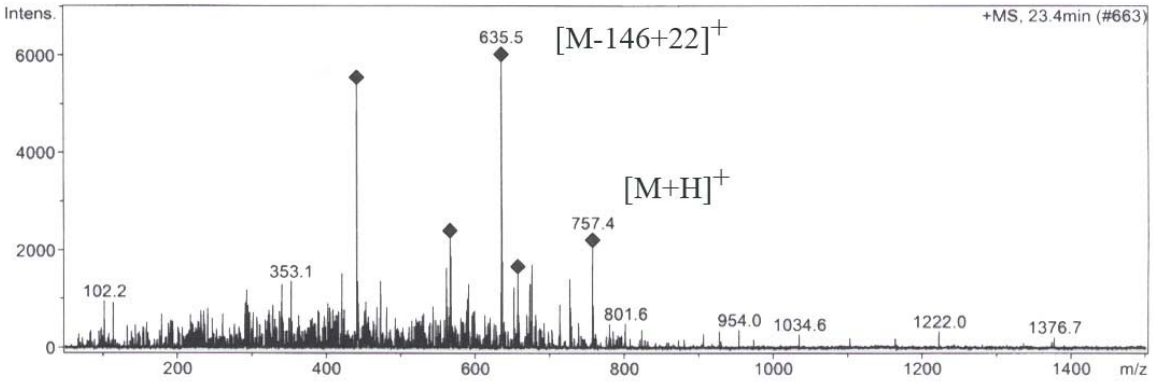

Figure 3.18: The LC/+MS analysis of isorhamnetin 3-*O*-α-L-rhamnosyl (1'''→6'')-*O*-*β*-D-galactopyranoside 7-*O*-*β*-L-apiofuranoside **(1A)**.

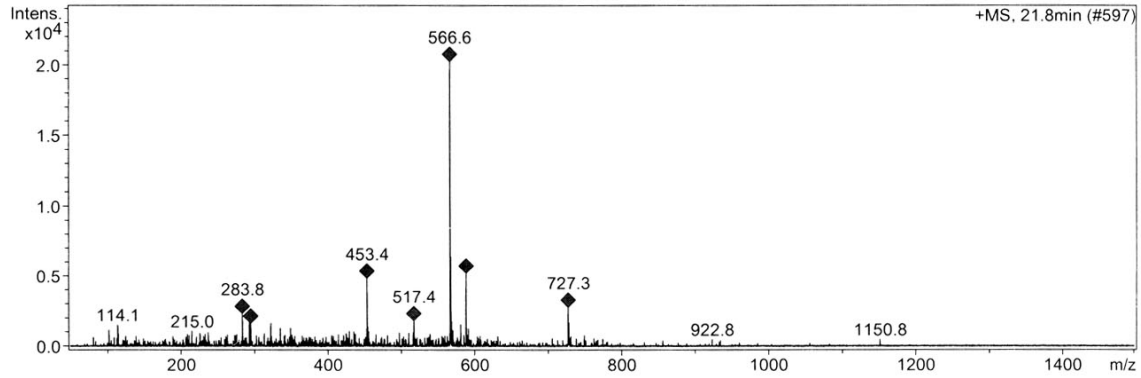

Figure 3.19: The LC/+MS spectrum of isorhamnetin 3-*O*-*β*-D-glucopyranoside **(2)**.

3.5 *Silphium integrifolium* (Fig. 3.20) is commonly known as Entire-leaved or Prairie rosinweed. This species is distributed among undisturbed open prairies and along rail right-of-ways. Molecularly, *S. integrifolium* is closely related to the species *S. perfoliatum* and *S. wasiotense* (Clevinger, 1999). Although it is found to hybridize with *S. asteriscus*, it is recognized as a distinct and separate species (Clevinger, 1999). Hybridization may be due to human interactions bringing both species in close contact.

Figure 3.20: *Silphium integrifolium* photographed with superimposed quercetin structure and flowers.

Results and Discussion

Many secondary metabolites, including essential oils, flavonoids, oleanosides, and sesquiterpenes, have been reported from *Silphium integrifolium* Michx. (Swanson *et al*., 1979). The leaves of this species contain high levels of essential oils (Kowalaski, 2004), which are currently being investigated as another source of natural rubber along with a hemaglutinating lectin that can be readily neutralized using N-acetyl-galactosamine (Hardman *et al.*, 1983).

The LC/MS+ analysis of the extracts of *S. integrifolium* show the presence of the following flavonoids: isorhamnetin 3-*O*-α-L-rhamnosyl (1'''→6'')-*O*-*β*-D-

galactopyranoside 7-*O*-*β*-L-apiofuranoside **(1A)**, *m/z* 757.4 $[M+H]^+$, (22.5 min); quercetin 3-*O*-*α*-L-rhamnosyl (1'''→6'')–*O*-*β*-D-galactopyranoside 7-*O*-*β*-L-apiofuranoside **(2A)**, *m/z* 743.4 $[M+H]^+$, (14.7 min); quercetin 3-*O*-*β*-D-galactopyranoside **(3)**, *m/z* 465.1 $[M+H]^+$, (18.8 min); kaempferol-3-*O*-*β*-D-apiofuranoside 7-*O*-α-L-rhamnosyl (1''''→6''')-*O*-*β*-galactopyranoside **(4A)**, *m/z* 727.3 $[M+H]^+$, (15.4 min); quercetin 3-*O*-rutinoside **(5)**, *m/z* 611.2 $[M+H]^+$**,** (14.7 min); quercetin 3-*O*-robinobioside **(6)**, *m/z* 611.2 $[M+H]^+$, (26.5 min); kaempferol 3-*O*-*β*-D-galactopyranoside **(7)**, *m/z* 449.2 $[M+H]^+$, (19.2 min); kaempferol 3-*O*-*β*-D-glucopyranoside **(8)**, *m/z* 449.2 $[M+H]^+$, (26.5 min); kaempferol 3-*O*-robinobioside **(9)**, *m/z* 595.4 $[M+H]^+$, (20.6 min); kaempferol 3-*O*-rutinoside **(10)**, *m/z* 595.2 $[M+H]^+$, (23.3 min).

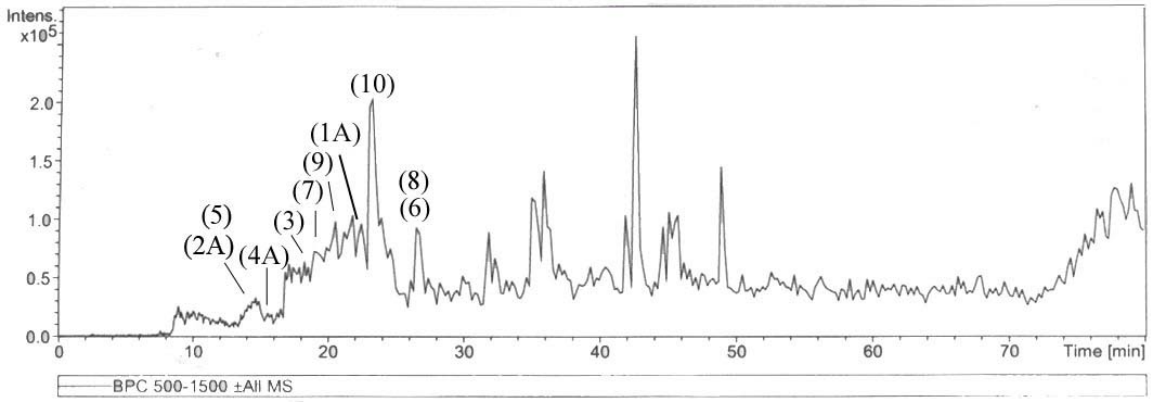

Figure 3.21: The LC/+MS spectrum for *S. integrifolium*.

The flavonoid chemistry for this species also includes the isolated compounds isorhamnetin 3-*O*-α-L-rhamnosyl (1'''→6'')-*O*-*β*-D-galactopyranoside 7-*O*-*β*-L-apiofuranoside **(1A)** and kaempferol-3-*O*-*β*-D-apiofuranoside 7-*O*-α-L-rhamnosyl (1''''→6''')-*O*-*β*-galactopyranoside **(4A)**.

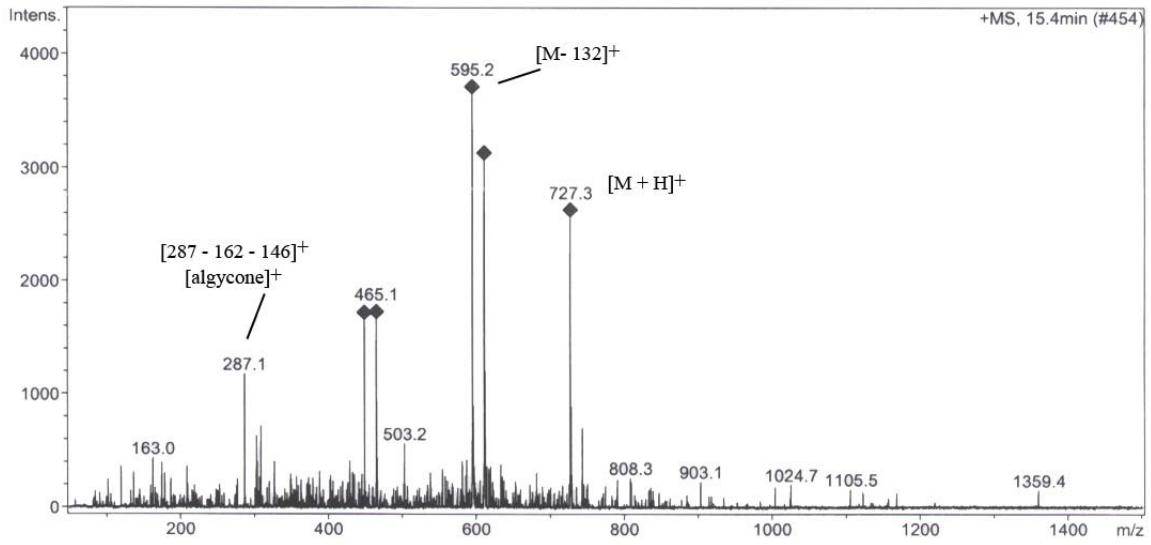

Figure 3.22: The LC/+MS analysis for kaempferol-3-*O*-*β*-D-apiofuranoside 7-*O*-α-L-rhamnosyl (1""→6")-*O*-*β*-galactopyranoside **(4A)**, *m/z* 727.3 $[M+H]^+$, (15.4 min).

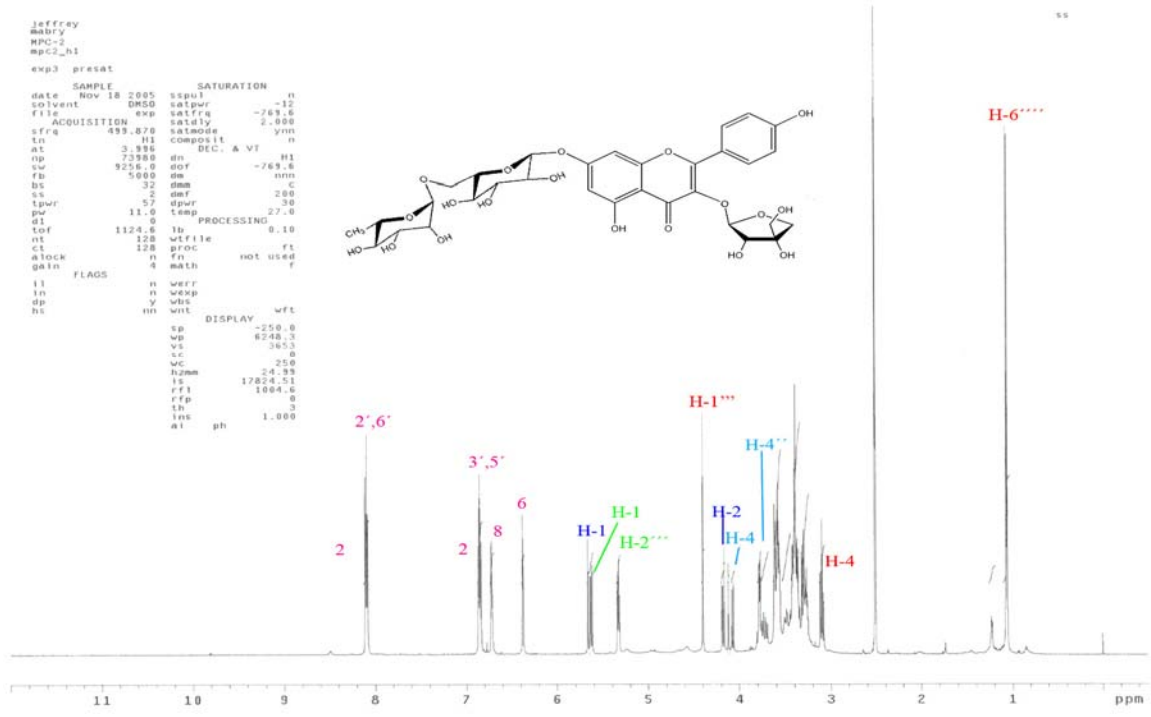

Figure 3.23: The ^{1}H NMR spectrum of kaempferol-3-*O*-*β*-D-apiofuranoside 7-*O*-α-L-rhamnosyl (1""→6")-*O*-*β*-galactopyranoside **(4A)**.

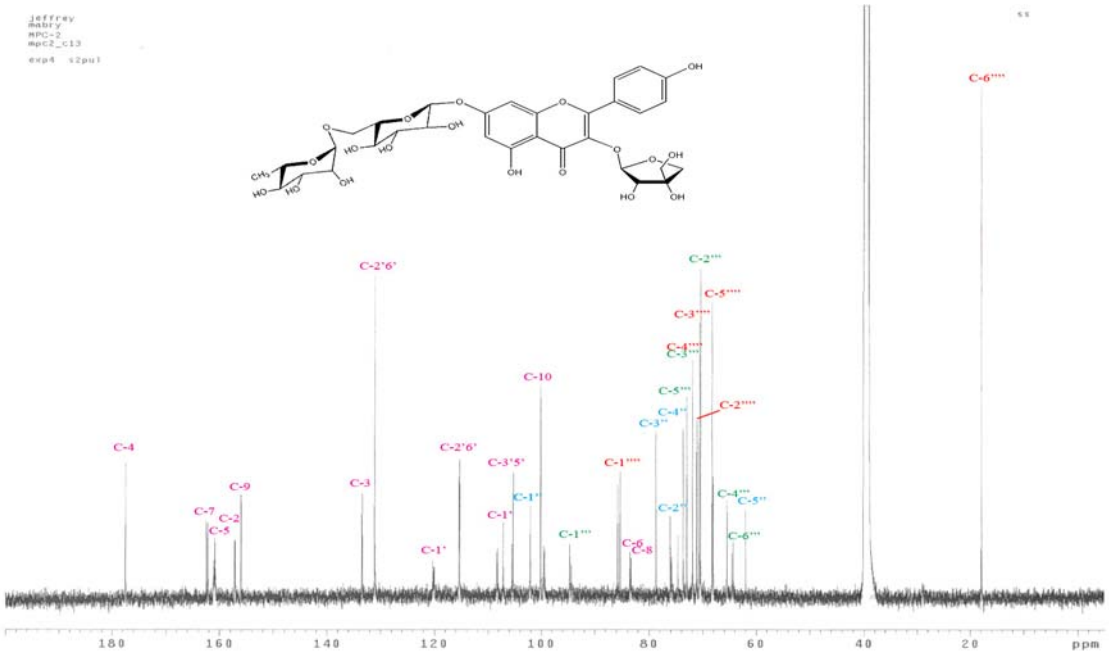

Figure 3.24: The ^{13}C NMR assignments for kaempferol-3-*O*-*β*-D-apiofuranoside 7-*O*-α-L-rhamnosyl (1''''→6''')-*O*-*β*-galactopyranoside **(4A)**.

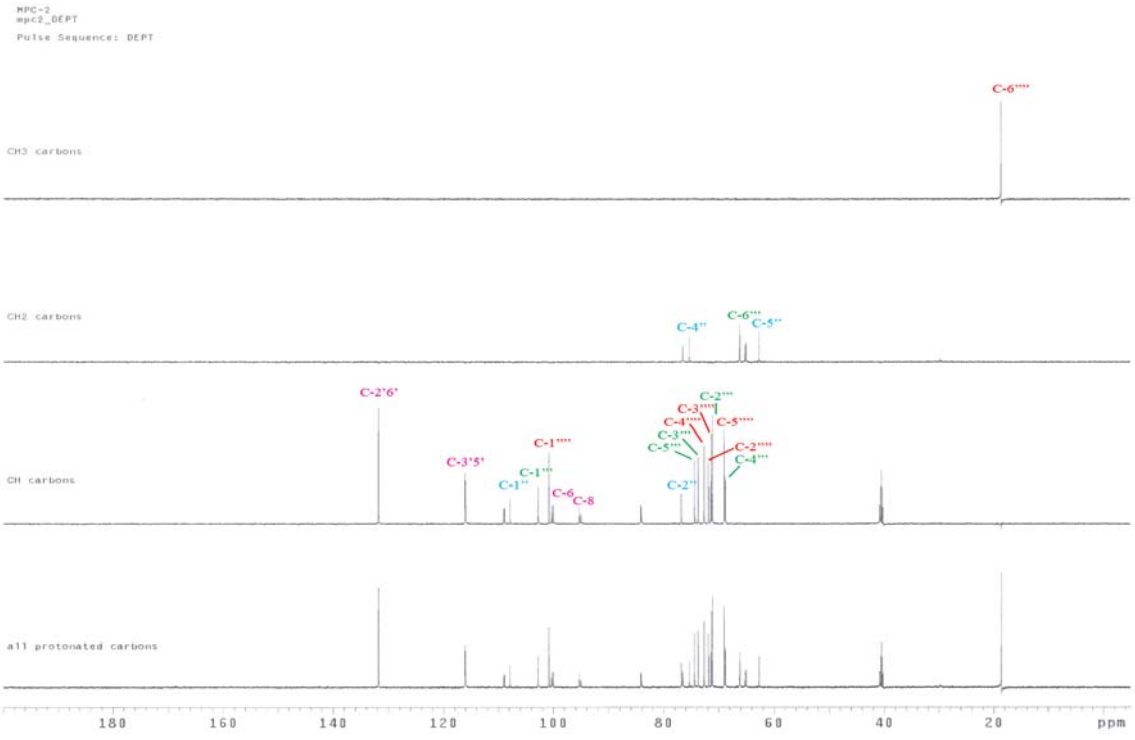

Figure 3.25: The DEPT analysis showing the three methylene, single methyl group, twenty-three methine and fourteen quaternary carbon moieties for **4A**.

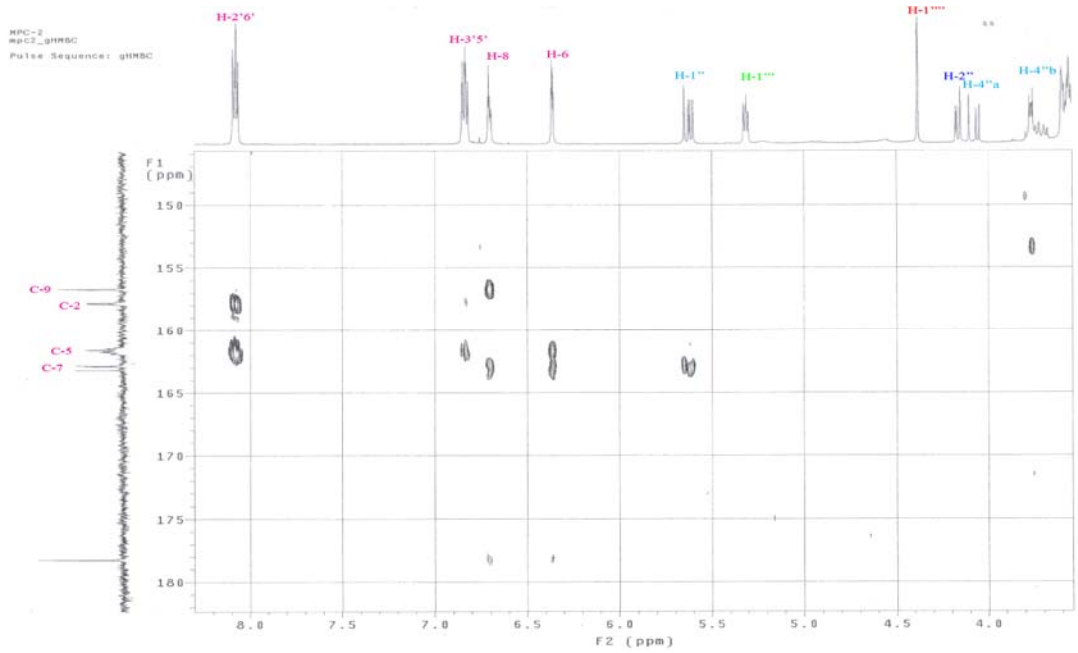

Figure 3.26: The HMBC enlargement showing the anomeric carbon/hydrogen relationships for the sugars galactose, rhamnose and apiose for **4A**.

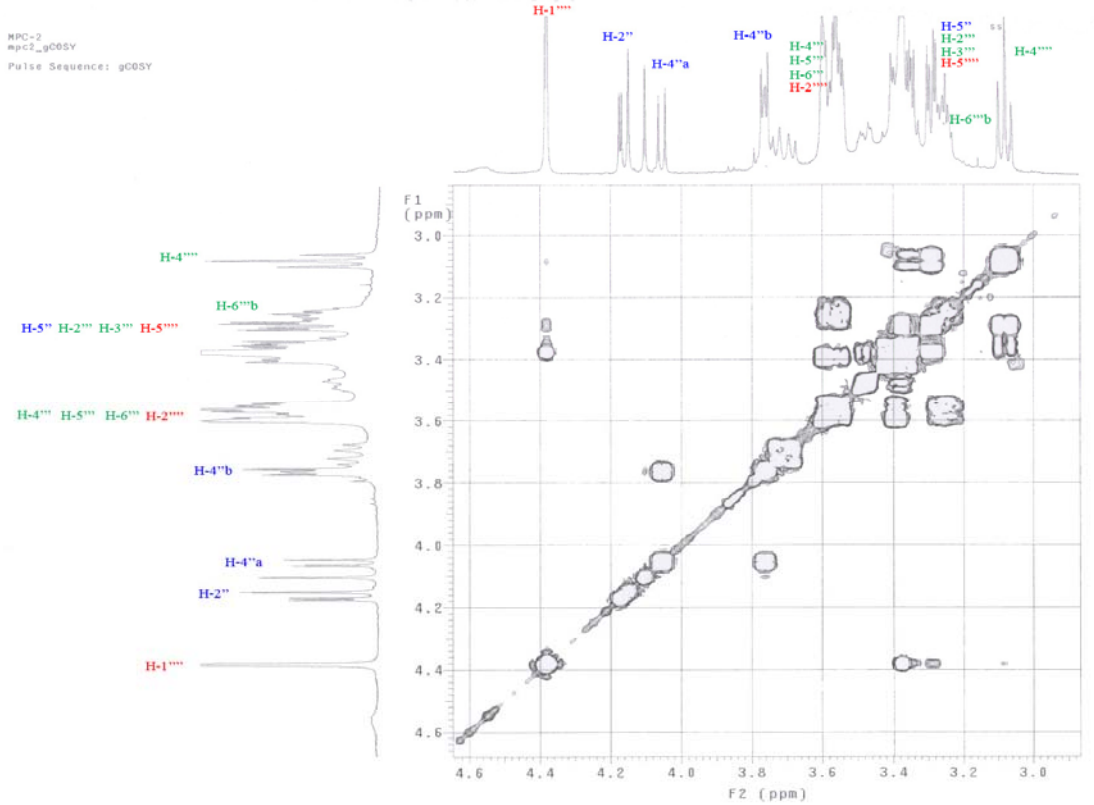

Figure 3.27: The grad-COSY analysis (ns=42, DMSO) of the anomeric region for **4A**.

3.6 *Silphium mohrii* (Fig. 3.28)**,** commonly known as Shaggy rosinweed, *Silphium mohrii* can be found growing along prairies, clearings and uncut rural fence lines. Similar to *S. brachiatum*, it is common to the lower Appalachian mountain regions of Alabama, Georgia and Tennessee. *S. asteriscus* and *S. brachiatum,* in an unresolved clade, have been reported as being related to *S. mohrii* (Clevinger 1999). There have been very few taxonomic studies of this species and no chemical analyses performed. This species also has a unique flower petal color. In fact, the cream-shaded corolla appears to be unique to the entire Asteraceae family.

Figure 3.28: The superimposed unique cream colored ray pedals of *S. mohrii* as taken in the field by Dr. Clevinger (jimmo.com).

Results and Discussion

The LC/MS positive mode analysis of *S. mohrii* provided for the following eleven flavonoids: isorhamnetin 3-*O*-*α*-L-galactosyl (1'''→6'') -*O*-*β*-D-rhamnosyl-7-*O*-*β*-L-apiofuranoside **(1A)**, *m/z* 757.4 $[M+H]^+$, (22.3 min); quercetin 3-*O*-*α*-L-galactosyl (1'''→6'') -*O*-*β*-D-rhamnosyl-7-*O*-*β*-L-apiofuranoside **(2A)**, *m/z* 743.4 $[M+H]^+$, (18.2 min); kaempferol triglycoside **(3)**, *m/z* 727.2 $[M+H]^+$, (19.7 min); kaempferol-3-*O*-*β*-D-

apiofuranoside7-*O*-α-L-rhamnosyl-(1""→6")-*O*-*β*-galactopyranoside **(4A)**, *m/z* 727.3 $[M+H]^+$, (21.4 min); quercetin 3-*O*- galactopyranoside **(5)**, *m/z* 465.1 $[M+H]^+$, (19.1 min); quercetin 3-*O*- glucopyranoside **(6)**, *m/z* 485.2 $[M\text{-}22\ Na^+]^+$, (21.4 min); quercetin 3-*O*-rutinoside **(7)**, *m/z* 611.2 $[M+H]^+$, (17.6 min); isorhamnetin 3-*O*-robinioside **(8)**, *m/z* 625.2 $[M+H]^+$, (24.3 min); isorhamnetin 3-*O*-rutinoside **(9)**, *m/z* 665.2 $[M\text{-}22\ Na^+\text{-}18\ H_2O]^+$, (27.5 min); kaempferol 3-*O*-rutinoside **(10)**, *m/z* 617.2 $[M\text{-}22\ Na^+]^+$, (25.7 min); and kaempferol 3-*O*-robinobioside **(11)**, *m/z* 595.2 $[M+H]^+$, (22.9 min).

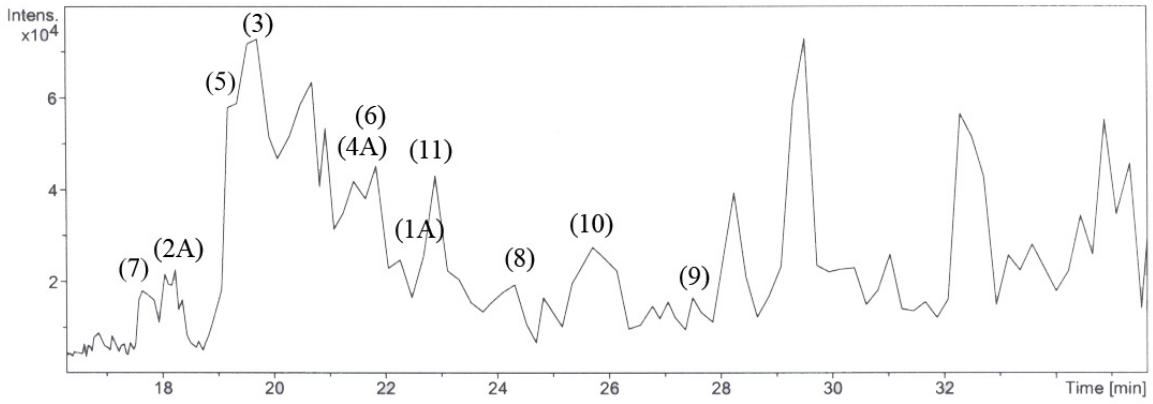

Figure 3.29: The LC/+MS spectrum for *S. mohrii*.

Three of the newly isolated flavonoids were detected in *S. mohrii*. These compounds were isorhamnetin 3-*O*-*α*-L-galactosyl (1'"→6")–*O*-*β*-D-rhamnosyl-7-*O*-*β*-L-apiofuranoside **(1A)**, quercetin 3-*O*-*α*-L-galactosyl (1'"→6") –*O*-*β*-D-rhamnosyl-7-*O*-*β*-L-apiofuranoside **(2A)** and kaempferol 3-*O*-*β*-D-apiofuranoside-7-*O*-α-L-rhamnosyl (1""→6")-*O*-*β*-galactopyranoside **(4A)** along with a fourth possibly unknown kaempferol triglycoside (**3**). This species contained the highest number of triglycosidic flavonoids detected using LC/MS injection.

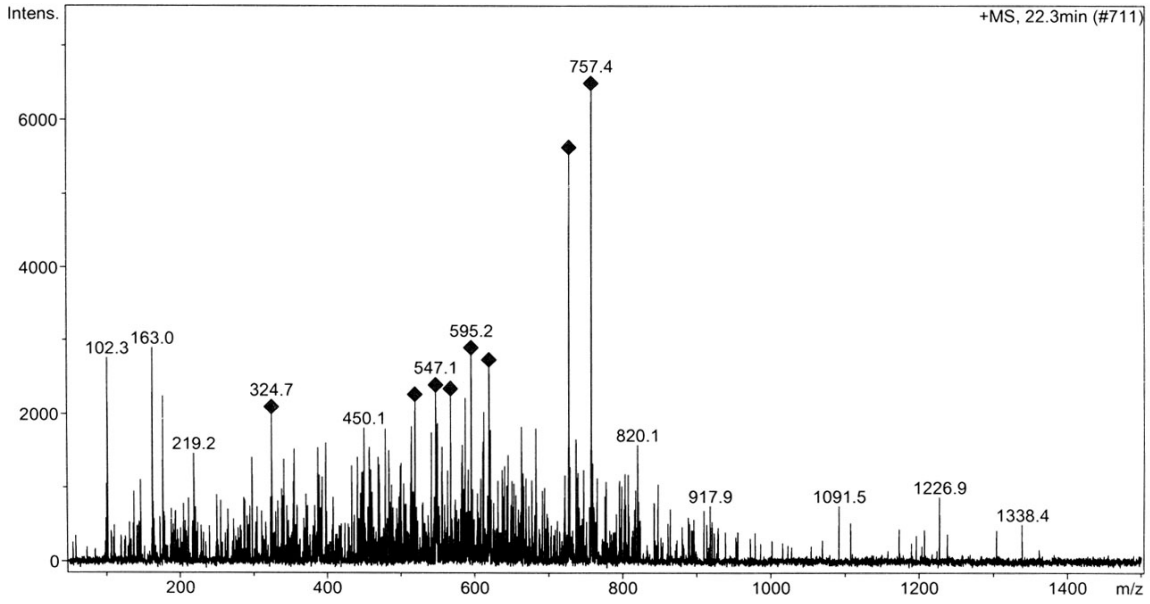

Figure 3.30: The LC/+MS spectrum for isorhamnetin 3-*O*-*α*-L-galactosyl (1'''→6'') –*O*-*β*-D-rhamnosyl 7-*O*-*β*-L-apiofuranoside **(1A)**.

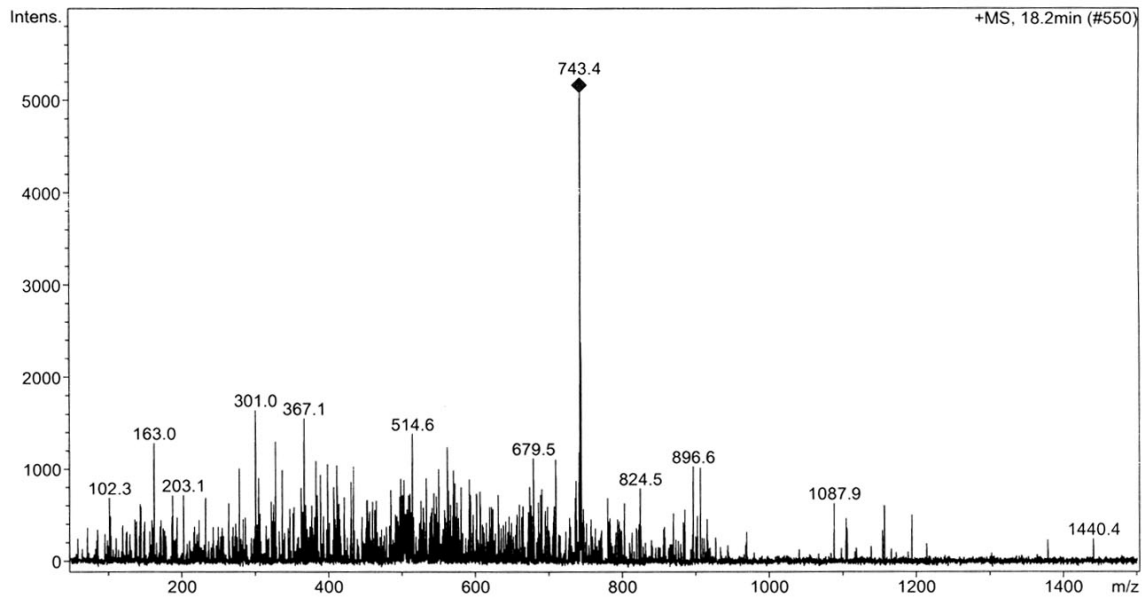

Figure 3.31: The LC/+MS spectrum for quercetin 3-*O*-*α*-L-galactosyl (1'''→6'') –*O*-*β*-D-rhamnosyl 7-*O*-*β*-L-apiofuranoside **(2A)**.

3.7 *Silphium perfoliatum* L. (Fig. 3.32) or Cup-plant, is a perennial herb ranging from south-central Texas to southern Canada (Britton and Brown, 1970). This species can be found on wet prairies, open forests, and along Midwestern highways (Clevinger, 1999). Previous chemical screening of *S. perfoliatum* detected a number of simple flavonoids, phenolic acids and terpenes (Davidyants and Abubakirov, 1992).

Figure 3.32: Nineteenth century sketch drawing of the species *Silphium perfoliatum* (flowersoncd.com).

Medicinally, the aerial parts of this herb have been used as a respiratory tonic, diaphoretic and diuretic (Heilpflanzen, 1996). Root poultices have been used to treat open wounds, backache and hemorrhaging (Hocking, 1997). Other compounds have been shown to have both hypocholesterolemic and hypotriglycerdemic effects (Wojcińska, 1998).

The anatomy of *Silphium perfoliatum* is unique in that it is the only species in the genus having square stems and connate-perfoliate leaves. Taxonomists have typically identified variants in this species based upon the connate-perfoliation of the leaves (Clevinger, 1999). *S. perfoliatum var. connatum* can be differentiated by its pubescent peduncle (Clevinger, 1999).

Results and Discussion

The LC/MS analysis of *S. perfoliatum* showed the presence of the following compounds: quercetin 3-*O*-glucopyranoside **(1)**, *m/z* 505.5 $[M-22Na-18H_2O]^+$, (21.5 min); quercetin 3-*O*- galactopyranoside **(2)**, *m/z* 481.2 $[M-18H_2O]^+$, (17.8 min); kaempferol 3-*O*-*β*-D-apiofuranoside **(3)**, *m/z* 417.3 $[M+H]^+$, (17.8 min); kaempferol-3-*O*-*β*-D-apiofuranoside7-*O*-α-L-rhamnosyl-(1''''→6''')-*O*-*β*-D-galactopyranoside (**4A**), *m/z* 727.6 $[M+H]^+$, (21.1 min); kaempferol 3-*O*-*β*-D-apiofuranoside 7-*O*-*α*-L-rhamnosyl-(1''''→6''')-*O*-*β*-D (2'''-*O*-*E*-caffeoylgalactopyranoside) **(5A)**, *m/z* 928.1 $[M-22Na-18\ H_2O]^+$, (22.8 min); kaempferol 3-*O*-*β*-D-galactopyranoside **(6)**, *m/z* 457 $[M-10H]^+$, (18.6 min); kaempferol 3-*O*-*β*-D-glucoside **(7)**, *m/z* 457 $[M-10H]^+$, (21.5 min); kaempferol 3-*O*- robinioside **(8)**, *m/z* 593.3 $[M+H]^+$, (17.8 min) and kaempferol 3-*O*- rutinoside **(9)**, *m/z* 593.3 $[M+H]^+$, (25.1 min). A possibly new, four-sugar flavonol might also be identified here when the mass of an apiose sugar is added *m/z* 1045.5 $[889-22(Na^+)-132\ apiose]^+$, (17.8 min). The LC/MS analysis from the field collection plants of *S. perfoliatum* did not show the compound quercetin 3-*O*- rutinoside as isolated from the botanical garden grown collection.

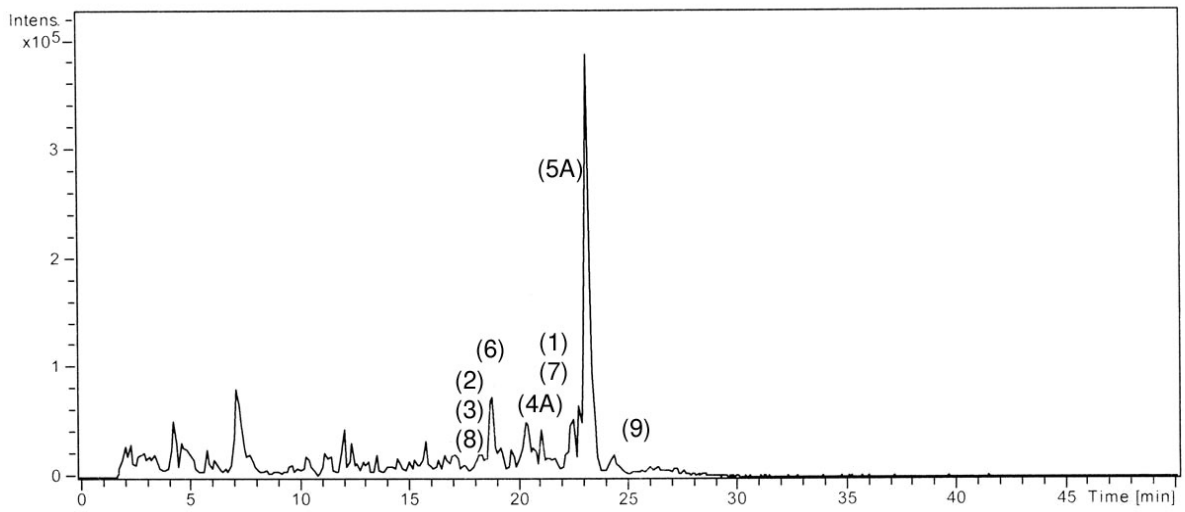

Figure 3.33: The LC/MS spectra for the species *Silphium perfoliatum***.**

The NMR chemistry of *Silphium perfoliatum* includes the isolation and identification of the two triglycosidic kaempferol flavonoids, kaempferol 3-*O*-*β*-D-apiofuranoside 7-*O*-*α*-L-rhamnosyl-(1''''→6''')-*O*-*β*-D-galactopyranoside **(4A)** and its caffeoyl ester **(5A)**, together with nine other known flavonoids.

The known compounds, kaempferol and its 3-*O*-glucoside (**7**) and 3-*O*-galactoside (**6**); 3-*O*-rutinoside (**9**) and 3-*O*-robinobioside (**8**); quercetin and its 3-*O*-galactoside (**2**), 3-*O*-glucoside (**1**) and 3-*O*-rutinoside, were all identified by comparison of their ^{1}H NMR, ^{13}C NMR, UV and LC/MS spectra (Agrawal and Bansal, 1989; Markham *et al*., 1978).

The ^{1}H NMR spectra for both compounds **4A** and **5A** exhibited the A and B ring signals characteristic of kaempferol 3, 7-di-*O*-substituted glycosides (Mabry *et al*., 1970). Signals for three anomeric protons were detected in both compounds: the 3-*O*-apiofuranosyl anomeric proton at δ 5.63 as *d, J* = 3.16 Hz for **4A** and δ 5.62 *d, J* = 3.65

Hz for **5A.** The presence of $J_{1,2}$ ~3–4 Hz confirms the *β*-D-*erythro*furanoside form of the sugar apiose (Angyal and Pickles, 1972; Angyal *et al*., 1977; Ranganathan *et al*., 1980; Ingham *et al*., 1986; and Silva *et al*., 2000).

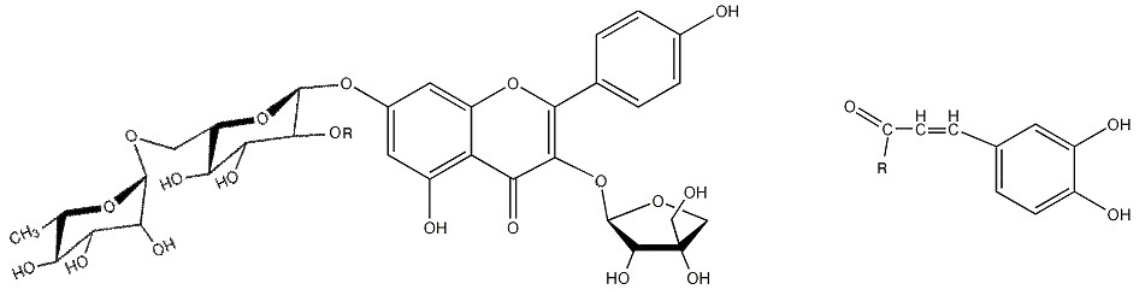

Figure 3.34: The structure of the two kaempferol triglycosides **4A** and **5A**.

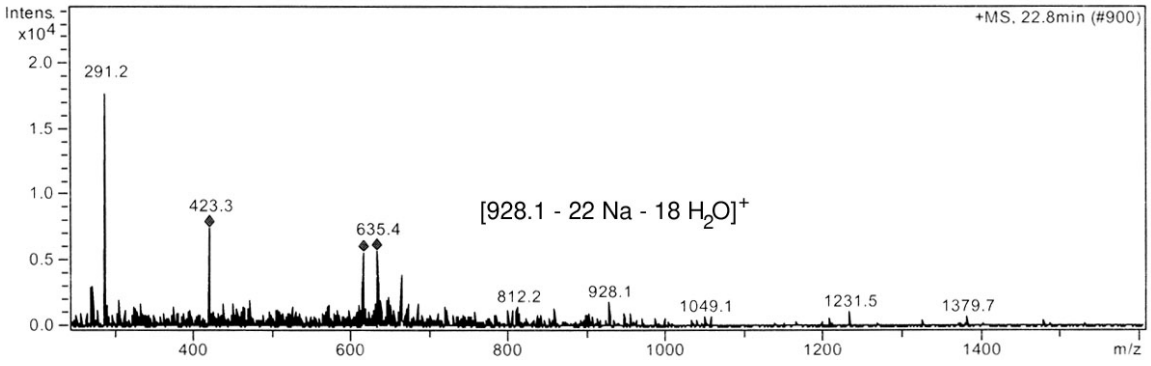

Figure 3.35 The LC/+MS detection of the kaempferol 3-*O*-*β*-D-apiofuranoside 7-*O*-*α*-L-rhamnosyl-(1""→6''')-*O*-*β*-D-(2'''-*O*-*E*-caffeoylgalactopyranoside)
(5A)

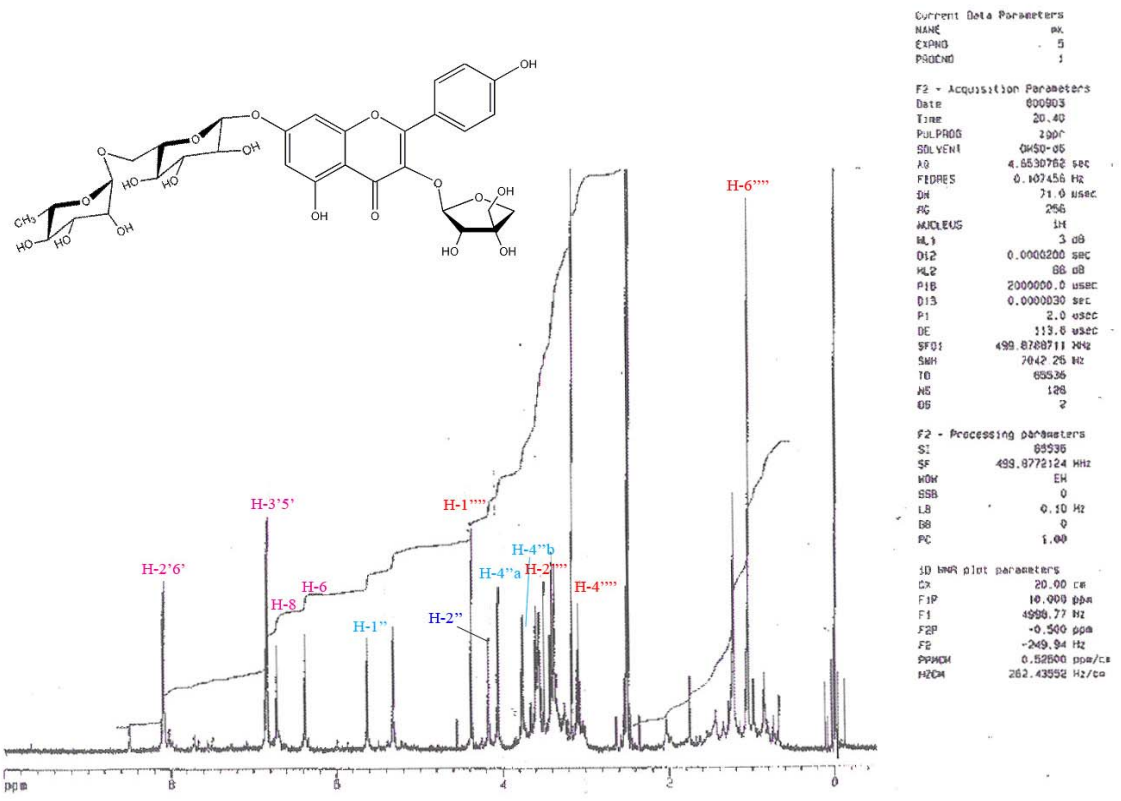

Figure 3.36: The ^{1}H NMR anomeric assignments for kaempferol 3-*O*-*β*-D-apiofuranoside 7-*O*-*α*-L-rhamnosyl-(1''''→6''')-*O*-*β*-D-galactopyranoside **(4A)**.

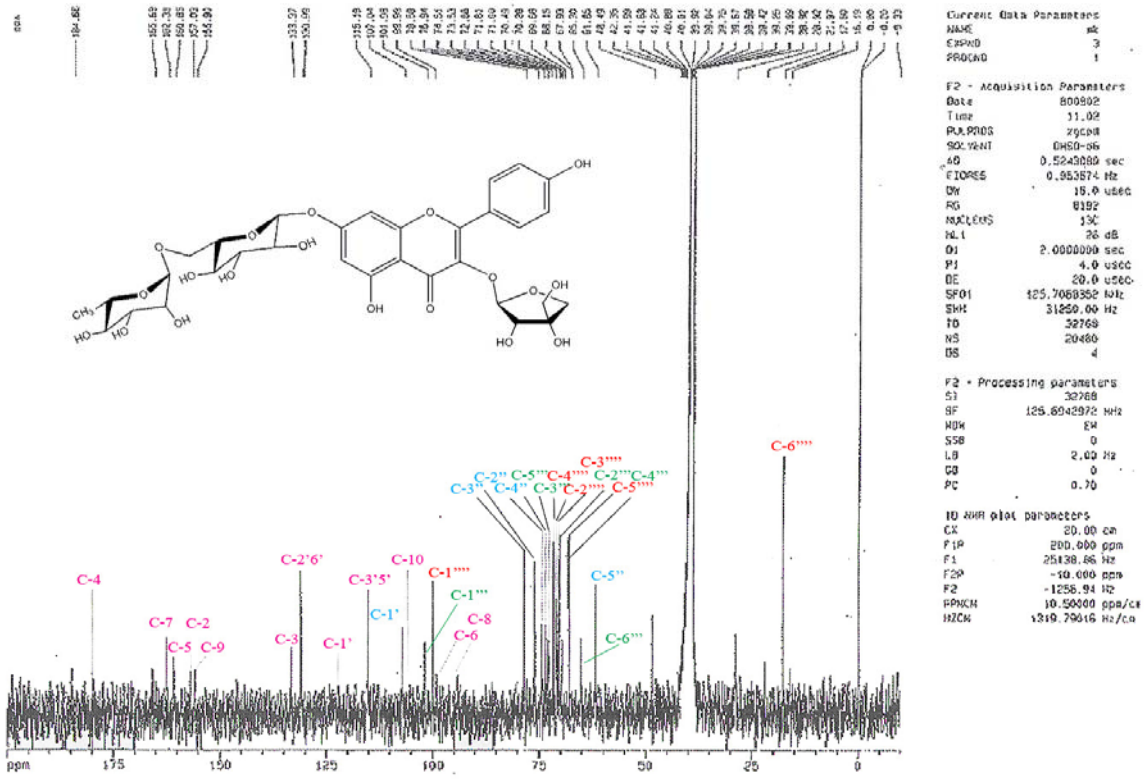

Figure 3.37: The ^{13}C NMR assignments for kaempferol 3-*O*-*β*-D-apiofuranoside 7-*O*-*α*-L-rhamnosyl-(1''''→6''')-*O*-*β*-D-galactopyranoside (**4A**).

The UV spectra for the kaempferol 3-*O*-*β*-D-apiofuranoside 7-*O*-*α*-L-rhamnosyl-(1''''→6''') –*O*-*β*-D-galactopyranoside (**4A**) in MeOH exhibited two bands at wavelengths λ 350 nm, band I, 267 nm, band II with a shoulder at 245, 292, 319 nm. On addition of $NaOCH_3$, band I showed an increase in absorbance and a shift in wavelength (+52 nm, band I, +0 nm, band II), results which are consistent with a 4' free OH. On addition of $AlCl_3$, both compounds showed an increase in wavelength (+49 nm, band I, +7 nm, band II) confirming the absence of the 3' hydroxyl. On addition of HCl similar wavelengths (398 nm, band I, 274 nm, band II) occurred. NaOAc exhibited a (+53 nm, band I, -1 nm,

band II) suggestive of a hydroxyl at the 7 position, and on addition of boric acid, a confirmation of the 4' OH (+3 nm, band I, -1 nm, band II) was observed.

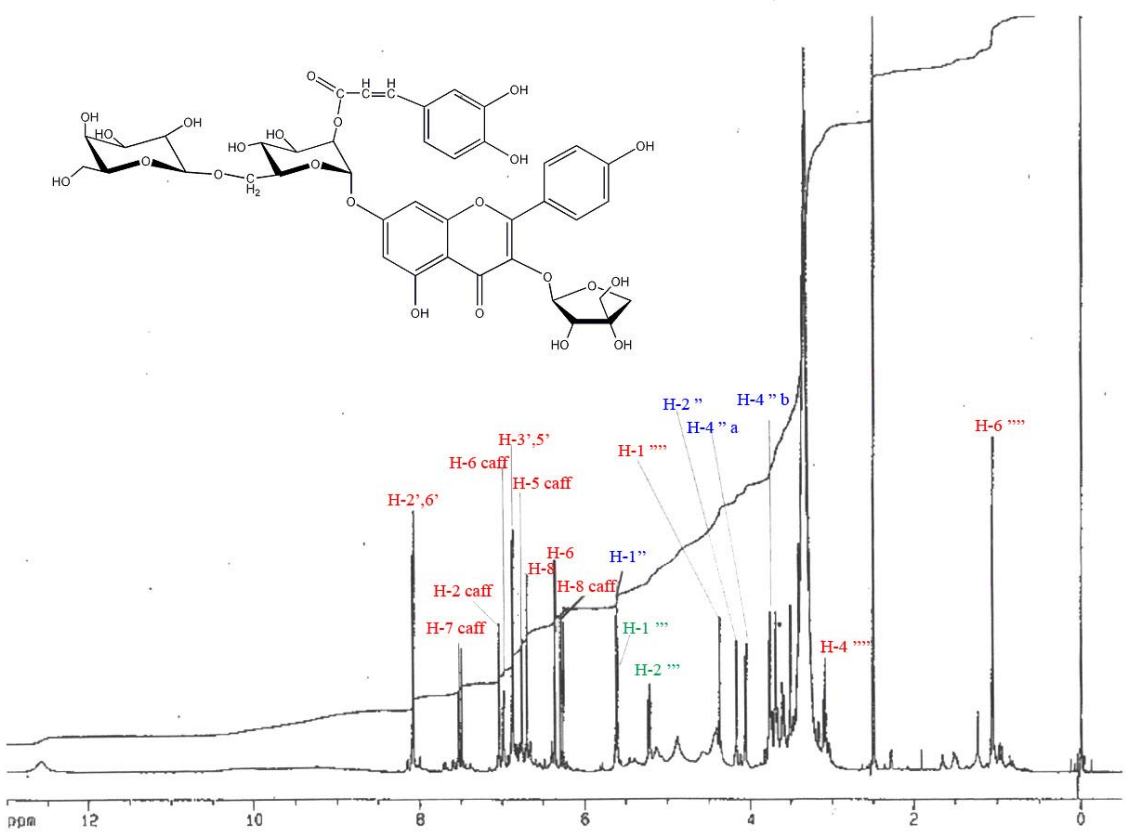

Figure 3.38: The[1]H NMR anomeric assignments for kaempferol 3-*O*-*β*-D-apiofuranoside 7-*O*-*α*-L-rhamnosyl-(1””→6”’)-*O*-*β*-D (2”’-*O*-*E*-caffeoylgalactopyranoside) (**5A**).

The *erythro* relationship for apiose in **5A** was suggestive from the chemical shift difference of 2.64 ppm observed for the C-2″ and C-3″ positions in both compounds (Bashir et al., 1990). The second signal for the anomeric proton of a 7-*O*-galactosyl was detected at *δ* 5.32 *d, J* = 7.75 Hz for **4A** and at *δ* 5.6 *d, J* = 7.98 Hz for **5A**. The third signal characteristic for a *O*-*α*- L -terminal rhamnosyl linkage with galactose was detected at *δ* 4.39 *d, J* = 1.26 Hz for **4A** and at *δ* 4.37 *d, J* = 1.21 Hz for **5A**. In addition,

compound **5A** exhibited *trans* olefinic proton signals at δ 7.5 *d, J* = 15.77 Hz and at δ 6.26 *d, J* = 15.92 Hz, along with a doublet at δ 6.76 *J* = 8.12 Hz for the caffeic proton H-5, a doublet of doublets for proton H-6 at δ 6.98 *J* = 1.93, 8.25 and at H-2, δ 7.04 *d, J* = 1.94 Hz. Each of these signals helps substantiate the caffeoyl moiety attachment of compound **5A** (Kraut *et al*., 1993).

The ^{13}C NMR and DEPT analysis provided for three methylene, one methyl, 18 methine and ten quaternary carbons for compound **4A** and three methylene, one methyl, 23 methine and 14 quaternary carbons for **5A**, which together with FAB negative at *m/z* 725 $[M–H]^-$ **(4A)** and 887 $[M–H]^-$ **(5A)** established the molecular ion formula of $C_{32}H_{38}O_{19}$ for **4A** and $C_{41}H_{44}O_{22}$ for **5A**.

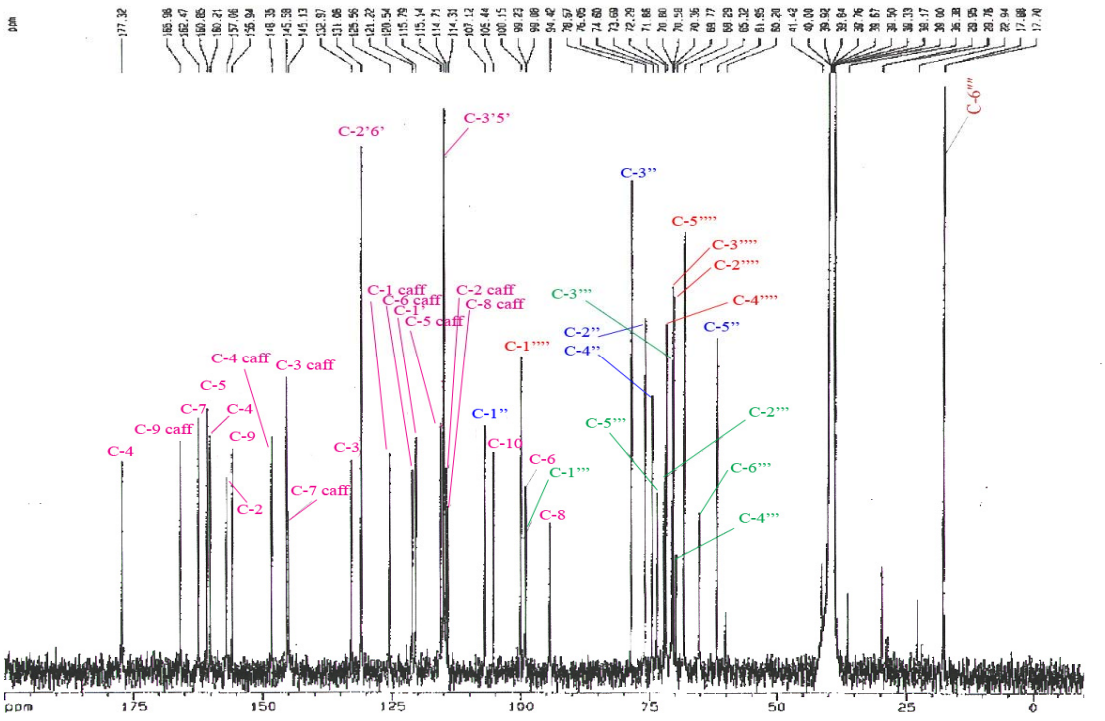

Figure 3.39: The ^{13}C NMR assignments for kaempferol 3-*O*-*β*-D-apiofuranoside 7-*O*-*α*-L-rhamnosyl-(1""→6''')-*O*-*β*-D (2'''-*O*-*E*-caffeoylgalactopyranoside) **(5A)**.

Proton Positions	Mf	Data Given From Literature		
		β-D-apiofuranoside	β-D-apiofuranoside	3,7 - Sugar Position kaempferol
Aglycone				
H-6	6.36d (*J*=2.5)	-	-	6.42d (*J*=1.4)
H-8	6.71d (*J*=2.8)	-	-	6.73d (*J*=1.4)
H-2′, 6′	8.08d (*J*=9.0)	-	-	8.02d (*J*=8.7)
H-3′, 5′	6.87d (*J*=8.9)	-	-	6.90d (*J*=8.7)
Attachments				
Apisose				
H-1′′	5.62d (*J*=3.5)	5.48d (*J*=3.5)	5.31d (*J*=2.0)	-
H-2′′	4.17d (*J*=3.4)	4.49d (*J*=3.5)	4.03d (*J*=2.0)	-
H-4′′a	4.05d (*J*=9.5)	4.15d (*J*=9)	4.18d (*J*=10.0)	-
H-4′′b	3.76d (*J*=9.4)	3.80d (*J*=9)	3.84d (*J*=10.0)	-
H-5′′a	3.35-3.75m*	3.61d (*J*=10)	3.64 br s	-
H-5′′b	3.35-3.75m*	3.43d (*J*=10)	-	-
Galalactose				
H-1′′′	5.6d (*J*=8.0)	-	-	-
H-2′′′	5.2sd (*J*=8.0; 8.0)	-	-	-
H-3′′′	3.74m*	-	-	-
H-4′′′	3.52m*	-	-	-
H-5′′′	3.66m*	-	-	-
H-6′′′a	3.66m*	-	-	t-*α*-*L*-rhamnopiranoside[3]
H-6′′′b	3.74m*	-	-	-
Rhamnose				
H-1′′′′	4.37d (*J*=1.2)	-	-	4.33d (*J*=1.2)
H-2′′′′	3.38m	-	-	-
H-3′′′′	3.30m	-	-	-
H-4′′′′	3.08t (*J*=9.3;9.3)	-	-	-
H-5′′′′	3.35-3.37m*	-	-	-
H-6′′′′	1.06d (*J*=6.2)	-	-	0.94d (*J*=6.2)
Caffeic Acid		Caffeic Acid (E)[4]	Caffeic Acid (Z)[5]	
H-2	7.04d (*J*=1.9)	7.07d (*J*=2.0)	6.92s	-
H-5	6.76d (*J*=8.1)	6.75d (*J*=8.1)	6.65d (*J*=8.8)	-
H-6	6.98dd (*J*=1.9; 8.2)	7.00dd (*J*=2.0; 8.2)	6.675d (*J*=8.8)	-
H-7	7.50d (*J*=15.8)	7.47d (*J*=15.8)	7.10d (*J*=16.1)	-
H-8	6.26d (*J*=15.9)	6.28d (*J*=15.9)	5.94d (*J*=15.6)	-

Table 3.1: Kaempferol proton assignments including their ppm shifts as recorded in the literature.

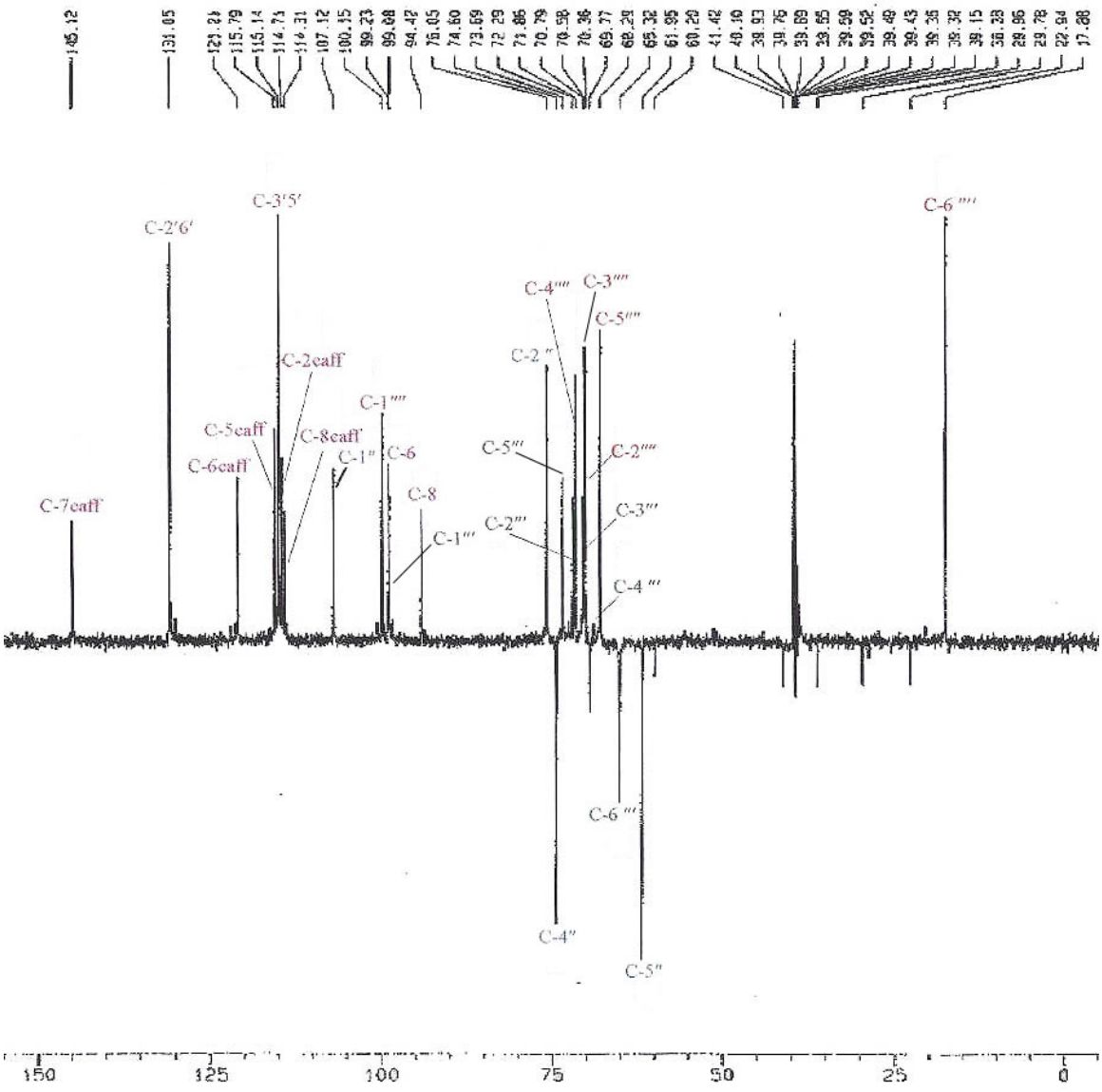

Figure 3.40: The DEPT analysis of **5A** showing the signals for three methylenes, single methyl group, twenty-three methines and fourteen quaternary carbon moieties.

The first mass unit loss of apiose *m/z* 593 $[M\text{-}l\text{-}132]^{-}$ for compound **4A** provides further support for the lack of apiose being linked to another sugar, supporting its direct attachment to the aglycone (El-Sayed, 2002).

The rhamnosyl terminal sugar is linked to galactose through a 1""→6"' bond for both **4A** and **5A** and is consistent with the galactosyl C-6"' 5.0 ppm downfield shift at δ 65.32 for **4A** and 65.30 ppm for **5A**. In addition an upfield shift of the rhamnosyl C-2"" carbon of 0.63 ppm (Markham *et al*., 1978) together with the HMBC correlation of the rhamnosyl H-l"" to the galactosy1 C-6"' confirm the 1""→ 6"' linkage between these two sugars. The caffeoyl moiety in **5A** is assigned to the galactosyl C-2"' based on the observed downfield shift of galactosyl H-l"' +0.29 and H-2"' +1.75 ppm and the downfield shifts of galactosyl C-2"' +2 ppm with the consequent upfield shift of both galactosyl C-1"' and C-3"' of −2.7 and −2.06 ppm, respectively. The correlation between caffeoyl C = 0 and both the galactosy1 H-l"' and galactosyl H-2"' by HMBC confirms the previous assignment.

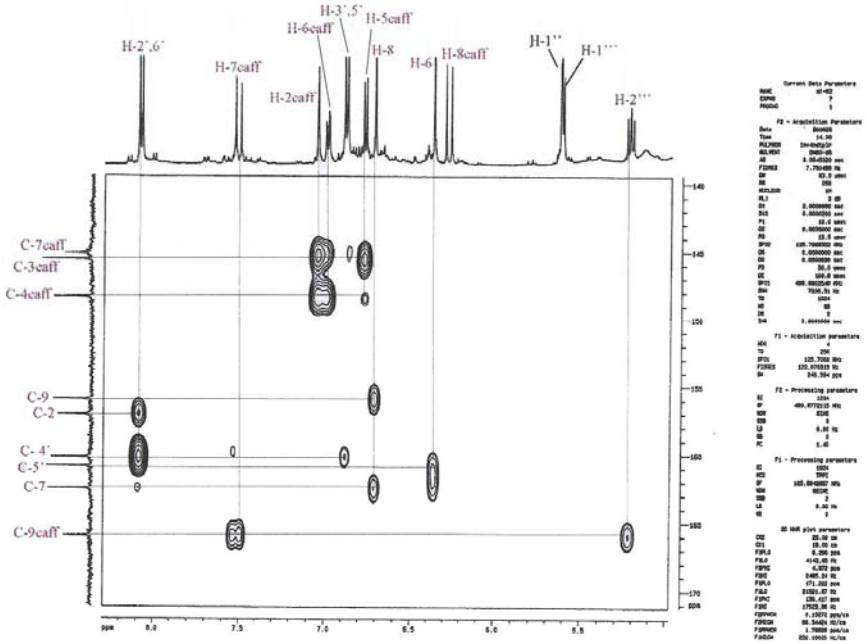

Figure 3.41: The HMBC analysis providing evidence for the caffeoyl galactosyl attachment in compound **5A.**

The data indicate that compound **4A** is indeed kaempferol 3-*O*-*β*-D-apiofuranoside 7-*O*-*α*-L-rhamnosyl-(1''''→ 6''')-*O*-*β*-D-galactopyranoside and **5A** is kaempferol 3-*O*-*β*-D-apiofuranoside7-*O*-*α*-L-rhamnosyl-(1''''→6''')-*O*-*β*-D-(2'''-O-*E*-caffeoyl-galactopyranoside).

The UV spectra for the kaempferol 3-*O*-β-D-apiofuranoside 7-*O*-α-L-rhamnosyl-(1→6) -*O*-β-D-(2'''-*O*-E-caffeoylgalactopyranoside) (**5A**) in MeOH exhibited two bands at wavelengths λ 333 nm, band I, 267 nm, band II with shoulders at 256, 294 nm. On addition of $NaOCH_3$, both bands showed an increase in absorbance and a shift in wavelength (+52 nm, band I, +2 nm, band II), results which are consistent with a 4' free OH. On addition of $AlCl_3$, both compounds showed an increase in wavelength (+76 nm, band I, +4 nm, band II) confirming the absence of the 3' hydroxyl. On addition of HCl similar wavelengths (397 nm, band I, 277 nm, band II) appeared. NaOAc treatment gave shifts of a (+1 nm, band I, +0 nm, band II) suggestive of a hydroxyl at the 7 position, and on addition of boric acid, confirmation of the 4' OH (+15 nm, band I, -2 nm, band II) was observed.

The remaining known mono and disaccharide compounds along with their respective spectra are listed below.

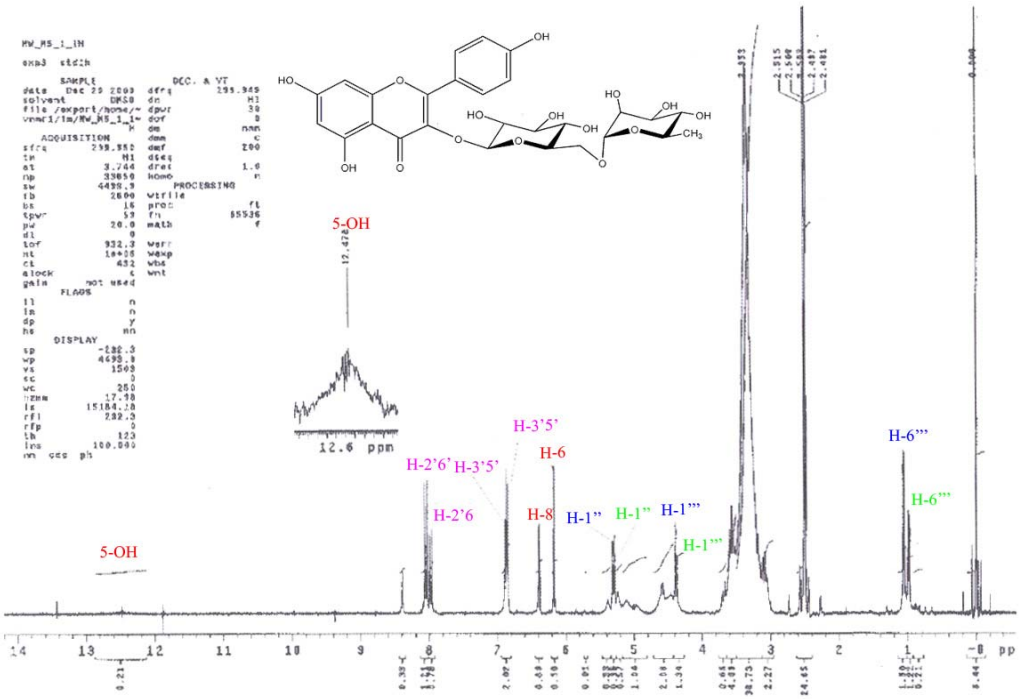

Figure 3.42: The ^{1}H NMR spectrum for kaempferol 3-*O*-*α*-L-rhamnosyl-(1""→6''')–*O*-*β*-D-galactopyranoside **(8)**.

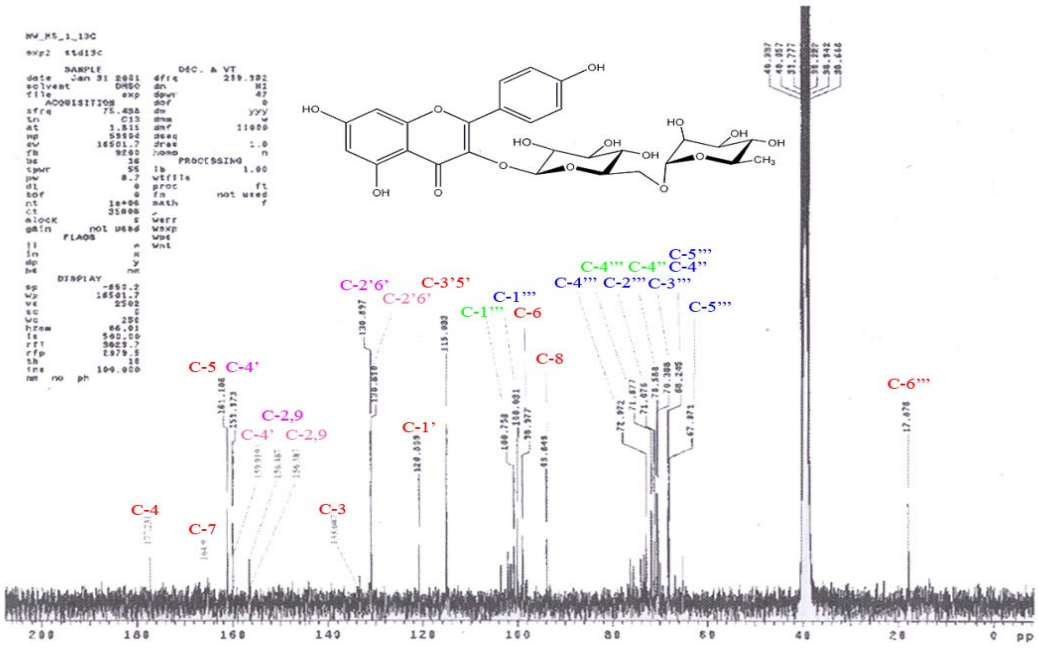

Figure 3.43: The ^{13}C NMR spectrum for kaempferol 3-*O*-α-L-rhamnosyl-(1""→6''')–*O*-*β*-D-galactopyranoside (**8**).

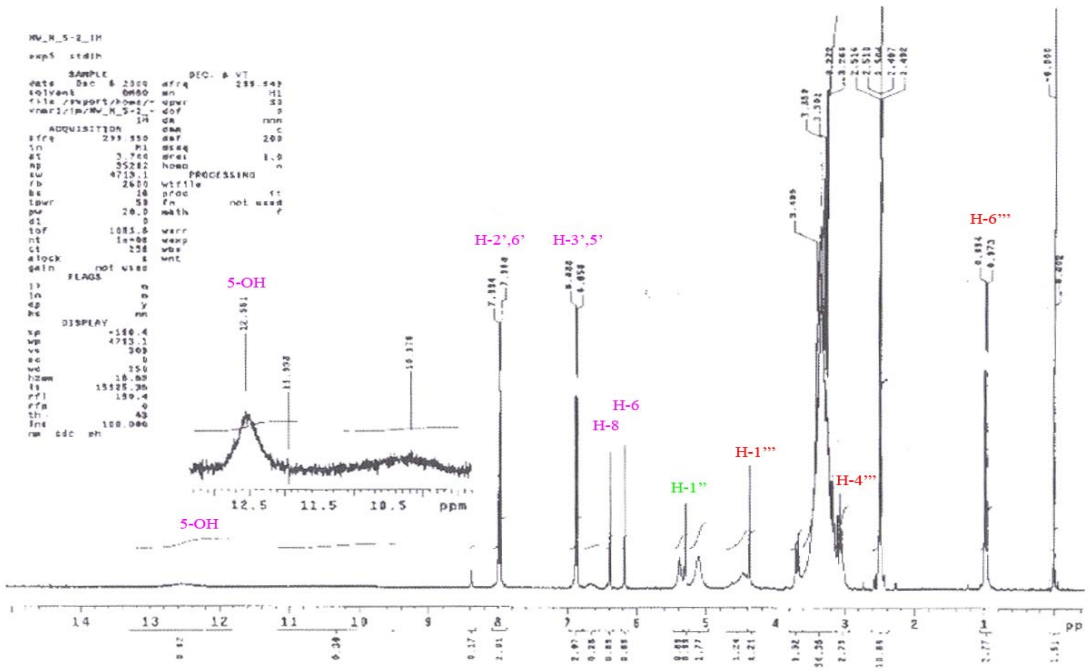

Figure 3.44: The ^{1}H NMR spectrum for kaempferol 3-*O*-α-L-rhamnosyl-(1""→6''')–*O*-*β*-D-glucopyranoside (**9**).

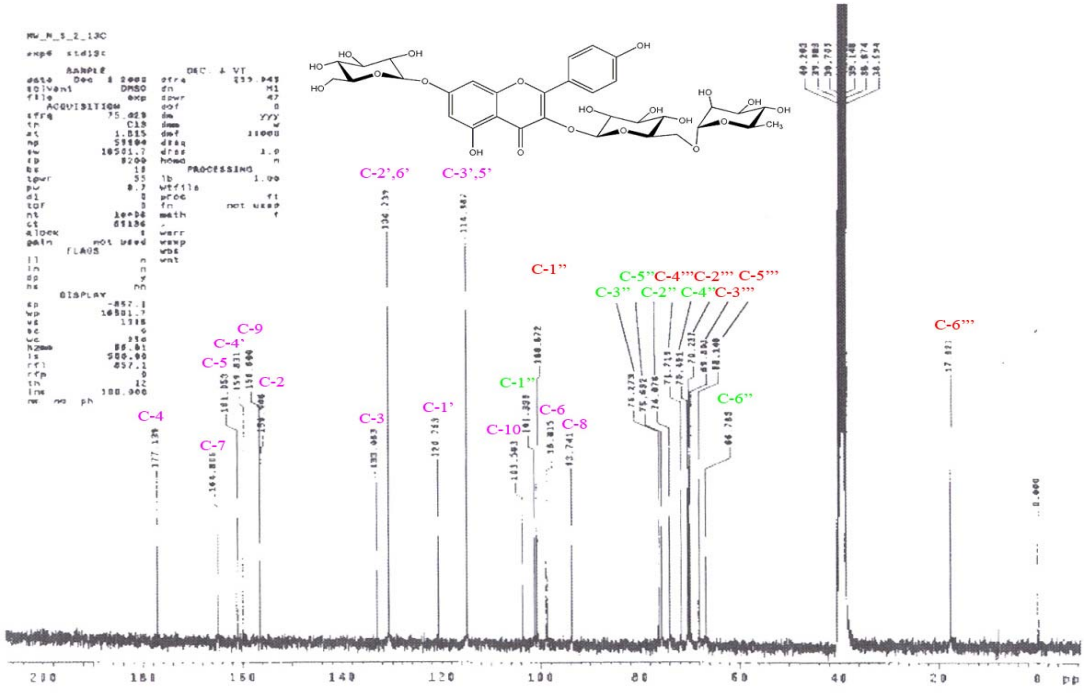

Figure 3.45: The ^{13}C NMR spectrum for kaempferol 3-*O*-*α*-L-rhamnosyl-(1""→6''')–*O*-*β*-D-glucopyranoside (**9**).

The UV spectra for both kaempferol 3-*O*-*α*-L-rahmnosyl-(1→6)–*O*-*β*-D-glucopyranoside **(9)** and galactopyranoside **(8)** in MeOH exhibited two bands at wavelengths (λ 349 nm **(9)**, λ 347 nm **(8)**, band I, λ 266 nm for **9**, λ 267 nm for **8**, band II) with a shoulder at 298 **(9)**, 246, 298 **(8)**. On addition of $NaOCH_3$, both bands showed an increase in absorbance and a shift in wavelength (+51 **(9)**, +52 **(8)** nm, band I, +8 **(9),** +8 **(8)** nm, band II), results which are consistent with a 4' free OH. On addition of $AlCl_3$, both compounds showed an increase in wavelength (+48 **(9)**, +49 **(8)** nm, band I, +8 **(9),** +8 **(8)** nm, band II) confirming the absence of the 3' hydroxyl. On addition of HCl similar wavelengths (392 **(9)**, 395 **(8)** nm band I, 275 **(9)**, 275 **(8)** nm band II) occurred. NaOAc exhibited a (+33 **(9)**, +26 **(8)** nm, band I, + 8 **(9)**, + 7 **(8)** nm, band II) suggestive of the hydroxyl presence at the 7 position, and on addition of boric acid, a confirmation of the 4' OH presence (+4 **(9),** +6 **(8)** nm, band I, + 1 **(9),** +0 **(8)** nm, band II) was observed.

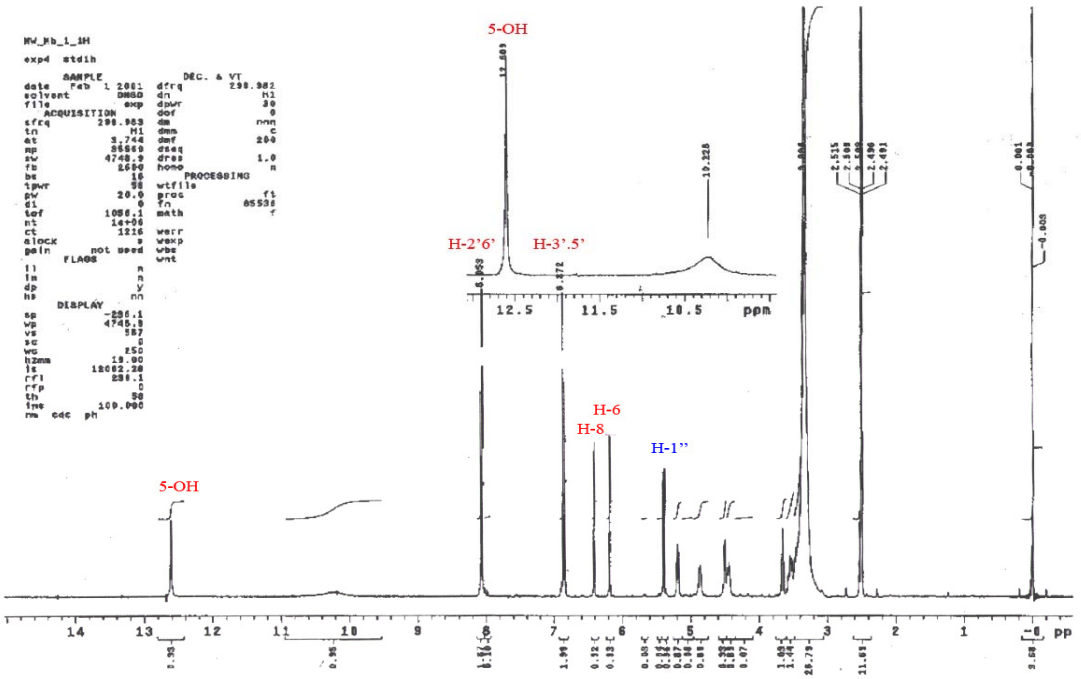

Figure 3.46: The ^{1}H NMR spectrum for kaempferol 3-*O*-*β*-D-galactopyranoside **(6)**.

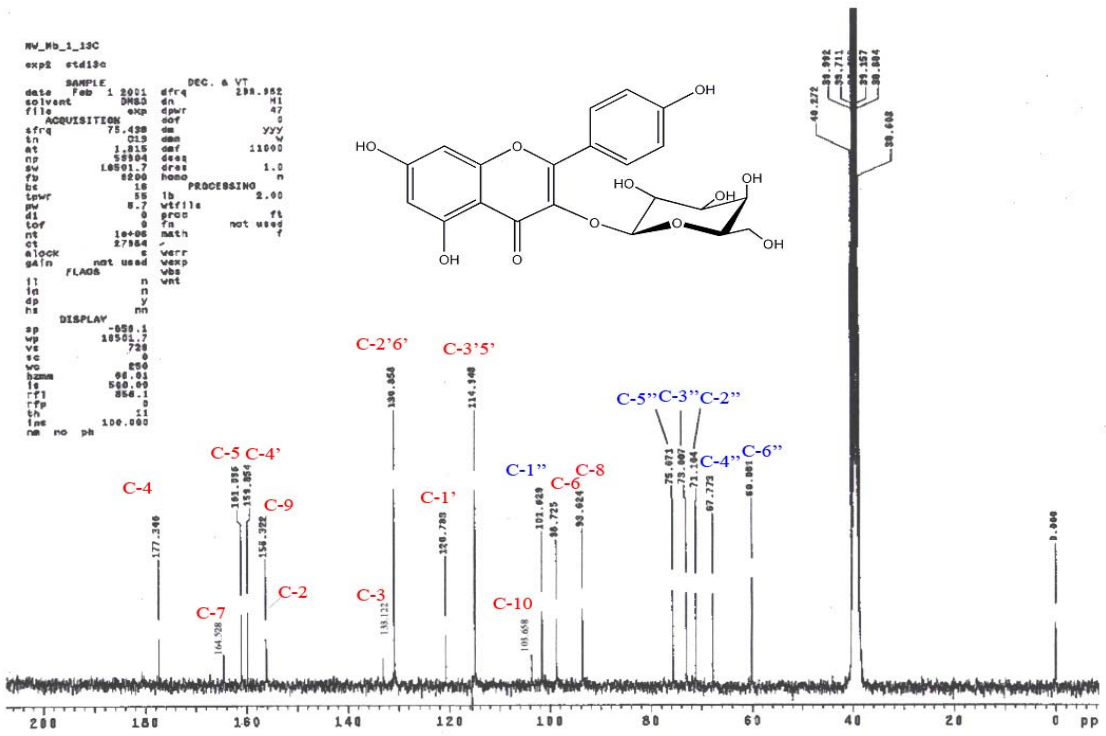

Figure 3.47: The ^{13}C NMR spectrum for kaempferol 3-*O*-*β*-D-galactopyranoside **(6)**.

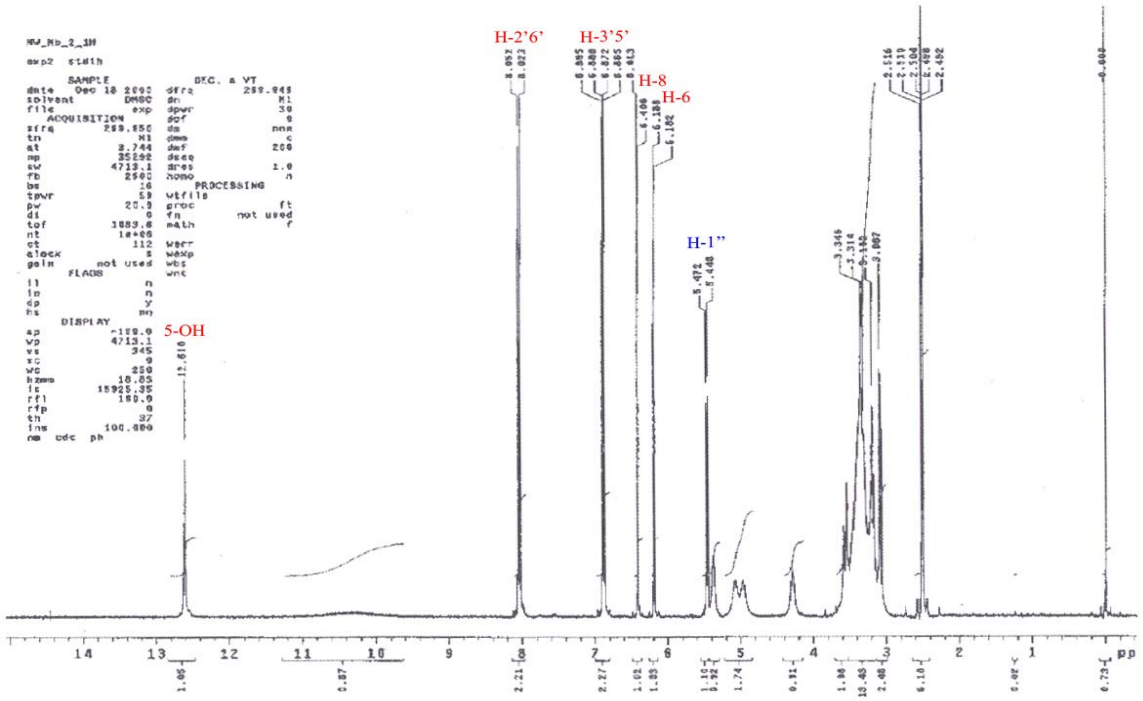

Figure 3.48: The ^{1}H NMR spectrum for kaempferol 3-*O*-*β*-D-glucopyranoside **(7)**.

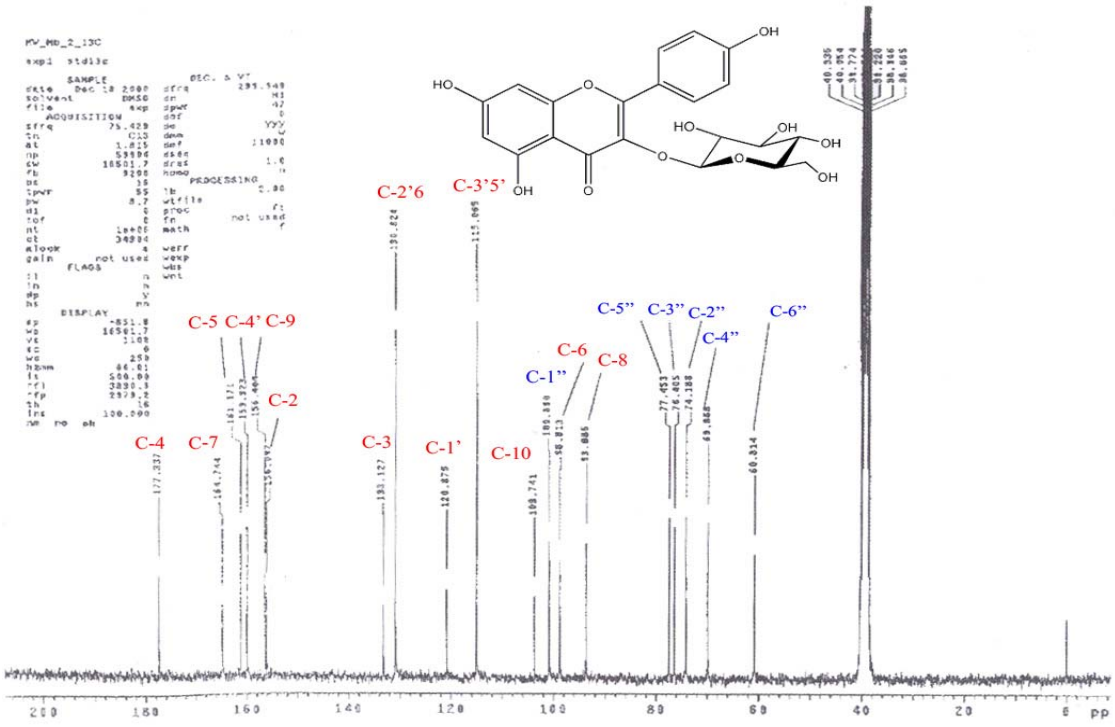

Figure 3.49: The ^{13}C NMR spectrum for kaempferol 3-*O*-*β*-D-glucopyranoside **(7)**.

The UV spectra for both kaempferol 3-*O*-*β*-D-glucopyranoside and **(7)** and galactopyranoside **(6)** in MeOH exhibited two bands at wavelengths (λ 348 **(7)**, λ 350 **(6)** nm, band I, λ 266 **(7)**, λ 266 **(6)** nm, band II) with a shoulder at 295 **(7)**, 295 **(6)**. On addition of $NaOCH_3$, both bands showed an increase in absorbance and a shift in wavelength (+48 **(7)**, +42 **(6)** nm, band I, +9 **(7),** +9 **(6)** nm, band II), results which are consistent with a 4' free OH. On addition of $AlCl_3$, both compounds showed an increase in wavelength (+48 **(7)**, +47 **(6)** nm, band I, +8 **(7),** +9 **(6)** nm, band II) confirming the absence of the 3' hydroxyl. On addition of HCl similar wavelengths (396 **(7)**, 397 **(6)** nm band I, 275 **(7)**, 275 **(6)** nm band II) occurred. NaOAc exhibited a (+28 **(7)**, +22 **(6)** nm, band I, + 8 **(7)**, + 8 **(6)** nm, band II) suggestive of the hydroxyl presence at the 7 position, and on addition of boric acid, a confirmation of the 4' OH presence (+5 **(7),** +2 **(6)** nm, band I, + 1 **(7),** +1 **(6)** nm, band II) was observed.

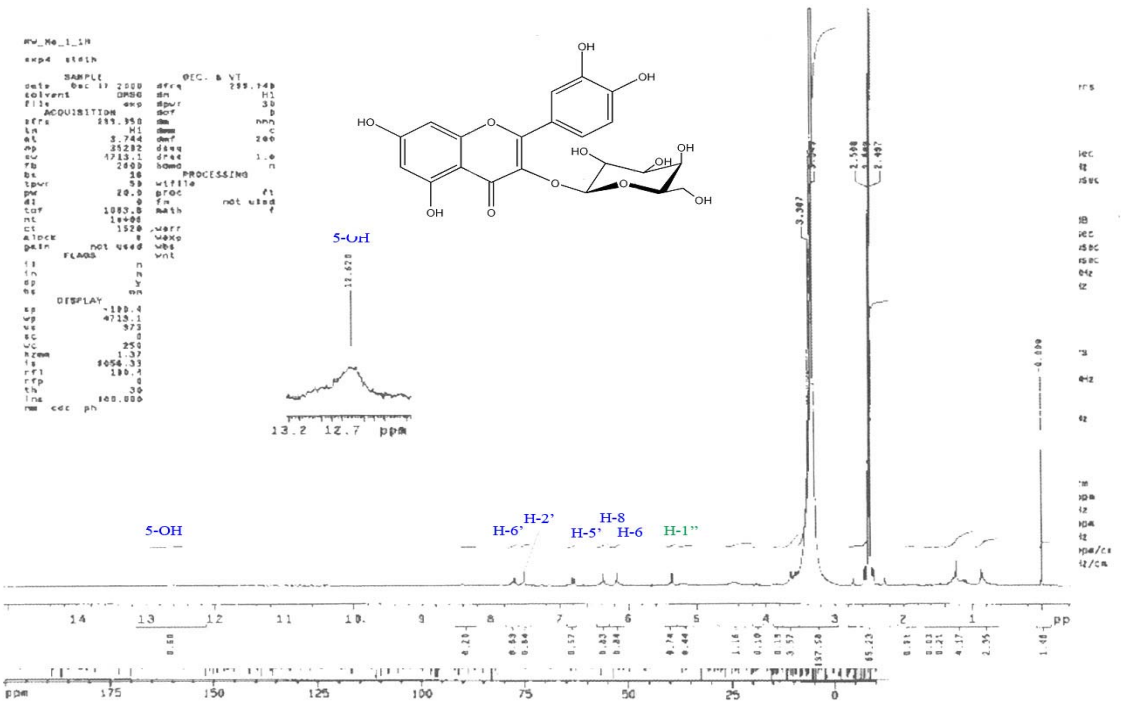

Figure 3.50: The ^{1}H NMR spectrum for quercetin-3-*O*-*β*-D-galactopiranoside **(2)**.

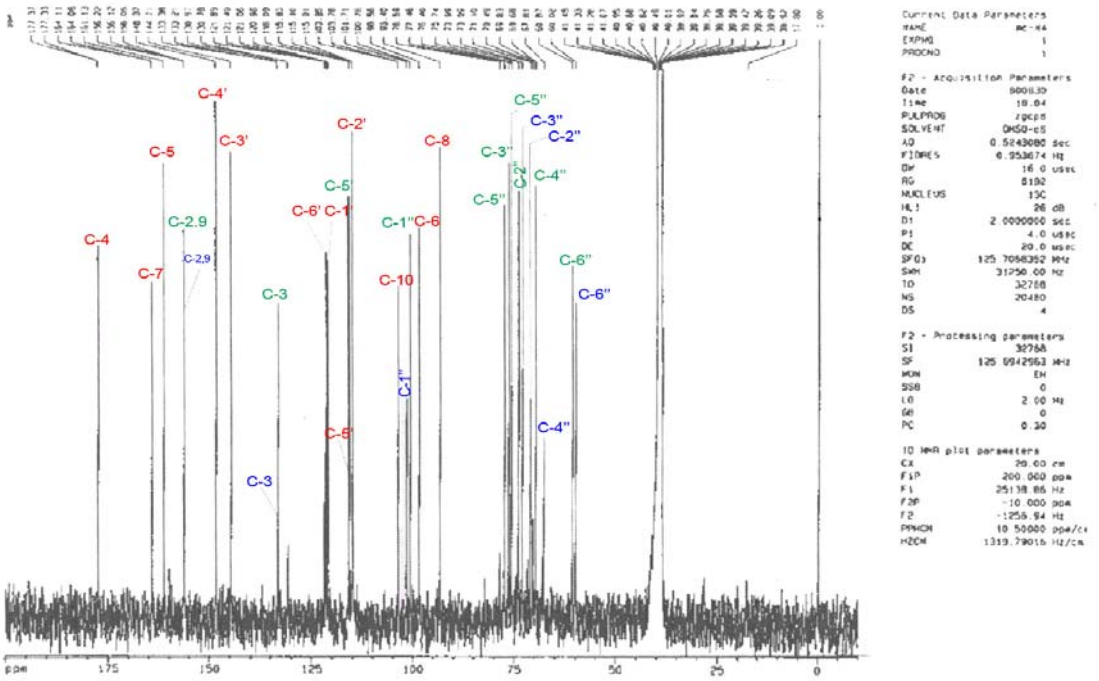

Figure 3.51: The ^{13}C NMR spectrum for quercetin-3-*O*-*β*-D-galactopyranoside **(2)**.

UV analysis of quercetin-3-*O*-*β*-D-galactopyranoside (**2**) in MeOH exhibited two bands at λ 362 band I, 258 band II and a shoulder at 296. On addition of $NaOCH_3$, both an increase stable in absorbance and wavelength occurred (+44 nm, band I, +14 nm, band II) in consistent with a 4′ free OH. The compound, on addition of $AlCl_3$, showed a bathochromic shift of (+71 nm, band I, +17 nm, band II) confirming the catecholic 3′,4′ OH presence. On addition of HCl, a decomposition and return to the wavelengths λ 357 and 269 nm occurred. Addition of NaOAc showed a (+23 nm, band I, +12 nm, band II) suggestive of an OH presence at the 7 position, and the addition of boric acid, resulted in the confirmation of the *ortho* 3′,4′ OH presence (+16 nm, band I, +4 nm, band II).

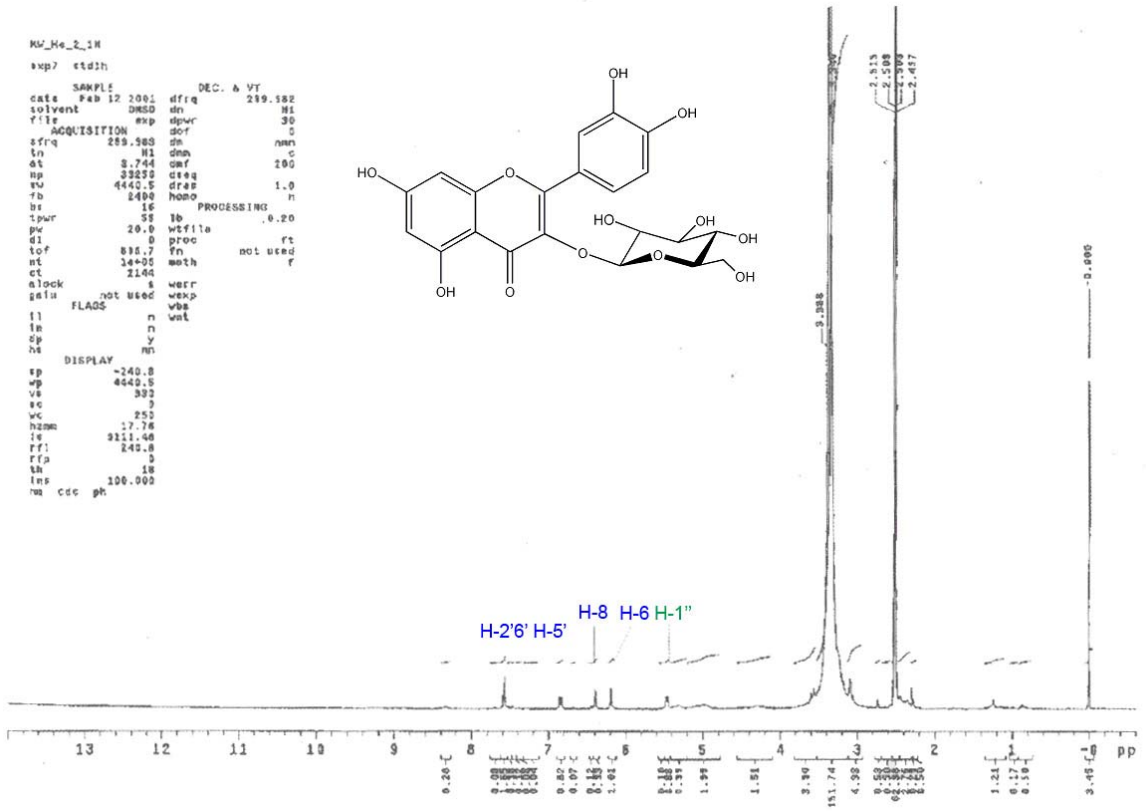

Figure 3.52: The ^{1}H NMR spectrum for quercetin 3-*O*-*β*-D-glucopyranoside **(1)**.

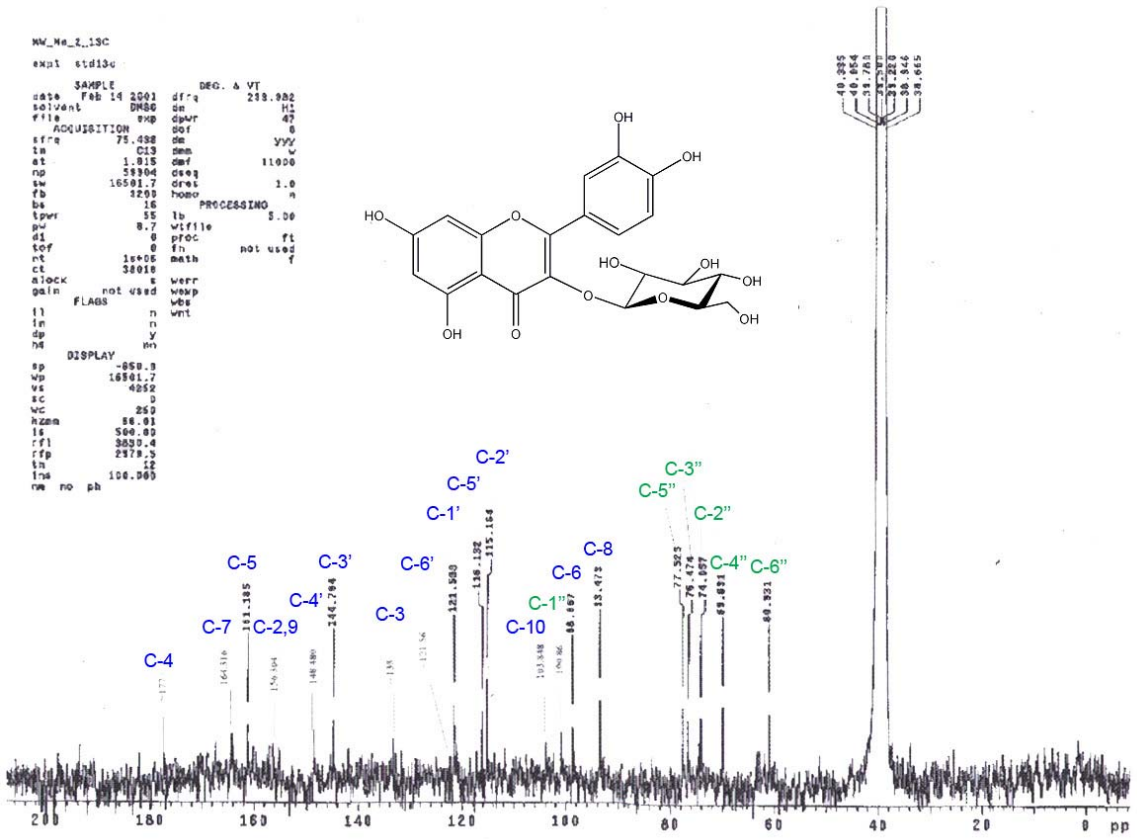

Figure 3.53: The ^{13}C NMR spectrum for quercetin 3-*O*-*β*-D-glucopyranoside **(1)**.

UV analysis of quercetin 3-*O*-*β*-D-glucopyranoside (**1**) in MeOH exhibited two bands at λ 360 band I, 258 band II and a shoulder at 297. On addition of $NaOCH_3$, both an increase stable in absorbance and wavelength occurred (+52 nm, band I, +15 nm, band II), consistent with a 4′ free OH. The compound, on addition of $AlCl_3$, showed a bathochromic shift of (+73 nm, band I, +17 nm, band II) confirming the catecholic 3′,4′ OH presence. On addition of HCl, a decomposition and return to the wavelengths λ 364 and 269 nm occurred. Addition of NaOAc showed a (+33 nm, band I, +14 nm, band II) suggestive of an OH presence at the 7 position, and on addition of boric acid, a reconfirmation of the *ortho* 3′,4′ OH presence (+18 nm, band I, +3 nm, band II) occurred.

UV analysis of quercetin-3-O-rutinoside (**2**) in MeOH exhibited two bands at λ 359 band I, 259 band II and a shoulder at 267, 301. On addition of $NaOCH_3$, both an increase stable in absorbance and wavelength occurred (+70 nm, band I, +17 nm, band II), consistent with a 4′ free OH. The compound, on addition of $AlCl_3$, showed a bathochromic shift of (+83 nm, band I, +21 nm, band II) confirming the catecholic 3′,4′ OH presence. On addition of HCl, a decomposition and return to the wavelengths λ 359 and 275 nm occurred. Addition of NaOAc showed a (+32 nm, band I, +16 nm, band II) suggestive of an OH presence at the 7 position, and on addition of boric acid, a reconfirmation of the *ortho* 3′-4′ OH presence (+29 nm, band I, +5 nm, band II) occurred.

3.8 *Silphium radula* (Fig. 3.54) is known to have two varieties: *Silphium radula* var. *gracile* and *Silphium radula* var. *radula*. *Silphium radula* var. *gracile*, commonly known as Slender rosinweed, can be found in Texas and is distinguished by its basal rosette (Clevinger, 2004). Molecular studies relate it to *S. asteriscus* var. *asperrimum*, *S. asteriscus* var. *asteriscus* and *S. asteriscus* var. *simpsonii*. *Silphium radula* var. *radula,* commonly known as Rough-stem rosinweed, is characterized by a caduceus basal rosette and is distributed in Arkansas, Louisiana, Oklahoma and Texas. Molecular studies link it to the species *S. asteriscus* and *S. integrifolium*, with closer relation to the former.

Figure 3.54: Superimposed image showing the slender growth form, tapered leaves and kaempferol chemistry of *Silphium radula.*

The LC/MS analysis detected the following compounds: an unknown quercetin diglycoside (**1**), *m/z* 611.2 $[M+H]^+$, (19.7 min); quercetin 3-*O*-*α*-L-galactosyl (1'''→6'') – *O*-*β*-D-rhamnosyl-7-*O*-*β*-L-apiofuranoside **(2A)**, *m/z* 743.4 $[M+H]^+$, (22.1 min); quercetin 3-*O*-galactopyranoside (**3**), *m/z* 487.4 $[M-22Na+H]^+$, (20.7 min); kaempferol-3-*O*-*β*-D-apiofuranoside7-*O*-α-L-rhamnosyl-(1''''→6''')-*O*-*β*-D-galactopyranoside (**4A**), *m/z* 727.4 $[M+H]^+$, (20.8 min); quercetin 3-*O*-glucopyranoside (**5**), *m/z* 487.4 $[M-22Na+H]^+$, (22.0

min); quercetin 3-*O*- *β*-D- rutinoside **(6)**, *m/z* 611.2 $[M+H]^+$, (22.1 min); quercetin 3-*O*- *β*-D- robinobioside **(7)**, *m/z* 633.2 $[M-22Na+H]^+$, (24.4 min); isorhamnetin 3-*O*-robinobioside **(8)**, *m/z* 625.1 $[M+H]^+$, (20.7 min); kaempferol 3-*O*-glucopyranoside (**9**), *m/z* 469.4 $[M+22Na+H]^+$, (21.3 min); kaempferol 3-*O*- robinioside **(10)**, *m/z* 595.2 $[M+H]^+$, (22.9 min); and kaempferol 3-*O*- rutinoside **(11)**, *m/z* 617.2 $[M-22\ Na^+]^+$, (25.7 min). An unknown kaempferol diglycoside **(12)**, appeared as *m/z* 595.3 $[M+H]^+$ at (28.8 min) along with an unidentified isorhamnetin triglycoside **(13)**, with mass *m/z* 757.3 $[M+H]^+$ at (33.2 min).

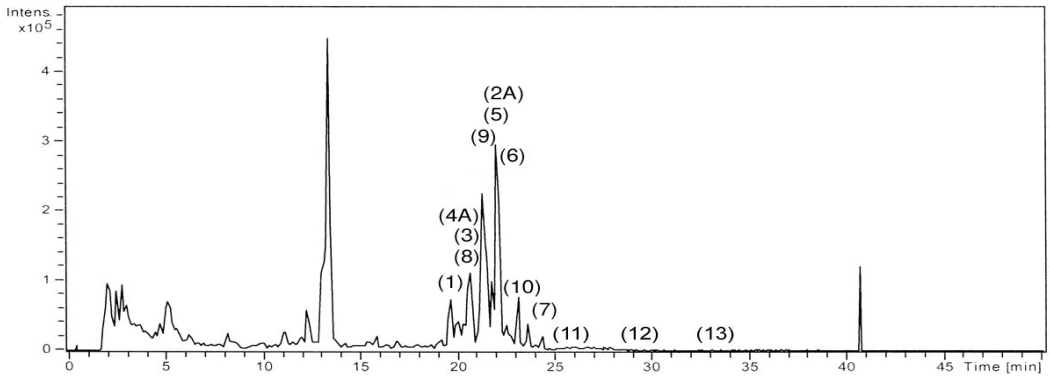

Figure 3.55: The LC/MS spectra for *Silphium radula***.**

The ^1H NMR analysis provided spectra for the two kaempferol diglycosides kaempferol 3-*O*- robinioside **(10)** and kaempferol 3-*O*- rutinoside **(11)**.

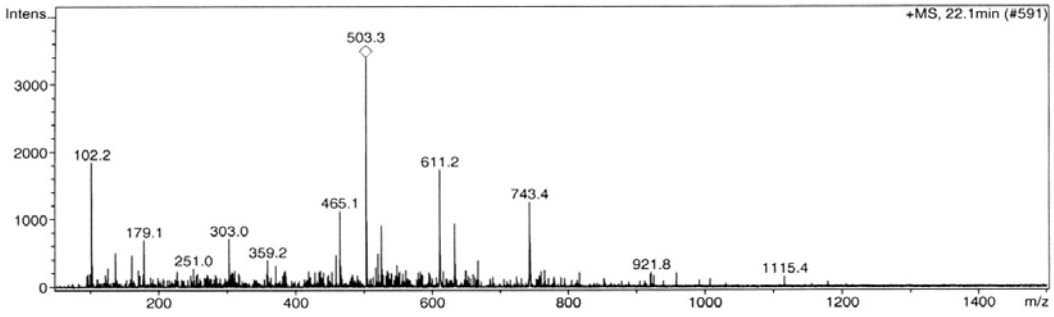

Figure 3.56: The MS spectra for quercetin 3-*O*-*α*-L-galactosyl (1'''→6'') –*O*-*β*-D-rhamnosyl 7-*O*-*β*-L-apiofuranoside **(2A)**, *m/z* 743.4 $[M+H]^+$, (22.1 min).

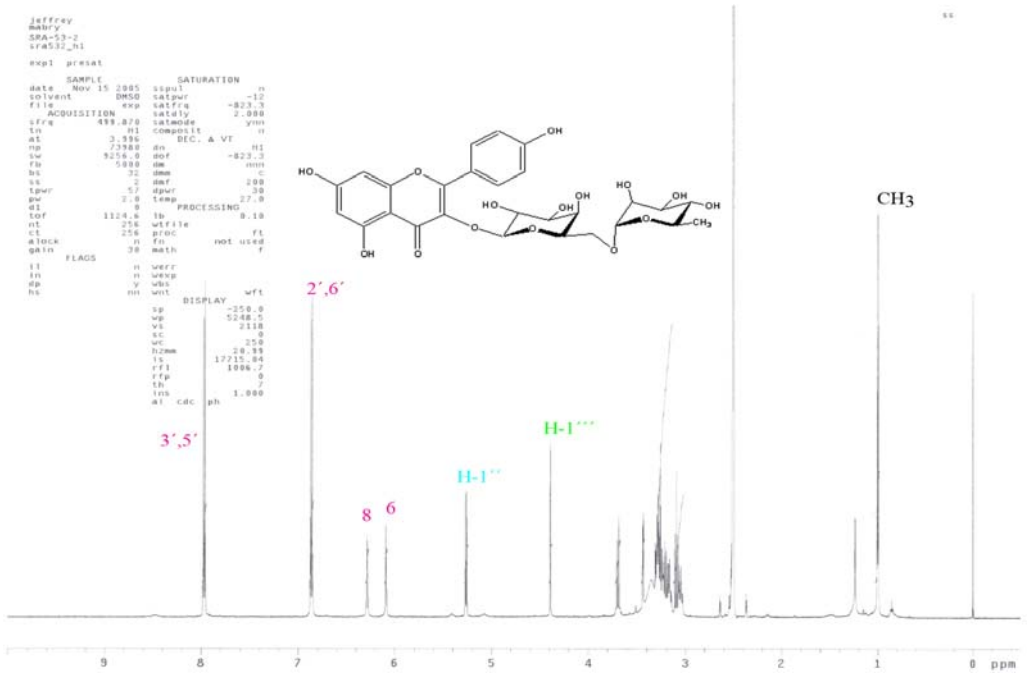

Figure 3.57: The ^{1}H NMR spectrum for the kaempferol 3-*O*- rutinoside **(11)**.

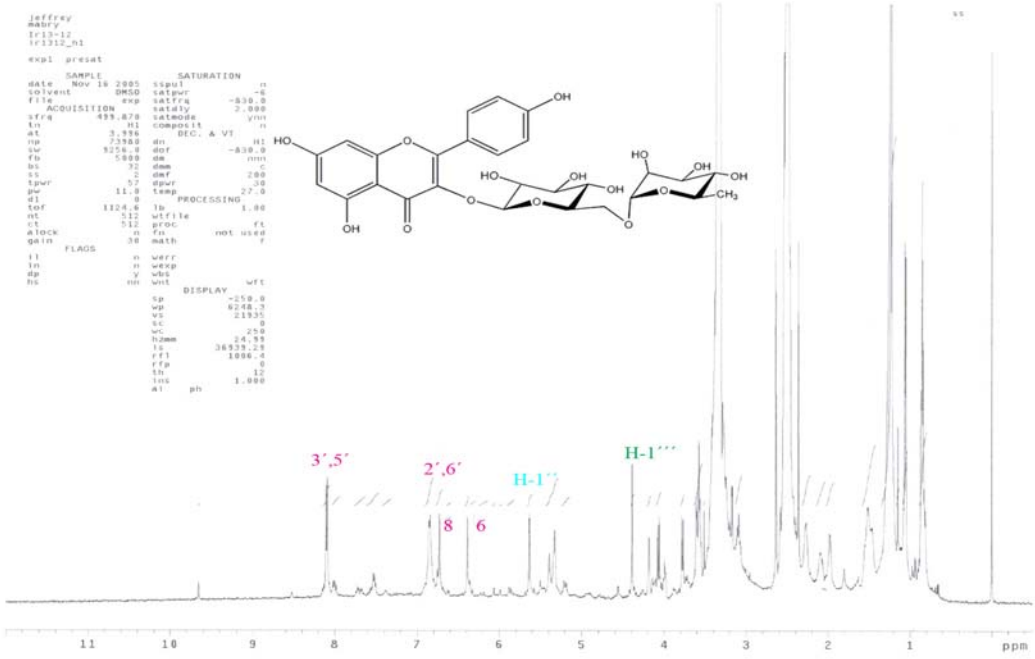

Figure 3.58: The ^{1}H NMR spectrum for the kaempferol 3-*O*- robinioside **(10)**.

3.9 *Silphium wasiotense* (Fig. 3.59), commonly known as Cumberland rosinweed, grows along clear patches of open forest and road cuts. This species is found exclusively in the mountain regions of Kentucky and Tennessee. *Silphium wasiotense* is a caulescent, fibrous rooted, perennial herb that is characterized by its persistent basal rosette. The ITS/ETS sequence analysis closely link *S. wasiotense* to the more commonly distributed species *S. perfoliatum* (Clevinger, 1999).

Figure 3.59: The broad dentate margined leaves of *Silphium wasiotense.* Similar in size and shape to the species *S. terebinthinaceum* the leaves can measure as wide as 16 cm.

Results and Discussion

The LC/MS flavonoid analysis detected the following compounds: isorhamnetin 3-*O*-α-L-rhamnosyl (1'''→6'')-*O*-*β*-D-galactopyranoside 7-*O*-*β*-L-apiofuranoside **(1A)**, *m/z* 757.4 $[M+H]^+$, (21.8 min); quercetin 3-*O*-galactopyranoside **(2)**, *m/z* 485.4 $[M-22\ Na^+]^+$, (19.1 min); quercetin 3-*O*-glucopyranoside **(3)**, *m/z* 485.4 $[M-22\ Na^+]^+$, (21.1 min); quercetin 3-*O*-rutinoside **(4)**, *m/z* 611.3 $[M+H]^+$, (23.3 min); kaempferol 3-*O*-*β*-D-apiofuranoside 7-*O*-α-L-rhamnosyl-(1''''→6''')-*O*-*β*-D (2'''-*O*-*E*-caffeoylgalactopyranoside) **(5A)**, *m/z* 888.2 $[M+H]^+$, (23.0 min); kaempferol 3-*O*-rutinoside **(6)**, *m/z* 595 $[M+H]^+$, (25.3 min); quercetin 3-*O*-robinobioside **(7),** *m/z* 611.3 $[M+H]^+$, (26.5 min); unknown

isorhamnetin triglycoside **(8)**, signal *m/z* 757.4 $[M+H]^+$, (26.5 min); and an unknown quercetin diglycoside **(9)**, signal *m/z* 611.2 $[M+H]^+$, (30.1 min).

Kaempferol 3-*O*-*β*-D-apiofuranoside 7-*O*-α-L-rhamnosyl-(1''''→6''')-*O*-*β*-D (2'''-*O*-*E*-caffeoylgalactopyranoside) **(5A)** was also detected in *S. perfoliatum*. Although this species has fewer detectable kaempferol derivatives, the rarer kaempferol triglycoside **5A** was detected in both species supporting Dr. Clevinger's studies relating *S. perfoliatum* with *S. wasiotense* rather than *S. mohrii* and *S. brachiatum* suggested by Medley (Clevinger 1999, Medley, 1989).

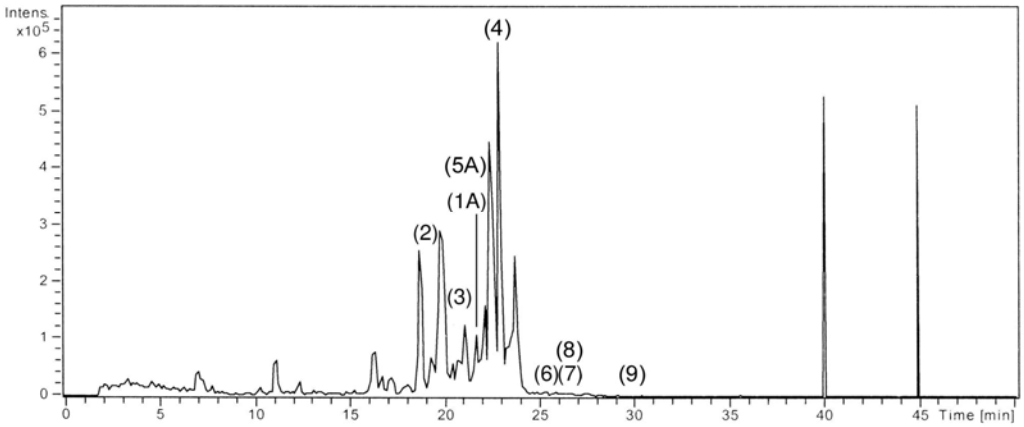

Figure 3.60: The LC/+MS spectrum for *Silphium wasiotense*.

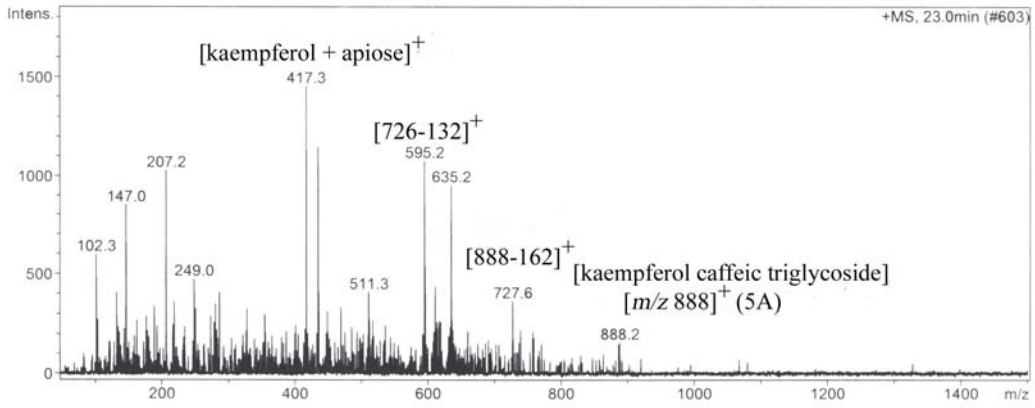

Figure 3.61: The LC/+MS spectrum for kaempferol 3-*O*-*β*-D-apiofuranoside 7-*O*-α-L-rhamnosyl-(1''''→6''')-*O*-*β*-D (2'''-*O*-*E*-caffeoylgalactopyranoside) **(5A)**.

Chapter 4

Experimental

4.1 Extraction and Isolation

Approximately 1000 grams of dried leaves from each species were extracted using an initial mixture of CH_2Cl_2/MeOH (1:1), MeOH and MeOH/H_2O (1:1), by cold percolation at room temperature. For the species *S. laciniatum* and *S. terebinthinaceum* a 50 g sample of dried leaf material was used. The combined methanolic and aqueous methanolic extracts were subjected to initial fractionation on a polyamide column, followed by repeated column chromatography on Sephadex LH-20 as well as RP-C_{18}, to yield the flavonoids.

The species *Silphium albiflorum* and *S. terebinthinaceum* provided the purified flavonols used as standards for the other analyses: isorhamnetin 3-*O*-*α*-L-rhamnosyl (1'''→6'') –*O*-*β*-D-galactopyranoside 7-*O*-*β*-L-apiofuranoside (**1A**), quercetin 3-*O*-*α*-L-rhamnosyl (1'''→6'') –*O*-*β*-D- galactopyranoside 7-*O*-*β*-L-apiofuranoside (**2A**), isorhamnetin 3-*O*-*β*-D-glucopyranoside, hyperoside, rutinoside, quercetin 3-*O*-*β*-D-galactopyranoside, quercetin 3-*O*-*β*-D-glucopyranoside, hyperoside and rutinoside. The species *S. astericus* provided the new compound quercetin 3-*O*-*β*-L-apiofuranoside 7-*O*-*α*-L-galactosyl (1'''→6'') –*O*-*β*-D-rhamnopyranoside (**3A**)**.** The species *S. perfoliatum* provided standards for four of the identified kaempferol flavonoids.

Identification of all of the flavonoids employed as standards from both *S. albiflorum*, *S. asteriscus* and *S. perfoliatum* were achieved by standard procedures outlined by Dr. Mabry and others (Mabry *et al*., 1970; Markham, 1982; Markham *et al*.,

1982; Markham and Geiger, 1994), including acid hydrolysis and spectral analysis (1D and 2D NMR, MS, UV). In some analyses, LC-MS^n with post-column manganese complexation was utilized (Davis and Brodbelt, 2005).

^1H (500 MHz) and ^{13}C NMR (125 MHz) spectra were measured in DMSO-d_6 at room temperature on a Bruker 500 MHz instrument. The chemical shifts are given in δ values (ppm) with TMS (0.03%) added as an internal standard. UV spectra were recorded on a Lambda 35 Perkin Elmer spectrophotometer. Mass spectra (CI, FAB and HR FAB) were recorded on a Finnigan MAT TSQ 70 spectrometer. Column chromotography was performed using both Polyamide (ICN Biomedical GmbH) and Sephadex LH 20 (Fluka). HPLC analysis were run using LiChroprep RP-18 (25-40 μm; Merck) columns equipped with a Beckman 110B Solvent Delivery Module pump; the flow rate was 0.2 ml/min. Paper chromotography was performed using Whatman No. 1 paper in (1) 15% HOAc; (2) BAW (*n*-BuOH-HOAc-H_2O, 4:1:5; upper layer), (3) EtOAc-HOAc-H2O (10:2:3, an organic layer). TLC was carried out on cellulose (Merck) plates in: 1, 2 and 4 [Bz-HOAc-H_2O (125:72:3)] and on silica gel 60 F_{254} (Merck) plates in: 5 [*n*-PrOH-EtOAc-H_2O (7:2:1)]. Solvent 4 was used for aglycones, whereas solvent 5 was applied for sugar analysis. The flavonoid spots were checked under UV_{360nm} light and visualized with 0.1% diphenyl-boric acid–ethanolamine complex in MeOH using Naturstoffreagenz A, (Roth). Aniline phthalate was employed as a spray for the color detection of the sugars.

LC conditions included approximately 0.1 mg of the mixture of compounds dissolved in 0.5 ml methanol. HPLC analysis was performed using an Alliance 2690

HPLC system (Waters, Milford, MA). The separation was performed on a Waters Symmetry C_{18}, (2.1 x 50 mm x 3.5 μm) column and guard column, with a flow rate of 0.3 ml/min, and injection volumes of 10-40 μL. The mobile phases were solvent A (water with 0.33% formic acid) and solvent B (acetonitrile with 0.33% formic acid). An isocratic separation method was used, holding the mobile phases at (86:14) A:B for 16 minutes. The column effluent was monitored by a UV detector at 280 nm, then lead without splitting into a LCQ Duo quadrupole ion trap mass spectrometer (ThermoFinnigan, San Jose, CA) equipped with electrospray ionization (ESI) source. The mass spectrometer was operated in negative ion mode in order to identify the aglycone portions of the unknowns. The following parameters were used: spray voltage, -4.5 V; sheath gas, 20 units; auxiliary gas, 5 units; heated capillary temp., 200 ˚C; capillary voltage, -45 V; tube lens offset, -45 V (Davis and Brodbelt, 2004, 2005). The analysis was run in positive mode with 500 μM $MnCl_2$ dissolved in methanol added at 20 μl/min via mixing between the UV detector and the mass spectrometer. The spray conditions were the same with the following exceptions: spray voltage, +4.5 kC; capillary voltage, +44 V; tube lens offset, +35 V.

Acid hydrolysis was performed using a solution of each compound in 1% aqueous HCl and heating for 90 minutes. The mixture was extracted in Et_2O to obtain the aglycone. The remaining aqueous layer was neutralized and the released sugar moieties determined. The Et_2O and aqueous fractions were concentrated and dried for identification (TLC, systems 4 and 5).

Analytical grade solvents were used for HPLC, UV and all NMR analysis. Commercial standards of kaempferol 3-*O*-glucoside and isorhamnetin 3-*O*-glucoside were purchased from Indofine (Somerville, NJ). The standards were dissolved in MeOH and stored in the dark at 4°C. Manganese (II) chloride was purchased from Aldrich (Milwaukee, WI).

Reversed Phase HPLC/MS/MS Tandem mass spectrometry was carried out using a micro-capillary gradient LC system (1100 series, Agilent Technologies, San Jose, CA) on-line with an Esquire-LC ion-trap (Bruker Instruments, Bellerica, MA). A reverse phase C_{18} MS column (Vydac 218 MS 3.1505, 150 um x 5 cm, purchased from the "Nest Group") was initiated at a flow rate of 2 um/minute. Mobile phase A consisted of 0.1% formic acid, 0.01% trifluoroacetic acid in LC grade water with mobile phase B consisting of 0.1% formic acid, 0.01% trifluoroacetic acid in LC grade water/acetonitrile (10/90) in gradient mode. The column was equilibrated at 5% phase B with the gradient starting at time 0 minutes at 5% phase B, increased to 95% phase B in 56 minutes, followed by an increase to 100% phase B in 2 minutes. Here it was held at 100% phase B for 4 minutes, followed by a gradual decrease to 5% phase B within 3 minutes. A total separation time of 65 minutes was applied. The effluent from HPLC separations was introduced on-line into the orthogonal Esquire-LC electrospray source. The ion spray experiment was performed in positive mode at +4000 V, end plate offset was -500V. Ions were scanned from 50 to 1500 *m/z*, the nebulizer gas was set to 23.0 psi, the dry gas to 7.00 L/min and the drying temperature at the capillary entrance was 150°C. Capillary exit was set to 76.1 V, skimmer 1 at 26.1 V, trap drive to 58, an average of 3 spectra were acquired over a

time period of 100 ms, the collision gas was helium, and MS/MS experiments were performed in the auto mode.

4.2 Plant Material, *Silphium* section *Composita*

S. albiflorum leaves were collected in Bosque Co., Norse Community, TX on dry upland *Juniperus* savannah approximately 52 mi. SW of the city of Clifton on the right side of Farm Road 219, TX, in July 2002. The plant material was identified by Prof. Mark W. Bierner (Boyce Thompson Arboretum, Superior, AZ 85273) and a voucher specimen (No. JW2002/7/1) was deposited at The University of Texas at Austin. The leaves were dried at room temperature prior to extraction.

S. laciniatum L. was collected in Greene Co., AL south of Eutaw at mile marker 44 on US Rt. 11, 2 miles south of the intersection US 43 and AL Rt. 14. The plants were growing with *Silphium asteriscus* var. *latifolium* and vouchered by Dr. Jennifer Clevinger (No. 232) July 26, 2003. The plant material was identified by Dr. Jennifer Clevinger and deposited at The University of Texas at Austin. The leaves were dried at room temperature prior to extraction.

S. compositum Michx. leaves were collected in Polk Co., TN Cherokee National Forest, along Oswald Dome between 1 to 2 miles Southwest of Oswald Dome, West of TN 30, SW of Reliance, June 19, 2003. The plant material was identified by Dr. Jennifer Clevinger, and a voucher specimen (No.228) was deposited at The University of Texas at Austin. The leaves were dried at room temperature prior to extraction.

The specimens used for *S. terebinthinaceum* Jacq. were collected in Dade Co., GA along the edge of a pine-oak forest 1.6 miles south of the town of Trenton, GA, June 19, 2003.

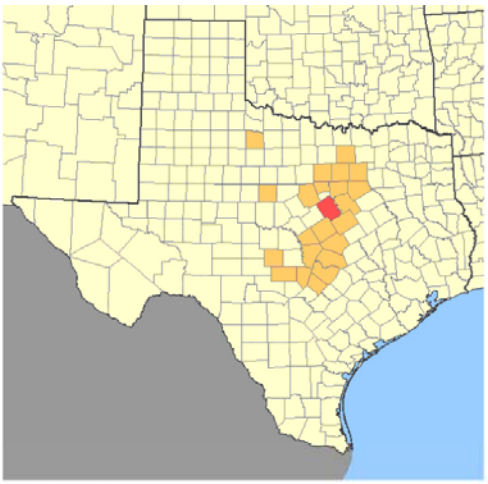

Silphium albiflorum
Bosque County, Texas:
Norse community, 52 miles Southwest of Clifton on the right side of FM 219.
June 16, 2002.
Voucher: M. Bierner (No. JW2002/7/1)

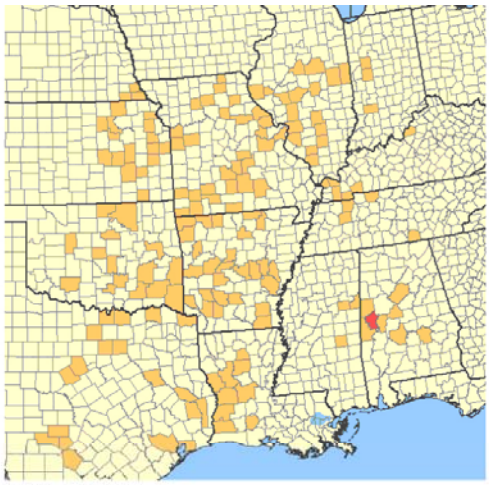

Silphium laciniatum
Green County, Alabama:
South of Eutaw at mile marker 44 on U.S. Route 11, 2 miles South of intersection U.S. Route 43.
July 26, 2003.
Voucher: J. Clevinger (No. 232).

Silphium compositum
Polk County, Tennessee:
Along Oswald Dome Road btw. 1 and 2 miles Southwest of Oswald Dome, Southwest of Reliance.
June 19, 2003.
Voucher: J. Clevinger (No. 228).

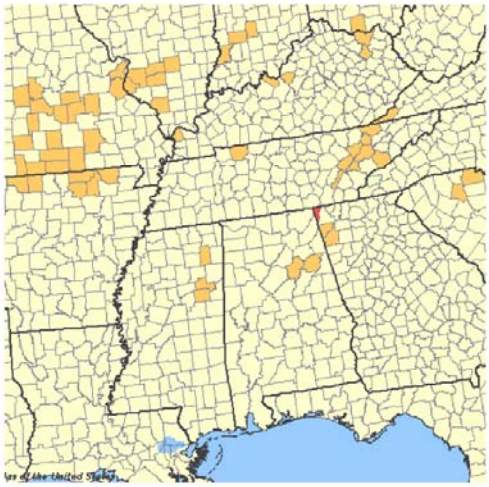

Silphium terebinthinaceum
Dade County, Georgia:
Along West side of U.S. 11, 1.6 miles South of Trenton on the edge of a pine forest.
June 19, 2003.
Voucher: J. Clevinger (No. 218).

Figure 4.1 Counties marked in red indicate the source of collections for each of the four species within *Silphium* section *Composita* (Clevinger 1999).

The plant material was identified by Dr. Jennifer Clevinger, S. and a voucher specimen (No.218) was deposited at The University of Texas at Austin. The leaves were dried at room temperature prior to extraction.

4.3 Plant Material, *Silphium* section *Silphium*

S. asteriscus leaves were collected in Dade Co., GA along the west side of US 11, 1.6 mi south of Trenton, GA at the edge of a pine-oak forest, growing with *S. terebinthinaceum* var. *pinnatifidum*, June 19, 2003. The plant material was identified by Dr. Jennifer Clevinger, and a voucher specimen (No. 219) was deposited at The University of Texas at Austin. The leaves were dried at room temperature prior to extraction.

S. brachiatum leaves were collected in Franklin Co., TN along the east side of TN 56, 5.1 mi south of Sewance, along the edge of the woods, some plants in deep shade, 4-6 ft. tall, June 19, 2003. The plant material was identified by Dr. Jennifer Clevinger and a voucher specimen (No. 224) was deposited at The University of Texas at Austin. The leaves were dried at room temperature prior to extraction.

S. integrifolium was collected in Bowie Co., TX, on the right side of Hwy. 30 approximately 10.5 miles southwest of the community of New Boston. Larger healthy populations were also found in Hunt Co., TX at the Mathews Prairie Preserve approximately 1.2 miles directly north of the town of Floyd. The plant material was identified by Jeffrey Williams, Małgorzata Wojcińska and vouchered by Dr. Mark

Bierner. A specimen was deposited as No. JW2002/7/2 at the University of Texas at Austin.

S. mohrii leaves were collected in Dade Co., GA along GA 136, 3.2 mi east of Trenton in a switchback curve, open area near the woods, growing with *S. asteriscus*, June 19, 2003. The plant material was identified by Dr. Jennifer Clevinger and a voucher specimen (No. 221) was deposited at The University of Texas at Austin. The leaves were dried at room temperature prior to extraction.

S. perfoliatum var. *connatum* leaves were collected in Giles Co. VA. along the New River on U.S. highway 460, northeast of Glen Lyn, 1.4 mi east of intersection 260 and 460, June 21, 2003. The plant material was identified by Dr. Jennifer Clevinger and a voucher specimen (No. 229) was deposited at The University of Texas at Austin. The leaves were dried at room temperature prior to extraction.

S. radula var. *gracile* was collected in Lee Co. TX. near rest area 20 ft. west of a historical marker along US 290, 4.85 miles West of the jct. of 290 and US 77, West of the city of Giddings. The plant populations numbered in the hundreds scattered along both sides of US 290 traveling east towards Giddings. The plant material was identified by Jeffrey Williams and vouchered by Dr. Mark Bierner (June 19, 2002). A specimen was deposited as No. JW2002/7/3 at the University of Texas at Austin.

S. wasiotense leaves were collected in Norris Co., Tennessee: Norris Dam State Park, along north side of Lower Clear Creek Road, 0.5 mi from junction of US 441 and the Norris Dam Grist Mill, on the edge of the woods near the road cut. Other species in the area included: *Platanus*, *Acer*, *Sassafras*, and *Quercus*, June 18, 2003. The plant

material was identified by Dr. Jennifer Clevinger and a voucher specimen (No. 217) was deposited at The University of Texas at Austin. The leaves were dried at room temperature prior to extraction.

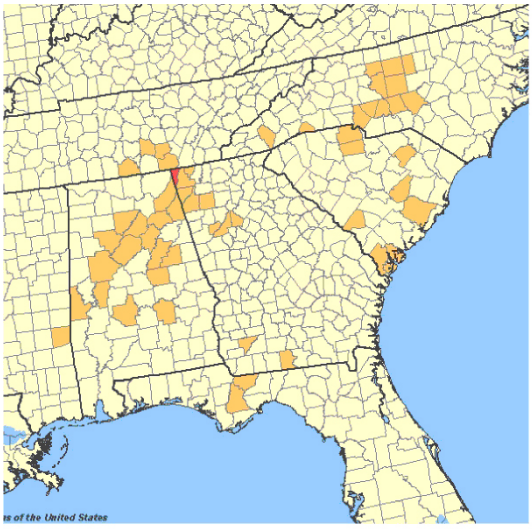

Silphium asteriscus
Dade County, Georgia:
Along the West side of U.S. 11, 1.6 mi South of Trenton.
June 19, 2003.
Voucher: J. Clevinger (No. 219).

Silphium mohrii
Dade County, Georgia:
Along GA 136, 3.2 miles East of Trenton.
June 19, 2003.
Voucher: J. Clevinger (No. 221).

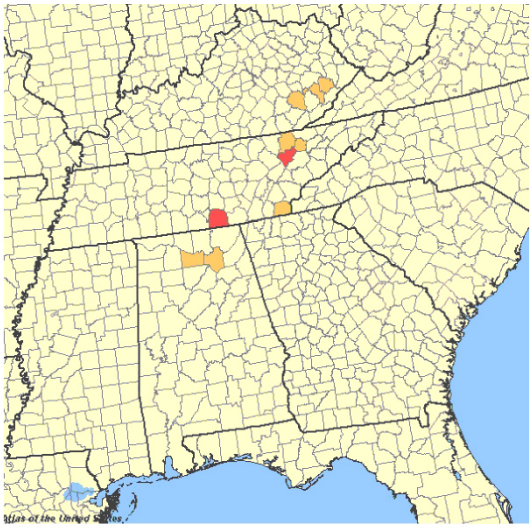

Silphium brachiatum
Franklin County, Tennesse:
Along East side of TN 56, 5.1 miles South of Sewanee.
June 19, 2003.
Voucher: J. Clevinger (No. 224).

Silphium wasiotense
Anderson County, Tennesse:
0.5 miles from junction of U.S. 441 and Norris Mill.
June 18, 2003.
Voucher: J. Clevinger (No. 217).

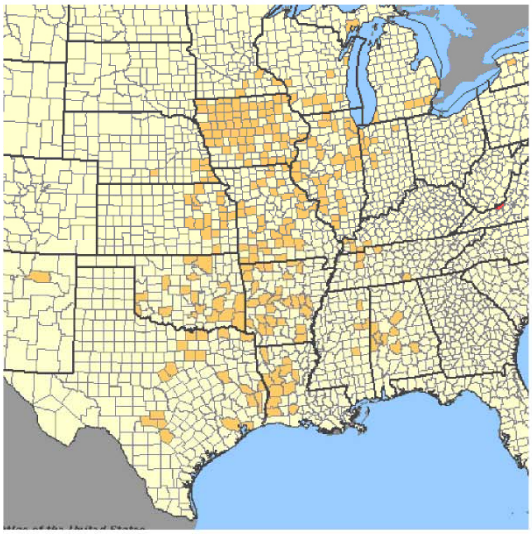

Silphium perfoliatum
Midwestern United States
Giles County, Virginia:
Along the New River on U.S. Highway 460, Northest of Glen Lyn, 1.4 miles East of intersection 260 and 460.
June 21, 2003
Voucher: J. Clevinger (No. 229).

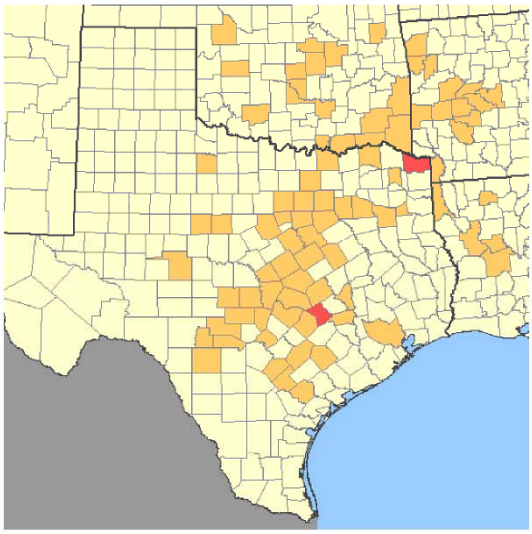

Silphium integrifolium
Bowie County, Texas:
10.5 miles Southwest of New Boston.
July 13, 2002.
Voucher: M. Bierner (JW2002/7/2).

Silphium radula
Lee County, Texas:
5 miles West of Giddings.
June 19, 2002.
Voucher: M. Bierner (JW2002/7/3).

Figure 4.2 Counties marked in red indicate the source of the collections for each of the seven species within *Silphium* section *Silphium* (Clevinger 1999).

Chapter 5

The Comparative Qualitative and Quantitative Distribution of Phenolic Acids in the Leaves of *Silphium* Species

High performance liquid chromatography of extracts from all eleven species in the genus *Silphium* showed the presence of both hydroxybenzoic and hydroxycinnamic phenolic acids. Within the genus *Silphium*, three of the four species in *Silphium* section *Composita*, namely *S. albiflorum*, *S. laciniatum* and *S. terebinthinaceum*, were higher in total phenolic acid concentration than other species in the genus except for *S. integrifolium* from section *Silphium*, which contained a similar amount. Members of section *Composita* provided higher concentrations specifically for hydrocaffeic, ferulic and protocatechuic acids (Figure 5.1a-b). The seven species comprising section *Silphium* showed only moderate levels of the phenolics hydrocaffeic, gallic and *p*-coumaric acids.

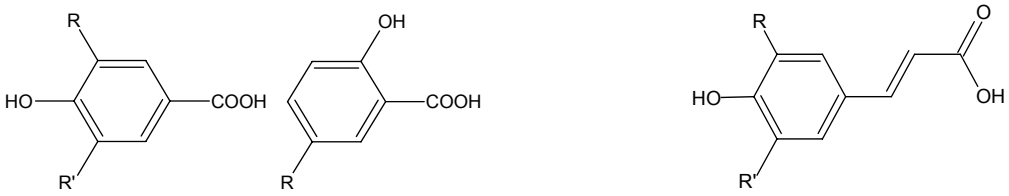

Figure 5.1: The chemical structures for types of hydroxybenzoic (A) and cinnamic acids (B), R groups = H, OH or OCH_3.

Each of the eleven species was extracted sequentially first using ether and then ethyl acetate (Wojcińska, 1998). The seven species in the section *Silphium* yielded more total phenolic extract using ether than did three of the four species in section *Composita*, *S.*

laciniatum, *S. composita* and *S. terebinthinaceum* when compared to their ethyl acetate extracts.

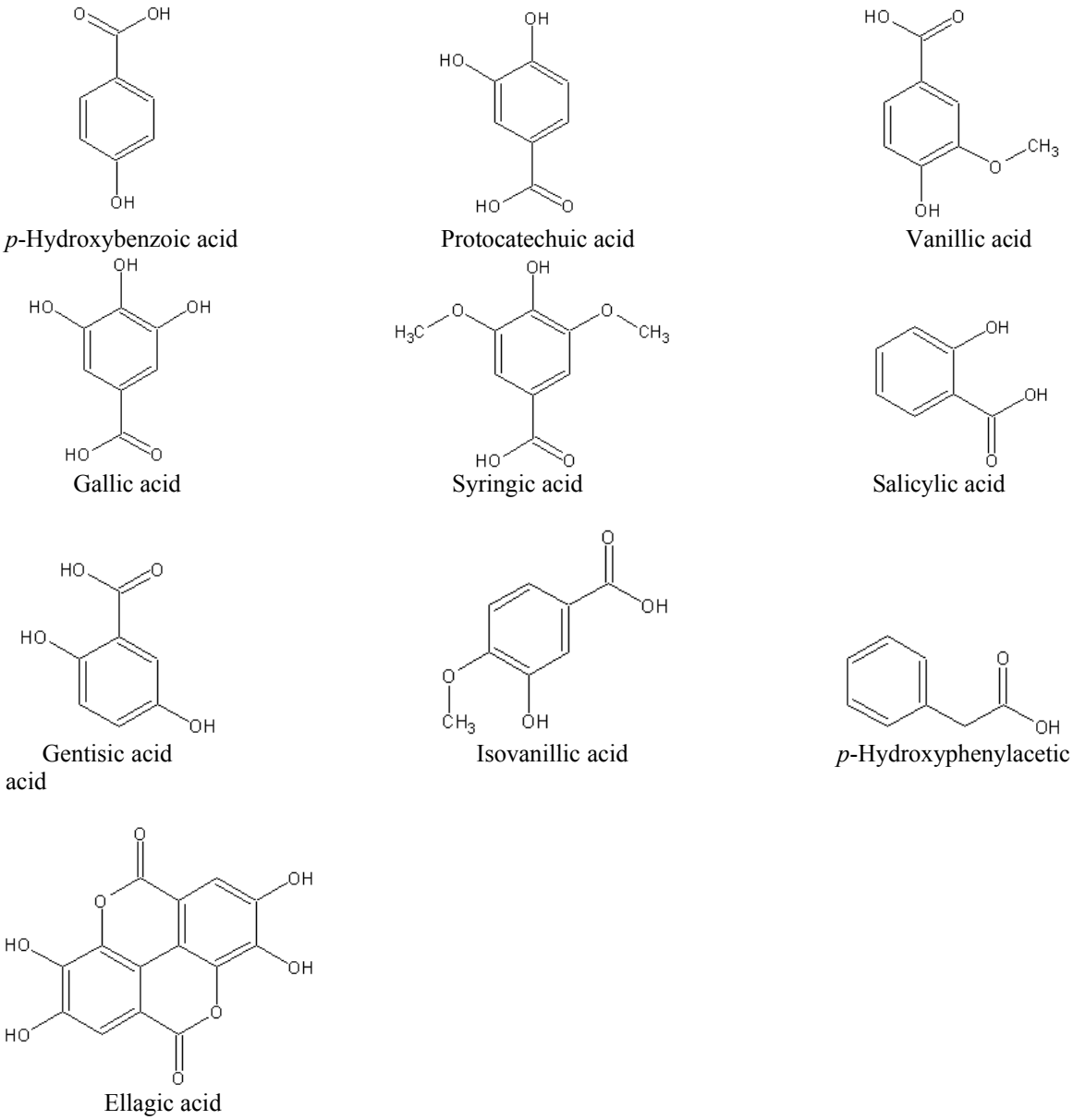

Figure 5.2: The hydroxybenzoic acids found in *Silphium*.

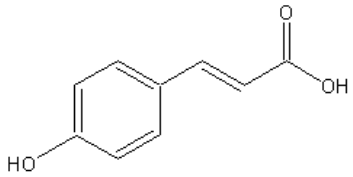

p-Coumaric acid

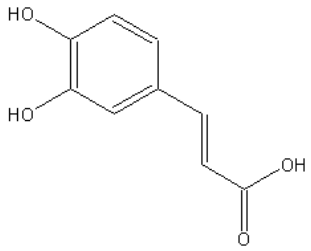

Caffeic acid

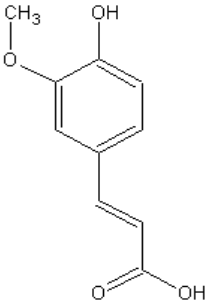

Ferulic acid

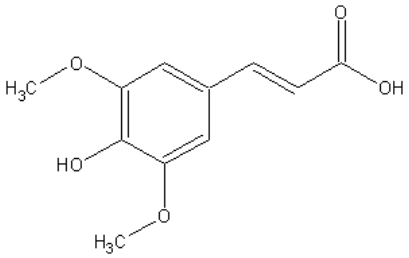

Sinapic acid

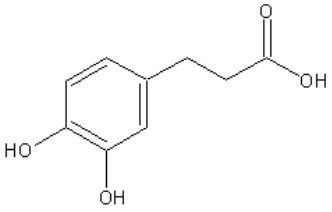

Hydrocaffeic acid

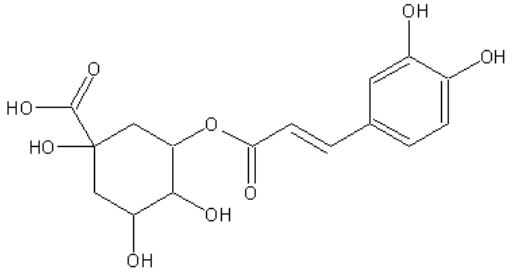

Chlorogenic acid

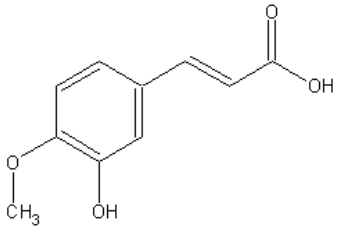

Isoferulic acid

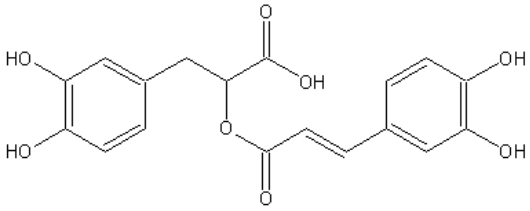

Rosmarinic acid

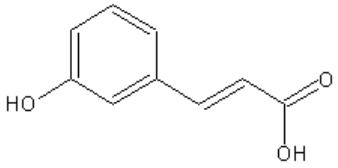

m-Coumaric acid

Figure 5.3: The hydroxycinnamic acids found in *Silphium*.

Phenolic acids, known for their roles as antiseptics, antioxidants and biochemical intermediates (Borkowski, 1993), are divided into two categories: the benzoic acids containing seven carbon atoms (C6-C1) and the cinnamic acids with nine carbon atoms (C6-C3) (Ribéreau-Gayon, 1972).

The benzoic acids are widely distributed among both angiosperms and gymnosperms and are direct precursors for lignin formation (Harborne and Simmons, 1964). Gallic and ellagic acids are precursors to many plant tannins and are present in as many as 40 orders of dicotyledons (Ribéreau-Gayon, 1972).

The second major category of phenolics is the cinnamic acids, which can exist as *cis* and *trans* isomeric forms. Biologically, most cinnamic acids are present in the more stable *trans* conformation, but are easily converted to the *cis* form on exposure to light (Ribéreau-Gayon, 1972). *Para*-coumaric acid is the most commonly encountered member of this group, which also includes the well-studied caffeic and chlorogenic acids, with caffeic acid having its name derived from early twentieth century extractions from coffee (Pictet and Brandenberger, 1960). Caffeic and protocatechuic acids have been shown to possess antiseptic activity and to stimulate immunoglobin G and immunoglobin M formation (Borkowski, 1993). Caffeic and ferulic acids exhibit choleretic and cholekinetic medicinal properties (Swiatek, 1998; Takeda, 1981).

Recent investigations of the species *S. perfoliatum* yielded seven major phenolic compounds. Using ether as the extracting solvent, one hydroxybenzoic acid (protocatechuic) and two hydroxycinnamic acids (*p*-coumaric and caffeic) were found in high concentration; three other hydroxybenzoic acids, namely *p*-hydroxybenzoic, syringic and vanillic acids, along with the cinnamic compound, ferulic acid, were obtained in smaller concentrations.

Leaf extract from this species have been reported to show hypocholesterolemic and hypotriglyceridemic circulatory effects (Syrov, 1992).

Leaves of the three *Silphium* species, *S. perfoliatum*, *S. trifoliatum* and *S. integrifolium*, were all analyzed for their free and released phenolic forms; all three species yielded caffeic, *p*-coumaric, protocatechuic and *p*-hydroxybenzoic acids. *S. trifoliatum* and *S. integrifoliatum* also afforded ferulic and salicylic acids while *S. perfoliatum* contained vanillic acid. *S. integrifolium* was found to contain the highest concentration of phenolic compounds with protocatechuic acid being the dominant component of the extract (at 21mg/100g of dry material).

Pharmacists and nutritionists are focusing on the uses of these important bioactive acids; their activity in inhibiting diseases caused by active free radicals is of particular interest and perhaps related to the use of *Silphium* extracts as folk remedies for upper respiratory disorders (Steinmetz, 1954).

5.1 Experimental Procedures

The plant samples for the phenolic acid analyses for all eleven *Silphium* species were collected in July 2002 (see Chapter 2 for details). Approximately 500-1000 grams of dry leaf material were removed from eleven separate populations. The leaves were collected in the field while the plants were in bloom. The individual species were vouchered by Dr. Jennifer Clevinger at both James Madison University in Harrisburg, VA and here at The University of Texas at Austin by Dr. Mark Bierner. The aerial parts were separated, dried and stored in the dark at room temperature.

The dried leaves were crushed and extracted in methanol and water (1:1) three times over a 72 hour period. The crude aqueous extract was filtered using 12.5 cm MFS

Qualitative filter paper and the extract was evaporated to dryness. A 50 g dried crude extract from each species was resuspended in 50 ml of water and then defatted using 50 ml of *n*-hexane four times followed by two 50 ml increment/washings with chloroform. The organic and water layers were further divided using a standard 1.0 liter separating funnel. The organic layer was concentrated and analyzed by thin layer chromatography and no detectable amounts of phenolic acids were observed. The acids were extracted from the 50 ml water layer under a standard fume hood on addition of 3-4 liters of ether and then approximately the same volume of ethyl acetate (Swiatek, 1977). The final purification of each ether and ethyl acetate sample was performed using Waters 6cc C_{18} solid phase silica gel cartridges. Both the ether and ethyl acetate dried samples were weighed and divided in half, with one half of each sample separated for further TLC examination and the remaining portion for HPLC analysis (Figure 5.3) (Appendix Table C.1). HPLC qualitative injection from each of the 22 samples was performed in Dr. Klaus Linse's laboratory here at the University of Texas at Austin.

Using the extraction procedure above, an applied quantitative approach was followed in comparing the proportions of each phenolic acid separated. Standard dilutions from 0.01mg/ml to 0.025mg/ml provided the calibration curves measuring the absorbencies common for phenolics λ 280 and λ 254 (Appendix Table C.2).

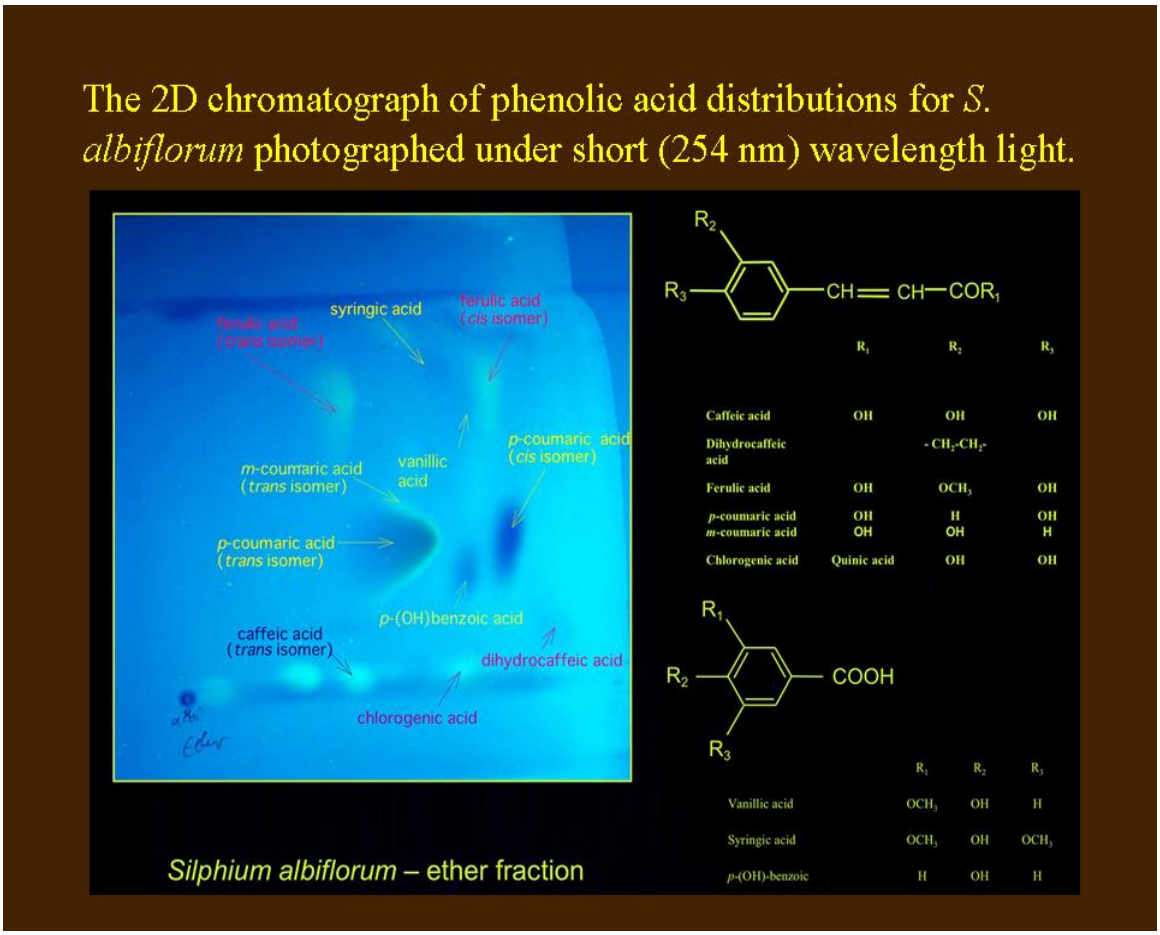

Figure 5.4: Each of the eleven species was analyzed using cellulose 2-D TLC plates ran in 15% acetic acid and BAW (butanol/acetic acid/ water, 4:1:5).

The phenolic acids were analyzed using 50% methanol HPLC/UV elution spectroscopy. The phenolics were eluted in a process using a C_{18} reverse-phase column by gradient analysis in 1.25% acetic acid and filtered using HPLC grade water (buffer A) and acetonitrile (buffer B) (0 min, 8% buffer B; 0.5 min, 11% buffer B; 50.5 min, 12% buffer B; and 61 min, 40% buffer B) as the mobile phase for recoveries were obtained for simultaneous determination of the phenolic compounds. This method was used for the material from all eleven *Silphium* species including the ether and ethyl acetate extracts and all samples were measured at wavelengths λ 280 and λ 254 (Appendix Table C.2).

The phenolic acid standards, chlorogenic, hydrocaffeic, isovanillic, *m*-coumaric, *p*-coumaric and protocatechuic, were purchased from Sigma (MO, USA). Gallic and sinapic acids were obtained from Roth (Germany). The water and acetonitrile were both HPLC grade. The stock solutions for each standard were prepared at a concentration of 1.0/mg/mL in methanol and stored at 2° C in darkness. Working dilutions were prepared in HPLC grade methanol and water. Calibration curves aided in the statistical analysis for the injections-thus the linear ranges for the curves are given as maximum and minimum values (Appendix Table C.3).

An individual species analysis at λ 280 for ether and ethyl acetate yielded different phenolic acids for each species (Appendix Table C.2). HPLC/UV analysis of the seven species contained in the second section, section *Silphium*, showed the presence of *p*-hydroxybenzoic acid in six of the seven species. Four species, *S. brachiatum*, *S. perfoliatum, S. mohrii* and *S. wasiotense* all included a peak consistent for ferulic acid. The same four species, in addition to *S. radula*, shared the same retention time for an unknown at just beyond 20 minutes.

5.2 Results and Discussion

The yield of total phenolic acids was greater for the species in section *Composita* than those in section *Silphium* (Table 5.1). The concentrations of the benzoic acids were clearly section specific with greater total amounts belonging to species in section *Composita* (Tables 5.2 and 5.3). For the cinnamic acids, the numbers of individual acids were more diversified, and higher total concentrations of these acids were also detected in section *Composita* (Tables 5.4 and 5.5).

Within the *Silphium* genus, members of the section *Composita* provided a considerably higher concentration of the acids hydrocaffeic, ferulic and protocatechuic (Appendix Table C.7). The seven species comprising section *Silphium* showed moderate levels of hydrocaffeic, gallic and *p*-coumaric acid, while HPLC/UV analysis of species in section *Composita* revealed the presence of protocatechuic, *p*-hydroxybenzoic and vanillic acids. The two closely related species, *S. albiflorum* and *S. laciniatum,* exhibited a complentary signal for ferulic acid (Figures 5.4 and 5.5, peak 7). *Silphium composita* and *S. terebinthinaceum* both contained five prominent peaks in the ethyl acetate extract with retention times between 8 and 15 minutes (Figures 5.6 and 5.7, peaks A, B, C, D, E). With the exception of protocatechuic acid in *S. terebinthinaceum*, all five peaks were unknowns and they were not detected in other *Silphium* species. At a retention time of approximately 30 minutes, two peaks were observed for all four species of section *Composita*- a smaller peak to the left dwarfed by a larger signal to its right (retention time ~32 min.). For the species *S. laciniatum* and *S. composita*, the larger peak to the right matched the retention time of *p*-coumaric acid (Figures 5.5 and 5.6, peaks 6 and 7, respectively). The size and area of this signal may also be overlapping the signal, possibly covering the presence of this same phenolic compound in *S. albiflorum* (Figure 5.4, peak C). These two peaks were detected throughout the genus with *S. wasiotense* (Figure 5.14) being the only exception (Figures 5.4 to 5.14); however, both peaks were lower in absorbance in three of the four species in section *Composita* relative to measurements for the seven species of section *Silphium* (Figures 5.4 to 5.14).

In section *Composita*, among the hydroxybenzoic acids, ethyl acetate extracted a greater variety of phenolics while ether extracted larger total concentrations. Among the

cinnamic acids, ether extraction provided for both a wider number and far greater concentration of phenolic acids. These acids included caffeic, hydrocaffeic and ferulic acids.

Ether extraction yielded for *S. terebinthinaceum* and *S. albiflorum* the highest amounts of hydrocaffeic acid while *S. laciniatum* provided high concentrations of ferulic acid. Higher amounts of *m*-coumaric acid were also obtained from the latter species; however more caffeic, chlorogenic and *p*-coumaric acids were recovered using ethyl acetate.

Ether was the solvent of choice with respect to members of section *Silphium*. Regarding the benzoic acid standards, extraction of all nine phenolic compounds were present among the species of this section. Of the nine benzoic acids identified, higher concentrations of 6 out of the 9 acids were detected using ether. Pertaining to the highest total phenolic acid concentrations collected, *S. radula* and *S. integrifolium* produced the highest at 0.42mg/100g and 0.35mg/100g respectively (Table 5.1). For the hydroxycinnamic acid concentrations collected in the seven plant species of section *Silphium*, *S. radula* produced the highest concentration consisting primarily of hydrocaffeic acid. *S. integrifolium* also contained moderate amounts of rosmarinic, p-coumaric and hydrocaffeic acids (Appendix C.7).

Among the hydroxybenzoic acid extracts, *S. brachiatum* again contained the least amounts of compound; however it had considerablyhigher cinnamic acid content. These data support the molecular/taxonomic difficulty of this plant as compared with the other eleven species of the genus.

Finally, notable among the total phenolic yields from *Silphium* section *Silphium* was the closely extractable amounts of compounds from the species *S. perfoliatum* and *S. wasiotense* (Table 5.1).

5.3 Summary and Conclusions

Although phenolic acids diverged early and down several biophysiological pathways, in the genus *Silphium*, their distribution among these eleven species supports Dr. Clevinger's molecular revision.

Qualitative and quantitative chemical analyses indicate a close relationship between the species *Silphium albiflorum* and its ancestral species *S. laciniatum* (Figures 5.4 and5..5). These same analyses involving both known and unknown compounds provide a chemotaxonomic phenolic acid link between the species *S. compositum* and S. *terebinthinaceum*; our findings also suggest that these two species may represent new commercial sources of *p*-hydroxybenzoic compounds (Figures 5.6 and 5.7). From *Silphium* section *Silphium*, *S. perfoliatum* and *S. wasiotense* contained similar total yields of the eighteen phenolic acids sampled, although *S. mohrii* contained closer extractable amounts to the former species than that of *S. integrifolium*. It may be that the isolation and identification of the glycosylated forms of these phenolic acids leads to greater taxonomic relevance especially involving section *Silphium*. These data support Dr. Clevinger's systematic revision providing comparative evidence between both types of hydroxy phenolic acids isolated in each of the two *Silphium* sections.

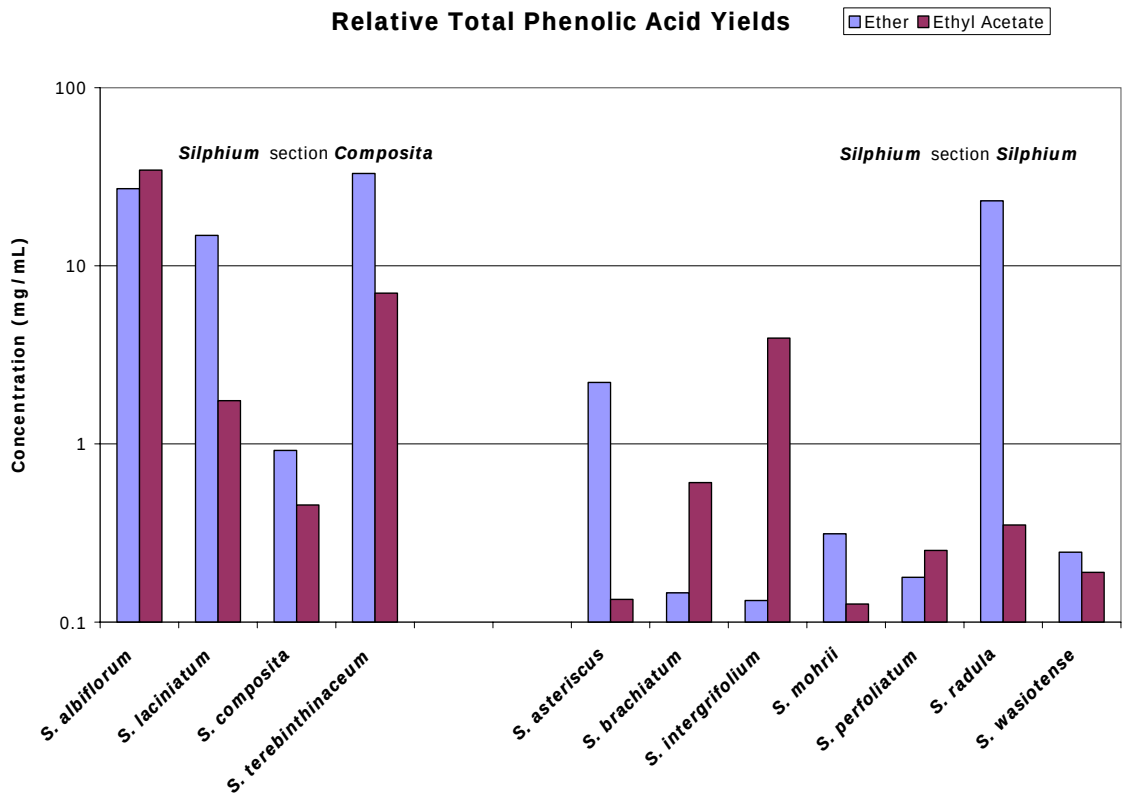

Table 5.1: Relative yields of phenolic acids for all 11 *Silphium* species with two solvents.

Observations taken during the extraction phase showed that the leaves from species of lighter chlorophyll coloration contained higher total phenolic acid yields (*S. albiflorum*, *S. laciniatum, S. compositum, S. terebinthinaceum, S asteriscus, S. integrifolium*). The species *S. brachiatum*, *S. mohrii* and *S. wasiotense* (all with leaves dark in color, thick in texture and containing heavy extract emulsifications) had the least collected amounts, with *S. mohrii* yielding as little as 0.5%. Four species, *S. albiflorum, S. laciniatum, S.terbinthinaceum* and *S. integrifolium,* provided 10% by weight greater amounts of extract using ethyl acetate.

Presence of benzoic acids in genus *Silphium* section *Silphium*

	S. asteriscus	*S. brachiatum*	*S. intergrif*	*S. mohrii*	*S. perforliatum*	*S. radula*	*S. Wasiotense*
p-OH-Benz	++	+	+	+	+	+	++
Protocatechuic	+	+	+	+	+++	+	++
Vanillic	+	-	+++	++	+	+	+
Isovanillic	+	+	+	+	+	++	+
Gallic	+	+	++	++	++	+++	+++
Ellagic	+	+	+	+	+	+	+
Syringic	+	-	+	+	+	+	+
Salicylic	+	+	+	++	++	+	++
P-OH-Phen	+	+	+	++	+	++	+

Table 5.2: Comparative data for the presence of benzoic acids within the genus S*ilphium* section *Silphium*. The symbol "-" indicates none detected, "+" indicates a minor presence (1-74 micrograms), "++" indicates a moderate presence (75-174 micrograms), and "+++" indicates a major presence (175 or more micrograms).

Presence of benzoic acids in genus *Silphium* section *Composita*

	S. albiforum	*S. laciniatum*	*S. composita*	*S. terebintanaceum*
p-OH-Benz	+	+	+	+
Protocatechuic	+++	+++	+++	+++
Vanillic	+	+	-	-
Isovanillic	++	+	+	++
Gallic	+++	+++	+	+++
Ellagic	+	+	+	+
Syringic	-	+	+	-
Salicylic	+	+	-	+
P-OH-Phen	+	+	+	++

Table 5.3: Comparative data for the presence of benzoic acids in the species of S*ilphium* section *Composita*. The symbol "-" indicates none detected, "+" indicates a minor presence (1-74 micrograms), "++" indicates a moderate presence (75-174 micrograms), and "+++" indicates a major presence (175 or more micrograms).

Presence of cinnamic acids in genus *Silphium* section *Silphium*

	S. asteriscus	*S. brachiatum*	*S. intergrif*	*S. mohrii*	*S. perforliatum*	*S. radula*	*S. Wasiotense*
p-Coumaric	+++	++	++	+	+	-	+
Caffeic	+	+	-	+	-	+	+
Hydrocaffeic	+++	++	+++	-	+++	+++	-
Ferulic	-	-	-	+	-	-	-
Chlorogenic	+	+	+	+	+	+	+
Isoferulic	-	-	-	-	-	-	-
Rosmarinic	+	+	+	+	+	+	+
m-Coumaric	-	-	+	+	-	-	+

Table 5.4: Comparative data for presence of cinnamic acids in species *Silphium* section *Silphium*. The symbol "-" indicates none detected, "+" indicates a minor presence (1-99 micrograms), "++" indicates a moderate presence (100-199 micrograms), and "+++" indicates a major presence (200 or more micrograms).

Presence of cinnamic acids in genus *Silphium* section *Composita*

	S. albiforum	*S. laciniatum*	*S. composita*	*S. terebintanaceum*
p-Coumaric	+	+	+	+
Caffeic	+	+	+	++
Hydrocaffeic	+++	+++	-	+++
Ferulic	-	+	-	-
Chlorogenic	+	+	+++	++
Isoferulic	+++	+++	-	-
Rosmarinic	+	++	+	++
m-Coumaric	+	+	-	+

Table 5.5: Comparative data for presence of cinnamic acids in genus S*ilphium* section *Composita*. The symbol "-" indicates none detected, "+" indicates a minor presence (1-99 micrograms), "++" indicates a moderate presence (100-199 micrograms), and "+++" indicates a major presence (200 or more micrograms).

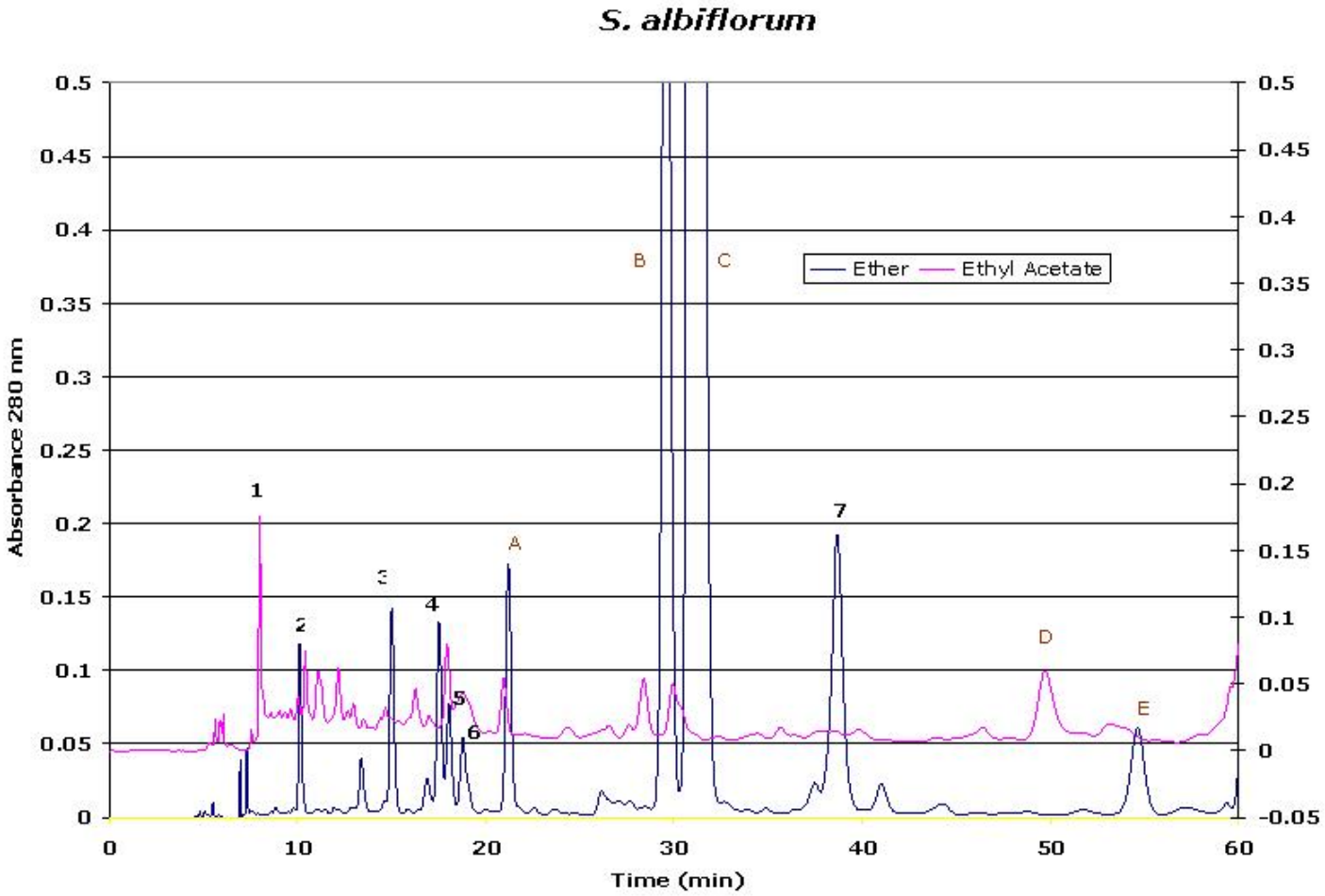

Figure 5.5: Standard phenolics denoted by number. 1. ellagic, 2. protocatechuic, 3. *P-hydroxyphenylacetic*, 4. vanillic, 5. caffeic, 6. hydrocaffeic, 7. ferulic. Unknowns are denoted by letters as follows: A, B, C, D, E.

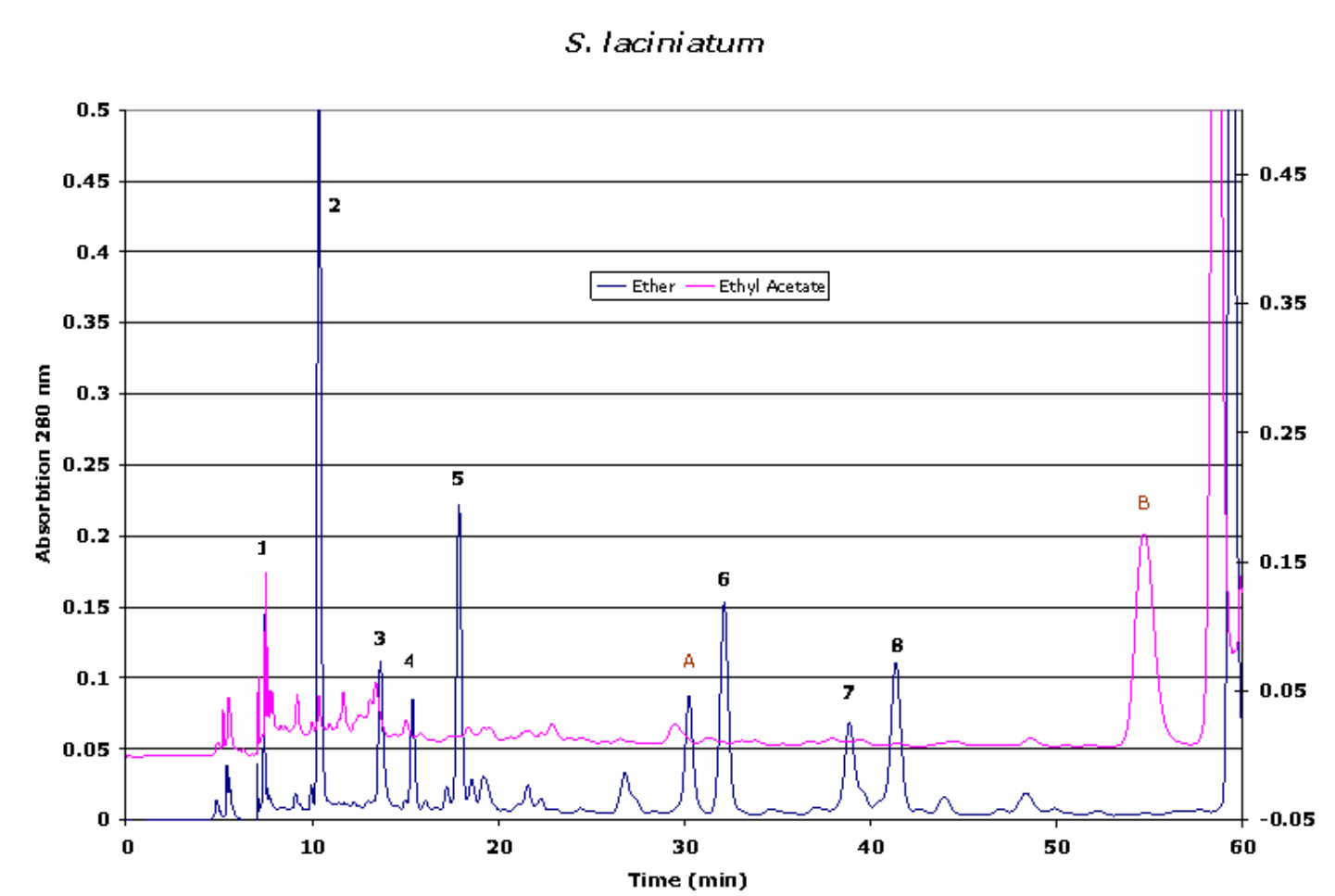

Figure 5.6: Standard phenolics denoted by number. 1. gallic, 2. protocatechuic, 3. chlorogenic, 4. *p*-OH benzoic, 5. vanillic, 6. *p*-coumaric, 7. ferulic, 8. *m*-coumaric. Unknowns are denoted by letters as follows: A, B.

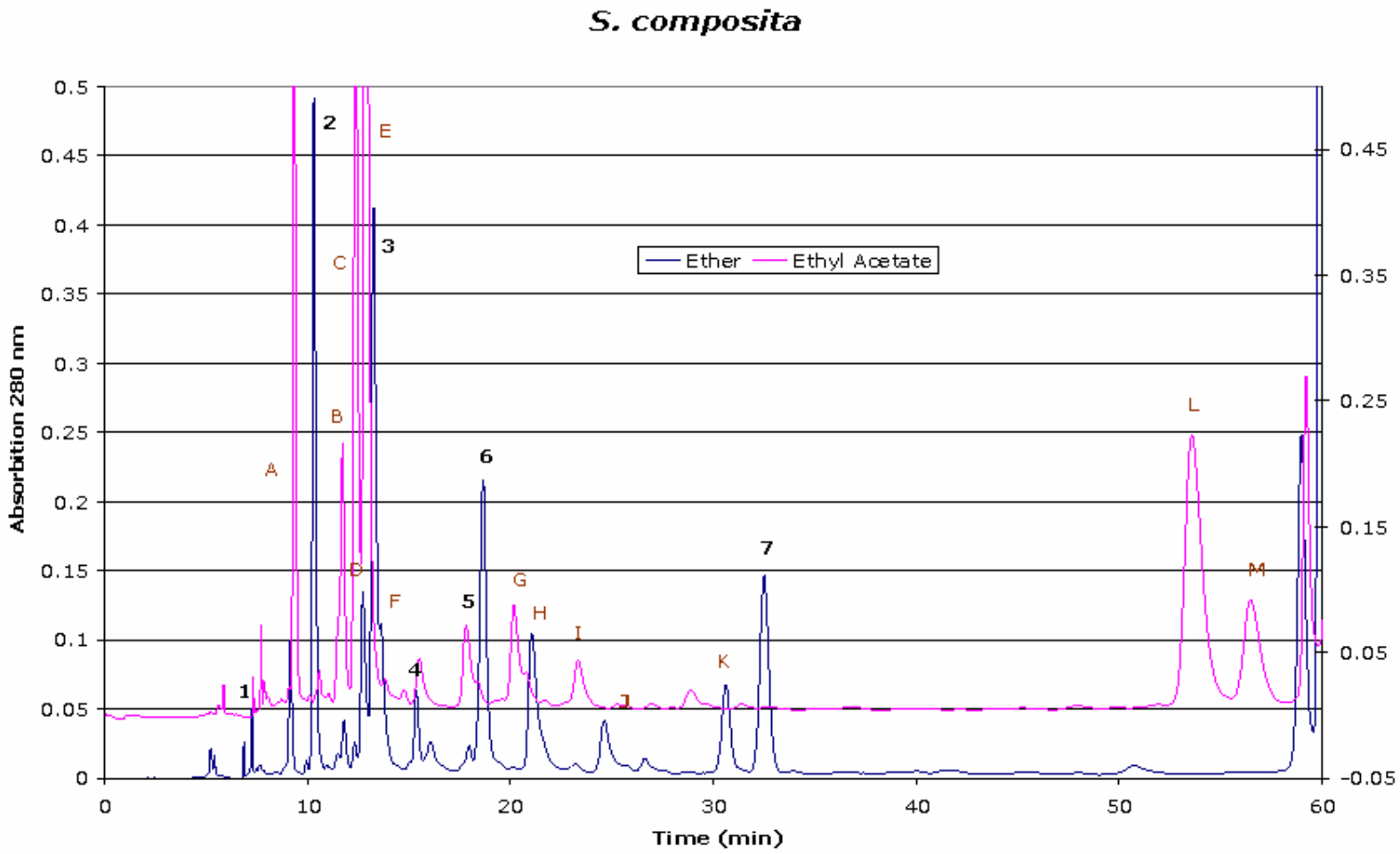

Figure 5.7: Standard phenolics denoted by number. 1. gallic, 2. protocatechuic 3. chlorogenic, 4. *p*-OH benzoic, 5. vanillic, 6. caffeic/hydrocaffeic, 7. *p*-coumaric. Unknowns are denoted by letters as follows: A, B, C, D, E, F, G, H, I, J, K, L, M.

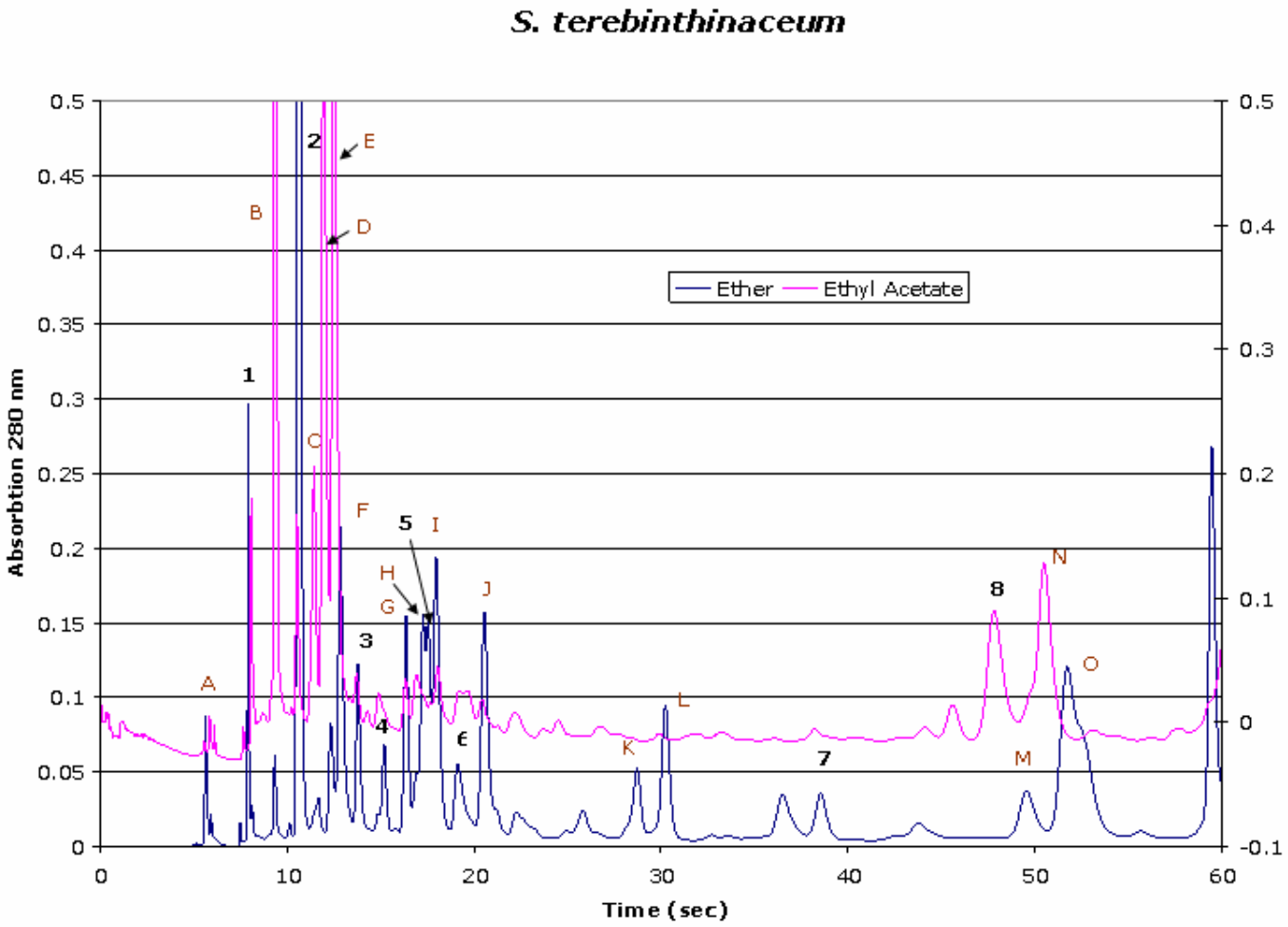

Figure 5.8: Standard phenolics denoted by number. 1. gallic, 2. protocatechuic 3. chlorogenic, 4. *p*-OH benzoic, 5. vanillic, 6. syringic, 7. ferulic, 8. salicylic acids. Unknowns are denoted by letters as follows: A, B, C, D, E, F, G, H, I, J, K, L, M, N, O.

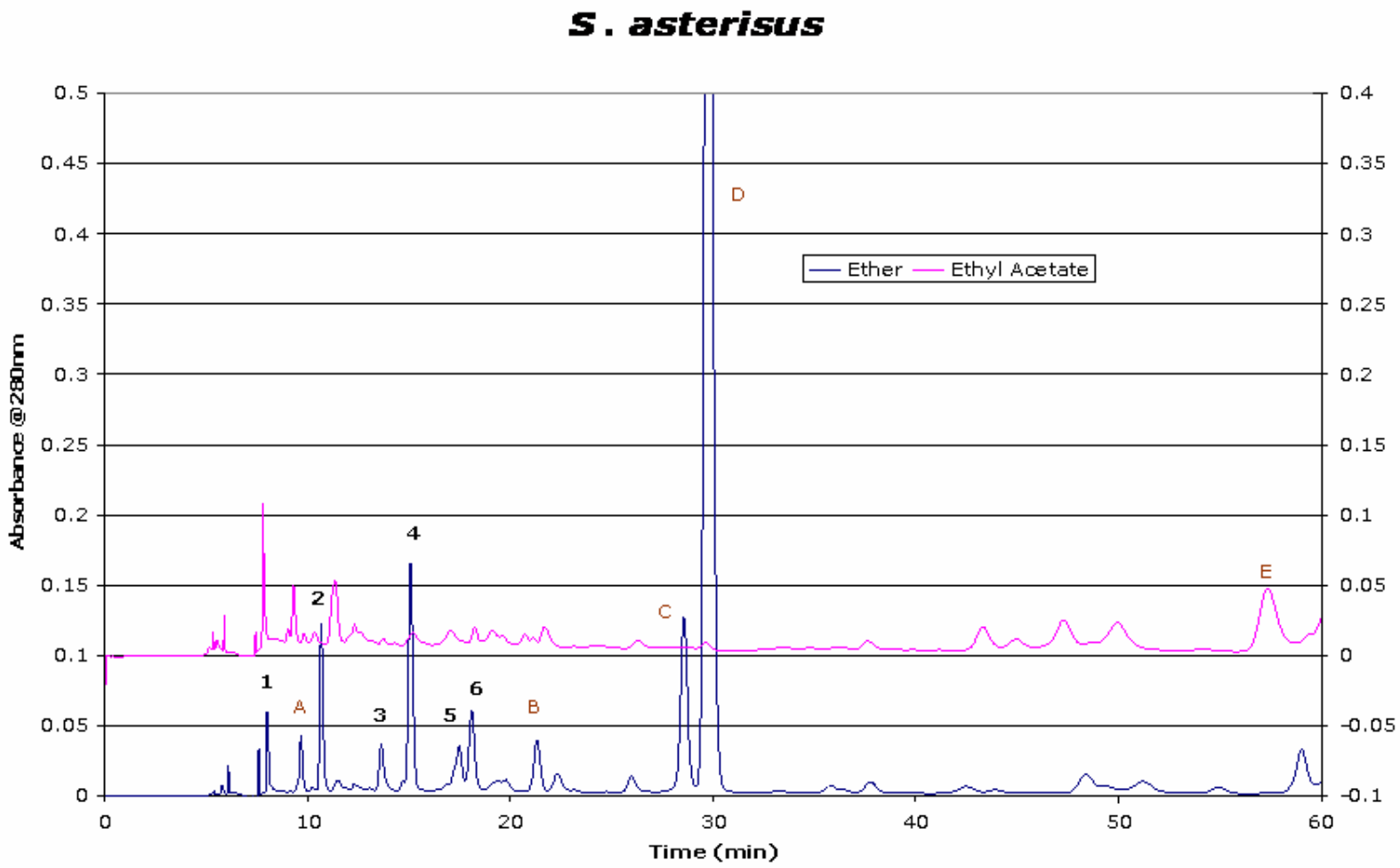

Figure 5.9: Standard phenolics denoted by number. 1. ellagic, 2. protocatechuic 3. *p*-OH-phenylactic, 4. *p*-OH benzoic, 5. vanillic, 6. caffeic/hydrocaffeic. Unknowns are denoted by letters as follows: A, B, C, D, E, F, G.

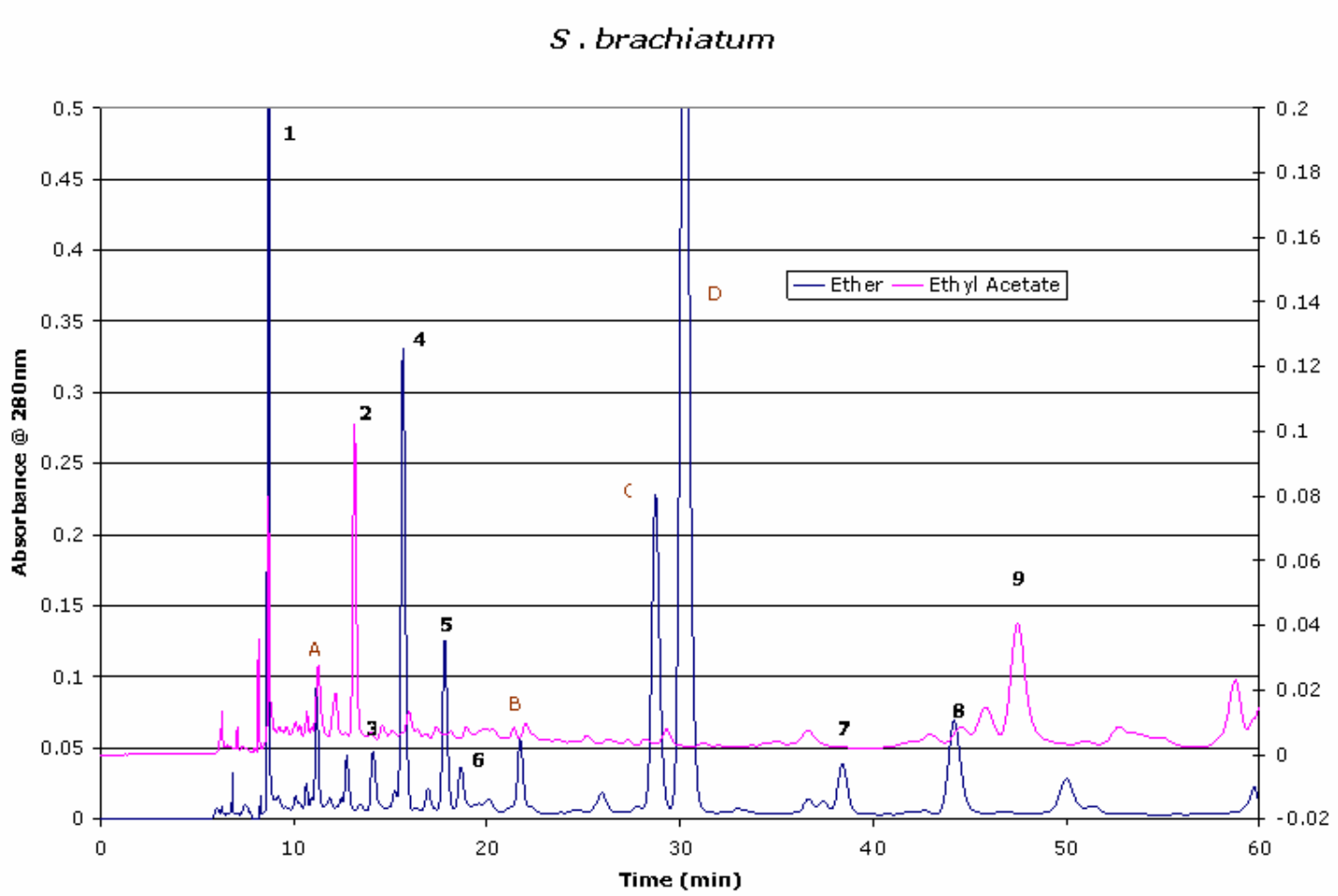

Figure 5.10: Standard phenolics denoted by number. 1. ellagic, 2. chlorogenic, 3. *p*-OH-phenylactic, 4. *p*-OH benzoic, 5. vanillic, 6. caffeic/hydrocaffeic, 7. ferulic, 8. sinapic, 9. salicylic. Unknowns are denoted by letters as follows: A. B. C. D.

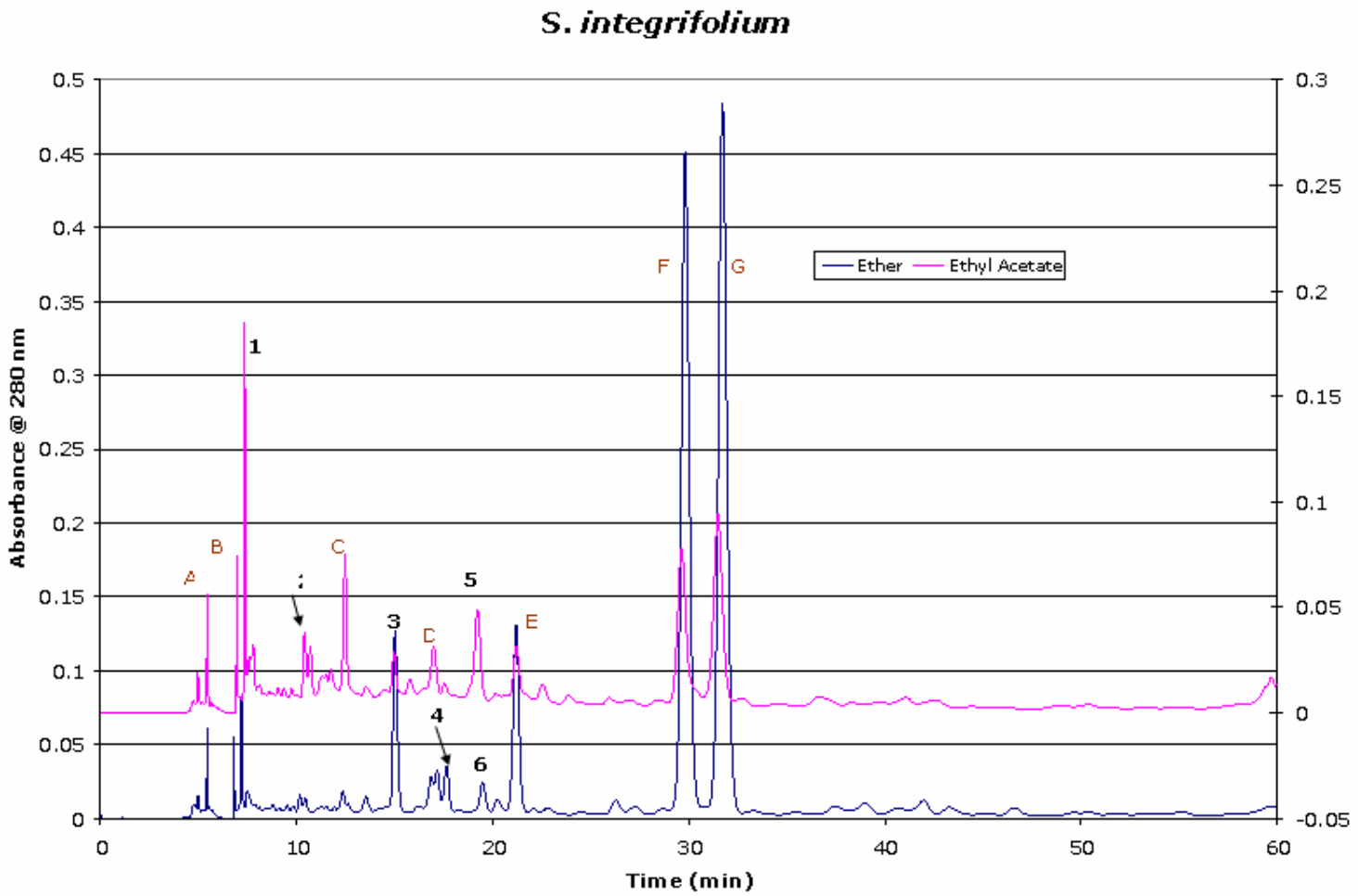

Figure 5.11: Standard phenolics denoted by number. 1. gallic, 2. protocatechuic 3. *p*-OH-benzoic, 4. vanillic, 5. syringic, 6. isovanillic. Unknowns are denoted by letters as follows: A, B, C, D, E, F, G.

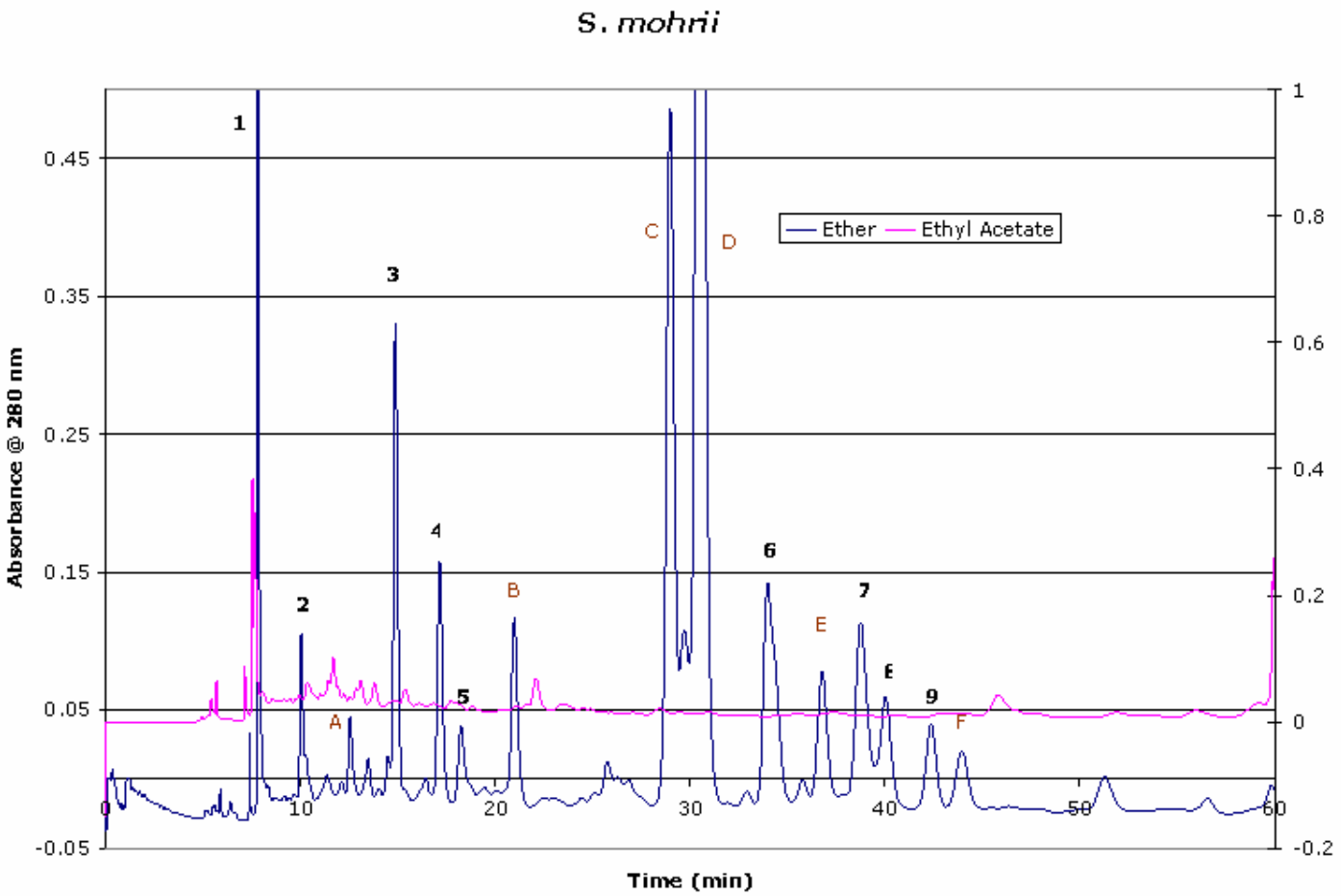

Figure 5.12: Standard phenolics denoted by number. 1. gallic, 2. protocatechuic 3. *p*-OH-benzoic, 4. vanillic, 5. caffeic/hydrocaffeic, 6. *p*-coumeric, 7. ferulic, 8. isoferulic, 9. sinapic. Unknowns are denoted by letters as follows: A, B, C, D, E, F, G.

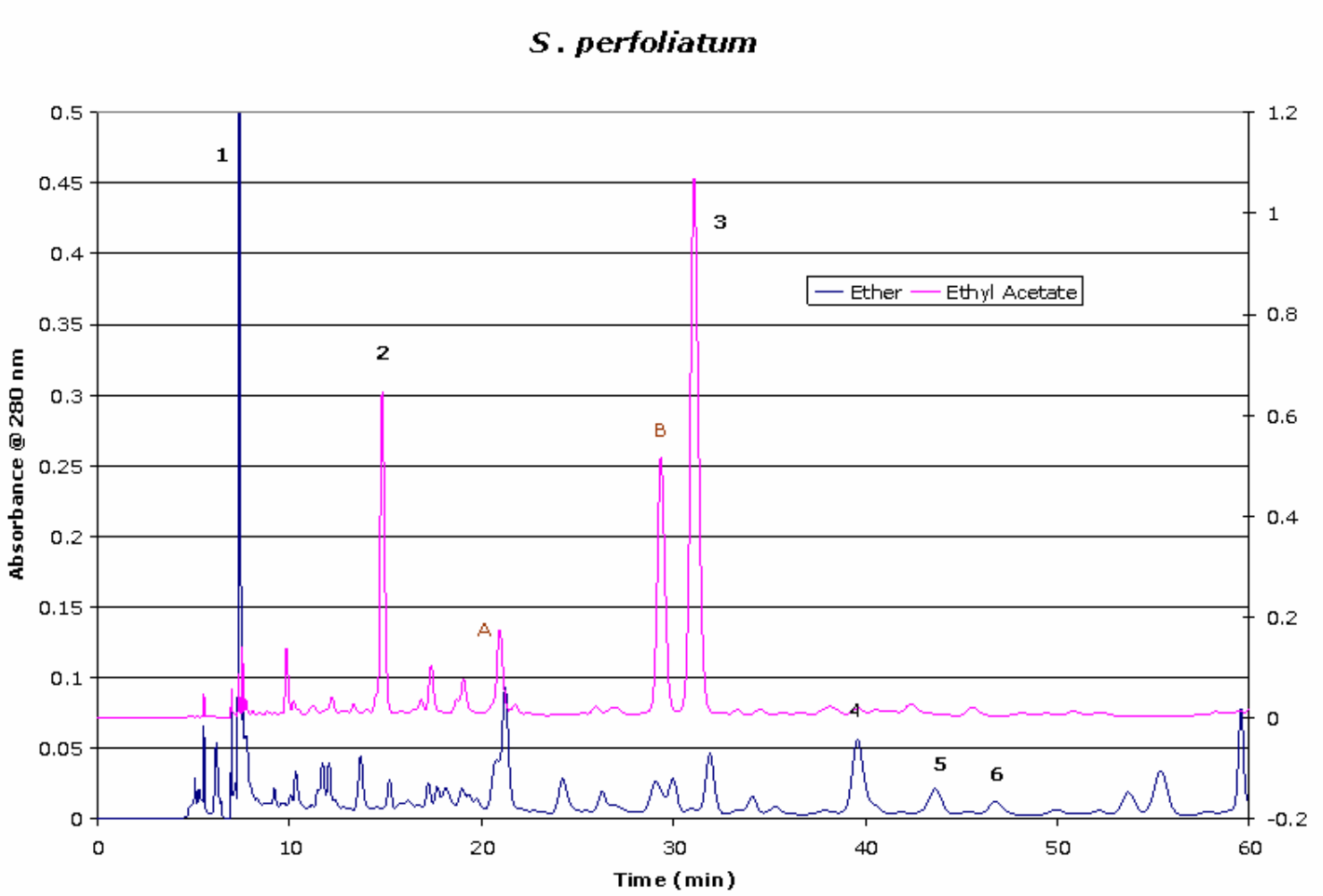

Figure 5.13: Standard phenolics denoted by number. 1. gallic, 2. *p*-OH-benzoic, 3. *p*-coumaric, 4. ferulic, 5. sinapic, 6. salicylic. Unknowns are denoted by letters as follows: A, B.

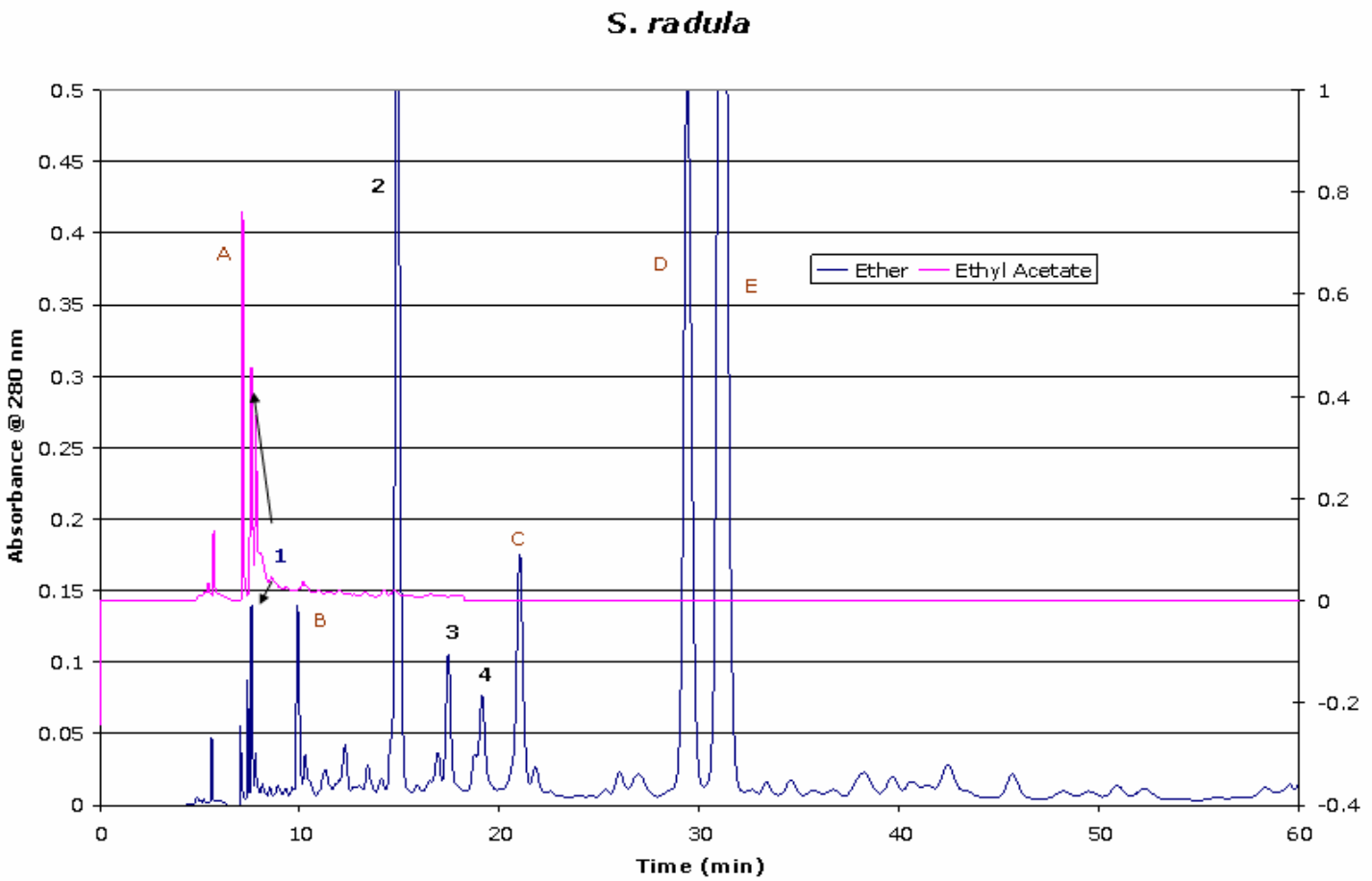

Figure 5.14: Standard phenolics denoted by number. 1. gallic, 2. *p*-OH-benzoic, 3. vanillic, 4. syringic. Unknowns are denoted by letters as follows: A, B, C, D, E.

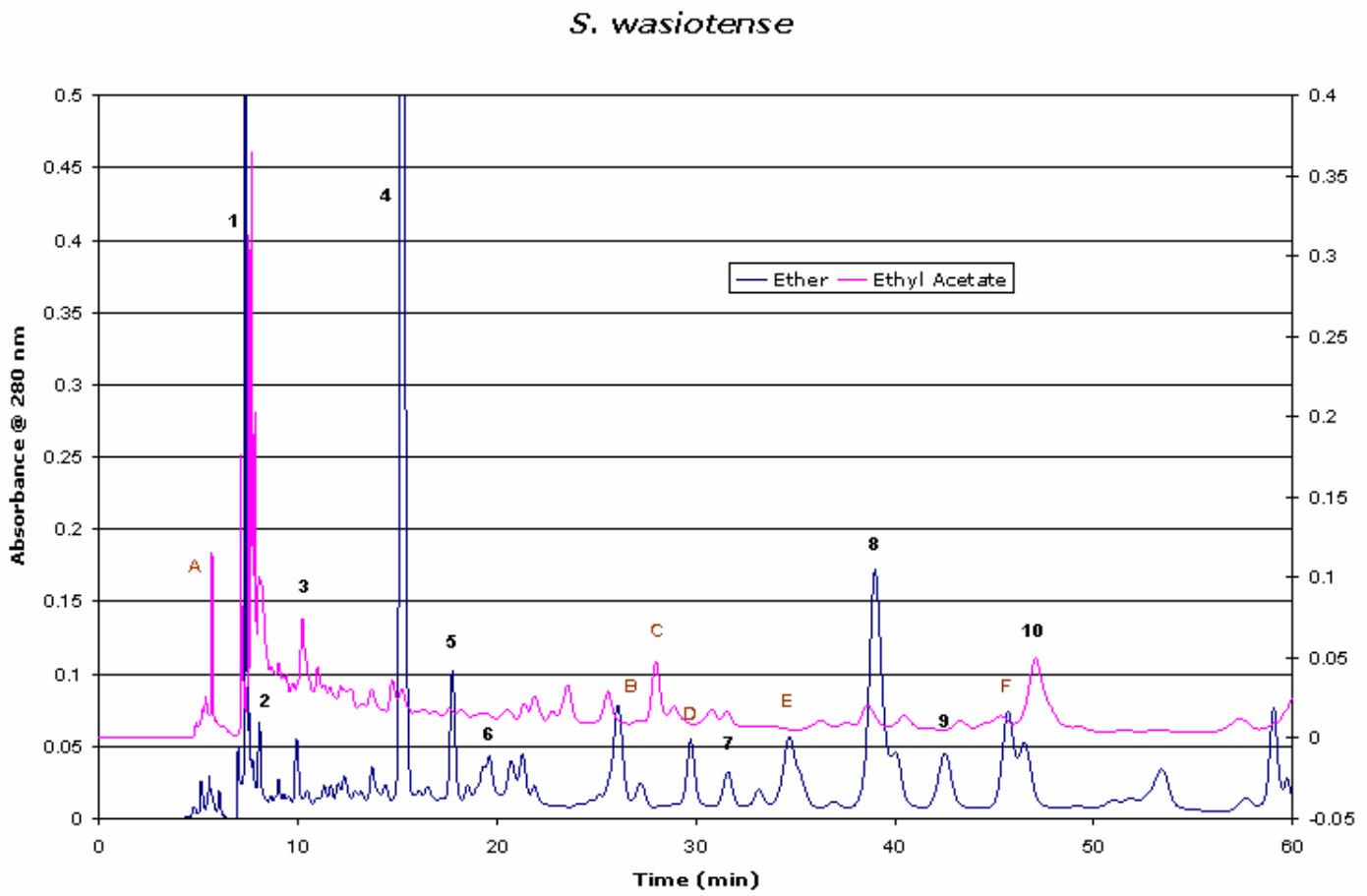

Figure 5.15: Standard phenolics denoted by number. 1. gallic, 2. ellagic, 3. protocatechuic 4. *p*-OH-benzoic, 5. vanillic, 6. isovanillic, 7. *p*-coumeric, 8. ferulic, 9. sinapic, 10. salicylic. Unknowns are denoted by letters as follows: A. B. C. D. E. F.

Chapter 6

Pharmacological Relevance and Medicinal Properties of Quercetin and Kaempferol Glycosides

Growth assay analysis of the five new triglycosidic flavonoids isolated from the genus *Silphium* were preformed in Dr. Suranganie F. Dharmawardhane's lab, the Department of Anatomy and Cell Biology, Universidad Central del Caribe, Puerto Rico. The protocol for the assay included 1, 750 MCF7 breast cancer cells. The experiment was conducted using a DMEM media containing 10% fetal bovine serum with the cells being grown two days prior to treatment. The MCF7 cells were treated for 96 hours using the aliquot amounts listed below (Table 6.1). From the analysis performed, three of the five newly isolated triglycosidic flavonoids gave a significant reduction in breast cancer cell growth.

6.1 Experimental

MCF7 Cells were treated every 24 hours for the first 48 hours (equaling 2 treatments), then left for an additional 48 hours before analysis. The cells were fixed with 3.7 % formaldehyde (20 min, room temp), stained with 0.23% crystal violet (20 min, room temp) to quantify their numbers. The crystal violet color was subsequently removed with 10% acetic acid and absorbencies were measured using a Beckman DU 520 spectrophotometer at 600 nm. The results are presented as the mean absorbance (N=4) for the combined treatments with their respective standard deviations (Table 6.1). Statistical analyses were used for "unpaired student t-tests" as the method for comparing control-

treated cells (1:1 DMSO: media) with each compound treatment individually. When the standard deviations were unequal between comparisons, a Welch's corrected t-test was applied.

Concentration	Compounds	Mean Abs.	SD
…	control	0.632	0.113
25uM	cmp **1A**	0.359	0.122
25uM	cmp **2A**	0.429	0.024
1uM	cmp **3A**	0.428	0.083
1uM	cmp **4A**	0.533	0.131
25uM	cmp **5A**	0.434	0.068

Table 6.1 Concentrations of the five flavonoid compounds along with their mean absorbance and standard deviations.

p-vals	Control	
1	0.14592	
2	0.03401	significant
3	0.02934	significant
4	0.29641	
5	0.03012	significant

Table 6.2 Compounds 2, 3, and 5 are significantly different from the control.

	Control	Treatment 1	Treatment 2	Treatment 3	Treatment 4	Treatment 5
Trial 1	0.520	0.585	0.423	0.36	0.477	0.357
Trial 2	0.589	…	0.423	0.404	0.524	0.395
Trial 3	0.633	0.346	0.463	0.548	0.718	0.497
Trial 4	0.786	0.506	0.408	0.399	0.413	0.485
Average	0.632	0.359	0.429	0.428	0.533	0.434
Std. Dev	0.113	0.122	0.024	0.083	0.131	0.068

Table 6.3 Absorbencies recorded for the growth assay providing averages and the standard deviations.

6.2 Results

The data from the tables above show the absorbencies of compounds 2, 3 and 5 as being significantly lower than the control, indicating reduced cell growth (Table 6.2). These compounds represented a reduction of approximately 30% cell growth as compared with the control. A significant growth reduction of approximately 50% was observed from isorhamnetin 3-*O*-*α*-L-rhamnosyl (1'''→6'') –*O*-*β*-D-galactopyranoside 7-*O*-*β*-L-apiofuranoside (**1A**); however, the high standard deviation indicates that it was not statistically significant. This experiment was performed one time with four replications of each treatment.

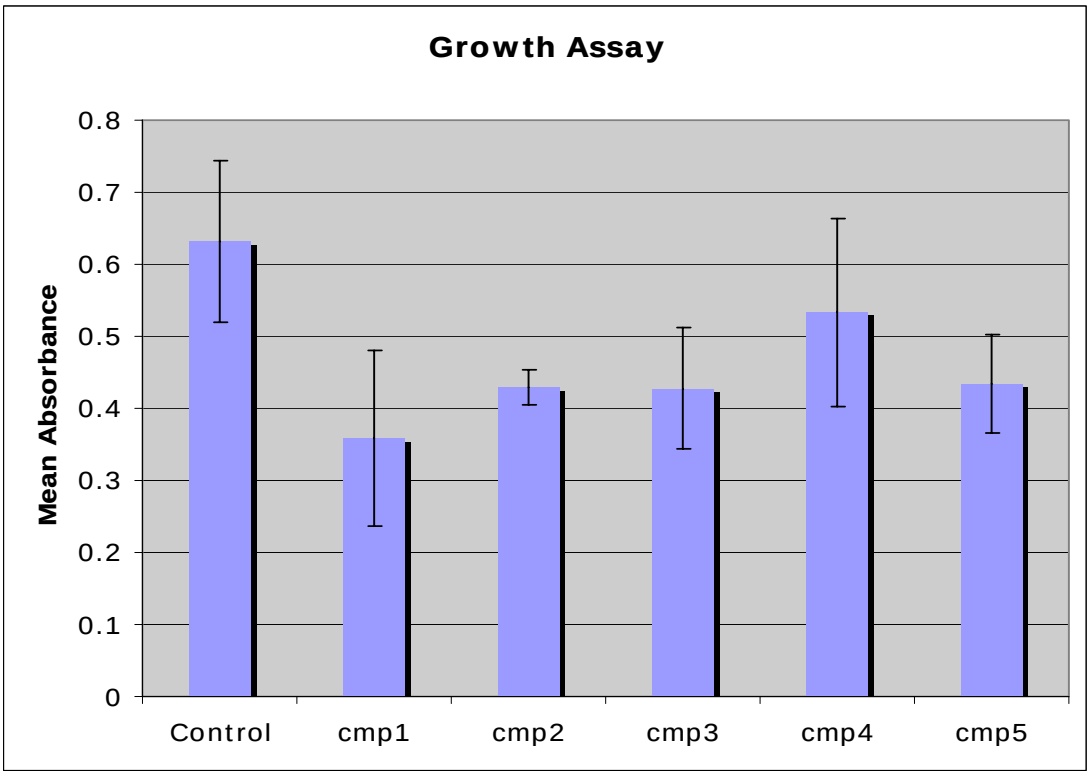

Table 6.4 Bar graph showing the mean absorbencies along with each compound's standard deviation.

6.3 Discussion

Quercetin and kaempferol glycosides may reduce the proliferation of several types of cancer; combination treatments of these compounds tend to decrease the expression of specific nuclear antigens along with reduce intercellular protein levels in both breast and intestinal cells (Akland, 2005).

Quercetin itself has been shown to inhibit the proliferation of tumor cells through cell cycle arrest, the up-regulation of tumor suppressor genes and influence MAPK transduction (Van Erk, 2005); moreover, it may also interfere with the expression of certain onco and tumor suppressor genes in mammary carcinoma (Avila, 1996).

Studies with quercetin and colon cancer have shown the inhibition of proliferative tumor cells, a reduction in the number of irregular crypt foci, and at 5 μm aliquots, down regulation of the expression of the cell cycle genes CDC6, CDK4 and cyclin D1. In addition, quercetin appears to up-regulate the expression of several tumor suppressor genes effecting both beta catenin/TCF signaling and MAPK transduction (van Erk, 2005).

As for its use directly in cancer treatment, flavonoids similar to quercetin are being investigated in relation to currently used chemotherapy agents. The agent *cis*-DDP (cis-diaminedichlorplatinum (II)) is now one of the most effective drug treatments prescribed, although its use must be monitored carefully due to side effects. The synergistic effects of quercetin and *cis*-DDP, when analyzed in *cis*-DDP- sensitive cancer cells have resulted in the lowered toxicity of *cis*-DDP. In addition, introduction of a flavonol-*cis*-DDP ligand altered the DNA-binding properties of the complex as compared

to *cis*-DDP alone. The T6 synergistic activities of these flavonols have sparked further research involving several commonly used chemotherapeutic agents (Kosmider, 2004).

Finally, Dr. Kiminori Matsubara at Okayama Prefectural University, found that quercetin 3-*O*-*β*-D-glucose specifically had a strong inhibiting effect involving *ex vivo* angiogenesis in comparison to other glycosylated forms of not only quercetin, but also isorhamnetin and kaempferol (Matsubara, 2004). Our highly polar, uniquely glycosylated five new flavonoids may not only directly add to further investigative treatments, but also encourage greater interest in the glycosidic mechanisms allowing for their effectiveness.

Chapter 7:

Summary and Conclusions

7.1 Flavonoid Studies

The analysis within this dissertation provides information for the extraction, identification and comparison of the flavonoid and phenolic acid chemistry for eleven species in the genus *Silphium*. The background for this project was based on the 1999 revision performed by Dr. Jennifer Clevinger and the medicinal uses of these plants by Native Americans.

Using comparative LC/MS analyses, the four species comprising section *Composita* showed the presence of various derivatives of the flavonols quercetin, isorhamnetin and kaempferol. Quercetin and isorhamnetin were especially prevalent among these species. *Silphium albiflorum* and *S. laciniatum* shared the same quercetin 3-monosaccharides, kaempferol 3-galactopyranoside as well as the newly isolated isorhamnetin 3-*O*-*α*-L-rhamnosyl (1'''→6'')-*O*-*β*-D-galactopyranoside 7-*O*- *β*-L-apiofuranoside (**1A**). This followed closely with Dr. Clevinger's sister grouping of *Silphium albiflorum* and *S. laciniatum*. The second newly isolated quercetin triglycoside, quercetin 3-*O*-*α*-L-rhamnosyl (1'''→6'') –*O*-*β*-D- galactopyranoside 7-*O*-*β*-L-apiofuranoside (**2A**), was detected in the species *S. albiflorum* and *S. compositum* but not in *S. laciniatum* or *S. terebinthinaceum.* The fact that this compound was detected in *S. compositum* suggests that the gene for this triglycoside exist among all four species of the section and may be activated upon environmental and or ecological stimuli. The pentose sugar apiose (*m/z* 132) was prevalent in the quercetin glycosides for all four species of

the section, while *S. laciniatum* also contained this sugar bound to the flavonol kaempferol.

Silphium section *Composita* contained two species, *S. albiflorum* and *S. terebinthinaceum*, with more derivatives of the flavonol isorhamnetin than found in any other species in the genus. *Silphium albiflorum*, *S. compositum* and *S. terebinthinaceum* all shared the isorhamnetin compound, isorhamnetin 3-*O*-*α*-L-rhamnosyl (1'''→6'')-*O*-*β*-D-galactopyranoside with *S. albiflorum* and *S. terebinthinaceum* both containing two additional isorhamnetin flavonols. In support of Dr. Clevinger's organization of *Silphium* section *Composita* the flavonol isorhamnetin was found more often among the plants of this section than in any other grouping. It is also important to note that the two-dimensional paper chromatograms revealed the largest extractable concentrations of three and possibly four glycosidic flavonoids in the species *S. terebinthinaceum,* considerably more than found in any other *Silphium* species (Figure 2.2).

In six of the seven species numbered among section *Silphium*, derivatives of the flavonol kaempferol were detected in greater numbers than in the species in section *Composita*. Also, extracted from the species of section *Silphium* were the newly isolated kaempferol 3-*O*-*β*-D-apiofuranoside 7-*O*-*α*-L-rhamnosyl-(1''''→6''')-*O*-*β*-D-galactopyranoside (**4A**) and its caffeoyl ester (**5A**).

In agreement with Dr. Clevinger's phylogenetic grouping of the three species *Silphium perfoliatum*, *S. wasiotense* and *S. integrifolium*, both *S. perfoliatum* and *S. wasiotense* were both found to produce the kaempferol triglycoside kaempferol 3-*O*- *β*-D-apiofuranoside 7-*O*-*α*-L-rhamnosyl (1''''→6''')-*O*- *β*-D-(2'''-*O*-*E*-caffeoylgalactopyranoside)

(**5A**), a compound not detected in any of the other species. Both species also contained quercetin 3-glucopyranoside, quercetin 3-galactopyranoside and kaempferol 3-rutinoside.

Less clear were the relationships drawn involving the four remaining species of section *Silphium*, which include the species *Silphium asteriscus*, *S. brachiatum*, *S. mohrii* and *S. radula.* The species *Silphium asteriscus*, *S. mohrii* and *S. radula* all contained the most individual numbers of flavonoids than any other *Silphium* species. Along with *Silphium integrifolium,* these three species shared the quercetin glycosides: quercetin 3-*O*-α-L-rhamnosyl (1'''$\rightarrow$6'') –*O*-β-D- galactopyranoside 7-*O*-β-L-apiofuranoside (**2A**), quercetin 3-*O*-rutinoside and quercetin 3-*O*-robinobioside. The two kaempferol diglycosides, kaempferol 3-*O*-rutinoside and kaempferol 3-*O*-robinobioside, were also detected and, in agreement with Dr. Clevinger's assignment, *Silphium asteriscus* and *S. mohrii* also share the most isorhamnetin mono and diglycosidic flavonols in the section.

The species *S. brachiatum* contained the least flavonoids with a sum total of four. This species also contained an unidentified, highly polar, brown material accompanying three separate extractions of this species.

7.2 Phenolic Acid Studies

The phenolic acid chemistry of section *Composita* followed closely the taxonomic assignments made by Dr. Clevinger. The cladistic relations between the species *S. albiflorum* and *S. laciniatum* were observed both qualitatively and quantitatively in our chemical studies. The HPLC chromatograms for both species showed approximately identical patterns for both known and unknown phenolic acids. Also present in greater

numbers and larger amounts were the hydroxycinnamic acids detected in both *S. albiflorum* and *S. laciniatum*. In section *Composita*, ethyl acetate extracted a greater variety of hydroxybenzoic acids while ether extracted larger total concentrations of these phenolic acids. Ether extraction provided for both a wider range of cinnamic acid types and a greater concentration of total compound, phenolics which included caffeic, hydrocaffeic and ferulic acids.

Along with the known phenolic acids, *S. compositum* and *S. terebinthinaceum* both contained five peaks extracted in ethyl acetate that were unique and identical for both species; all five peaks had the same retention times and their consecutive positions were not detected in other *Silphium* species. The closely related patterns of *S. albiflorum* with *S. laciniatum* along with *S. compositum* with *S. terebinthinaceaum* all appear to support Clevinger's placement of these four species in their own section although also from these chemical findings it might be argued that both *S. compositum* and *S. terebinthinaceaum* could be sub-grouped into their own section.

The phenolic acid analysis of *Silphium* section *Silphium* showed more diversity among the individual phenolic compounds than the species in section *Composita*; for example, all nine hydroxybenzoic acids in the seven species of this section were present (Table C.6). Of the nine benzoic acids identified, higher concentrations of six out of the nine were detected in ether. The species *Silphium radula* and *S. wasiotense* produced the highest total phenolic acid amounts in section *Silphium*. *Silphium radula* produced the highest concentration of hydroxycinnamic acids consisting primarily of hydrocaffeic acid. *Silphium integrifolium* also contained moderate amounts of the acids rosmarinic, *p*-coumaric and hydrocaffeic acids

7.3 Comparison of the Chemical Findings with Clevinger's Molecular Data

Chloroplast DNA (cpDNA) and morphologic cladistic analyses support *Silphium*'s revision and placement in the subtribe Engelmanniinae. From the data collected from the Internal Transribed Spacer regions, a phylogeny has been constructed that helps clarify the taxonomy of the genus. Clevinger, who used this DNA analysis in her Ph.D. studies, currently continues her investigations on the *Silphium* genus and the tribe Heliantheae. This project focuses on the view that plant secondary metabolites, while in no way diminishing the necessity of molecular data, can be used as a supplemental genomic reference for modern taxonomic alignments and revisions.

7.4 Bioassays and the Medical Value of the Chemical Findings

The isolation of mono and disaccharide flavonoids have been categorized and documented for decades. Modern techniques for flavonoid extraction are now providing for the separation of the more complex three and four sugar derivatives of flavonols, compounds which may exhibit more useful pharmaceutical properties than previously investigated aglycones.

Significantly, five new triglycosidic flavonoids were isolated in the course of these studies. The structures for these flavonoids were determined using modern spectral analysis including ^{1}H NMR, ^{13}C NMR, HMQC, HMBC, COSY, LC/MS and other techniques. **These new compounds were submitted for chemotoxic analysis, namely MCF7 breast cancer cell research, and notable reductions in the cell growth of the cancer cells were observed.**

In regards to the medical value of natural products, my studies were limited to the submission of the five new complex flavonoid triglycosides to Dr. Nico Azios for bioassays to test their ability to control the growth of breast cancer cells. Three compounds afforded a reduction of cell growth by approximately 30% and may open a new area of research, namely, studies of highly glycosylated antioxidants that travel more effectively through aqueous solutions delivering their active components to the problem cell. Such complex flavonoid triglycosides have been little studied, not only because of their structural complexity but also because natural products research often focuses on other well known classes of compounds. Now we know that the triglycosides of isorhamnetin, quercetin and kaempferol have unusually high capabilities for inhibiting proliferation of breast cancer cells, at least in lab studies, a finding that might have remained unknown without our work with Dr. Azios.

7.5 Final Comments on My Research

There is no doubt that molecular data must always be used in erecting reliable phylogentic trees, but chemical patterns can provide useful information for many aspects of systematics.

My own investigations suggest that patterns of both flavonoids and simple phenolics can be useful in evaluating relationships among plant populations, especially when environmental and ecological factors cause taxonomic confusion due to their effects on morphological characters. Of course the natural products chemistry of a plant is also affected by environmental and ecological factors, but most frequently the changes

are in the quantity of each compound produced; thus with today's highly sensitive analytical equipment it is possible to detect even trace amounts of compounds. These analyses allow scientists to establish and confirm that certain biosynthetic pathways are indeed present and therefore the genes for the enzymes for these pathways must also be present.

In the course of my studies here at the University of Texas at Austin, I discovered several research concerns in the plant sciences, including one which has been experienced by previous phytochemistry students, namely that only well-funded Chemistry and Molecular Biology Departments have the modern equipment available to adequately investigate the chemistry of natural products. There are many knowledgeable and gifted natural products scientists whose resources are increasingly constrained due to limited funding and poor access to the required technology. Dr. Mabry's connections to chemical and molecular programs allowed me to have access to advanced analytical facilities thus allowing me to establish the flavonoid and phenolic acid chemistry for eleven species within the genus *Silphium*. Funding needs to be increased with greater emphasis placed upon supporting medically important natural products discoveries and providing more modern facilities for analysis.

Appendix A

The chemical structures of flavonoids are diverse and they are of the largest classes of plant secondary metabolites. Two separate biosynthetic pathways involving a series of condensation reactions are employed in their creation. Different types of flavonoids perform different functions thus the proper identification of the aglycone along with the types, attachments and arrangements of the sugars must be analyzed. Several spectra where used in order to elucidate the correct triglycosidic compounds. Here are presented further in depth spectral data for the triosides for the compounds **1A** and **2A** extracted from *Silphium* section *Composita.*

The flavonol aglycones quercetin and isorhamnetin were determined for the two triglycosides isolated from *Silphium* section *Composita.* Modern NMR, UV and MS fragmentation analyses where used in determining the correct structures. For each of the two triglycosides **1A** and **2A**, DEPT, HMBC, HMQC, COSY, ROESY and TOCSY where employed.

The DEPT analysis identified the carbon/hydrogen types; 2 methines, 2 methylenes and 1 quaternary carbon for compound **1A** (Figure A.1). The H-1''' anomeric proton of rhamnose was supported through the cross peak between the rhamnose H-1''' and galactose C-6'' as observed in the HMBC spectrum (Figure A.2). Three protons substantiating the isorhamnetin aglycone provided cross links with C-3' (HMBC) and C-2' (COSY) providing for the 3', 4' disubstituted B-ring at the C-3' methoxyl. The sites of the glycosylation involving the 1H and 13C signals where supported from TOCSY as well as the 2D NMR analysis (Figure A.6).

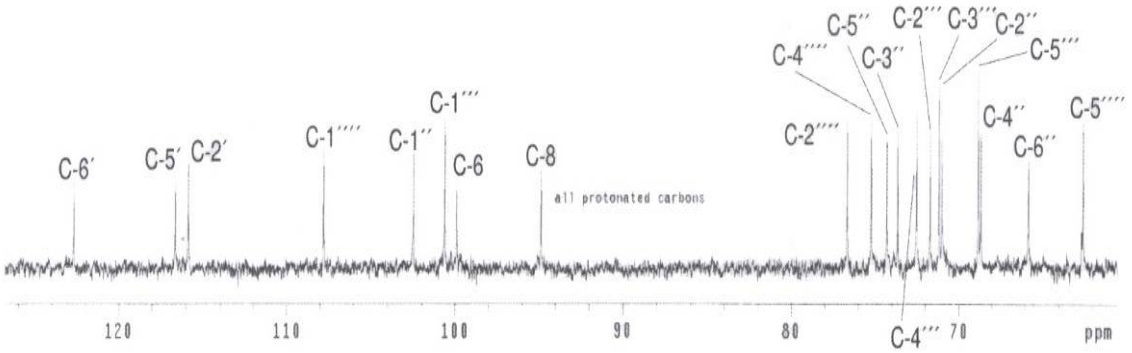

Figure A.1: DEPT Scan for the *S. albiflorum* isorhamnetin trioside **1A.**

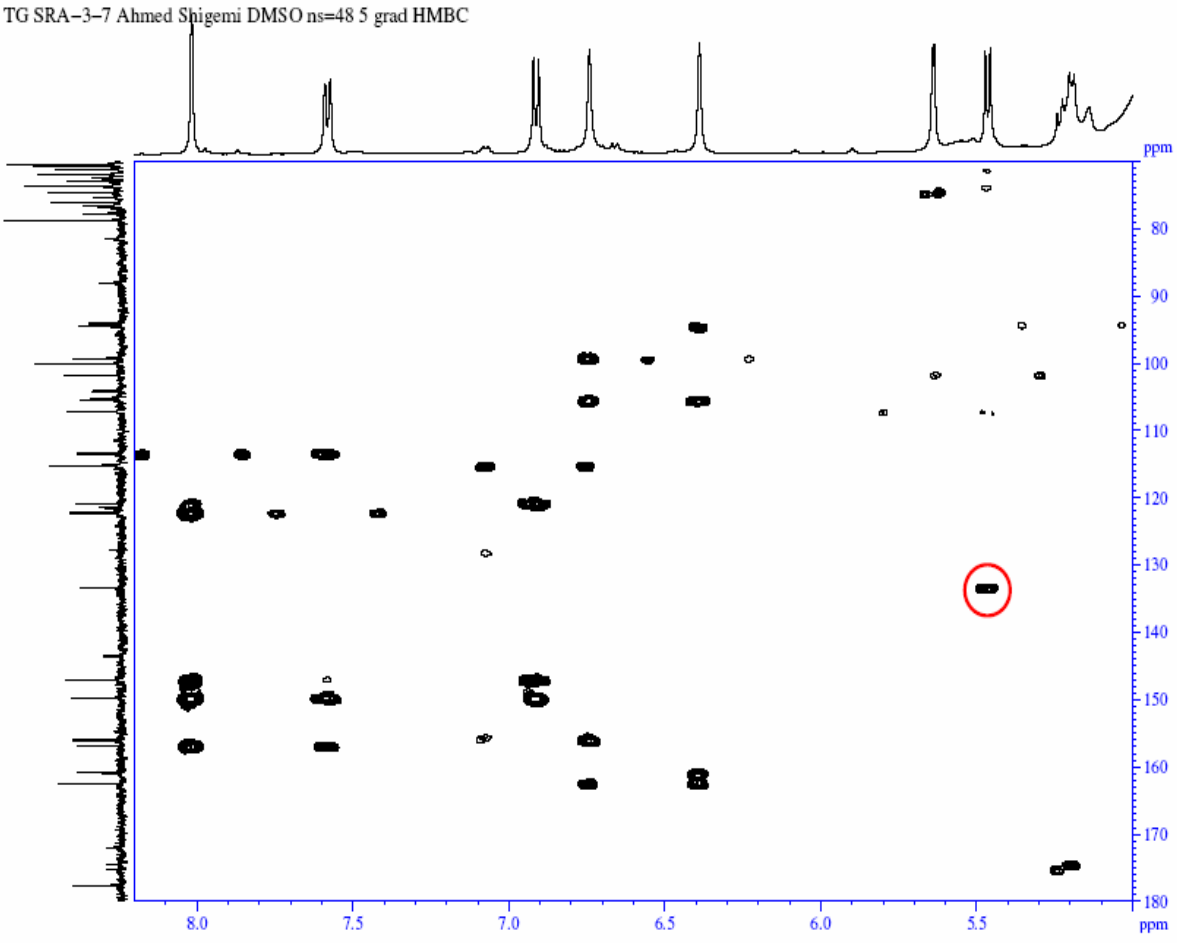

Figure A.2: HMBC long-range scan for the *S. albiflorum* isorhamnetin trioside **1A.**

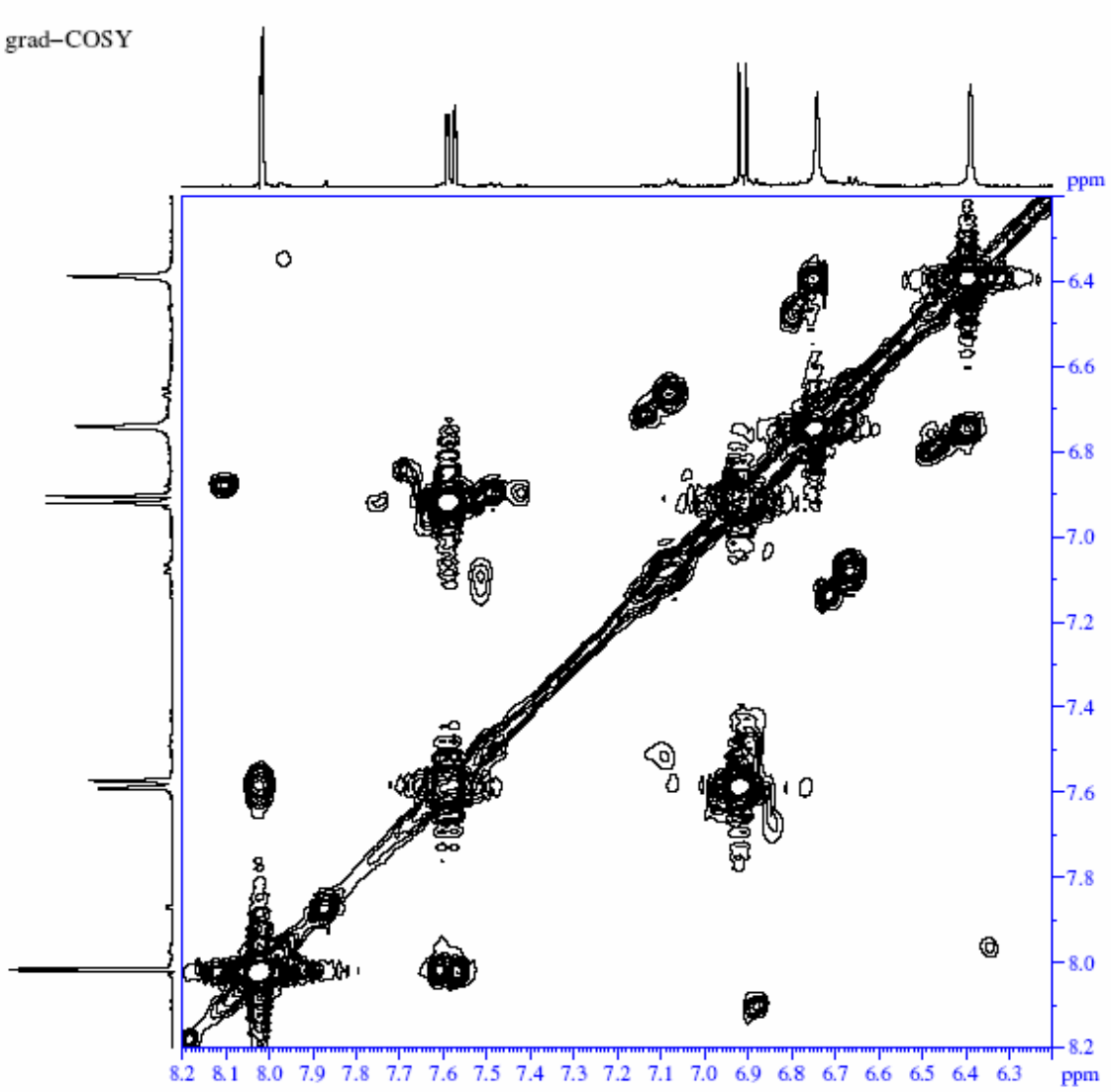

Figure A.3: COSY scan for the *S. albiflorum* isorhamnetin trioside **1A.**

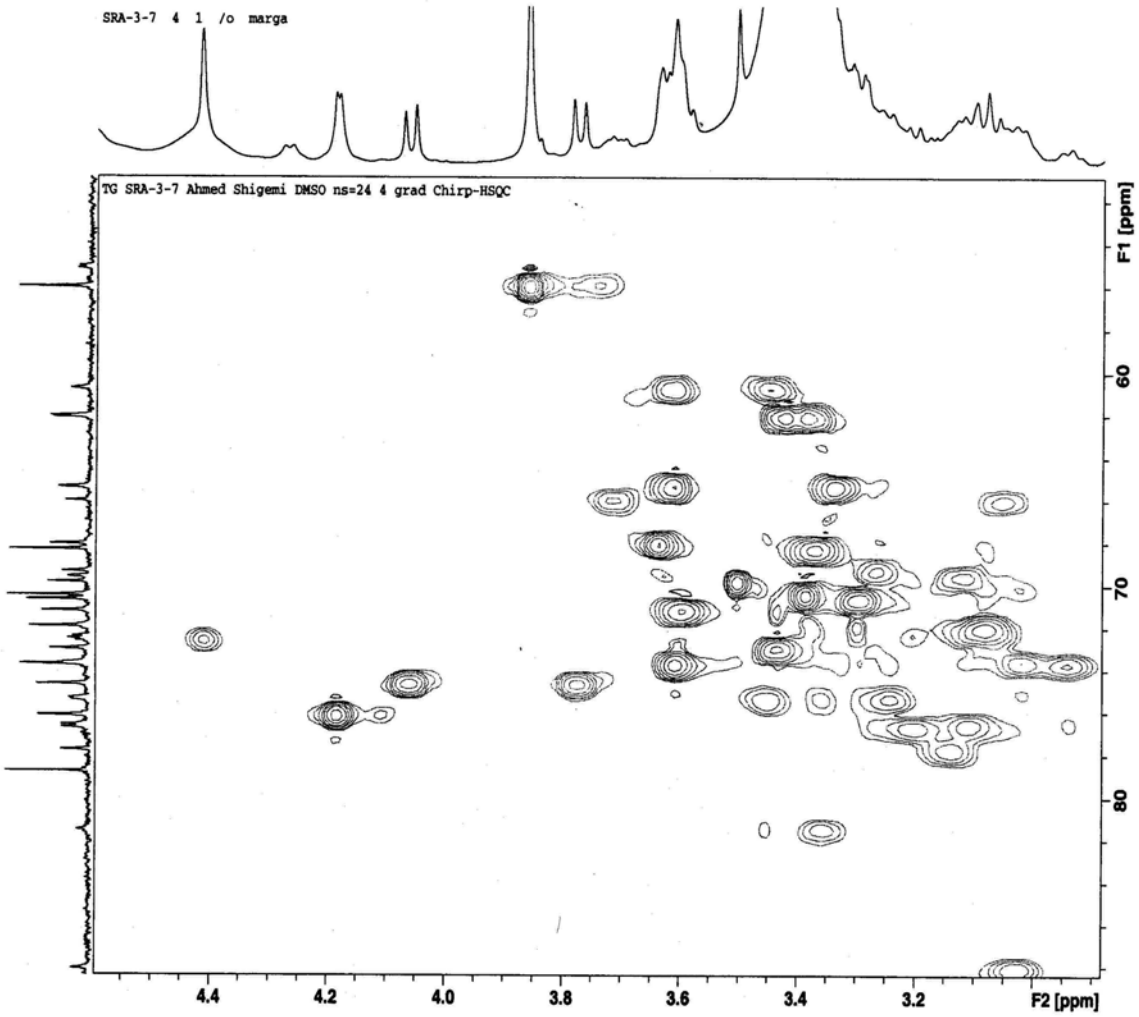

Figure A.4: HSQC Scan for the *S. albiflorum* isorhamnetin trioside **1A.**

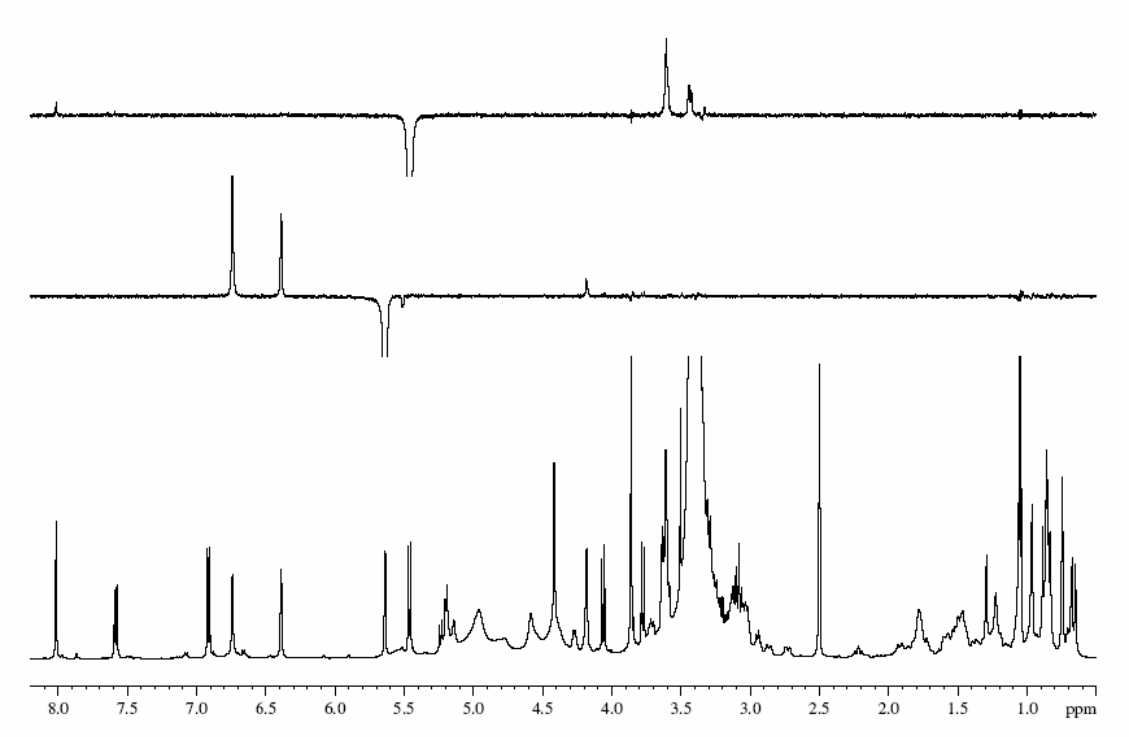

Figure A.5: ROESY Scan for the *S. albiflorum* isorhamnetin trioside **1A.**

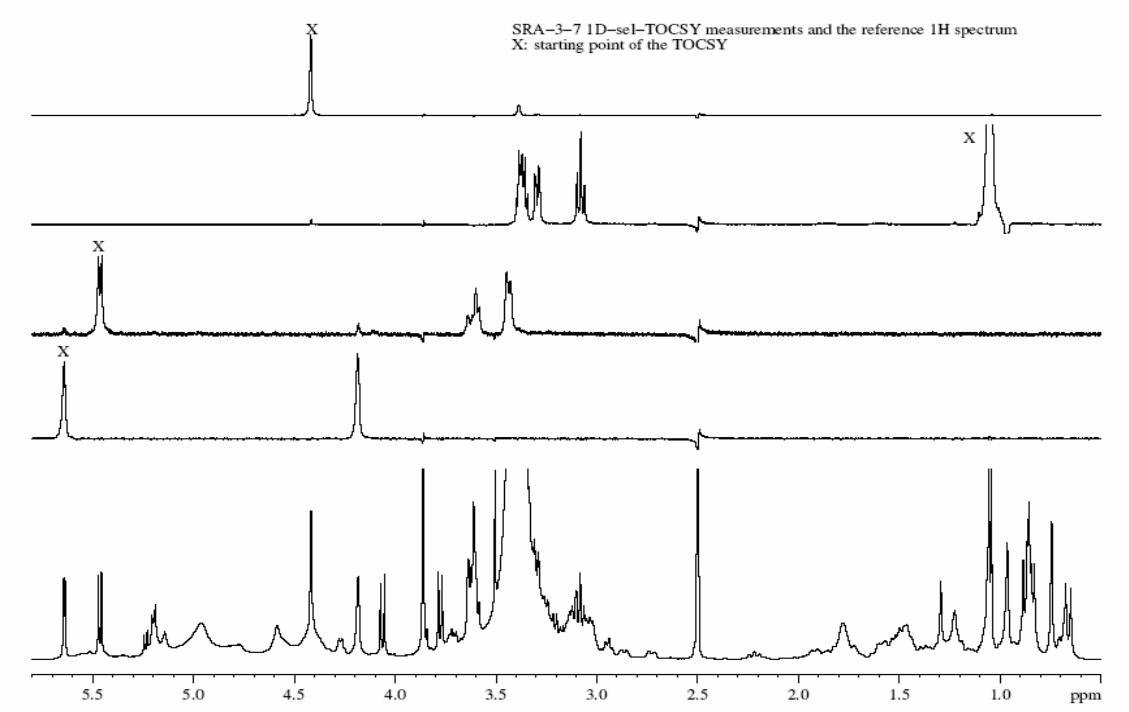

Figure A.6: TOCSY Scan for the *S. albiflorum* isorhamnetin trioside **1A.**

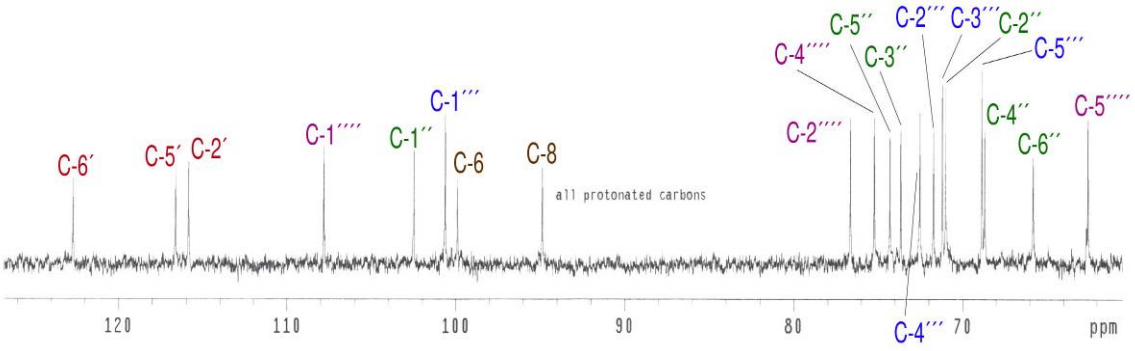

Figure A.7: DEPT Scan for the *S. albiflorum* quercetin trioside **2A.**

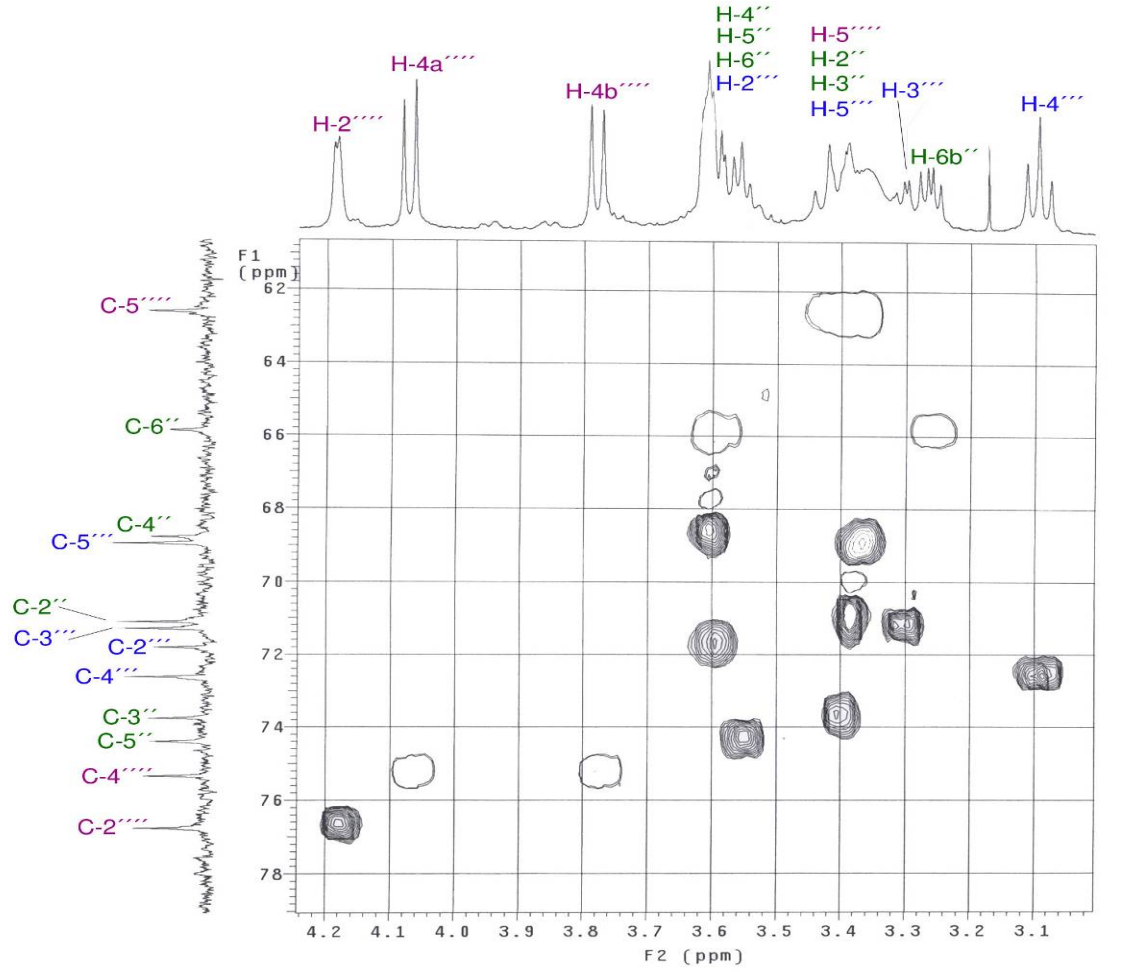

Figure A.8: HSQC direct C-H correlations of the sugars moieties in the quercetin trioside **(2A).**

Appendix B

The two triglycosidic kaempferol compounds isolated for the first time from *Silphium* section *Silphium* consisted of the compounds **4A** and **5A**. Additional analyses supporting the 3 sugar attachments, their C-H functionality and the caffeoyl group placement on 5A were performed. 13C and DEPT analysis showed three methylene, one methyl, eighteen methane and ten quaternary carbons for **4A** and three methylene, one methyl, twenty three methane and fourteen quaternary carbons for **5A** (Figure B.1). The caffeoyl moiety in 5A was attached to the galactosyl C-2''' and the correlation between the caffeoyl C=O and both the galactosyl H-1''' and galactosyl H-2''' can be supported by the HMBC cross patterns (Figures B.2, B.7, B.8 and B.9).

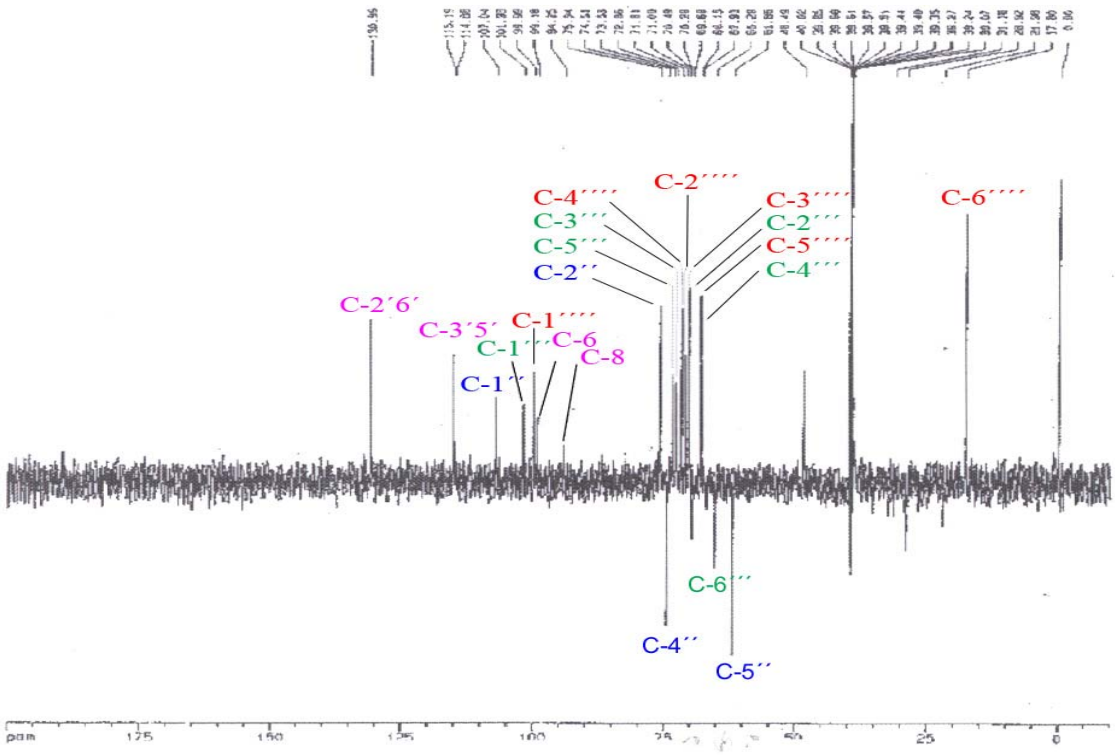

Figure B.1: DEPT Scan for the *S. perfoliatum* kaempferol trioside **4A.**

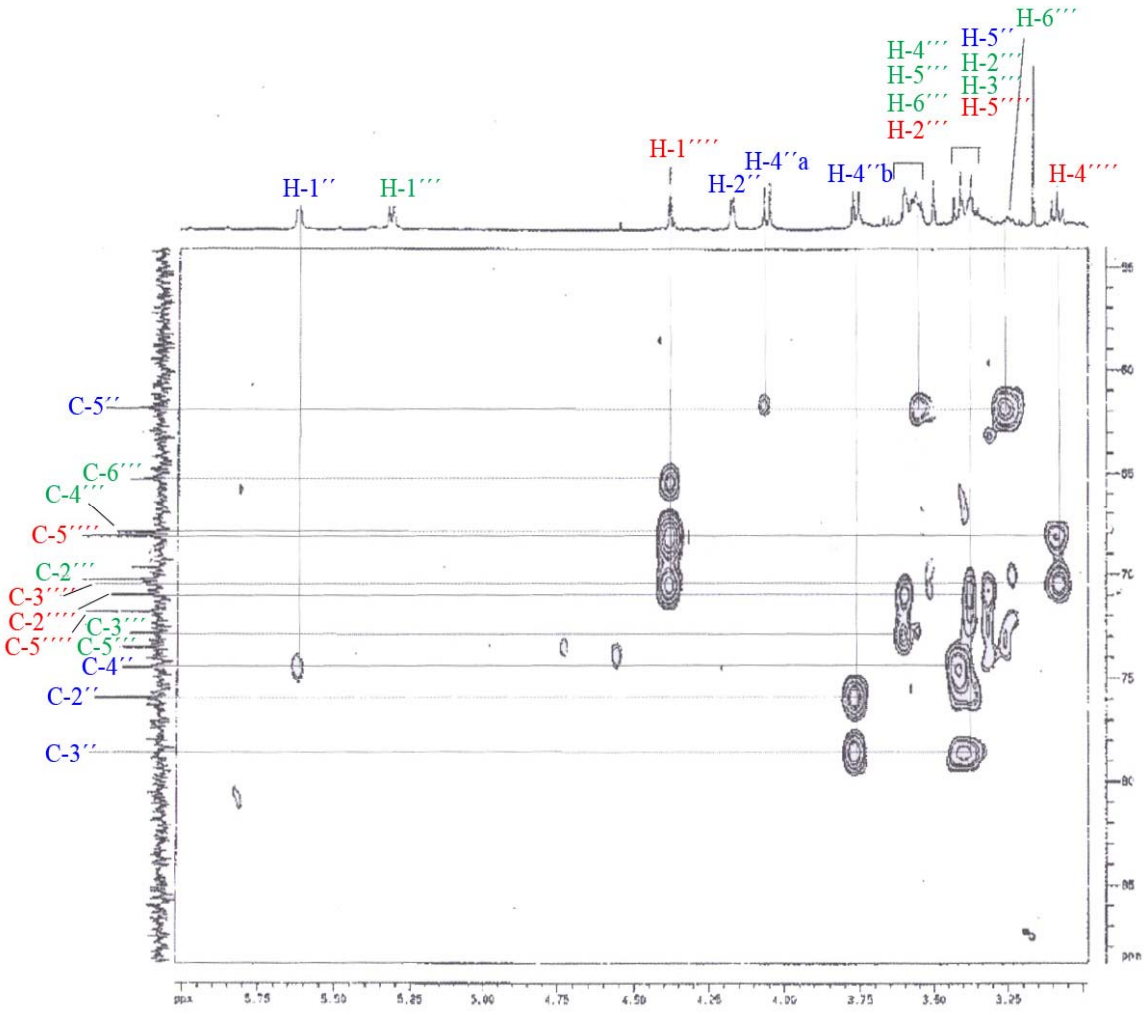

Figure B.2: HMBC Scan for the *S. perfoliatum* kaempferol trioside **4A.**

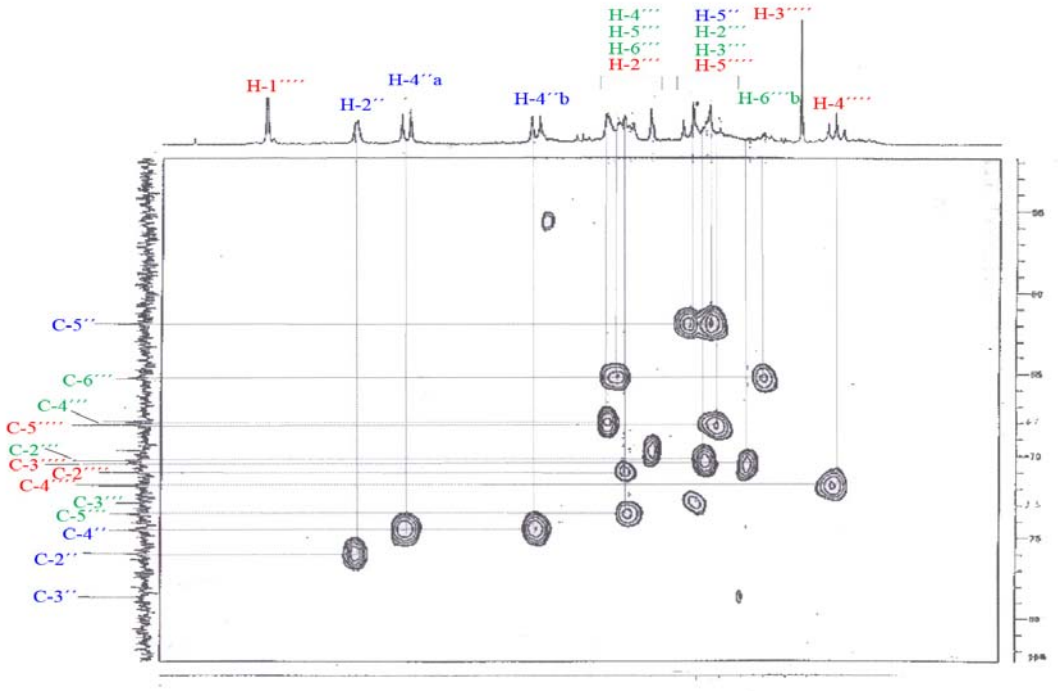

Figure B.3: HMQC Scan for the *S. perfoliatum* kaempferol trioside **4A.**

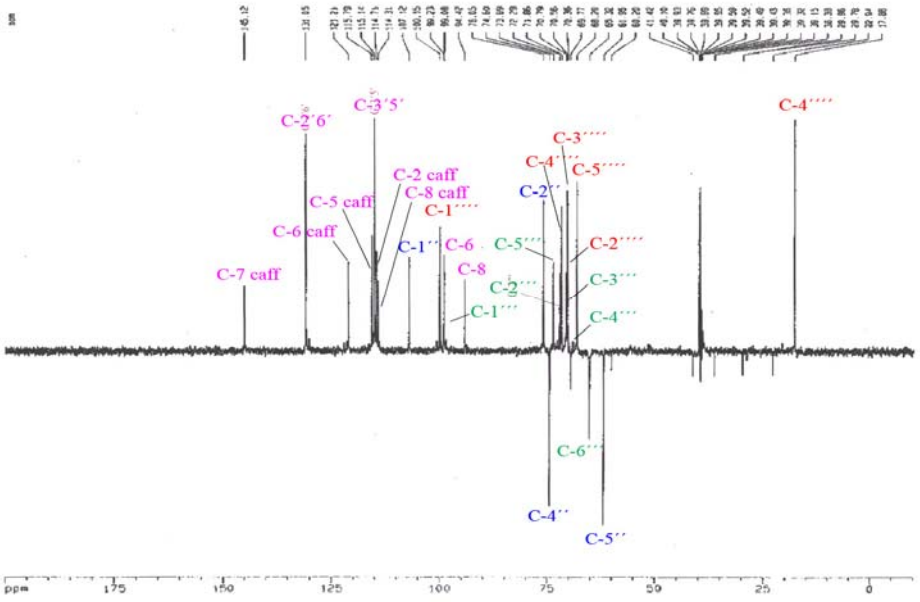

Figure B.4: DEPT Scan for the *S. perfoliatum* kaempferol caffeic acid trioside **5A.**

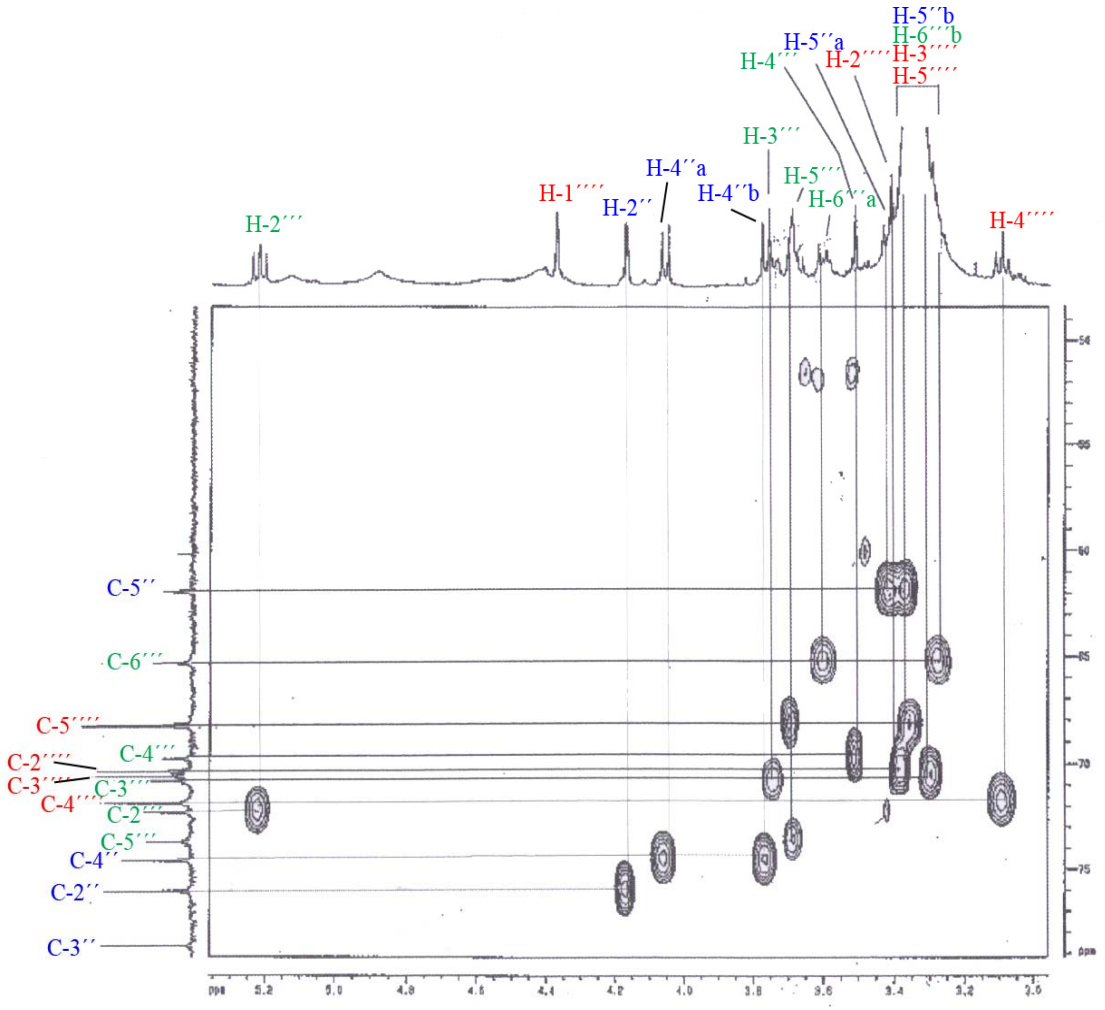

Figure B.5: HMQC Scan for the *S. perfoliatum* kaempferol caffeic trioside **5A** showing the proton carbon correlations of the three sugars**.**

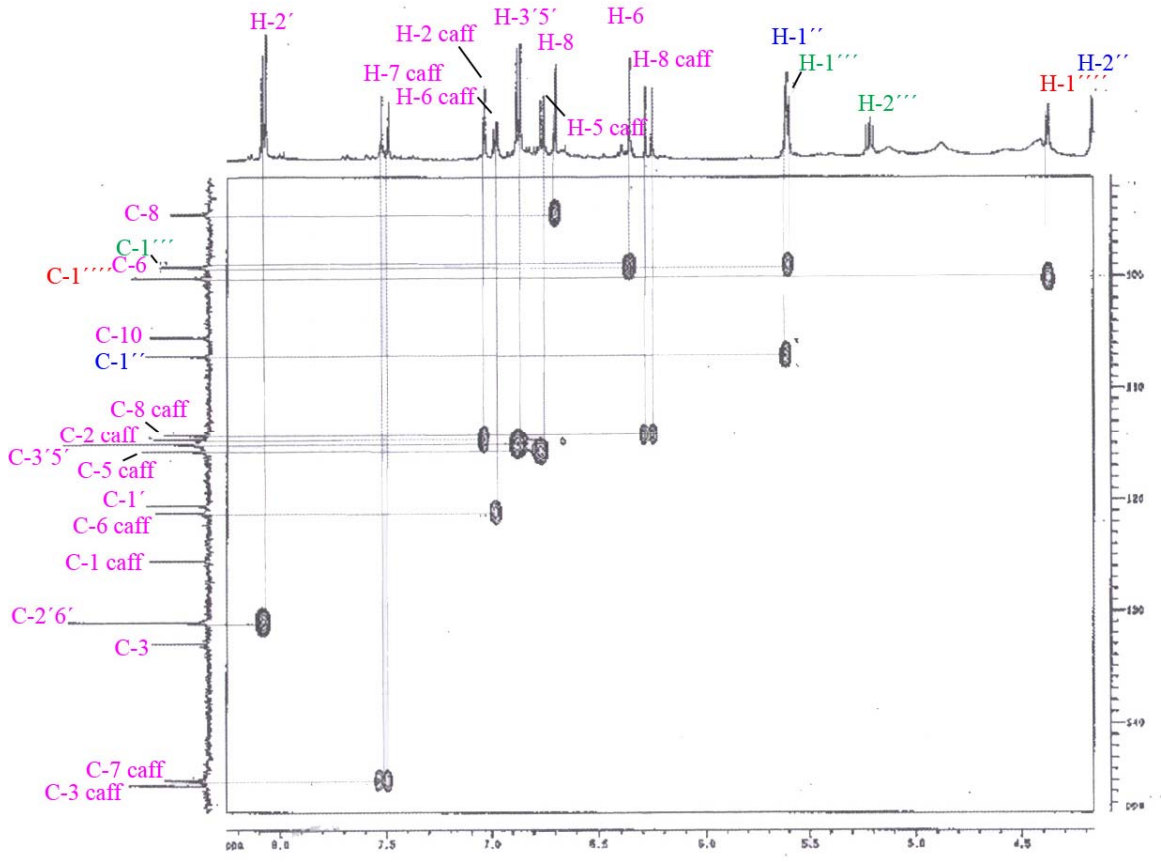

Figure B.6: HMQC Scan for the *S. perfoliatum* kaempferol caffeic acid trioside **5A** showing the proton carbon correlations of the caffeic moiety**.**

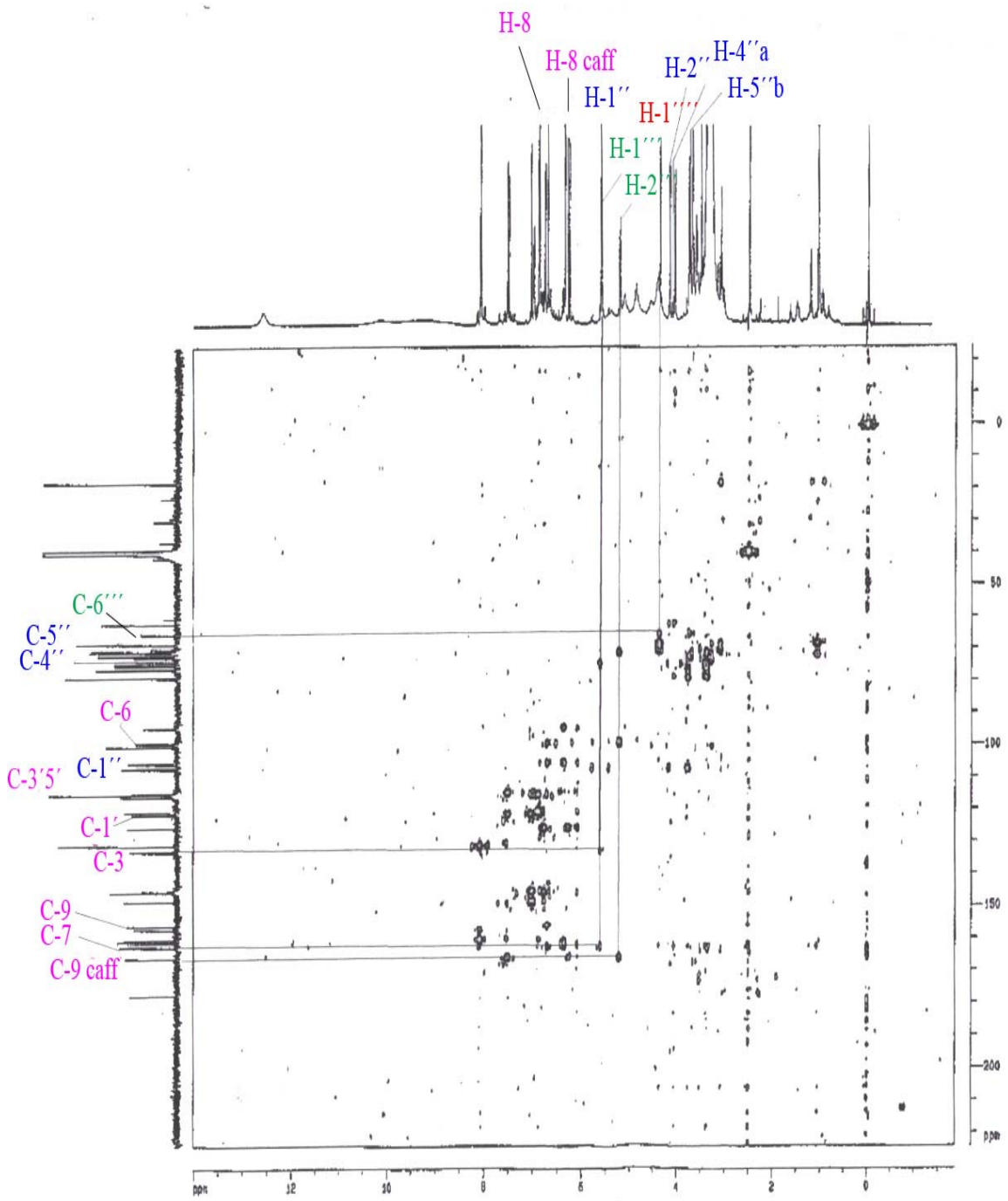

Figure B.7: The complete HMBC scan for the *S. perfoliatum* kaempferol caffeic acid trioside **5A** showing the long range correlations of the anomeric rhamnose proton with the galactose 6 carbon, the anomeric apiose proton with the caffeic 1-carbon and the anomeric galactose proton with the caffeic 7-carbon**.**

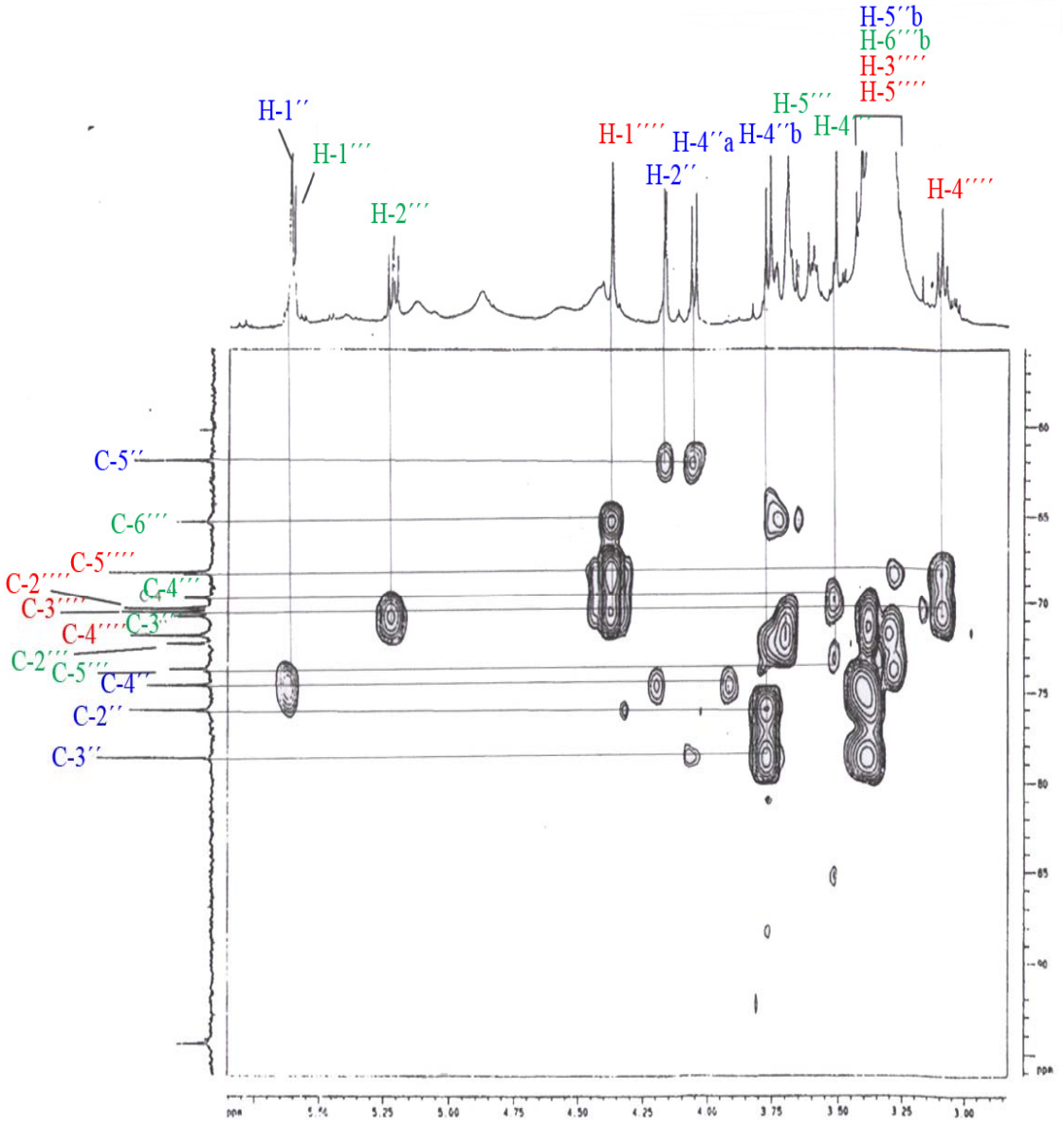

Figure B.8: The abridged proton 3.00-5.75 ppm HMBC scan for the *S. perfoliatum* kaempferol caffeic acid trioside **(5A)** showing both anomeric and sugar proton/carbon correlations.

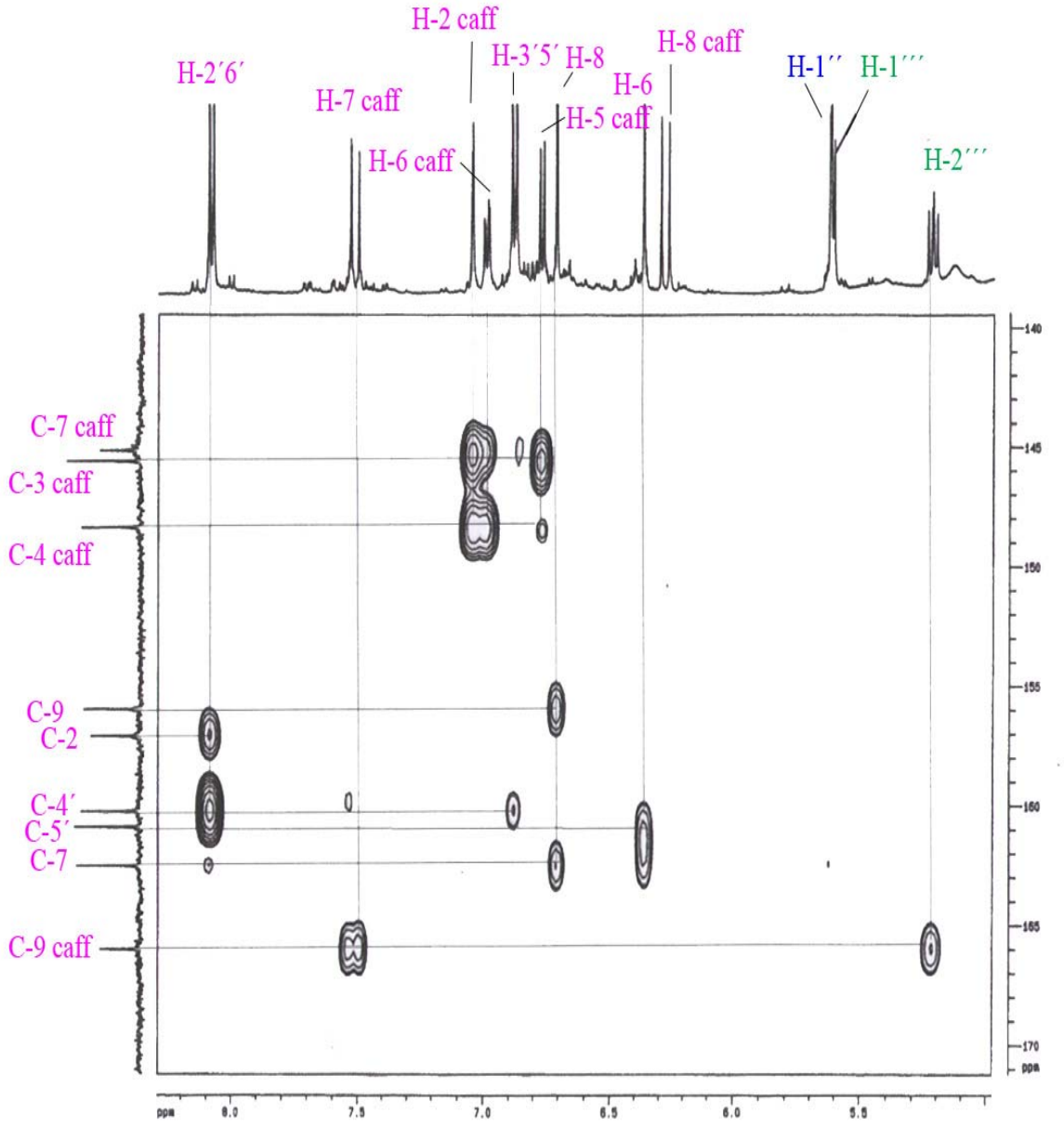

Figure B.9: The HMBC scan for the *S. perfoliatum* kaempferol caffeic acid trioside **(5A)** showing specifically the long range caffeic proton-carbon correlations.

Appendix C

Eighteen standards of the phenolic acids commonly found in the plants of the family Asteraceae where measured. A 50g crude sample of the eleven Silphium species were used in the quantification of the varying phenolic acid compounds. Unknown phenolics, most likely glycosolated forms of the knowns detected, where marked on each of the chromatograms at the end of chapter 5 (Figures 5.5-5.15). Known quantities where extracted using two solvent systems Ether and EtOAc and their amounts measured against calibration curves crated from industrial purchased standards.

sect. *Silphium*		
sect. Silphium		Total Weight
S. asteriscus	Ether	63.30 mg
S. asteriscus	EtOH	68.46 mg
S. brachiatum	Ether	116.73 mg
S. brachiatum	EtOH	95.91 mg
S. intergrifolium	Ether	86.11 mg
S. intergrifolium	EtOH	39.07 mg
S. mohrii	Ether	465.77 mg
S. mohrii	EtOH	345.06 mg
S. perfoliatum	Ether	40.33 mg
S. perfoliatum	EtOH	31.57 mg
S. radula	Ether	283.33 mg
S. radula	EtOH	212.54 mg
S. wasiotense	Ether	245.66 mg
S. wasiotense	EtOH	273.82 mg

sect. *Composita*		
		Total Weight
S. albiforum	Ether	97.15 mg
S. albiforum	EtOH	92.94 mg
S. laciniatum	Ether	146.7 mg
S. laciniatum	EtOH	378.86 mg
S. composita	Ether	127.73 mg
S. composita	EtOH	410.25 mg
S. terebintanaceum	Ether	155.21 mg
S. terebintanaceum	EtOH	415.97 mg

Table C.1: The purified phenolic/unknown extract mixtures were weighed, separated and then stored at 2° C in the dark. One half of the extract was used for TLC chromatography and the second half for HPLC analysis. The HPLC data were submitted and collected from two separate laboratories.

	Std. Phenolics	280λ A 0.01mg/ml	Ret. Time	0.0075mg/ml	Ret. Time	0.005mg/ml	Ret. Time	0.0025mg/ml	Ret. Time
	Ellagic	0.56	8.38	0.06	8.33	0.14	8.5	0.19	8.42
	Gallic	20.9	7.65	15.43	7.5	10.79	7.59	5.5	7.61
	Isovanillic	8.6	19.41	7.07	19.49	4.63	19.72	2.13	19.46
Benzoic	p-OH-Benzoic	15.6	15.07	12.27	15.23	7.86	15.37	3.91	15.24
Acids	Protocatechuic	13.9	10.09	10.93	10.28	6.89	10.3	3.47	10.4
	Salicylic	17.93	47.12	14.97	46.83	9.1	47.33	4.51	46.82
	Syringic	16.23	19.35	12.8	18.98	8.6	19.32	4.45	19.26
	Vanillic	16.78	17.91	13.44	17.61	8.82	17.89	4.68	17.89
	Caffeic	25.6	18.4	20.27	18.5	12.87	18.78	6.2	18.49
	Chlorogenic	10.13	13.46	7.89	12.95	4.98	13.37	2.44	13.4
	Ferulic	11.24	39.78	8.46	39.78	5.47	40.22	0.3	39.92
	Isoferuliuc	2.98	40.55	2.62	40.29	1.7	40.7	0.81	40.38
Cinnamic	Hydrocaffeic	1.89	18.56	1.6	18.26	1	18.66	0.52	18.47
Acids	m-Coumaric	42.39	41.36	33.48	41.36	20.99	41.77	10.54	41.52
	p-Coumaric	32.26	32.69	25.81	32.05	16.7	32.22	8.79	32.53
	p-OH-Phenylacetic	9.59	14.24	6.12	13.97	3.96	14.15	1.93	14.12
	Rosmarinic		59.57						
	Sinapic	11.82	43.29	8.9	42.4	6.01	42.49	0.12	42.93

	Std. Phenolics	254λ B 0.01mg/ml	Ret. Time	0.0075mg/ml	Ret. Time	0.005mg/ml	Ret. Time	0.0025mg/ml	Ret. Time
	Ellagic	0.07	8.38	0.054	8.15	0.38	0.83	1.21	7.72
	Gallic	14.15	7.65	10.94	7.5	7.97	7.59	4.49	7.61
	Isovanillic	19.46	19.41	15.04	19.49	9.84	19.72	4.8	19.46
Benzoic	p-OH-Benzoic	56.33	15.07	44.53	15.23	28.52	15.37	14.11	15.24
Acids	Protocatechuic	28.82	10.09	22.75	10.28	14.33	10.3	7.16	10.4
	Salicylic	9.56	47.12	6.9	46.83	5.3	47.34	2.15	46.83
	Syringic	7.41	19.35	5.94	18.98	3.93	19.33	2.02	19.26
	Vanillic	30.31	17.91	24.5	17.61	16.04	17.89	8.57	17.89
	Caffeic	18.31	18.4	14.06	18.5	8.9	18.78	4.31	18.49
	Chlorogenic	8.05	13.46	6.15	12.95	3.83	13.37	1.75	13.4
	Ferulic	7.55	39.78	5.79	39.78	3.71	40.22	0.13	39.93
	Isoferuliuc	0.16	40.55	0.13	40.29	1.41	40.7	0.74	40.36
Cinnamic	Hydrocaffeic	1.32	18.56	1.08	18.26	0.73	18.66	0.37	18.48
Acids	m-Coumaric	16.93	41.36	13.47	41.37	8.33	41.78	4.13	41.52
	p-Coumaric	5.33	32.69	4.33	32.05	2.86	32.22	0.14	32.53
	p-OH-Phenylacetic	1.15	14.24	0.72	13.9	0.51	15.15	0.2	14.12
	Rosmarinic	1.28	59.57						
	Sinapic	12.26	43.29	9.23	42.4	6.33	42.49	0.21	42.93

Table C.2: The calibration tables of the 18 phenolic acid standards at wavelengths λ 280 and λ 254.

	Linear Range (mg/mL)	Regression Equation	R^2
Gallic	.1-.0025	y=2032x+.45	0.9989
Ellagic	.1-.0025	y=32x+.25	0.0865
Protocatechuic	.1-.0025	y=1408+1E-14	0.9973
Chlorogenic	.1-.0025	y=1040x-.15	0.9973
p-OH-Phenylacetic	.1-.0025	y=1008x-.9	0.9818
p-OH-Benzoic	.1-.0025	y=1568x+.1	0.9963
Vanillic	.1-.0025	y=1636x+.7	0.9968
Caffeic	.1-.0025	y=2798x-.5	0.9985
Hydrocaffeic	.1-.0025	y=192x+.05	0.9846
Syringic	.1-.0025	y=1584x+.6	0.9976
Isovanillic	.1-.0025	y=952x-.2	0.9983
p-Coumeric	.1-.0025	y=3184x+1	0.9962
Ferculic	.1-.0025	y=1428x-2.5	0.9734
Isoferculic	.1-.0025	y=300x+.15	0.974
m-Coumaric	.1-.0025	y=4328x-.2	0.9962
Sinapic	.1-.0025	y=1520x-2.8	0.964

Table C.3: The regression analysis for each phenolic standard.

	Ellagic		Gallic		p-OH-Benz		p-Oh-Phen		Protocat.		Salicyl.		Vanillic		Isovanil.		Syringic	
	Eth	*EA*	*Eth*	*EA*	*Eth*	*EA*	*Eth*	*EA*	*Eth*	*EA*	*Eth*	*EA*	*Eth*	*EA*	*Eth*	*EA*	*Eth*	*EA*
S. albiflorum	√	√	√	√	√	√	√	√	√	√	√	√		√	√	√		
S. laciniatum	√	√	√	√	√	√	√	√	√	√	√	√	√	√	√	√	√	
S. composita	√	√	√	√	√	√	√	√	√	√		√				√		√
S. terebintana	√	√	√	√	√	√	√	√	√	√	√	√			√	√		
S. asteriscus	√	√	√	√	√	√	√	√	√	√	√	√			√	√	√	√
S. brachiatum	√	√	√	√	√	√		√	√	√	√	√				√		√
S. integrifolium	√	√	√	√	√	√	√	√	√	√	√	√	√	√	√	√	√	√
S. mohrii	√	√	√	√	√	√	√	√	√	√	√	√				√	√	√
S. perfoliatum	√		√	√	√	√	√	√	√	√	√	√	√		√		√	
S. radula	√	√	√	√		√	√	√	√	√	√	√		√	√		√	
S. wasiotense	√	√	√	√	√	√	√	√	√	√	√	√	√		√			√

Table C.4: Presence of benzoic acids by species and extraction solution (check mark indicates compound was detected).

	Caffeic		Hydrocaff		Chloro		Ferrulic		Isofer		m-Coum		p-Coum		Rosmar	
	Eth	*EA*	*Eth*	*EA*	*Eth*	*EA*	*Eth*	*EA*	*Eth*	*EA*	*Eth*	*EA*	*Eth*	*EA*	*Eth*	*EA*
S. albiflorum	√	√	√		√	√				√	√	√		√	√	√
S. laciniatum	√	√	√		√	√	√			√	√	√	√		√	√
S. composita	√	√			√	√		√						√	√	√
S. terebintana	√	√	√	√	√						√			√	√	√
S. asteriscus		√	√		√	√							√	√	√	√
S. brachiatum	√			√	√	√	√	√					√		√	√
S. integrifolium				√	√						√		√	√	√	√
S. mohrii		√	√	√	√	√		√			√	√	√		√	√
S. perfoliatum				√	√	√							√		√	√
S. radula	√	√	√		√	√									√	√
S. wasiotense	√				√	√	√				√	√	√		√	√

Table C.5: Presence of cinnamic acids by species and extraction solution (check mark indicates compound was detected).

Benzoic Acids									
	p-OH-Benz	**Protocat.**	**Vanillic**	**Isovanil.**	**Gallic**	**Ellagic**	**Syringic**	**Salicyl**	**P-Oh-Phen**
S. asteriscus	67	0	0	5	7	2	8	19	13
S. asteriscus	19	13	27	23	33	4	3	56	20
TOTAL	**86**	**14**	**27**	**28**	**40**	**6**	**11**	**74**	**33**
S. brachiatum	8	3	0	0	1	3	0	7	0
S. brachiatum	2	2	0	3	2	2	0	8	10
TOTAL	**10**	**6**	**0**	**3**	**3**	**5**	**0**	**15**	**10**
S. intergrif	51	6	184	1	32	1	0	20	6
S. intergrif	2	14	28	54	70	2	1	15	25
TOTAL	**53**	**20**	**212**	**55**	**102**	**3**	**1**	**35**	**31**
S. mohrii	10	6	146	0	128	6	13	142	76
S. mohrii	32	31	7	23	38	20	3	12	33
TOTAL	**41**	**37**	**153**	**23**	**166**	**26**	**16**	**155**	**109**
S. perforliatum	11	156	16	18	48	5	4	63	13
S. perforliatum	2	31	0	0	116	0	0	19	8
TOTAL	**13**	**187**	**16**	**18**	**164**	**5**	**4**	**82**	**21**
S. radula (ether)	0	5	0	80	13	3	1	8	50
S. radula (EtOAch)	2	11	2	0	599	34	0	8	30
TOTAL	**2**	**16**	**2**	**80**	**613**	**37**	**1**	**16**	**80**
S. Wasiotense	111	68	8	18	5	5	0	109	27
S. Wasiotense	11	9	0	0	289	16	8	16	8
TOTAL	**122**	**78**	**8**	**18**	**295**	**21**	**8**	**125**	**35**
	p-OH-Benz	**Protocat.**	**Vanillic**	**Isovanil.**	**Gallic**	**Ellagic**	**Syringic**	**Salicyl**	**P-Oh-Phen**
S. albiforum (ether)	61	428	0	8	12	1	0	31	20
S. albiforum (EtOAch)	11	346	26	96	368	4	0	6	36
TOTAL	**72**	**774**	**26**	**104**	**380**	**5**	**0**	**37**	**56**
S. laciniatum	6	171	1	11	194	5	2	5	3
S. laciniatum	38	2886	16	48	29	2	0	8	8
TOTAL	**44**	**3058**	**17**	**59**	**223**	**7**	**2**	**13**	**10**
S. composita (ether)	25	1684	0	0	22	1	0	0	9
S. composita (EtOAch)	41	38	0	10	43	4	4	0	45
TOTAL	**66**	**1722**	**0**	**10**	**65**	**4**	**4**	**0**	**54**
S. terebintanaceum (ether)	31	7723	0	84	320	7	0	11	9
S. terebintanaceum (EtOAch)	23	898	0	64	397	5	0	6	84
TOTAL	**54**	**8621**	**0**	**147**	**716**	**12**	**0**	**17**	**93**

Table C.6: The total concentration of phenolic benzoic acids extracted in micrograms by species (rounded to nearest whole number).

Cinnamic Acids								
	p-Coum.	Caffeic	Hydrocaff	Ferulic	Chloro	Isofer	Rosmar	m-Courm
S. asteriscus	241	0	4054	0	2	0	10	0
S. asteriscus	1	1	0	0	12	0	56	0
TOTAL	**242**	**1**	**4054**	**0**	**15**	**0**	**66**	**0**
S. brachiatum	194	37	0	0	24	0	6	0
S. brachiatum	0	0	117	0	2	0	7	0
TOTAL	**194**	**37**	**117**	**0**	**26**	**0**	**13**	**0**
S. intergrif	110	0	0	0	1	0	4	3
S. intergrif	21	0	7584	0	0	0	34	0
TOTAL	**131**	**0**	**7584**	**0**	**1**	**0**	**38**	**3**
S. mohrii	32	0	0	0	2	0	13	51
S. mohrii	0	11	0	3	23	0	9	0
TOTAL	**32**	**11**	**0**	**3**	**26**	**0**	**22**	**51**
S. perforliatum	6	0	0	0	5	0	13	0
S. perforliatum	0	0	312	0	6	0	11	0
TOTAL	**6**	**0**	**312**	**0**	**11**	**0**	**23**	**0**
S. radula (ether)	0	3	46089	0	7	0	10	0
S. radula (EtOAch)	0	1	0	0	4	0	11	0
TOTAL	**0**	**4**	**46089**	**0**	**10**	**0**	**21**	**0**
S. Wasiotense	23	16	0	4	16	0	12	71
S. Wasiotense	0	0	0	0	16	0	8	6
TOTAL	**23**	**16**	**0**	**4**	**32**	**0**	**20**	**77**
	p-Coum.	**Caffeic**	**Hydrocaff**	**Ferulic**	**Chloro**	**Isofer**	**Rosmar**	**m-Courm**
S. albiforum (ether)	0	24	53478	0	5	0	21	67
S. albiforum (EtOAch)	12	27	0	0	16	67956	20	3
TOTAL	**12**	**51**	**53478**	**0**	**21**	**67956**	**41**	**69**
S. laciniatum	1	1	1752	27380	8	0	96	1
S. laciniatum	0	66	0	0	10	3379485	42	23
TOTAL	**1**	**67**	**1752**	**27380**	**18**	**3379485**	**138**	**24**
S. composita (ether)	0	5	0	0	78	0	16	0
S. composita (EtOAch)	1	34	0	3	662	0	22	0
TOTAL	**1**	**39**	**0**	**3**	**740**	**0**	**38**	**0**
S. terebintanaceum (ether)	0	72	57628	0	149	0	15	12
S. terebintanaceum (EtOAch)	3	36	12442	0	0	0	85	0

Table C.7: The total concentration of phenolic cinnamic acids extracted in micrograms by species (rounded to nearest whole number).

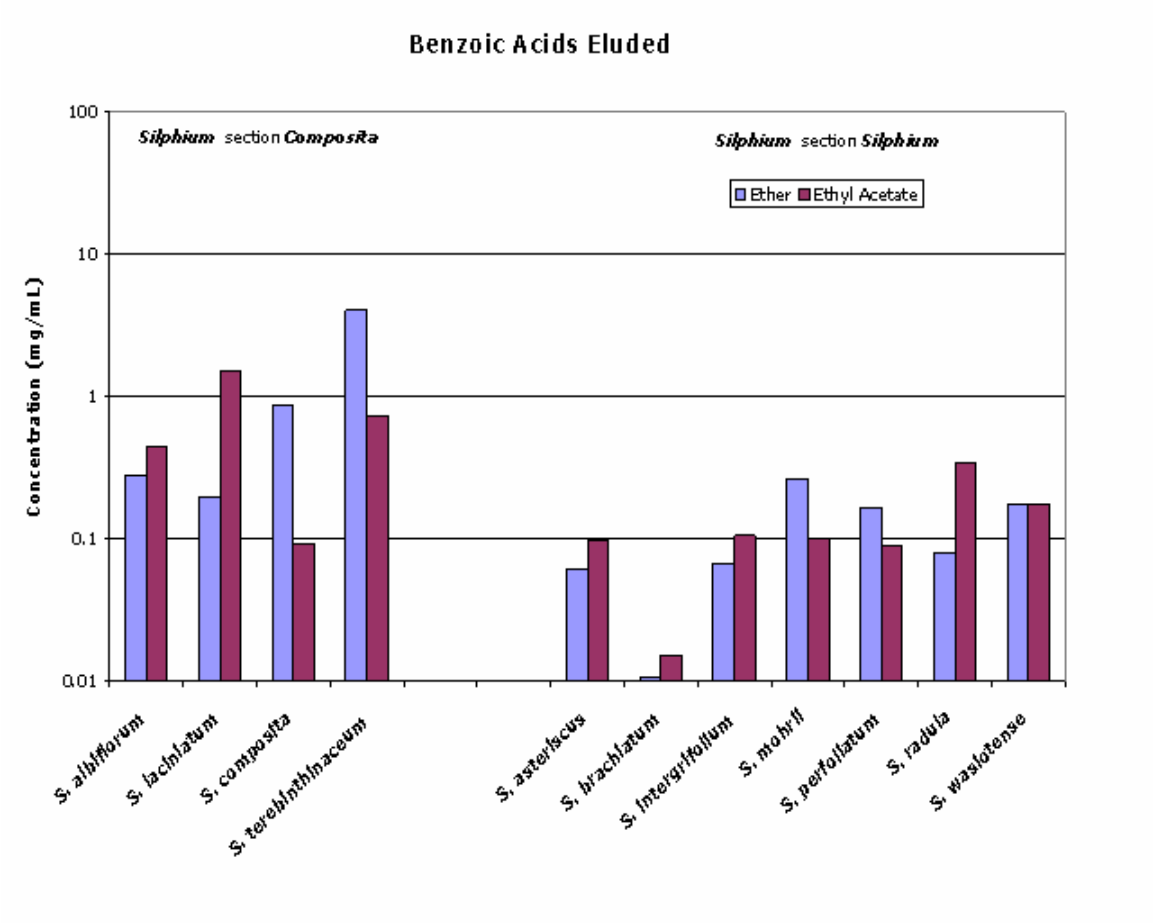

Benzoic Acids

1. R=R'=H; *p*-hydroxybenzoic acid
2. R=OH, R'=H; protocatechuic acid
3. R= OCH_3, R'=H; vanillic acid
4. R=R'=OH; gallic acid
5. R=R'= OCH_3; syringic acid
6. R=H; salicylic acid (*o*-hydroxybenzoic acid)
7. R=OH; gentisic acid

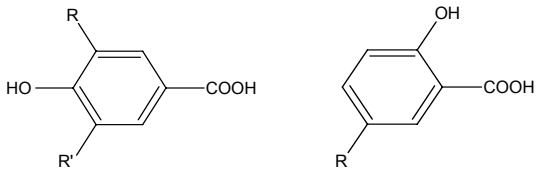

Figure C.1: The concentration comparison across the genus *Silphium* involving the hydroxybenzoic acids. The data for both the ether and ethyl acetate extracts are included along with the substitution patterns for the standards used.

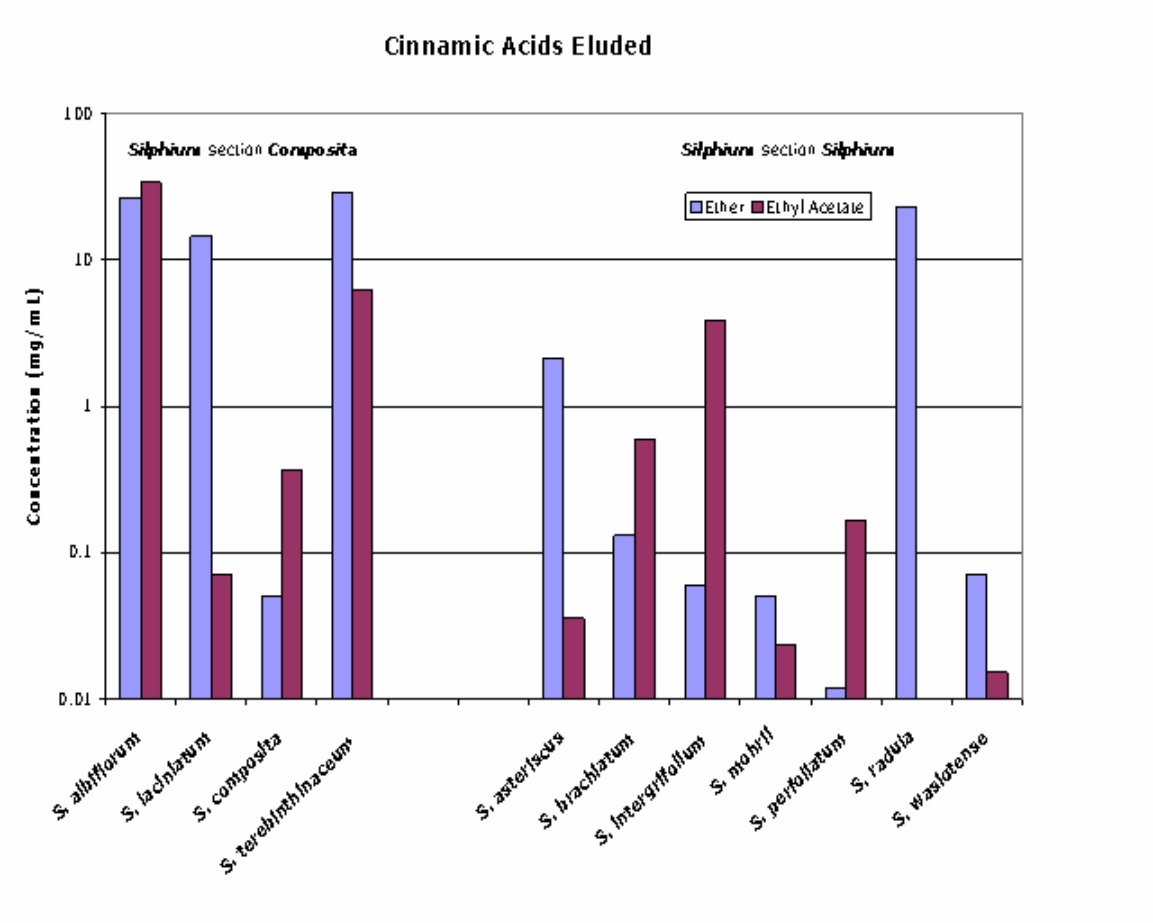

Cinnamic Acids

1. R=R'=H; *p*-coumaric acid
2. R=OH, R'=H; caffeic acid
3. R=OCH_3, R'=H; ferulic acid
4. R=R'= OCH_3; sinapic acid

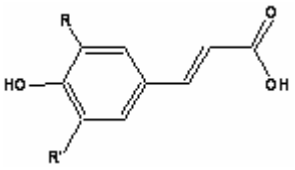

Figure C.2: The distribution of hydroxycinnamic compounds in both ether and ethyl acetate extracts.

References:

Agrawal, P. K. and Bansal, M. C. (1989). Carbon 13 NMR of Flavonoid Glycosides. Elsevier, New York. pp. 283-364.

Agrawal, P. K. (1992). NMR spectroscopy in the structural elucidation of oligosaccharides and glycosides. Phytochem. *31*, 3307-3330.

Agrawal, P. K. and Bansal, M. C. (1989). Flavonoid glycosides. In: Agrawal. P.K. (Ed.), Carbon-13 NMR of Flavonoids. Elsevier, Amsterdam, pp. 283-364.

Ajilvsgi, G. (1984). Wildflowers of Texas. Shearer Publishing, Fredericksburg, Texas, p. 33.

Akland, M. L., Van De Waarsenburg S. and Jones, R. (2005). Synergistic antiproleferative action of the flavonols quercetin and kaempferol in cultured human cancer cell lines. In Vivo, *19* (1, spec. Iss.), 69-76.

Angyal, S. J., Bodkin, C. L., Mills, J. A. and Pojer, P. M. (1977). Complexes of carbohydrates with metal cations. IX. Synthesis of the methyl D-tagatosides, D-psicosides, D-apiosides and D-erythrosides. Aust. J. Chem. *30*, 1259–1268.

Angyal, S. J. and Pickles, V. A. (1972). Equilibria between pyranoses and furanoses. Aust. J. Chem. *25,* 1695-1710.

Auffenorde, T. M. and Wistendahl, W. A. (1982). Demography and persistence of *Silphium laciniatum* at the O. E. Anderson compass plant prairie. In Proceedings of the Eighth North American Prairie Conference. Ed. R. Brewer. Western Michigan University, Kalamazoo, pp. 30-32.

Avila, M. A., Cansado, J., Harter, K. W., Velasco, J. A. and Notario, V. (1996). Quercetin as a modulator of the cellular neoplastic phenotype. Dietary Phytochemicals in Cancer Prevention and Treatment, Adv. Eep. Med. Biol. 101-110.

Baily, L. H. (1951). Manual of Cultivated Plants. MacMillan Publishing, New York. p. 974.

Barberá, O., Sanz, F. J., Sánchez-Parareda, J. and Marco, J. A. (1986). Further flavonol glycosides from *Anthyllis onobrychioides*. Phytochem. *25*, 3781-3784.

Bashir, A., Hamburger, M., Gupta, M. P., Solis, P. N. and Hostettmann, K. (1990). Flavonol glycosides from *Monnina sylvatica*. Phytochem. *30*, 3781–3784.

Benke, H. D. and Mabry, T. J. (1994). *Caryophyllales*: Evolution and Systematics. Springer-Verlag, Heidelberg, p. 276.

Borkowski, B. (1993). Fenolokwasy i ich estry. Cz.II. Herba Polon. *39*,139.

Britton, N. L. and Brown, H. A. (1970). Illustrated Flora of the Northern United States and Canada. Vol.III. Dover Publications Inc, New York, pp. 459-462.

Buschi, C. A. and Pomilio, A. B. (1982). Isorhamnetin 3-*O*-robinobioside from *Gomphrena martiana*. J. Nat. Prod. *45*, 557-559.

Charting Nature. Compass Plant: *Silphium laciniatum*. Flower print: p. 6170.

Clevinger, J. A. (2004). New Combinations in *Silphium* (Asteracaceae: Heliantheae), Novon *14*, pp. 275-277.

Clevinger, J. A. (1999). Dissertation: Systematics of *Silphium* and its Subtribe Engelmanniinae (Asteraceae: Heliantheae). The University of Texas at Austin.

Clevinger, J. A. and Panero, J. L. (2000). Phylogenetic relationships in Engelmaniinae and the genus *Silphium* (Asteraceae: Heliantheae) based on ITS and ETS sequence data. Am. J. Bot. *87*, 565-572.

Correll, D. S. and Johnston, M. C. (1970). Manual of the Vascular Plants of Texas. Renner Texas Research Foundation, pp. 1622-1623.

Cronquist, A. (1980). *Silphium*. In Vascular Flora of the Southeastern United States, Vol. I: Asteraceae. University of North Carolina Press, Chapel Hill, NC, pp. 67-72.

Curtis, S. (1836). Curtis's Botanical Magazine. *63*: plate 3525.

Davidyants, E. S. and Abubakirov, N. K. (1992). Chemical composition of species of the genus *Silphium* L. and prospects of its utilization. Rastit. Resur. *28*, 118–128.

Davis, B. D. and Brodbelt, J. S. (2004). Determination of the glycosylation site of flavonoid monoglucosides by metal complexation and tandem mass spectrometry. J. Am. Soc. Mass Spectrom. *15*, 1287-1299.

Davis, B. D. and Brodbelt, J. S. (2005). LC-MS^n Methods of saccharide characterization of monoglycosyl flavonoids using post-column manganese complexation. Anal. Chem. *77*, 1883-1890.

Densmore, F. (1929). Uses of plants by the Chippewa Indians. Annual report of the Bureau of American Ethnology to the Secretary of the Smithsonian Institute. Washington, G.P.O. 44th, pp. 340-358.

Dings, G. M. Jr., Lipscomb, B. L. and O'Kennon, R. J. (1999). Shinner's Mahler's Illustrated Flora of North Central Texas. Botanical Research Institute of Texas and Austin College, p. 404.

Dragondorff, G. (1898). Die Heilflanzen der Verscheiden Völker und Zeiten. Ihre Anwendung, Wesentlichen Bestandtheile und Geschichte. Verlag von Enke, Stuttgart, Germany, p. 668.

El-Sayed, N. H., Wojcińska, M., Drost-Karbowska, K., Matławska, I., Williams, J. and Mabry, T. J. (2002). Kaempferol trioside from *Silphium perfoliatum*. Phytochem. *60*, 835-838.

Felter, H. W. and Lloyd, J. U. (1898). King's American Dispensatory. Ohio Valley Co., Cincinnatti, p. 652.

Ferrandina, G., Scambia, G., Panici, P. B., Ranelletti, F. O., De Vincenzo, R., Piantelli, M., Masciullo, V., Bonanno, G. and Mozzetti, S. (1994). Quercetin induces transforming growth factor β1 secretion by human overian cancer cells. Acta Medica Romana. *32*, 566-572.

Fielder, M. (1975). Plant Medicine and Folklore. Winchester Press, New York, p. 100.

Flowersoncd.com. *Silphium perfoliatum*. Flower print: p..

Geissmam, T. A. (1962).The Chemistry of Flavonoid Compounds, The MacMillian Company, New York. pp. 317-319.

Gleason, H. A. and Cronquist, A. (1991). *Silphium*. In Manual of Vascular Plants of the northeastern United States and adjacent Canada. New York Botanical Garden, NY, 545-547.

Halim, A. F., Saad, H. F. and Hashish, N. E. (1995). Flavonol glycosides from *Nitraria retusa.* Photochem. *40*, 349-351.

Halsted, B.D. (1887). Dry weather foliage of the compass plant. Bot. Gaz. *12*, 161-162.

Harborne, J. B. and Simmons, N. W. (1964). Biochemistry of Phenolic Compounds, ed. by J. B. Harborne. Academic Press, New York . pp. 82.

Heilpflanzen—Herbal Remedies, (1996–1999). CD. Files: *Silphium perfoliatum* L., *S. laciniatum* L., Medpharm.

Hocking, G. M. (1997). A Dictionary of Natural Products. Plexus Publishing Old Marlton Pike Medford, NJ. pp.724-725.

Ingham, J. L., Markham, K. R., Dziedzic, S. Z., and Pope, G. S. (1986). Puerarin 6-*O*-*β*-apiofuranoside A, C-Glycosyloisoflavone *O*-glucoside from *Pueraria mirifica*. Phytochem. *25*, 1772–1775.

Ishii, T. and Yanagisawa, M. (1988). Synthesis, separation and NMR spectral analysis of methyl apiofuranoside. Carbohydr. Res. *313*, 189-192.

Jimmo.com. *Silphium mohrii*, drawing.

Kosmider, B. and Osiecka, R., (2004). Flavonoid compounds: a review of anticancer properties and interactions with cis-diamminedichloroplatinum(II). Drug Dev. Res. *63*, 200-211.

Kowalski, R. (2004). Secondary metabolites in *Silphium integrifolium* in the first 2 years of cultivation. N. Z. J. Crop and Hort. Sci. *32*, 397-406.

Kowalski, R. and Wiercinski, J. (2003). Pol. J. Food Nutr. Sci. *12*, 17-20.

Kraut, L., Mues, R. and Sim-Sim, M. (1993). Acylated flavone and glycerol glucosides from two *Frullania* species. Phytochem. *34*, 211–218.

Linnaeus, C. (1826). Systema Vegetabilium, Gottingae, Sumtibus Librariae Dieterichianae, Vol.3. pp.16-23.

Mabry, T. J., Markham, K. R. and Thomas, M. B. (1970). The Systematic Identification of Flavonoids. Springer-Verlag, New York, pp.292-298

"Mallorn Plant of the Month.: *Silphium perfoliatum*.htm."; http:www.Mallorn.com./pon/Aug99.

Markham, R. K. (1982). Techniques of Flavonoid Identification. Academic Press, London. pp. 5-7.

Markham, R. K., Chari, V. M. and Mabry, T. J. (1982). Carbon-13 NMR spectroscopy of flavonoids. In: Markham, K. R. and Mabry, T. J. (Eds.), The Flavonoids: Advances in Research. Chapman and Hall, New York, pp.19-134.

Markham, R. K. and Geiger, H. (1994). ^{1}H nuclear magnetic resonance spectroscopy of flavonoids and their glycosides in hexadeuterodimethylsufoxide. In: Harborne, J.

B. (Ed.), The Flavonoids: Advances in Research Since 1985. Chapman and Hall, London, pp. 441-449.

Markham, R. K. and Ternai, B. (1976). ^{13}C NMR of flavonoids – II. Flavonoids and other than flavone and flavonol aglycones. Tetrahedron *32*, 2607-2612.

Markham, K. R., Ternai,B., Stanley, R., Geiger, H. and Mabry T. J. (1978). ^{13}C NMR studies of flavonoids. III. Naturally occuring flavonoid glycosides and their acylated derivatives. Tetrahedron *34*, 1389–1397.

Medley, M. E. (1989). *Silphium wasiotense* (Asteraceae), a new species from the Appalachian Plateau in Eastern Kentucky. Sida *13*: 285-291.

Mohr, C. (1901). Plant life of Alabama an account of the distribution, modes of association, and adaptations of the flora of Alabama, together with a sy / Theodore, 1824-1901. , Washington ,.

Matsubara, K., Ishihara, K., Mizushina, Y., Mori, M. and Nobuyoshi, N. (2004). Anti-angiogenic activity of quercetin and its derivatives. Lett. Drug Des. Discovery *1*, 329-333.

Oszmianski, J. (1995). Polifenole jako naturalne przeciwutleniacze w zywnosci. Przem. Spoz *3*, 94-96.

Perry, L. M. (1937). Notes on *Silphium*. Rhodora *39*, 281-297.

Pictet, C. and Brandenberger, H. (1960). J. Chromatogr. *4*, 396.

Pcolinski, M. J. (1992). Dissertation: Structural Studies of Natural Products from *Silphium perfoliatum* L. *Amphiachyris amoena* (Shinners) Solbrig and *Amphiachyris dracunculoides* DC. Nutt. The Ohio State University.

Pleasants, J. M. and Jurik, T. W. (1992). Dispersion of seedlings of the prairie compass plant, Silphium laciniatum (Asteraceae). Am. J. Bot. *79*, 133-137.

Ranganathan, R., Nagarajan, S., Mabry, T. J., Yong-Long, L. and Neuman, P. (1980). 6-hydroxyluteolin 7-*O*-apioside from *Lepidagathis cristata.* Phytochem. *19*, 2505-2506.

Rastrelli,L., Saturnino, O. and Dini, A. (1995). Studies on the constituents of *Chenopodium pallidicaule* (Cañihua) seeds. Isolation and characterization of two new flavonol glycosides. J. Agri. Food Chem. *43*, 2020-2024.

Ribéreau-Gayon, P. (1972). Plant Phenolics. Institut d' Oenologie, Universite de Bordeaux II *3*, 82.

Riesenberg, L. H. and Brouillet, L. (1994). Are many species paraphyletic? Taxon *43,* 21-32.

Robards, K. and Antolovich, M. (1997). Analytical chemistry of fruit bioflavonoids – A review. Analyst *122*, 11-34.

Santos-Buelga, C., García-Viguera, C. and Tomás-Bareran, F. A. (2003). On-line identification of flavonoids by HPLC coupled to Diode Array Detection. In: C. Santos-Buelga and G. Williamson (Eds), Methods in Polyphenol Analysis. Royal Society of Chemistry, Cambridge, pp. 92-127.

Schieber, A., Keller, P., Streker P., Klaiber, I. and Carle, R. (2002). Detectoin of isorhamnetin glycosides in extracts of apples (*Malus domestica* cv. "Brettacher") by HPLC-PDA and HPLC-APCI-MS/MS. Phytochem. *13*, 87-94.

Silva, B. P., Velozos, L. S. M. and Parente, J. P. (2000). Biochanin A triglycoside from *Andira inermis*. Fitoterapia *71*, 663–667.

Small, J. K. (1933). *Silphium*. In Manual of the Southeastern Flora. University of North Carolina Press, Chapel Hill, NC, pp.1408-1415.

Steinmetz, J .A. (1954). Materia medica vegetabilis, Part II. Amsterdam, p.1292.

Swanson, C. L., Buchanan, R. A. and Otey, F. H. (1979). Molecular weights of natural rubbers from selected temperate zone plants. J. Appl. Polym. Sci. *23*, 743-748.

Swiatek, L. (1977). Herba Polon. *23*, 201.

Swiatek, L., Grabias, B., and Kalemba, D. (1998). Phenolic acids in certain medicinal plants of the genus *Artemisia*. Pharm. Pharmacol. Lett. *8*, 158-160.

Syrov, V. N., Khushabaktova, Z. A., and Davidyan, X. (1992). Triterpenoid glycosides from *Silphium perfoliatum* L.: hypolipidemic activity of silphioside. Khim.-Farm. Zh. *26*, 66–69.

Takeda, S. and Aburada, M. (1981). The choleretic mechanism of coumarin compounds and phenolic compounds. Journal of Pharmacobio-dynamics *4*, 724-734.

Tyman, J. H. P. and Jacobs, N. (1971). Composition of the unsaturated phenolic components of anacardic acid. J. Chromatogr. *54*, 83-90.

van Erk, M. J., Roepman, P., van der Lende, T. R., Stierum, R. H., Aarts, J. M., van Bladeren, P. J., and van Ommen, B. (2005). Integrated assessment by multiplegene expression analysis of quercetin bioactivity on anticancer-related mechanisms in colon cancer cells *in vitro*. Eur. J. Nutr. *44*, 143-156.

Wink, M. (2003). Evolution of secondary metabolites from an ecological and molecular phylogenetic perspective. Phytochem. *64*, 3-19.

Wojcińska, M. (1998). Phenolic Acids in *Silphium perfoliatum* L. flowers (Asteraceae/ Composita). Acta Poloniae Pharmaceutica. *55*, 413-416.

Yasukawa, K. and Takido, M. (1987). A flavonol glycoside from *Lysimachia mauritiana*. Phytochem. *24*, 1224-1226.

Zhang, H., Pleasants J. M. and Jurik, T. W. (1991). Development of leaf orientation in the prairie compass plant, *Silphium laciniatum* L. Bull. Torrey Bot. Club *118*, 33-42.

VITA

Jeffrey Douglas Williams was born August 23, 1968 in Baton Rouge, LA to Sharon Jaunita Child and Douglas Robert Williams. He completed his secondary schooling graduating in 1987. After High School he completed a two year foreign mission to Berlin, Germany returning to complete his B.S. in European/German Studies at Brigham Young University, UT, graduating in 1995. While at BYU, he certified his language proficiency through the German Goethe Institute, worked as a transmission assembler for the BMW Corporation in Munich and completed his honors thesis involving German film of the 1930's. In 1998 he began the study of medicine at the Louisiana State Medical Center, New Orleans, LA opting to leave the medical field at the completion of his dermatology rotation in the spring of 2000. He began the study of natural products chemistry under the direction of Dr. Tom Mabry at the University of Texas at Austin in the spring of 2000. After entering the Plant Biology Graduate Program, he has been a Teaching Assistant and taught a number of biology labs and lectures for several professors and lecturers. He also completed the graduate course work required for his teaching certification in secondary education through the UTeach Natural Sciences Graduate Program. His doctorate studies were supported by awards provided by Dr. Tom Mabry, Undergraduate Coop Fellowships and the Welch Foundation. His publications include: Phytochemistry 60 (8): 835-837 (2002), Phytochemistry 2006 (*in press*), Natural Products Communications 2006 (*in press*).

Permanent address: 111 Bridle Path, Kyle, TX, 78640

This dissertation was typed by Jeffrey Williams.